frontiers | Research Topics

Case reports in radiation oncology 2022

Edited by
Benjamin Clasie, Tao Song, Haibo Lin and Ianik Plante

Published in
Frontiers in Oncology

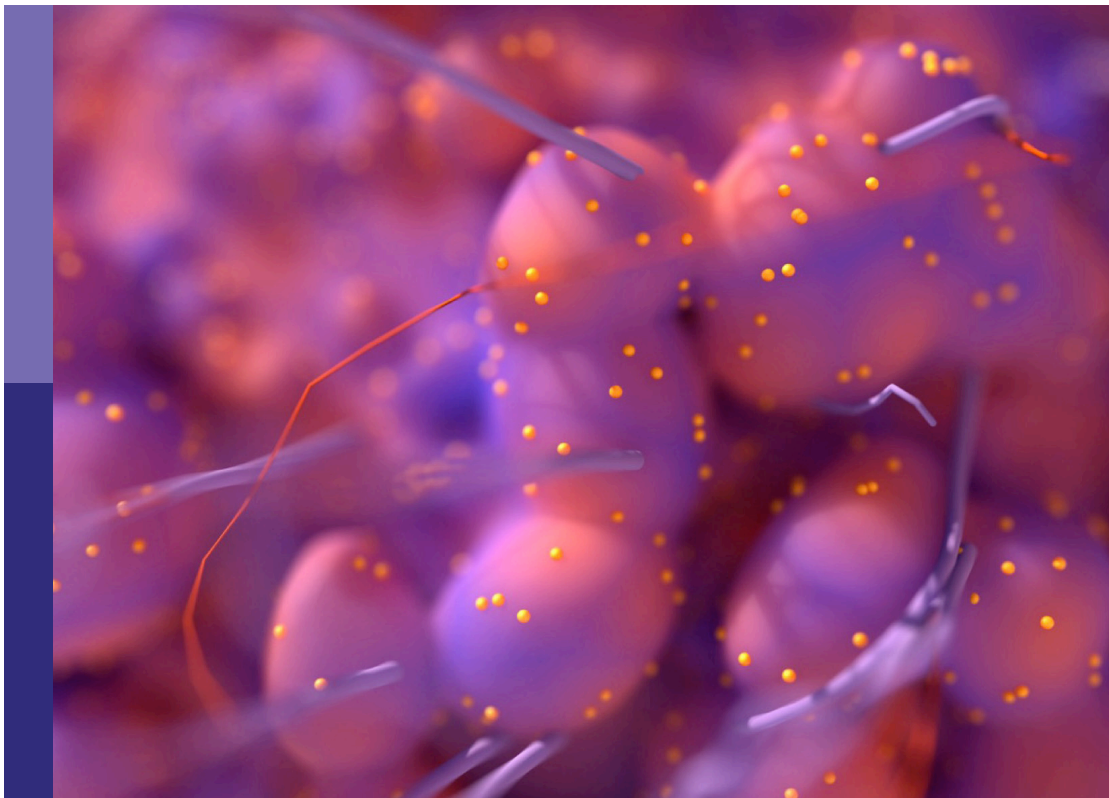

ISSN 1664-8714
ISBN 978-2-8325-3222-5
DOI 10.3389/978-2-8325-3222-5

About Frontiers

Frontiers is more than just an open access publisher of scholarly articles: it is a pioneering approach to the world of academia, radically improving the way scholarly research is managed. The grand vision of Frontiers is a world where all people have an equal opportunity to seek, share and generate knowledge. Frontiers provides immediate and permanent online open access to all its publications, but this alone is not enough to realize our grand goals.

Frontiers journal series

The Frontiers journal series is a multi-tier and interdisciplinary set of open-access, online journals, promising a paradigm shift from the current review, selection and dissemination processes in academic publishing. All Frontiers journals are driven by researchers for researchers; therefore, they constitute a service to the scholarly community. At the same time, the *Frontiers journal series* operates on a revolutionary invention, the tiered publishing system, initially addressing specific communities of scholars, and gradually climbing up to broader public understanding, thus serving the interests of the lay society, too.

Dedication to quality

Each Frontiers article is a landmark of the highest quality, thanks to genuinely collaborative interactions between authors and review editors, who include some of the world's best academicians. Research must be certified by peers before entering a stream of knowledge that may eventually reach the public - and shape society; therefore, Frontiers only applies the most rigorous and unbiased reviews. Frontiers revolutionizes research publishing by freely delivering the most outstanding research, evaluated with no bias from both the academic and social point of view. By applying the most advanced information technologies, Frontiers is catapulting scholarly publishing into a new generation.

What are Frontiers Research Topics?

Frontiers Research Topics are very popular trademarks of the *Frontiers journals series*: they are collections of at least ten articles, all centered on a particular subject. With their unique mix of varied contributions from Original Research to Review Articles, Frontiers Research Topics unify the most influential researchers, the latest key findings and historical advances in a hot research area.

Find out more on how to host your own Frontiers Research Topic or contribute to one as an author by contacting the Frontiers editorial office: frontiersin.org/about/contact

Case reports in radiation oncology: 2022

Topic editors

Benjamin Clasie — Massachusetts General Hospital, Harvard Medical School, United States

Tao Song — Zhejiang Provincial People's Hospital, China

Haibo Lin — New York Proton Center, United States

Ianik Plante — KBRwyle, United States

Citation

Clasie, B., Song, T., Lin, H., Plante, I., eds. (2023). *Case reports in radiation oncology: 2022*. Lausanne: Frontiers Media SA. doi: 10.3389/978-2-8325-3222-5

Table of contents

frontiers | Frontiers in Oncology

TYPE Editorial
PUBLISHED 31 July 2023
DOI 10.3389/fonc.2023.1264297

OPEN ACCESS

EDITED AND REVIEWED BY
Timothy James Kinsella,
Brown University, United States

*CORRESPONDENCE
Ianik Plante
ianik.plante-1@nasa.gov

RECEIVED 20 July 2023
ACCEPTED 21 July 2023
PUBLISHED 31 July 2023

CITATION
Plante I (2023) Editorial: Case reports in radiation oncology: 2022.
Front. Oncol. 13:1264297.
doi: 10.3389/fonc.2023.1264297

Editorial: Case reports in radiation oncology: 2022

Ianik Plante*

Human Health and Performance Contract, KBR, Houston, TX, United States

KEYWORDS

radiation oncology, chemotherapy, radiotherapy, medical imaging, machine learning

Editorial on the Research Topic
Case reports in radiation oncology: 2022

This Case Reports series of Frontiers in Oncology highlights unique cases of patients that present with an unexpected diagnosis, treatment outcome, or clinical course. The cases reported are either rare cases with typical features, frequent cases with atypical features, and cases with a convincing response to new treatments.

In Laurino et al., a literature review of radio-induced sarcomas (RIS) found in patients referred to the IRCCS CROB Centro di Riferimento Oncologico della Basilicata from January 2009 to May 2022 is presented. Amongst 186 patients with histologically proven soft tissue and bone sarcomas, seven patients received a histological diagnosis of secondary RIS. This review has shown that RIS represents a possible complication for long-survivor cancer patients.

In Amidon et al., a perfusion-weighted MRI (PWI) was performed in four patients with glioblastoma to create fractional tumor burden (FTB) maps to spatially distinguish active tumors from treatment-related effects. PWI was performed prior to re-resection on those who had undergone upfront pulsed low-dose-rate radiotherapy (pLDR) concurrent with temozolomide (TMZ) and who had radiographic suspicion for tumor progression at a median of 3 months (0–5 months or 0–143 days) post-pLDR. Pathologic diagnosis revealed treatment effect (n=2), a mixture of viable tumor and treatment effect (n=1), or viable tumor (n=1). In 3 of 4 cases, FTB maps were indicative of lesion volumes being comprised predominantly of treatment effect with enhancing tumor volumes comprised of a median of 6.8% vascular tumor (6.4–16.4%). This case series provides insight into the radiographic response to upfront pLDR and TMZ and the role for FTB mapping to distinguish tumor progression from treatment effect prior to redo-surgery and within 20 weeks post-radiation.

In Wu et al., the case of a 56-year-old woman with a mass on the right breast discovered in May 2015 is reported. The treatment by modified radical mastectomy and lymph node biopsy revealed that the tumor was a metaplastic squamous cell carcinoma with axillary lymph node metastasis. The following treatment was traditional adjuvant chemotherapy and radiotherapy. A recurrence in the right chest wall was found in May 2017, so the recurring lesion was resected, then the patient was given postoperative adjuvant radiotherapy and chemotherapy. In August 2019, new pulmonary and mediastinal lymph node metastases were found on the PET/CT examination. After 4 cycles of albumin paclitaxel plus cisplatin chemotherapy combined with nivolumab

immunotherapy, the patient achieved complete response, then switched to nivolumab immune maintenance therapy. At the time of writing, no obvious recurring metastasis has been observed.

In Zhou et al., the first case of choroidal melanoma complicated with a macular hole and vitreous hemorrhage after stereotactic hypofractionated radiotherapy in Japan is reported. An 83-year-old male with choroidal melanoma was treated with stereotactic hypofractionated radiotherapy in January 2021. Five months later, a full-thickness macular hole developed, followed by an acute massive vitreous hemorrhage about 2 weeks later. Following confirmation of tumor regression, the patient underwent a pars plana vitrectomy and internal limiting membrane peeling. The macular hole was closed postoperatively, and the patient's best-corrected visual acuity improved to 20/125. There was no evidence of intraocular tumor dissemination or distant metastases during follow-up. A systematic literature search only identified 10 previous cases of choroidal melanoma with a macular hole in eight reports worldwide, mainly in females. Most patients who underwent vitrectomy for complications after tumor regression achieved a good prognosis.

In Bentahila et al., the first case of second retreatment of a spinal metastasis initially irradiated with standard radiotherapy and stereotactic body radiation therapy (SBRT), who subsequently progressed with imaging-confirmed local tumor progression at the same level, is presented. After a third course of irradiation with SBRT, a complete response was achieved. After 8 months of follow-up, the patient remains free of local recurrence. A third course of vertebral irradiation for a recurrent vertebral metastasis could be used in a selected group of patients if an adequate dose is delivered to the target while observing critical tissue tolerance limits.

In Du et al., a machine learning (ML) model based on pre-treatment multimodal magnetic resonance imaging (MRI) radiomics and clinical risk factors for brain metastasis (BM) was developed and validated. In this study, 337 BM patients were included (247, 60, and 30 in the training set, internal validation set, and external validation set, respectively). Four clinical features and 223 radiomics features were selected using least absolute shrinkage and selection operator (LASSO) and Max-Relevance and Min-Redundancy (mRMR) filters. The ML model using the selected features and the support vector machine (SVM) classifier was used to predict the treatment response of BM patients to SRS therapy. In the training set, the SVM classifier that uses a combination of clinical and radiomics features demonstrates outstanding discriminative performance given the area under curve (AUC) (AUC=0.95, 95% CI: 0.93-0.97). Moreover, this model also achieves satisfactory results in the validation sets (AUC=0.95 in the internal validation set and AUC=0.93 in the external validation set), demonstrating excellent generalizability. This ML model enables a non-invasive prediction of the treatment response of BM patients receiving stereotactic radiosurgery (SRS) therapy, which can in turn assist neurologist and radiation oncologists in the development of more precise and individualized treatment plans for BM patients.

Author contributions

IP: Writing – original draft, Writing – review & editing.

Funding

This work was supported by the Human Health and Performance contract NNJ15HK11B.

Conflict of interest

The author declares that the research was conducted in the absence of any commercial or financial relationships that could be construed as a potential conflict of interest.

Publisher's note

frontiers | Frontiers in Oncology

TYPE Case Report
PUBLISHED 01 August 2022
DOI 10.3389/fonc.2022.884491

OPEN ACCESS

EDITED BY
Silvia Cammelli,
University of Bologna, Italy

REVIEWED BY
Gianandrea Pasquinelli,
University of Bologna, Italy
Andrea Ronchi,
University of Campania Luigi Vanvitelli, Italy

*CORRESPONDENCE
Hongtao Zhang
hongtaozhangmd@163.com

SPECIALTY SECTION
This article was submitted to Radiation Oncology, a section of the journal Frontiers in Oncology

RECEIVED 26 February 2022
ACCEPTED 07 July 2022
PUBLISHED 01 August 2022

CITATION
Gao Z, Yu H, Di X, Zhao J, Liang Y, Liu Z, Wang J and Zhang H (2022) Case report: ^{125}I seed implantation for rare malignant solitary fibrous tumor in the pelvic cavity: A case report. *Front. Oncol.* 12:884491. doi: 10.3389/fonc.2022.884491

Case report: ^{125}I seed implantation for rare malignant solitary fibrous tumor in the pelvic cavity: a case report

Zhen Gao, Huimin Yu, Xuemin Di, Jinxin Zhao, Yansong Liang, Zezhou Liu, Juan Wang and Hongtao Zhang*

Department of Oncology, The Hebei General Hospital, Shijiazhuang, China

Solitary fibrous tumor (SFT) is a rare spindle cell tumor, benign or low-grade malignant, with an extremely low possibility of occurrence of malignant solitary fibrous tumor (MSFT). Surgery is an effective way for treating SFT, but it is often difficult to resect completely due to a large size, with a high recurrence rate and mortality rate after operation. Additionally, SFT is relatively resistant to chemotherapy, and there is a lack of effective systemic drug treatment. These lead to certain difficulties in the treatment of SFT. We report a case of a rare MSFT in the pelvic cavity. With a history of recurrence after two surgeries, this patient underwent surgical removal combined with ^{125}I seed implantation at our hospital in the context that the tumor could not be completely removed because it was large and adhered to surrounding tissues; after up to 43 months of progression-free survival (PFS), the patient underwent ^{125}I seed implantation alone, and achieved a complete remission, with a PFS up to 35 months. ^{125}I seed implantation can be a safe and effective treatment option for unresectable MSFT as well as a potential solution to repeated local recurrence.

KEYWORDS

^{125}I seeds, brachytherapy, malignant solitary fibrous tumor, recurrence, MSFT

Introduction

Solitary fibrous tumor (SFT) is a rare spindle cell tumor originating from CD34-positive dendritic mesenchymal cells (1). It has three typical primary sites: the pleura, the meninges, and extrathoracic soft tissues (2), and can also occur at a wide variety of sites including the head and neck, extremities, kidneys, liver, prostate, adrenal glands, and skin and soft tissues (3–5). It usually affects middle-aged people (6). Generally, SFT, benign or low-grade malignant, behaves in a benign or borderline fashion, and in very rare cases, it can develop as a malignant tumor (7). For the treatment of SFT, surgery is an effective approach, but a complete resection often becomes difficult due to a large size of tumor,

and postoperative relapse and death events become frequent; SFT is relatively resistant to chemotherapy, and thus there is a lack of effective systemic drugs, making the treatment further challenging. While previous literature has mostly focused on the imaging and molecular pathological features of SFT (8, 9), there are few reports on the adjuvant therapy for MSFT, and there is no treatment guideline for MSFT. ^{125}I seeds, a radioactive material of brachytherapy, can be placed into tumors during surgery or under imaging guidance, and then continuously release low-energy gamma rays to destroy the DNA double strands of tumor cells. This approach can increase the radiation dose to the tumor target, and dramatically decrease the dose to surrounding normal tissues, showing great advantages of safety, minimal invasion, definite benefit, few complications, low level of radioactive contamination, and convenience for protection. In recent years, it has been used for treating solid tumors at various sites and has achieved good performance (10–13). We report a case of MSFT undergoing ^{125}I seed implantation and attaining a good therapeutic effect, and we have yet to find such reports in China and abroad.

Case report

A 57-year-old women was first admitted to our hospital on June 29, 2015, complaining that she had undergone surgery for pelvic masses 7 years before admission and had experienced a recurrence 1 year before admission. In 2008, the patient initially presented with irregular vaginal bleeding; her gynecological ultrasound suggested multiple uterine fibroids, and her pelvic magnetic resonance imaging displayed abnormal signal intensity in the left wall of the cervix. In September 2008, she underwent total hysterectomy and removal of the tumor between the vagina and bladder; postoperative pathology demonstrated multiple uterine fibroids and vaginal fibroma. At the beginning of 2014, the patient felt distension in the lower abdomen, with multiple pelvic masses on computed tomography (CT). On April 8, 2014, she underwent pelvic mass resection; postoperative pathology showed a borderline or low-grade malignant spindle cell tumor, consistent with SFT, and the immunohistochemistry results were as follows: Ki-67 (5% positive), Bcl-2 (-), Desmin (-), SMA (-), DOG-1 (-), CD68 (-), CD117 (-), S-100 (-), CD34 (blood vessels +), CD99 (+), and Calretinin (-). Two months later, her CT displayed a walnut-size mass each under the abdominal wall and in the vaginal stump, with no specific treatment. On June 29, 2015, the patient visited our hospital and had abdominal and pelvic CT examination, which indicated multiple space-occupying lesions in the abdominal wall and pelvic cavity (Figure 1). On July 7, 2015, she underwent exploratory laparotomy under general anesthesia; the tumors were distributed in the right wall of the abdomen, in the left pelvic cavity, near the right iliac vessels, and behind the bladder; considering the large size of tumors as well as adhesion between the abdominal wall tumor and the small intestine and between the pelvic tumors and iliac vessels, the tumors could not be resected completely, so in addition to removal of the tumors in the abdominal wall and pelvic cavity. Postoperative microscopic observation: the tumor cells were spindle with unclear boundaries and diffuse hyperplasia, with large, fusiform, round or oval nuclei, pathological mitosis of 5 per 10HPF, intercellular collagen fibers, scattered lymphocytes, bleeding and necrosis, and small vascular hyperplasia. Postoperative pathology showed recurrent solitary fibrous tumor, considered low-grade malignancy, and the immunohistochemistry results were as follows:CD99 (Weak +), CD34 (blood vessels+), SMA (-), Bcl-2 (+), Vimentin(+), Wide CK(-), S-100(-), Desmin(-), CR(-), MC(-), Ki-67 (10% positive) (Figures 2A–C).^{125}I seed implantation was performed, in which 30 seeds (0.3 mCi) were implanted into the tumor bed near the right iliac vessels, with D_{90} of 62.0 Gy, and 32 seeds (0.5 mCi) into the tumor bed of the left pelvic cavity, with D_{90} of 58.0 Gy; the operation was smooth, and postoperative pathology came back as a recurrent low-grade MSFT. In August 2015, a residual tumor was observed on CT in the posterior wall of the bladder. On August 27, 2015, under the guidance of CT, 50 ^{125}I seeds (0.3 mCi) were placed percutaneously into the tumor in the left posterior wall of the bladder, with D_{90} of 64.8 Gy measured post implant. On September 21, 2015, under CT guidance, 28 ^{125}I seeds (0.3 mCi) were implanted into the tumor in the right posterior wall of the bladder, with D_{90} of 49.7 Gy measured post implant. Dose-volume histogram parameters were applied for the evaluation of target volume and organs at risk (OARs).The patient's regular examinations after implants revealed a complete remission (Figure 3). No major complication (fever, hemorrhage, bone marrow suppression, liver/kidney dysfunction, skin/mucosal radiation reaction, radiation enteritis, or cystitis) was observed during our follow-up period. No seeds migrated to other tissues or organs.

In January 2016, CT showed that a tumor recurred in the abdominal wall, with a size of about 4.0×2.5×4.5 cm. On January 6, 2016, she underwent implantation of 29 ^{125}I seeds (0.4 mCi) into the wall tumor, with D_{90} of 77.8 Gy. Her regular examinations thereafter demonstrated a complete remission all the way until October 2018, when CT displayed recurrent tumors in the abdominal wall and pelvic cavity. On October 16, 2018, with the help of CT guidance, 54 ^{125}I seeds (0.5 mCi) were embedded into the SFT (5.0×3.0×5.0 cm) under the right side of the bladder, with D_{90} of 97.6 Gy; on October 23, 2018, 30 ^{125}I seeds (0.5 mCi) were embedded into the SFT (3.6×1.5×3.0 cm) in the abdominal wall, with D_{90} of 101.3 Gy. The patient achieved a complete remission, no complications were found, and the brachytherapy was well tolerated by the patient, The patient had no recurrence of abdominal and pelvic tumors during the 4-month follow-up (Figure 4).

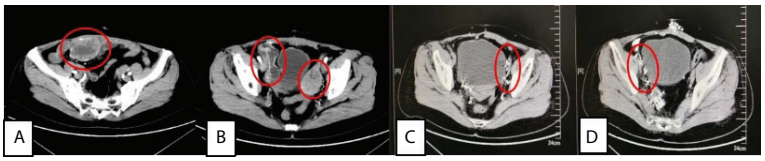

FIGURE 1
(A) and **(B)** were abdominal wall tumor(7×5×8 cm), left pelvic tumor(5.5×3.5×7 cm) and right iliac paravascular tumor(8.5×3×5 cm) before treatment, while **(C)** and **(D)** were left pelvic and right iliac paravascular tumors without recurrence 43 months after surgery+^{125}I seed implantation.

Discussion

The diagnosis of SFT mainly depends on the pathologic features and immunophenotypes. Histologically the tumor was composed of abundant and dense cells, which were separated by rope like collagenous fibrous stroma. The tumor cells were spindle to short-spindle shaped with marked nuclear atypia and increased mitotic activity. The tumor cells arranged in fascicular or swirl pattern. In focal areas, hemangiopericytoma-like structure, coagulative necrosis, focal hemorrhage and invasive margin were presented. MSFT is usually grossly indistinguishable from conventional forms, but it may also show a more irregular cut surface, with evidences of necrotic areas or infiltration of the nearest tissues (14). Immunohistochemistry plays a pivotal role in differentiating SFTs from other spindle cell mesenchymal tumors. SFTs are immunoreactive to Vimentin, CD34, CD99 and bcl-2 and they are negative for actin, desmin (in smooth muscle tumors), keratin and CD117 (in GISTs) (15, 16). Recently, the discovery of the NAB2-STAT6 fusion gene in SFT led to development of a STAT6 antibody that is a reliable immunohistochemical marker with a high level of sensitivity and specificity. Therefore, nuclear expression of STAT6 is currently the most useful marker (17).In this case, we do not perform STAT6 immunohistochemistry initially, because the marker was not widely used at that time. But some years later, we perform STAT6 immunohistochemistry and the diffuse STAT6 nuclear positivity further confirmed the diagnosis (Figure 2D). SFT is mostly benign. Malignant transformation may also occur within histologically benign SFTs even after several years of diagnosis (18). The diagnosis of malignant solitary fibrous tumors in the 2020 edition of WHO soft tissue pathology classification continues to follow the previous criteria (19), mainly including: (1) The presence of high cellularity;(2) Cellular pleomorphism; (3) high mitotic count, usually more than 4/10HPF; (4) neoplastic necrosis. The case met the diagnostic criteria of MSFT.

Generally, the most effective treatment for SFT is surgical resection. However, in most cases, when patients feel discomfort and visit doctors, tumors have grown to large masses — beginning to press on adjacent organs to produce the warning symptoms — and there are usually abundant blood vessels and collateral circulation around the tumors, often making surgery difficult. Relevant literature has shown that patients with benign SFT undergoing surgical removal have a median 10-year overall survival rate of 54%-89% (20–23), and 20%-30% of the patients will experience local recurrence or metastasis. Reoperation can be considered in some patients with advanced SFT, but the recurrence rate and mortality rate are still very high. SFT is generally insensitive to chemotherapy, and sensitive to only a

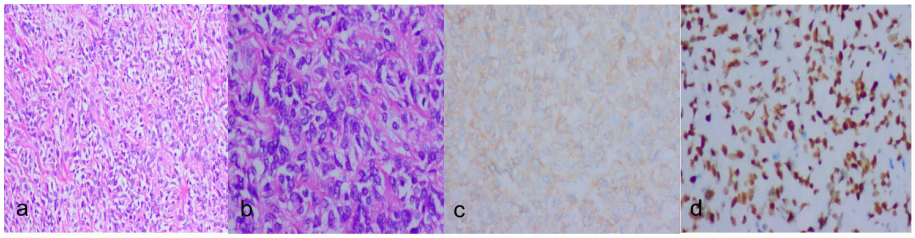

FIGURE 2
(A):hypercellular areas(HE ×100). **(B)**:hypercellular area with atypical nuclei and some evident mitotic figures(HE ×200). **(C):**Tumor cells are diffusely positive for CD99(IHC×200). **(D):**Tumor cells are diffusely positive for STAT6 (IHC ×100).

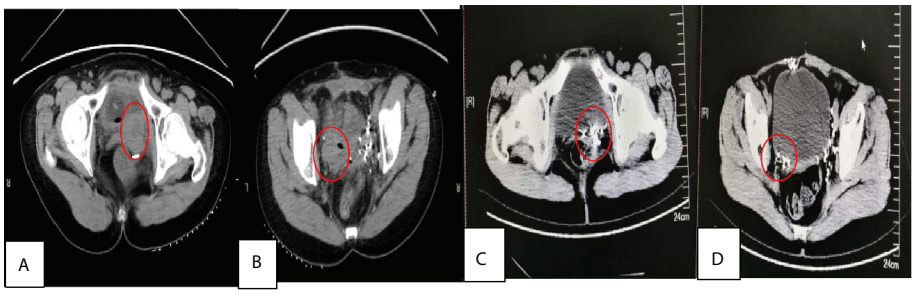

FIGURE 3
(A) and **(B)** were behind bladder tumors before treatment with size of about 4×3×5.0 cm, 3.0×2.0×2.5cm respectively, and **(C)** and **(D)** were two years after ^{125}I seed implantation.

few chemotherapy drugs, according to European and American studies. Therefore, it is important to find a safe and effective treatment approach based on the characteristics of SFT. We report our application of ^{125}I seed implantation in MSFT, providing a novel solution to the treatment of the disease.

This patient was initially diagnosed with SFT in 2014 and then underwent tumor removal, but relapsed just two months later. In July 2015, surgical resection alone was performed on the tumor in the abdominal wall, and the tumor recurred in the abdominal wall six months later. While surgery alone failed to improve the outcome, surgical removal combined with ^{125}I seed implantation for the tumors in the left pelvic cavity and near the right iliac vessels showed a surprising benefit: the patient attained a complete remission, and no relapse was observed as of the end of follow-up, with a PFS of 43 months (Table 1). ^{125}I seed implantation alone for the tumor behind the bladder continued to work: a complete remission was achieved, with a PFS of 35 months (Table 1). The PFS of 43 months and 35 months after seed implantation was far longer than the PFS of 2 months and 6 months after surgery alone. Seed implantation-yielded PFS in this case also showed notable superiority compared with the data of systemic drugs from previous research. Levard *et al.* described that the median PFS with doxorubicin alone and combined with ifosfamide was 4.0 months and 6.7 months, respectively (24). Park *et al.* evaluated the efficacy of temozolomide combined with bevacizumab in 14 patients with advanced SFT, and the median PFS was 10.8 months (25). A phase II clinical trial of sorafenib for treating five cases of advanced SFT showed a median PFS of 178 days (about 5.9 months) (26). Compared with surgery, seed implantation is more minimally invasive, and patients can recover more quickly; and it can be repeatedly performed if necessary. Patients have better tolerance to ^{125}I seeds than to chemotherapy, which often causes severe side effects. Moreover, seed implantation costs less than chemotherapy and targeted drug therapy. However, seed implantation is a local therapy. If there is widespread metastasis, a combination of seed implantation and chemotherapy or targeted drug therapy may be a possible solution.

In this report, the patient experienced repeated recurrence after surgery, but benefited from ^{125}I seed implantation, which supports seed implantation as a potential solution to repeated

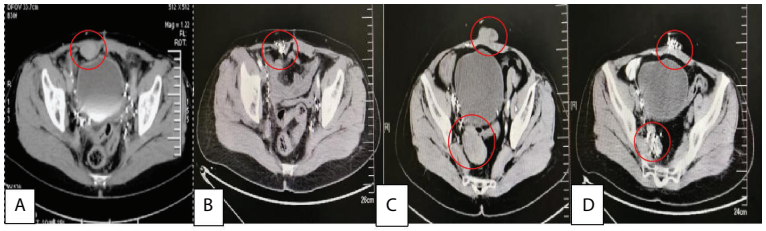

FIGURE 4
(A) was the recurrence of abdominal wall tumor with a size of about 4.0×2.5×4.5 cm before treatment in 2016/1, **(B)** was 6 months after ^{125}I seed implantation, **(C)** was the recurrence of abdominal wall tumor(3.6×1.5×3.0 cm) and behind bladder tumors(5.0×3.0×5.0 cm) before treatment in 2018/10, **(D)** was 4 months after ^{125}I seed implantation.

TABLE 1 The characteristics of treatment methods and efficacy.

Date	Tumor location	Treatment	Tumorresponse	PFS (months)
2015-7	the right wall of the abdomen	surgery	CR	6
	the left pelvic cavity	surgery+^{125}I seed implantation	CR	43
	near the right iliac vessels	surgery+^{125}I seed implantation	CR	43
2015-8/2015-9	behind the bladder	^{125}I seed implantation	CR	35
2016-1	recurrent tumor in abdominal wall	^{125}I seed implantation	CR	32
2018-10	recurrent tumor behind the bladder	^{125}I seed implantation	CR	4
	recurrent tumor in abdominal wall	^{125}I seed implantation	CR	4

local recurrence. As MSFT is very rare, there has been no more research than case reports, not to mention clinical randomized controlled trials. Our report could provide a reference for the treatment of MSFT.

Data availability statement

The original contributions presented in the study are included in the article/supplementary material. Further inquiries can be directed to the corresponding author.

Author contributions

ZG performed the bibliographic search and wrote the manuscript; ZG, HY, XD and JW revised the manuscript; YL, JZ and ZL took part to the equipment preparation and follow-up; HZ made the decision to submit the article for publication. All authors read and approved the final manuscript.

Conflict of interest

The authors declare that the research was conducted in the absence of any commercial or financial relationships that could be construed as a potential conflict of interest.

Publisher's note

All claims expressed in this article are solely those of the authors and do not necessarily represent those of their affiliated organizations, or those of the publisher, the editors and the reviewers. Any product that may be evaluated in this article, or claim that may be made by its manufacturer, is not guaranteed or endorsed by the publisher.

References

1. Martin-Broto J, Stacchiotti S, Lopez-Pousa A, Redondo A, Bernabeu D, de Alava E, et al. Pazopanib for treatment of advanced malignant and dedifferentiated solitary fibrous tumour: a multicentre, single-arm, phase 2 trial. *Lancet Oncol* (2019) 20(1):134–44. doi: 10.1016/S1470-2045(18)30676-4

2. Penel N, Amela EY, Decanter G, Robin YM, Marec-Berard P. Solitary fibrous tumors and so-called hemangiopericytoma. *Sarcoma* (2012) 2012:690251. doi: 10.1155/2012/690251

3. Ghasemi-Rad M, Wang KY, Jain S, Lincoln CM. Solitary fibrous tumor of thyroid: a case report with review of literature. *Clin Imaging* (2019) 53:105–7. doi: 10.1016/j.clinimag.2018.09.011

4. Sorrenti G, Pelligra I, Albertini R, Piccin O. Solitary fibrous tumor of the tongue: An uncommon cause of obstructive sleep apnea. *J Maxillofac Oral Surg* (2018) 17(4):441–3. doi: 10.1007/s12663-017-1053-4

5. Meyer D, Riley F. Solitary fibrous tumor of the orbit: a clinicopathologic entity that warrants both a heightened awareness and an atraumatic surgical removal technique. *Orbit* (2006) 25(1):45–50. doi: 10.1080/01676830500506101

6. Thway K, Ng W, Noujaim J, Jones RL, Fisher C. The current status of solitary fibrous tumor: Diagnostic features, variants, and genetics. *Int J Surg Pathol* (2016) 24(4):281–92. doi: 10.1177/1066896915627485

7. Robinson LA. Solitary fibrous tumor of the pleura. *Cancer Control* (2006) 13 (4):264–9. doi: 10.1177/107327480601300403

8. Kratiras Z, Spapis V, Koniaris E, Kozyrakis D, Skriapas K. Malignant solitary fibrous tumor of urinary bladder: A rare clinical entity. *Arch Ital Urol Androl* (2019) 91(2):135–6. doi: 10.4081/aiua.2019.2.135

9. Ronchi A, La Mantia E, Gigantino V, Perdonà S, De Sio M, Facchini G, et al. A rare case of malignant solitary fibrous tumor in prostate with review of the literature. *Diagn Pathol* (2017) 12(1):50. doi: 10.1186/s13000-017-0640-5

10. Tanderup K, Ménard C, Polgar C, Lindegaard JC, Kirisits C, Pötter R. Advancements in brachytherapy. *Adv Drug Delivery Rev* (2017) 109:15–25. doi: 10.1016/j.addr.2016.09.002

11. National Comprehensive Cancer Network. *NCCN clinical practice guidelines in oncology-prostate cancer . version 2. 2017*. Washingten DC: NCCN (2017).

12. Li J, Zhang L, Xie Q, Wang W, Hua Y, Zhou L, et al. 125I seeds implantation for treating residual hepatocellular carcinoma located beneath the diaphragm after transcatheter arterial chemoembolization. *Brachytherapy* (2019) 18(3):420–5. doi: 10.1016/j.brachy.2018.12.008

13. Duan F, Su XL, Wei ZX, Kong DW, Huang TY, Wang S. Efficacy of computed tomography-guided implantation of 125I seeds in the treatment of refractory malignant tumors accompanied with cancer pain and its influence on tumor markers in the serum. *Eur Rev Med Pharmacol Sci* (2018) 22(6):1595–601. doi: 10.26355/eurrev_201803_14564

14. Ronchi A, Cozzolino I, Marino FZ, Accardo M, Montella M, Panarese I, et al. Extrapleural solitary fibrous tumor: A distinct entity from pleural solitary fibrous tumor. an update on clinical, molecular and diagnostic features. *Ann Diagn Pathol* (2018) 34:142–50. doi: 10.1016/j.anndiagpath.2018.01.004

15. Varaldo M, Ferrarazzo C, Tunesi G, Mencoboni M. Solitary fibrous tumor. *Rare Tumors* (2010) 2:e64. doi: 10.4081/rt.2010.e64

16. Spairani C, Squillaci S, Pitino A, Ferrari M, Montefiore F, Rossi C, et al. A case of concomitant occurrence of solitary fibrous tumor and urothelial high-grade invasive carcinoma of the urinary bladder. *Int J Surg Path* (2014) 22:252–9. doi: 10.1177/1066896913481061

17. Doyle LA, Vivero M, Fletcher CD, Mertens F, Hornick JL, et al. Nuclear expression of STAT6 distinguishes solitary fibrous tumor from histologic mimics. *Modern Pathol* (2014) 27):390–5. doi: 10.1038/modpathol.2013.164

18. de Perrot M, Kurt A-M, Robert JH, Borisch B, Spiliopoulos A. Clinical behavior of solitary fifibrous tumors of the pleura. *Ann Thorac Surg* (1999) 67 (5):1456–9. doi: 10.1016/s0003-4975(99)00260-x

19. *The WHO classification of tumours editorial board. WHO classificaton of tumours soft tissue and bone tumours. 5thed*. Lyon France: Iarc press (2020).

20. Espat NJ, Lewis JJ, Leung D, Woodruff JM, Antonescu CR, Shia J, et al. Conventional hemangiopericytoma:modem analysis of outcome. *Cancer* (2002) 95 (8):1746–51. doi: 10.1002/cncr.10867

21. Spitz FR, Bouvet M, Pisters PW, Pollock RE, Feig BW. Hemangiopericytoma: a 20-year single-institution experience. *Ann Surg Oncol* (1998) 5(4):350–5. doi: 10.1007/BF02303499

22. Magdeleinat P, Alifano M, Petino A, Le Rochais JP, Dulmet E, Galateau F, et al. Solitary fibrous tumors of the pleura: clinical characteristics, surgical treatment and outcome. *Eur J Cardiothorac Surg* (2002) 21(6):1087–93. doi: 10.1016/s1010-7940(02)00099-4

23. Harrison-Phipps KM, Nichols FC, Schleck CD, Deschamps C, Cassivi SD, Schipper PH, et al. Solitary fibrous tumors of the pleura: results of surgical treatment and long-term prognosis. *J Thorac Cardiovasc Surg* (2009) 138(1):19–25. doi: 10.1016/j.jtcvs.2009.01.026

24. Levard A, Derbel O, Méeus P, Ranchère D, Ray-Coquard I, Blay JY, et al. Outcome of patients with advanced solitary fibrous tumors: the centre léon bérard experience. *BMC Cancer* (2013) 13:109. doi: 10.1186/1471-2407-13-109

25. Park MS, Patel SR, Ludwig JA, Trent JC, Conrad CA, Lazar AJ, et al. Activity of temozolomide and bevacizumab in the treatment of locally advanced, recurrent, and metastatic hemangiopericytoma and malignant solitary fibrous tumor. *Cancer* (2011) 117(21):4939–47. doi: 10.1002/cncr.26098

26. Valentin T, Fournier C, Penel N, Bompas E, Chaigneau L, Isambert N, et al. Sorafenib in patients with progressive malignant solitary fibrous tumors: a subgroup analysis from a phase II study of the French sarcoma group (GSF/GETO). *Invest New Drugs* (2013) 31(6):1626–7. doi: 10.1007/s10637-013-0023-z

frontiers | Frontiers in Oncology

TYPE Case Report
PUBLISHED 05 August 2022
DOI 10.3389/fonc.2022.906812

OPEN ACCESS

EDITED BY
Tao Song,
Zhejiang Provincial People's Hospital, China

REVIEWED BY
Bilgin Kadri Aribas,
Bülent Ecevit University, Turkey
Takeaki Ishizawa,
Osaka Metropolitan University, Japan

*CORRESPONDENCE
Xiaoli Yang
344920646@qq.com
Bo Li
liboer2002@126.com

†These authors have contributed equally to this work

SPECIALTY SECTION
This article was submitted to Radiation Oncology, a section of the journal Frontiers in Oncology

RECEIVED 29 March 2022
ACCEPTED 06 July 2022
PUBLISHED 05 August 2022

CITATION
Peng Y, Fan J, Zhu G, Fang C, Peng F, Zhang Z, Tian J, Su S, Yang X and Li B (2022) First case report of spontaneous biliary pleural fistula diagnosed using near infrared region I/II fluorescence of indocyanine green. *Front. Oncol.* 12:906812. doi: 10.3389/fonc.2022.906812

First case report of spontaneous biliary pleural fistula diagnosed using near infrared region I/II fluorescence of indocyanine green

Yisheng Peng[1,2,3†], Jun Fan[1,2,3†], Gang Zhu[1,2,3†], Cheng Fang[1,2,3], Fangyi Peng[1,2,3], Zeyu Zhang[4], Jie Tian[4], Song Su[1,2,3], Xiaoli Yang[1,2,3*] and Bo Li[1,2,3*]

[1]Department of General Surgery (Hepatobiliary Surgery), The Affiliated Hospital of Southwest Medical University, Luzhou, China, [2]Nuclear Medicine and Molecular Imaging Key Laboratory of Sichuan Province, The Affiliated Hospital of Southwest Medical University, Luzhou, China, [3]Academician (Expert) Workstation of Sichuan Province, The Affiliated Hospital of Southwest Medical University, Luzhou, China, [4]Key Laboratory of Molecular Imaging, Institute of Automation, Chinese Academy of Sciences, Beijing, China

We report a rare case of spontaneous biliary pleural fistula in a patient whose diagnosis was aided by the use of near-infrared I/II fluorescence imaging. When both 99mTc-mebrofenin hepatobiliary scintigraphy and CT examination were diagnostically difficult, we found strong fluorescent signals in the patient's pleural drainage fluid and sputum using NIR I/II fluorescence imaging, and therefore diagnosed the patient with a biliary pleural fistula. This provides a safe and effective test for diagnosing biliary pleural fistulas.

KEYWORDS

biliary pleural fistula, NIR fluorescence, ICG, diagnosis, case report

Introduction

Biliary pleural fistula is a pathological traffic between the biliary system and the pleura, through which bile enters the pleural cavity and travels as a biliary pleural effusion, and is one of the serious complications of biliary disease (1). Because of its insidious symptoms and clinical rarity, it is highly susceptible to misdiagnosis and underdiagnosis, and its mortality rate may exceed 50% (2). The main causes of biliary pleural fistulae are amoebic liver abscess, hepatic peritonitis, post-radiofrequency ablation, trauma, post-pneumonectomy, and complications after hepatectomy (3, 4). The common tests currently used for biliary pleural fistula include 99mTc-mebrofenin hepatobiliary scintigraphy, cholangiography, CT of the chest and abdomen, and MRCP

(5–7). However, cholangiography may trigger risks such as cholangitis and radiation in patients. CT and MRCP have low diagnostic efficacy for microfistulae and are highly likely to be missed (8).

Near-infrared window I (NIR-I, 700-900 nm) fluorescence imaging has good spatial and temporal resolution and has been widely used in clinical applications such as: real-time intraoperative fluorescence navigation and diagnostic imaging (9). Near Infrared Window II (NIR-II, 1000-1700 nm) fluorescence imaging offers better imaging quality and its sensitivity is higher (10). Indocyanine green is widely used in the preoperative assessment of liver function. It is first bound to plasma proteins in the blood, then taken up by the parenchymal cells of the liver and finally excreted from the biliary system *via* the bile (10, 11).

However, so far, there is no research on the near-infrared window region I/II fluorescence technique for diagnosing biliary pleural fistula. Therefore, this study aimed to evaluate the feasibility and effectiveness of the near-infrared window region I/II fluorescence technique in the diagnosis of biliary pleural fistula.

Case report

A 53-year-old female was admitted to the hospital on 18/08/2021 with "yellowish staining of the skin and sclera with dyspnea after activity for 20+ days". Past history: 9+ years ago, he underwent the combined splenectomy with left lobe resection of the liver for calculus of bile duct and 1+ years ago, he underwent endo scopic haemostasis for cirrhosis with ruptured oesophagogastric fundic varices. The patient presented two days after admission with worsening dyspnea and coughing up of yellowish-brown sputum. The patient's serum bilirubin was 316 umol/L, and the thoracentesis showed yellow-green pleural effusion, and the pleural effusion examination showed a mildly elevated bilirubin level of 76 umol/L. The patient was then suspected of having a possible biliary pleural fistula. Therefore, CT examination (Figure 1) and 99mTc-mebrofenin hepatobiliary scintigraphy (Figure 2) were performed and no significant fistulae were found. Indocyanine green (0.5mg/kg) was then injected intravenously and the patient waited for 24 hours. Pleural effusion and sputum were collected again and the presence of fluorescent signals in them was detected using a near-infrared I-region fluorescence imaging system provided by the Beijing Key Laboratory of Molecular Imaging (Digital Precision Medicine). Interestingly, we can clearly observe a strong fluorescent signal in both pleural effusion and sputum (Figure 3). Also, we found strong fluorescent signals in pleural effusions and sputum using near-infrared region II fluorescence imaging (Figure 4). Therefore, the patient was considered to be diagnosed with a biliary pleural fistula. We recommend that the patient is dissected for a definitive diagnosis of a biliopleural fistula and that a repair of the fistula hole is performed if available. Unfortunately, after assessment of the patient's general condition and multidisciplinary consultation and discussion, it was concluded that the patient's current poor general underlying condition, with liver failure, severe lung infection and severe morphological deformation of the liver, made surgical treatment an extremely high risk and endoscopic nasobiliary drainage (ENBD) treatment could be considered. After communication with the patient and his family, they refused to undergo further investigations and treatment due to the risks of surgery and financial reasons. After 20 days in hospital, the patient did not improve significantly and the sufferer chose to abandon treatment. The patient unfortunately passed away after 1 month of follow-up.

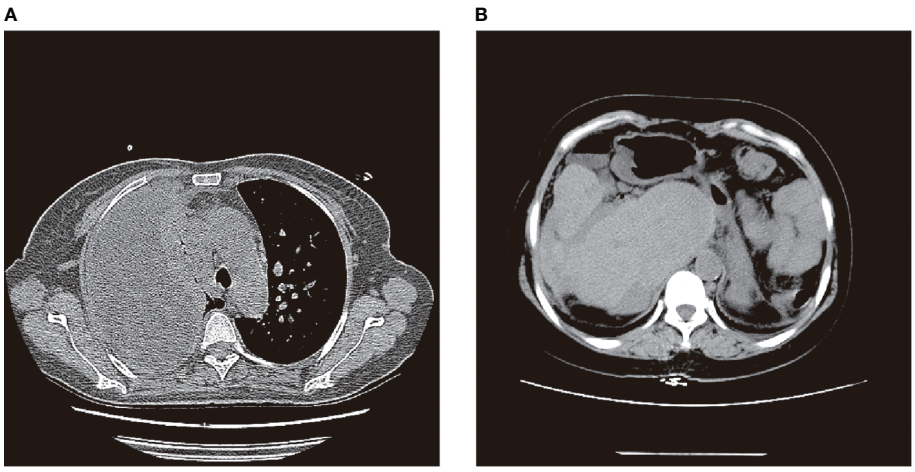

FIGURE 1
CT examination: **(A)** patient with massive right pleural effusion and inflammatory lesions; **(B)** post-hepatectomy, post-splenectomy, severe liver deformation, intrahepatic bile duct stones and dilated intrahepatic bile ducts.

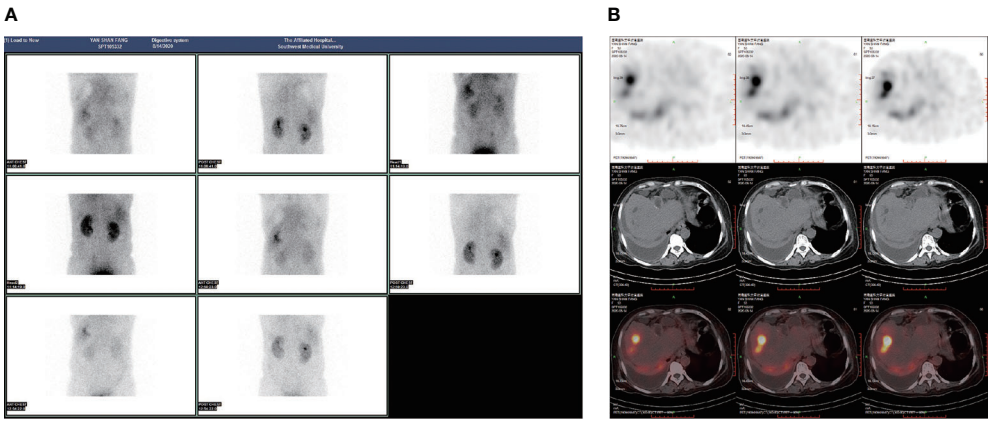

FIGURE 2
99mTc-mebrofenin hepatobiliary scintigraphy: **(A, B)** Impaired liver function and large right pleural effusion with no obvious developer distribution within it.

Discussion

Fluorescence imaging following intravenous injection of ICG has already been used widely for cholangiography (12). Compared with the first near-infrared (NIR-I) optical window (650-950 nm), the fluorescence imaging of the second near-infrared optical window (NIR-II, 950-1700 nm) has better tissue penetration, with facilitates *in vivo* deep tissue imaging and real-time localization of tumors (13). NIR II imaging is widely used in surgery, such as real-time guided liver cancer resection, lung tumor resection, lymph node dissection, photothermal therapy, etc (10). It has good application prospects.

In this case, we consider a spontaneous biliary pleural fistula caused by a long-term diffuse intra- and extra-hepatic bile duct stone causing biliary obstruction, which raised the biliary pressure and then formed a leak of hepatic peritoneum into the thoracic cavity. The biliary pleural fistula in this patient may be very small, so neither the 99mTc-mebrofenin hepatobiliary scintigraphy nor CT examination found the existence of the patient's fistula. At the same time, the bilirubin level in the patient's pleural effusion was only slightly elevated and did not reach the level (triple) for diagnosing bile leakage (14). Therefore, it is difficult to judge whether it is a biliary pleural fistula from the color and nature of the pleural effusion. We

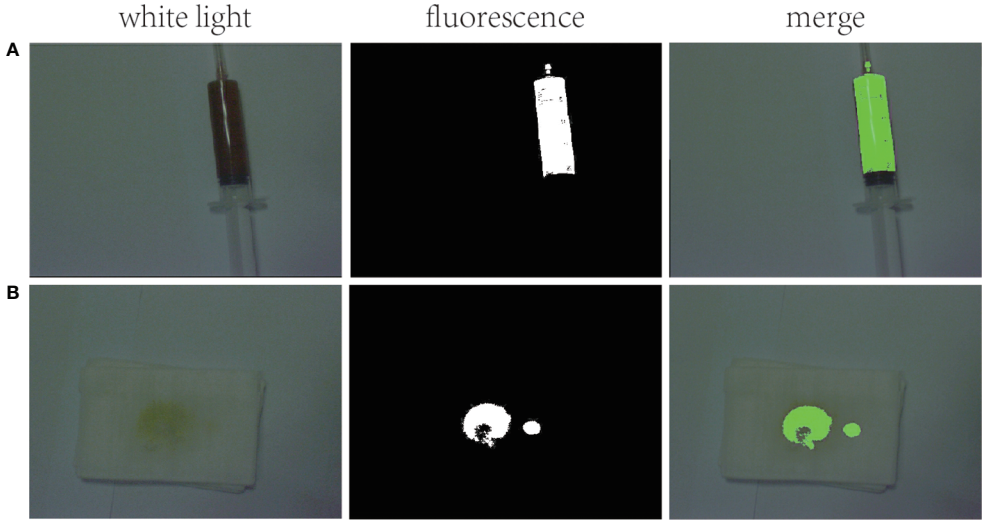

FIGURE 3
Fluorescence imaging in the NIR I region: **(A)** strong fluorescent signal seen in pleural effusion; **(B)** strong fluorescent signal seen in sputum.

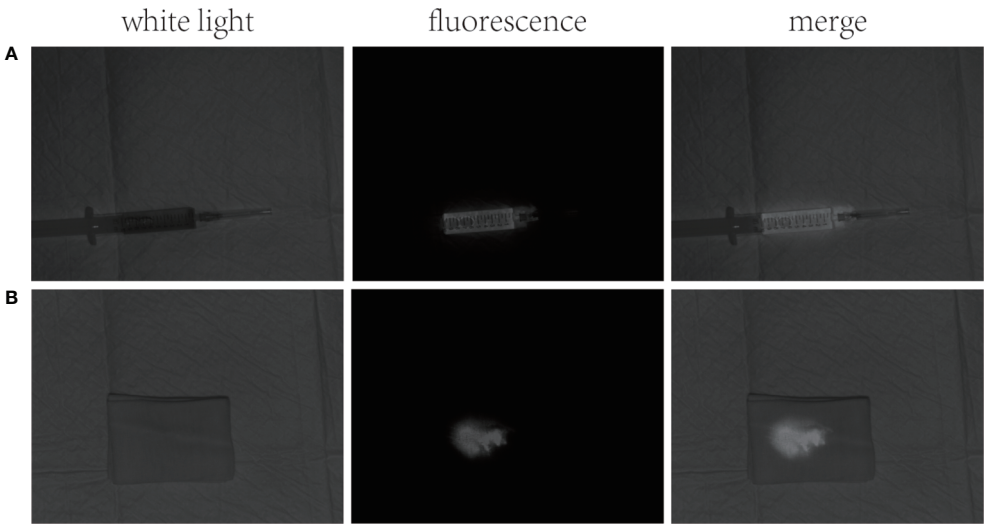

FIGURE 4
NIR region II fluorescence images: **(A)** strong fluorescent signal in pleural effusion; **(B)** strong fluorescent signal in sputum.

considered arranging a cholangiogram to definitively diagnose a biliopleural fistula. However, the patient declined to undergo cholangiography due to his poor general underlying condition. It is currently difficult to diagnose this patient with a biliary pleural fistula. At this time, there is a great need to find a new and safe method to aid in the diagnosis of biliary pleural fistula. One study reported the successful application of ICG fluorescence technique for the diagnosis of biliary leakage during hepatectomy (15). Therefore, for the first time, we successfully assisted in the diagnosis of the presence of bile in both the pleural fluid and sputum of this patient using near-infrared region I/II fluorescence imaging based on the metabolic characteristics of ICG. In the patient's pleural fluid and sputum, we can clearly observe the presence of strong fluorescent signals. It shows that NIR region I/II fluorescence imaging is highly sensitive and that it is very easy and safe to use. Furthermore, NIR Region I/II fluorescence imaging avoids the risk of exposing the patient to radiation and allows for diagnosis through a non-invasive approach. This provides another new way to diagnose biliary pleural fistulas.

However, the location of the fistula in the abdominal cavity is difficult to detect due to the weak penetration of NIR region I/II fluorescence imaging. In the future, if ICG fluorescence and 99mTc-mebrofenin hepatobiliary scintigraphy are combined, this will further improve the diagnosis of biliopleural fistulas.

Near-infrared region I/II fluorescence imaging is a new method for the diagnosis of biliary pleural fistulas, which has the advantage of being safe, convenient and sensitive. It has very promising applications in the future to assist in the diagnosis of biliary pleural fistulae.

Data availability statement

The original contributions presented in the study are included in the article/supplementary material. Further inquiries can be directed to the corresponding authors.

Ethics statement

The studies involving human participants were reviewed and approved by Ethics Committee of Affiliated Hospital of Southwest Medical University. The patients/participants provided their written informed consent to participate in this study. Written informed consent was obtained from the individual(s) for the publication of any potentially identifiable images or data included in this article.

Author contributions

BL and XY conceived the idea of the project. YP, JF and GZ wrote the manuscript in addition to designing, performing all experiments. CF and FP performed the experiments. ZZ and JT collected the information on patients with biliary pleural fistulae. SS assisted with experimental design, manuscript preparation and image analysis. BL and XY designed, supervised and analyzed all experiments, in addition to assisting with manuscript preparation. All authors contributed to the article and approved the submitted version.

Funding

This work was supported by Key Research and Development Project of the Science & Technology Department of Sichuan Province (Nos.2021YFS0231, 22ZDYF1898), China Postdoctoral Science Foundation Funded Project (Grant Nos. 2020M673096).

Conflict of interest

The authors declare that the research was conducted in the absence of any commercial or financial relationships that could be construed as a potential conflict of interest.

Publisher's note

All claims expressed in this article are solely those of the authors and do not necessarily represent those of their affiliated organizations, or those of the publisher, the editors and the reviewers. Any product that may be evaluated in this article, or claim that may be made by its manufacturer, is not guaranteed or endorsed by the publisher.

References

1. Karabulut N, Cakmak V, Kiter G. Confident diagnosis of bronchobiliary fistula using contrast-enhanced magnetic resonance cholangiography. *Korean J Radiol* (2010) 11(4):493–6. doi: 10.3348/kjr.2010.11.4.493

2. Joh HK, Park SY. Surgical treatment of bronchobiliary fistula with pulmonary resection and omentopexy. *Korean J Thorac Cardiovasc Surg* (2020) 53(1):38–40. doi: 10.5090/kjtcs.2020.53.1.38

3. Xi XJ, Zhang Y, Yin YH, Li H, Ma DD, Qu YQ. Bronchobiliary fistula following radiofrequency ablation for liver metastases from breast cancer: a case report and literature review. *Med (Baltimore)* (2018) 97(43):e12760. doi: 10.1097/MD.0000000000012760

4. Liao GQ, Wang H, Zhu GY, Zhu KB, Lv FX, Tai S. Management of acquired bronchobiliary fistula: a systematic literature review of 68 cases published in 30 years. *World J Gastroenterol* (2011) 17(33):3842–9. doi: 10.3748/wjg.v17.i33.3842

5. Acquasanta M, Spadarella G, Civelli EM. Spontaneous bronchobiliary fistula: case report. *J Radiol Case Rep* (2020) 14(10):10–5. doi: 10.3941/jrcr.v14i10.3743

6. Annovazzi A, Viceconte G, Romano L, Sciuto R, Maini CL. Detection of a suspected bronchobiliary fistula by hepatobiliary scintigraphy. *Ann Nucl Med* (2008) 22(7):641–3. doi: 10.1007/s12149-008-0154-z

7. Kobayashi M, Nakanishi T, Nishi K, Higaki Y, Okudaira H, Ono M, et al. Transport mechanisms of hepatic uptake and bile excretion in clinical hepatobiliary scintigraphy with 99mTc-N-pyridoxyl-5-methyltryptophan. *Nucl Med Biol* (2014) 41(4):338–42. doi: 10.1016/j.nucmedbio.2014.01.004

8. Girard E, Messager M, Sauvanet A, Benoist S, Piessen G, Mabrut JY, et al. Anastomotic leakage after gastrointestinal surgery: diagnosis and management. *J Visc Surg* (2014) 151(6):441–50. doi: 10.1016/j.jviscsurg.2014.10.004

9. Tichauer KM, Samkoe KS, Gunn JR, Kanick SC, Hoopes PJ, Barth RJ, et al. Microscopic lymph node tumor burden quantified by macroscopic dual-tracer molecular imaging. *Nat Med* (2014) 20(11):1348–53. doi: 10.1038/nm.3732

10. Hu Z, Fang C, Li B, Zhang Z, Cao C, Cai M, et al. First-in-human liver-tumour surgery guided by multispectral fluorescence imaging in the visible and near-infrared-I/II windows. *Nat BioMed Eng* (2020) 4(3):259–71. doi: 10.1038/s41551-019-0494-0

11. Ishizawa T, Tamura S, Masuda K, Aoki T, Hasegawa K, Imamura H, et al. Intraoperative fluorescent cholangiography using indocyanine green: a biliary road map for safe surgery. *J Am Coll Surg* (2009) 208(1):e1–4. doi: 10.1016/j.jamcollsurg.2008.09.024

12. Pavel MC, Boira MA, Bashir Y, Memba R, Llácer E, Estalella L, et al. Near infrared indocyanine green fluorescent cholangiography versus intraoperative cholangiography to improve safety in laparoscopic cholecystectomy for gallstone disease-a systematic review protocol. *Syst Rev* (2022) 11(1):36. doi: 10.1186/s13643-022-01907-6

13. Meng X, Pang X, Zhang K, Gong C, Yang J, Dong H, et al. Recent advances in near-Infrared-II fluorescence imaging for deep-tissue molecular analysis and cancer diagnosis. *Small* (2022) e2202035. doi: 10.1002/smll.202202035

14. Koch M, Garden OJ, Padbury R, Rahbari NN, Adam R, Capussotti L, et al. Bile leakage after hepatobiliary and pancreatic surgery: a definition and grading of severity by the international study group of liver surgery. *Surgery* (2011) 149 (5):680–8. doi: 10.1016/j.surg.2010.12.002

15. Kaibori M, Ishizaki M, Matsui K, Kwon AH. Intraoperative indocyanine green fluorescent imaging for prevention of bile leakage after hepatic resection. *Surgery* (2011) 150(1):91–8. doi: 10.1016/j.surg.2011.02.011

frontiers | Frontiers in Oncology

TYPE Case Report
PUBLISHED 05 August 2022
DOI 10.3389/fonc.2022.923579

OPEN ACCESS

EDITED BY
Ira Ida Skvortsova,
Innsbruck Medical University, Austria

REVIEWED BY
Maria Elena Samar,
National University of Cordoba, Argentina
Sisir Kumar Patra,
LLH Hospital, United Arab Emirates

*CORRESPONDENCE
Fu-rong Hao
hkc515@163.com
Yun-xiang Zhang
zhangbing199592@163.com

SPECIALTY SECTION
This article was submitted to Radiation Oncology, a section of the journal Frontiers in Oncology

RECEIVED 19 April 2022
ACCEPTED 30 June 2022
PUBLISHED 05 August 2022

CITATION
Zhang W, Wang X-x, Wang X-l, Zhang Y, Li X-f, Li Y, Cai Y-y, Ren H-q, Zhang Y-x and Hao F-r (2022) Epithelial–myoepithelial carcinoma of the nasopharynx: A case report and review of the literature. *Front. Oncol.* 12:923579. doi: 10.3389/fonc.2022.923579

Epithelial–myoepithelial carcinoma of the nasopharynx: A case report and review of the literature

Wei Zhang[1], Xiao-xiao Wang[2], Xiao-li Wang[2], Yan Zhang[1], Xiu-feng Li[3], Yang Li[2], Yuan-yuan Cai[2], Hui-qi Ren[2], Yun-xiang Zhang[3]* and Fu-rong Hao[2,4]*

[1]Clinical School, Weifang Medical University, Weifang, China, [2]Department of Radiation Oncology, Weifang People's Hospital, Weifang, China, [3]Department of Pathology, Weifang People's Hospital, Weifang, China, [4]Weifang Key Laboratory of Radiophysics and Oncological Radiobiology, Weifang, China

Background: Epithelial–myoepithelial carcinoma (EMCa) is a rare low-grade malignant tumor that most commonly occurs in the salivary glands, with approximately 320 cases having been reported worldwide. Here, we report the third case of EMCa occurring in the nasopharynx. Rare cases in the breast, pituitary gland, lacrimal gland, nose, paranasal sinus, nasal cavity, trachea and bronchus, lung, and even the pleura mediastinalis have also been reported. Histopathology and immunohistochemistry are useful for confirming the diagnosis of EMCa, which is characterized by biphasic tubular structures composed of inner ductal and outer clear myoepithelial cells and stains for different markers in each layer. However, because of the rarity of EMCa, the clinicopathological characteristics and treatment of these patients remain unclear.

Case presentation: We report a rare case of EMCa of the nasopharynx. A 51-year-old man presented with a 5-month history of pain while swallowing and aggravation accompanied by right ear tinnitus lasting for 1 month. Nasopharyngoscopy and magnetic resonance imaging (MRI) of the nasopharynx and neck revealed a 5.6 cm × 3.4 cm × 3.1 cm mass in the nasopharyngeal space, invasion of the right cavernous sinus, and lymph node enlargement in the right retropharyngeal space. On 17 April 2019, based on the histopathological and immunohistochemical features, a final diagnosis of EMCa of the right nasopharynx was made. The patient underwent concurrent chemoradiotherapy (CCRT), and his symptoms were relieved after treatment. On 10 January 2022, nasopharynx MRI and biopsy revealed local recurrence, but chest and abdominal computed tomography (CT) showed no obvious signs of metastasis. The local recurrence-free survival (LRFS) period was 33 months.

Conclusion: To the best of our knowledge, this is the third reported case of EMCa in the nasopharynx and the only case of EMCa in the nasopharynx treated with CCRT, and a partial response was achieved. Therefore, to improve the quality of life and prognosis of patients with unresectable tumors, we believe that CCRT is a suitable option. Further clinical observations are required to elucidate the pathophysiology and prognosis of EMCa.

KEYWORDS

epithelial–myoepithelial carcinoma, nasopharynx, immunohistochemistry, concurrent chemoradiotherapy, case report

Background

Epithelial–myoepithelial carcinoma (EMCa) is a rare low-grade malignant epithelial neoplasm composed of variable proportions of ductular cells with large, clear cytoplasmic myoepithelial cells arranged around the periphery of the ducts (1–4). EMCa predominantly arises from the parotid gland, accounting for less than 1% of all salivary gland tumors and approximately 2% of malignant salivary gland neoplasms (3–12). Of all the types of nasopharyngeal malignancies treated at our center, the incidence of EMCa is 1/315 (0.3%) as of 2021. This tumor can occur in unusual sites, such as the breast (13–15), pituitary gland (16), paranasal sinus (9, 17, 18), lacrimal gland (19–22), nasal cavity (1, 3, 6, 23–25), trachea and bronchus (26, 27), lung (28–34), nasopharynx (4, 5), and even the pleura mediastinalis (35). EMCa was first reported by Donath in 1972, and 8 patients have been reported with a salivary gland tumor that was termed EMCa (36). However, it was described in the literature as early as 1956 (2, 7, 37). Only approximately 320 cases have been reported thus far (2, 11, 38). The domestic and foreign literature mostly consist of case reports, with two cases of nasopharyngeal EMCa being reported by Imate et al. in 2000 (5) and Kim et al. in 2015 (4). Here, we report the third case of EMCa of the nasopharynx in a 51-year-old man who was treated with concurrent chemoradiotherapy (CCRT).

Case presentation

On 14 April 2019, a 51-year-old man presented with a 5-month history of pain while swallowing and aggravation accompanied by right ear tinnitus lasting for 1 month. He was admitted to the otolaryngology department of our hospital. Nasopharyngoscopy revealed a mass on the right nasopharyngeal wall, and a partial tissue sample was obtained *via* biopsy. Magnetic resonance imaging (MRI) of the nasopharynx and neck on 15 April 2019 revealed a 5.6 cm × 3.4 cm × 3.1 cm mass within the right parietal and lateral walls of the nasopharynx, accompanied by skull base bone erosion, and invasion of the oropharyngeal lateral wall and right parapharyngeal space, the right medial pterygoid muscle and musculus longus capitis, and the cavernous sinus and the posterior nostril. Simultaneously, lymph node enlargement was found in the right retropharyngeal space (Figure 1). A final diagnosis of EMCa was made based on the histological and immunohistochemical (IHC) features of nasopharyngeal biopsy on 17 April 2019. Hematoxylin and eosin staining showed a classical biphasic pattern with typical epithelial cells and myoepithelial cells (Figure 2) without nerve invasion or vascular cancer embolus. The patient was transferred to our department for further treatment. The tumor was staged as IVa (cT4N1M0) according to the 8th edition of the AJCC staging system (39).

Treatment and outcomes

The patient received CCRT in our department. Target volumes were delineated according to the consensus (40), and intensity-modulated radiation therapy (IMRT) was performed from 24 April 2019 to 10 June 2019. Over a total of 33 fractions, a dose of 7,000 cGy was delivered to the tumor, and a dose of 6,800 cGy was delivered to the metastatic lymph node in the right retropharyngeal space; the dose delivered to high-risk regions was 6,006 cGy, referred to as clinical target volume 1 (CTV1), and the dose delivered to low-risk regions was 5,775 cGy, referred to as CTV2. During radiation therapy, 80 mg/m^2 cisplatin was administered every 3 weeks for up to 3 cycles. On 29 July 2019, 1.5 months after the end of treatment, nasopharynx and neck MRI revealed that the nasopharyngeal lesions on the right side had shrunk significantly, but there was a 4.8 cm × 3.0 cm × 2.7 cm residual area of low signal and no enhancement, which suggested necrosis (Figure 3). In September 2019, the patient suffered from massive nasopharyngeal

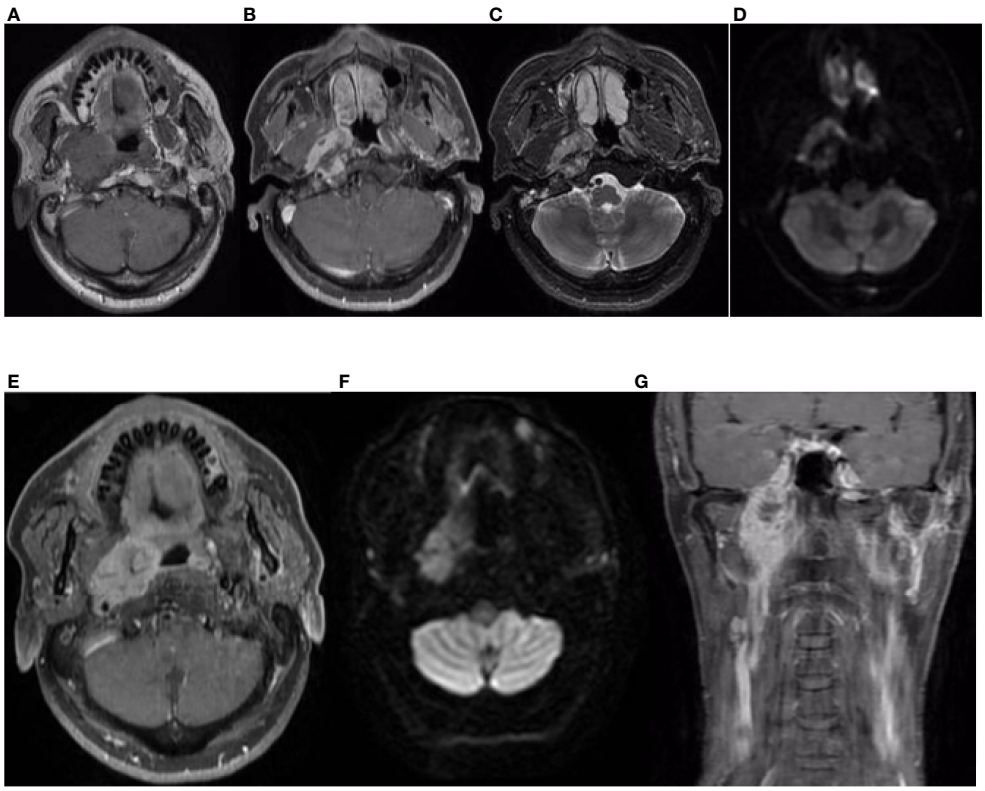

FIGURE 1
Nasopharynx and neck MRI findings from 15 April 2019. **(A–D)** The axial planes of T1-weighted, enhanced T1-weighted, T2-weighted, and diffusion-weighted imaging (DWI) MRI of the nasopharynx, showing a 5.6 cm × 3.4 cm × 3.1 cm mass within the right parietal and lateral walls of the nasopharynx, accompanied by skull base bone invasion, invasion of the oropharyngeal lateral wall and right parapharyngeal space, the right medial pterygoid muscle, and the musculus longus capitis. **(E, F)** The axial planes of enhanced T1-weighted DWI MRI revealed enlargement of the right retropharyngeal lymph node. **(G)** The coronal plane of enhanced T1-weighted imaging showed tumor involvement with the cavernous sinus.

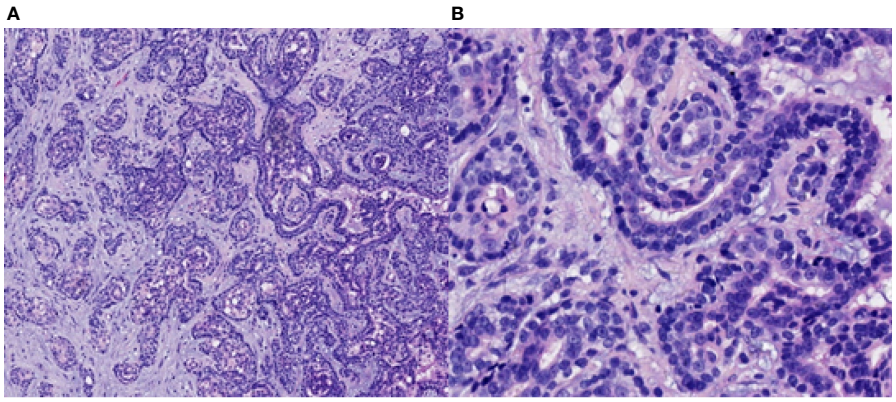

FIGURE 2
Pathological findings of the nasopharyngeal biopsy obtained on 17 April 2019. The EMCa of the nasopharynx was mainly composed of an inner layer of epithelial cells and an outer layer of clear cytoplasmic myoepithelial cells. H&E staining; magnification, ×10 **(A)** and ×40 **(B)**. EMCa, epithelial–myoepithelial carcinoma; H&E, hematoxylin and eosin.

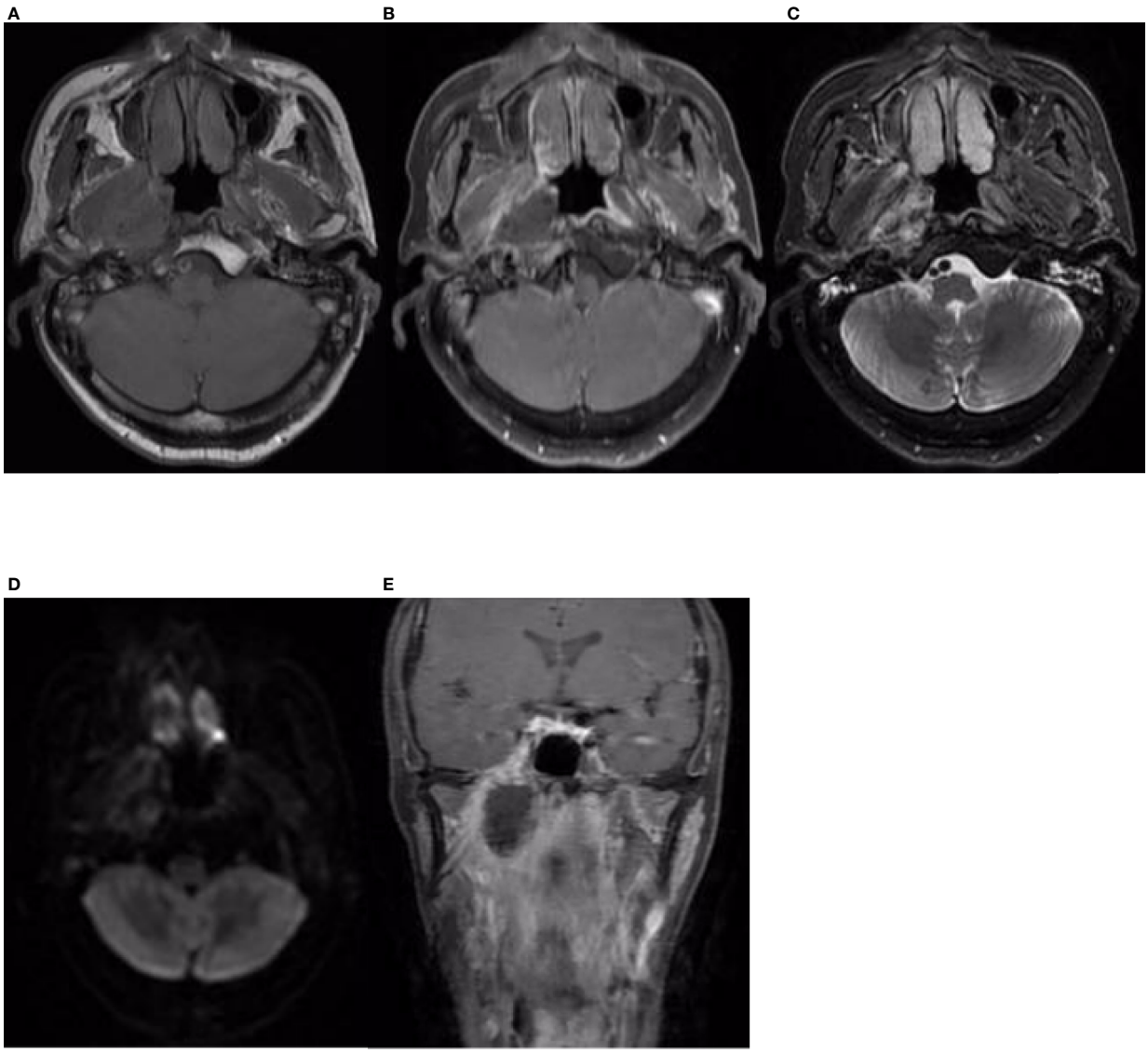

FIGURE 3
Nasopharynx and neck MRI findings from 29 July 2019. **(A–D)** The axial planes of T1-weighted, enhanced T1-weighted, T2-weighted, and DWI and **(E)** the coronal plane of enhanced T1-weighted MRI, showing that the nasopharyngeal lesions on the right side subsided significantly, but there was a 4.8 cm × 3.0 cm × 2.7 cm residual area of low signal and no enhancement, which suggested necrosis.

hemorrhage at home, which improved after receiving symptomatic treatment such as hemostasis in a local hospital. Then, follow-up of the patient became irregular. On 7 July 2020, 1 year after the end of treatment, nasopharynx and neck MRI revealed that the nasopharyngeal lesions had subsided significantly, but there was still an area of inhomogeneous residual enhancement of the right nasopharynx and parapharyngeal space (Figure 4). The residual area of inhomogeneous enhancement had shrunk to a smaller size, and there were no obvious signs of recurrence or metastasis on reexamination on 27 April 2021 (Figure 5). The patient's pain while swallowing was completely relieved, and his symptoms of right tinnitus were partially relieved. On 10 January 2022, the patient was examined at our department, and nasopharynx and neck MRI revealed that the nasopharyngeal enhancement area was more obvious than before, which was considered recurrence (Figure 6). Chest and abdominal computed tomography (CT) showed no obvious signs of metastasis. Nasopharyngeal biopsy was performed that same day, and the pathological (Figure 7) and IHC findings on 18 January 2022 suggested EMCa recurrence of the nasopharynx. In summary, the follow-up at 33 months revealed recurrence but no distant metastasis.

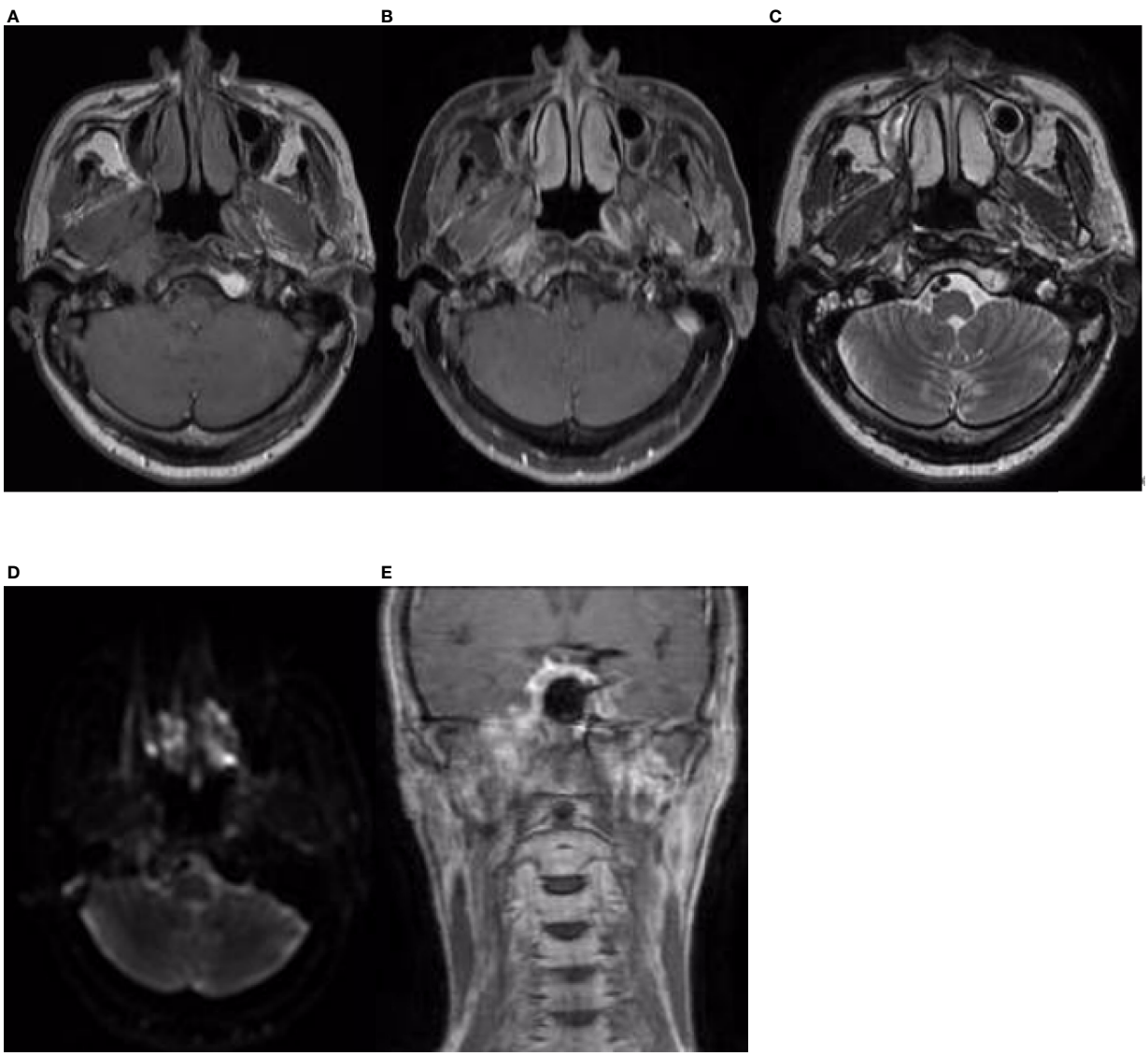

FIGURE 4
Nasopharynx and neck MRI findings from 7 July 2020. **(A–D)** The axial planes of T1-weighted, enhanced T1-weighted, T2-weighted, and DWI and **(E)** the coronal plane of enhanced T1-weighted MRI, showing that the nasopharyngeal lesions and the necrotic area had subsided significantly. However, there was still a residual area of inhomogeneous enhancement in the right nasopharynx and parapharyngeal space, demonstrating restricted diffusion on DWI.

IHC findings

On 17 April 2019, at first admission, IHC staining revealed that cytokeratin (CK) was widely positive, and the inner epithelial cells were positive for CK7, an epithelial cell marker. The outer myoepithelial cells were positive for P63, smooth muscle actin (SMA) and vimentin (VIM), consistent with a myoepithelial phenotype, confirming the diagnosis of EMCa. Epidermal growth factor receptor (EGFR) and CD117 staining was also positive, while S-100, actin, and glial fibrillary acidic protein (GFAP) staining was negative. The expression of programmed death ligand-1 (PD-L1) was less than 1% in tumor cells and 10% in stromal cells. The expression of MLH1, MSH2, MSH6, and PMS2 and all four mismatch repair (MMR) proteins was positive, which was interpreted as proficient mismatch repair (pMMR). Ki-67 was positive in 35% of the neoplastic cells (Figure 8).

On 18 January 2022, at the second admission, IHC staining revealed that CK was wildly positive, and the inner epithelial cells were positive for CK7. The outer myoepithelial cells were positive for P63, SMA, and VIM. S-100 was positive in some

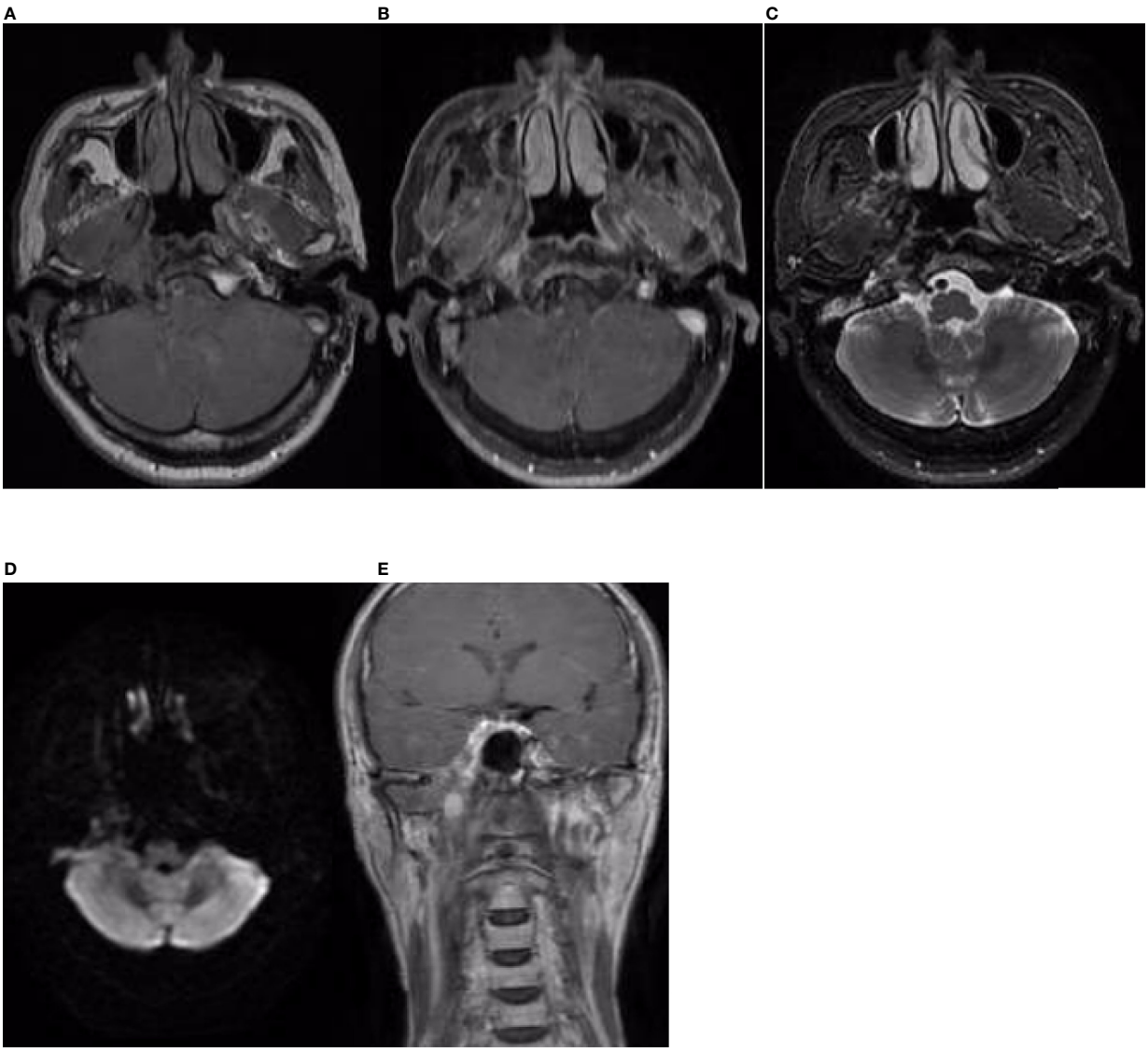

FIGURE 5
Nasopharynx and neck MRI findings from 27 April 2021. **(A–D)** The axial planes of T1-weighted, enhanced T1-weighted, T2-weighted, and DWI and **(E)** the coronal plane of enhanced T1-weighted MRI, showing that the residual area of inhomogeneous enhancement had shrunk.

cells, and CK5/6 was positive in most cells. Ki-67 was positive in 15% of the neoplastic cells (Figure 9). The IHC results of the inner epithelial cells and the outer myoepithelial cells are summarized in Table 1.

Discussion

EMCa is a rare and unique tumor that most commonly occurs in the salivary glands (7, 11, 12). The average age at diagnosis is approximately 60 years old, and the incidence is higher in women than in men, with a ratio of 1.34-2:1 (2, 7). These tumors have a propensity for infiltration but low malignancy (4). Thus, they invade nerves, blood vessels, and bone, and local recurrence is often observed (0–56%) (5), but the mortality rate is low (11). The mean times to recurrence and metastases are 5 years (41) and 15 years (42), respectively. The median disease-free survival (DFS) time is 11.34 years, and the 5- and 10-year disease-specific survival (DSS) rates are 93.5% and 81.8%, respectively (2). Factors associated with overall survival include the following: tumor size < 4 cm, absence of regional nodal or distant metastases, patient age <

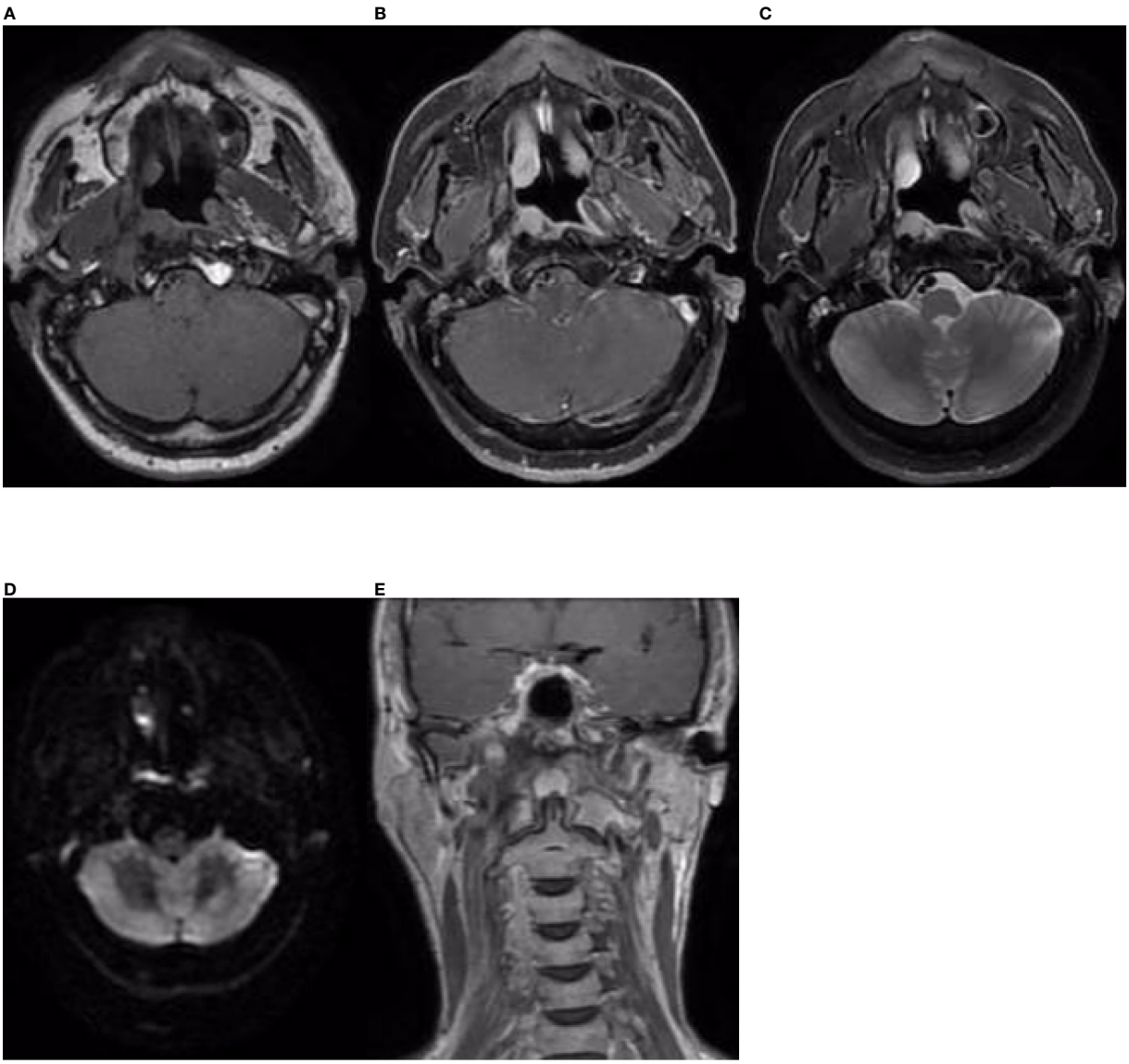

FIGURE 6
Nasopharynx and neck MRI findings from 10 January 2022. **(A–D)** The axial planes of T1-weighted, enhanced T1-weighted, T2-weighted, and DWI and **(E)** the coronal plane of enhanced T1-weighted MRI, showing an area of enhancement in the right nasopharyngeal and parapharyngeal space. DWI demonstrated slightly restricted diffusion, which was considered indicative of recurrence.

80 years at diagnosis, surgical treatment, and Ki-67 index less than 3.5% (7, 10, 43, 44). Age younger than 80 years was the only factor associated with a good prognosis in the case reported herein. Clinical manifestations of EMCa are usually nonspecific and can vary depending on the site of origin and extent of the tumor (10). Tumors involving the nasopharynx may cause symptoms such as nose blockage, epistaxis, tinnitus, hearing loss and pain in the ear (4, 5). In our case, the patient presented with pain while swallowing and tinnitus, for which the main cause was the lesion occupying the surrounding tissues.

The confirmative diagnosis of EMCa depends on the histopathological and IHC results (11). EMCa exhibits a biphasic histological morphology, with the inner layer being a single layer of cubic sacral epithelial cells and the peripheral layer being composed of clear cytoplasmic myoepithelial cells, with a duct-like structure and infiltrating margins (7, 11). Compared with the low specificity of radiologic imaging,

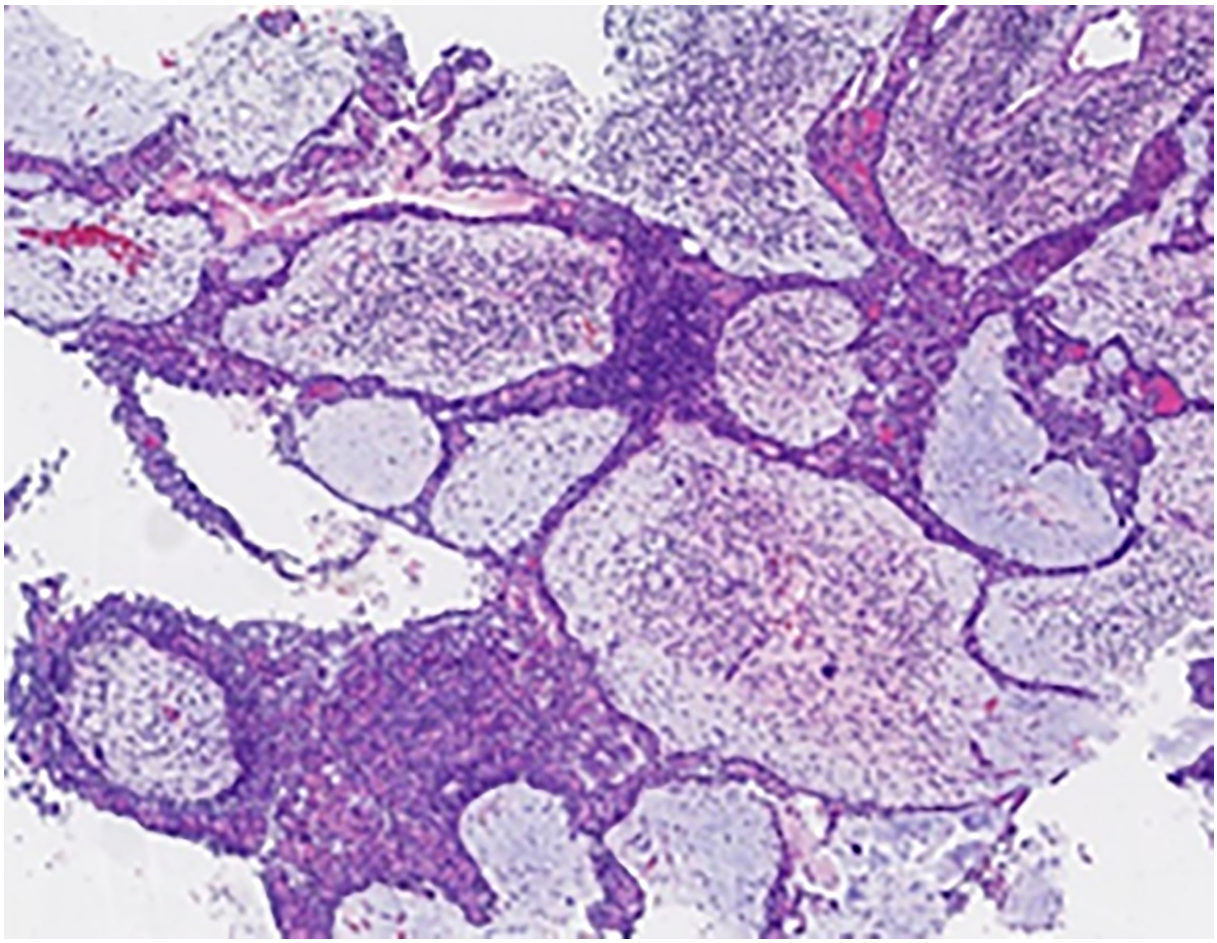

FIGURE 7
Pathological findings of the nasopharyngeal biopsy obtained on 12 January 2022. Nasopharyngeal EMCa recurrence was considered. H&E staining; magnification, ×4. EMCa, epithelial–myoepithelial carcinoma; H&E, hematoxylin and eosin.

immunohistochemistry is useful for distinguishing EMCa, as it can depict the characteristic biphasic epithelial–myoepithelial phenotype and the differential staining of markers in each layer; thus, it plays a major role in the final diagnosis (2, 10). IHC staining of glandular epithelial markers such as CK, epithelial membrane antigen (EMA), and CD117 (11) and myoepithelial markers such as SMA, S-100 protein, Actin, VIM, CK14, GFAP and Calponin, and P63 is observed (45–47). Kawahara et al. suggested that P63 is an especially useful marker of myoepithelial cells with naked nuclei in EMCa (48). Nevertheless, studies have shown that VIM and calponin, especially the latter, are sensitive markers for salivary myoepithelial tumor cells. SMA and P63 are relatively less sensitive than calponin (11, 49, 50). In our case, we observed positive CK7 staining in the inner epithelial cells along with P63, SMA, and VIM in the outer myoepithelial cells.

There is currently no consensus regarding the optimal treatment of this disease, largely due to its rarity (24). For other malignant tumors of the head and neck (51), surgery is the preferred method (11). Studies have shown that the true survival benefit of radiotherapy is unclear (7), but others have argued that it may be effective at preventing local recurrence, particularly for neoplasms with a diameter larger than 4 cm (6, 24, 52). A recent study suggested that the complete remission (CR) rate could be improved by consecutive radiotherapy, and if tumors are deemed primarily unresectable, definitive radiotherapy may be used with or without chemotherapy (44). To the best of our knowledge, two cases of EMCa in the nasopharynx reported in the literature were treated by surgical

10.3389/fonc.2022.923579

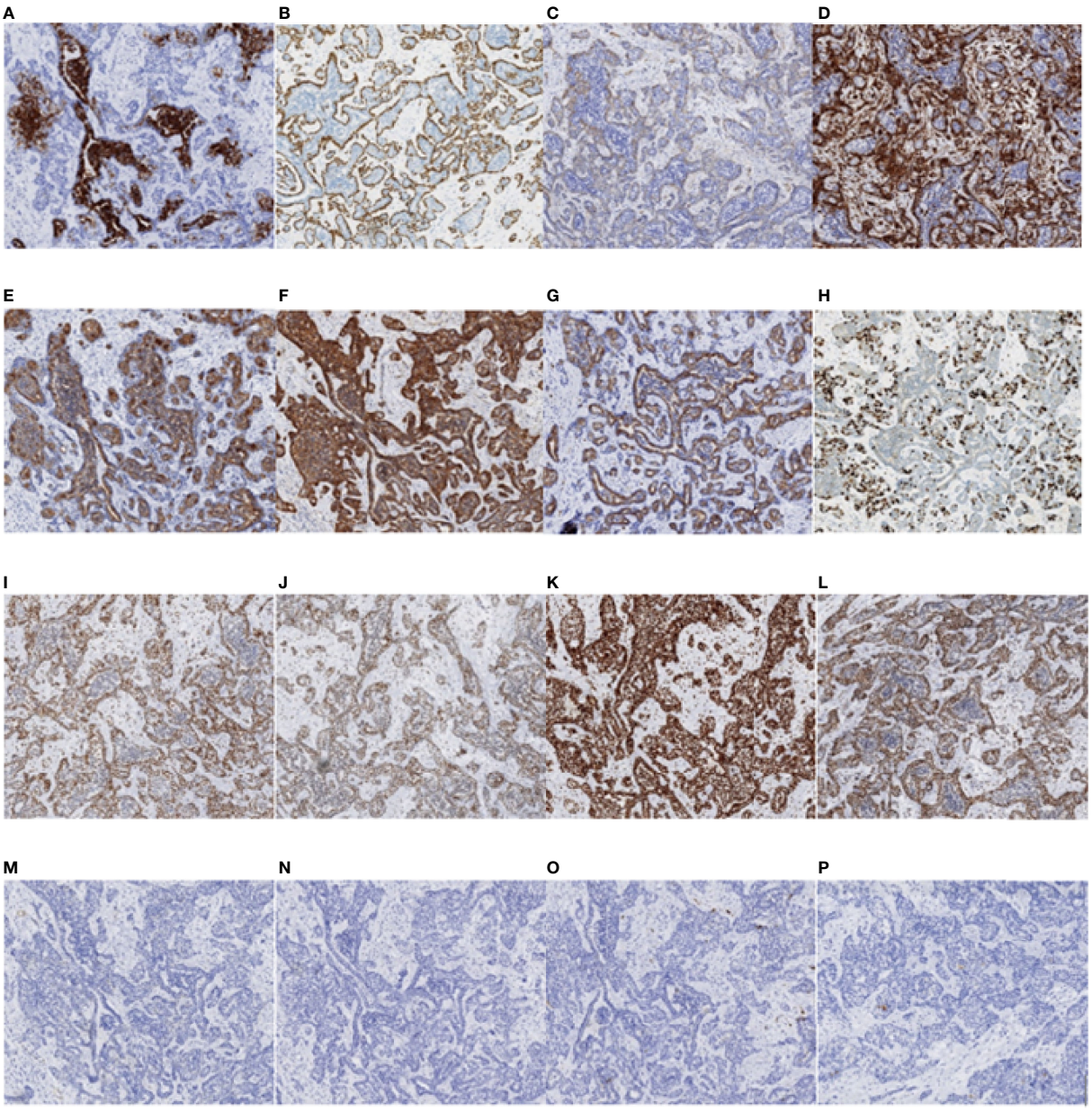

FIGURE 8
Immunohistochemistry test results of the nasopharyngeal biopsy obtained on 17 April 2019. **(A)** CK7 positivity was observed in epithelial cells. **(B–D)** P63, SMA, and VIM positivity was observed in myoepithelial cells. **(E–G)** CK, EGFR, and CD117 positivity was observed in tumor cells. **(H)** Ki-67 positivity was observed in 35% of the tumor cells. **(I–L)** MLH1, MSH2, MSH6, and PMS2 positivity was observed in tumor cells. **(M–O)** Actin, GFAP, and S-100 negativity was observed in tumor cells. **(P)** PD-L1 positivity was observed in less than 1% of tumor cells and in 10% of stromal cells (magnification, ×10). CK, cytokeratin; SMA, smooth muscle actin; VIM, vimentin; EGFR, epidermal growth factor receptor; GFAP, glial fibrillary acidic protein; PD-L1, programmed death ligand-1.

resection (5), and another was treated with CCRT followed by systemic chemotherapy (4), which resulted in a partial response. In our case, due to the anatomical location and the clinical stage of the patient being locally advanced, the tumor was unresectable; thus, CCRT was suggested.

Conclusion

Although it is a low-grade malignancy, EMCa should be treated aggressively, as it has a tendency for both local recurrence and distant metastasis. Although the optimal

10.3389/fonc.2022.923579

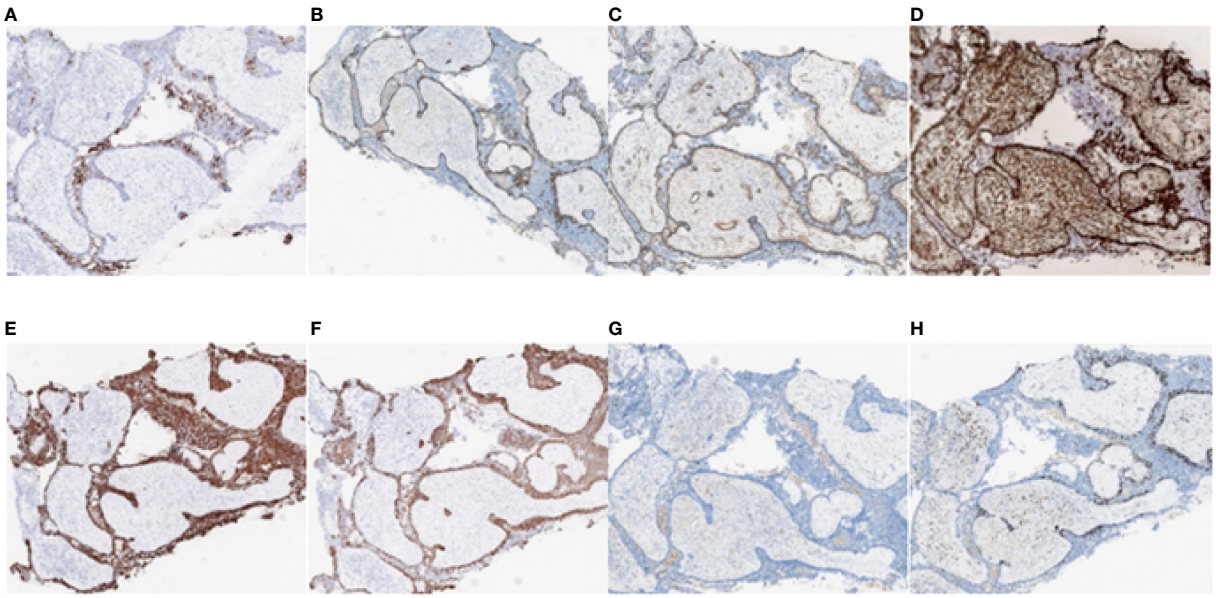

FIGURE 9
Immunohistochemistry test results of the nasopharyngeal biopsy obtained on 18 January 2022. **(A)** CK7 positivity was observed in epithelial cells. **(B–D)** P63, SMA, and VIM positivity was observed in myoepithelial cells. **(E–G)** CK, CK5/6, and S-100 positivity was observed in tumor cells. **(H)** Ki-67 positivity was observed in 15% of tumor cells (magnification, ×4). CK, cytokeratin; SMA, smooth muscle actin; VIM, vimentin.

TABLE 1 Immunohistochemistry findings from 17 April 2019 and 18 January 2022.

Antibody	17 April 2019		18 January 2022	
	Inner cells	Outer cells	Inner cells	Outer cells
CK7	Positive	Negative	Positive	Negative
P63	Negative	Positive	Negative	Positive
SMA	Negative	Positive	Negative	Positive
VIM	Negative	Positive	Negative	Positive
CK	Positive	Positive	Positive	Positive
EGFR	Positive	Positive	-	-
CD117	Positive	Positive	-	-
MLH1	Positive	Positive	-	-
MSH2	Positive	Positive	-	-
MSH6	Positive	Positive	-	-
PMS2	Positive	Positive	-	-
Actin	Negative	Negative	-	-
GFAP	Negative	Negative	-	-
S-100	Negative	Negative	Positive	Positive
CK5/6	-	-	Positive	Positive
KI-67	Positive	Positive	Positive	Positive

CK, cytokeratin; SMA, smooth muscle actin; VIM, vimentin; EGFR, epidermal growth factor receptor; GFAP, glial fibrillary acidic protein; "-", this test was not performed.

treatment strategy for EMCa remains poorly defined due to its rarity, the present study reports the only case of EMCa in the nasopharynx treated with CCRT, and a partial response was achieved. Therefore, to improve the quality of life and prognosis of patients with unresectable tumors, we believe that CCRT is a suitable option. Further accumulation of cases and long-term follow-up data are needed to elucidate the pathophysiology and prognosis of epithelial–myoepithelial carcinoma.

Data availability statement

The original contributions presented in the study are included in the article/supplementary

material. Further inquiries can be directed to the corresponding authors.

Ethics statement

The studies involving human participants were reviewed and approved by the Ethics Committee of Weifang People's Hospital. Written informed consent was obtained from the individual(s) for the publication of any potentially identifiable images or data included in this article.

Author contributions

WZ, X-XW, X-LW, and YZ drafted the manuscript and performed the literature review. X-FL and Y-XZ retrieved and analyzed pathological and immunohistochemistry information. Y-YC and F-RH performed the chemoradiotherapy in this case. YL and H-QR retrieved the imaging data, and WZ and F-RH performed patient follow-up. F-RH and Y-XZ conceived, designed, and supervised the study. This paper properly credits the meaningful contributions of all coauthors and coresearchers. All authors have been personally and actively involved in substantial work leading to the publication of this paper and take public responsibility for its content.

Funding

This work was supported by Weifang Science and Technology Development Project (Grant NO. 2019YX003).

Conflict of interest

The authors declare that the research was conducted in the absence of any commercial or financial relationships that could be construed as a potential conflict of interest.

Publisher's note

References

1. Jin X, Ding C, Chu Q. Epithelial-myoepithelial carcinoma arising in the nasal cavity: a case report and review of literature. *Pathology* (1999) 31(2):148–51. doi: 10.1080/003130299105340

2. Seethala R, Barnes E, Hunt J. Epithelial-myoepithelial carcinoma: a review of the clinicopathologic spectrum and immunophenotypic characteristics in 61 tumors of the salivary glands and upper aerodigestive tract. *Am J Surg Pathol* (2007) 31(1):44–57. doi: 10.1097/01.pas.0000213314.74423.d8

3. Yamanegi K, Uwa N, Hirokawa M, Ohyama H, Hata M, Yamada N, et al. Epithelial-myoepithelial carcinoma arising in the nasal cavity. *Auris Nasus Larynx* (2008) 35(3):408–13. doi: 10.1016/j.anl.2007.10.001

4. Kim S, Park S, Bae H, Song D, Oh H, Cho K, et al. Epithelial-myoepithelial carcinoma of the nasopharynx: A case report and review of the literature. *Oncol Lett* (2015) 10(2):927–30. doi: 10.3892/ol.2015.3314

5. Imate Y, Yamashita H, Endo S, Okami K, Kamada T, Takahashi M, et al. Epithelial-myoepithelial carcinoma of the nasopharynx. *ORL J Oto-Rhino-Laryngology Its Related Specialties* (2000) 62(5):282–5. doi: 10.1159/000027761

6. Park J, Jung C, Sun D, Kim M. An unusual presentation of aggressive epithelial-myoepithelial carcinoma of the nasal cavity with high-grade histology. *J Laryngology Otology* (2011) 125(12):1286–9. doi: 10.1017/s0022215111002222

7. Vázquez A, Patel T, D'Aguillo C, Abdou R, Farver W, Baredes S, et al. Epithelial-myoepithelial carcinoma of the salivary glands: An analysis of 246 cases. *Otolaryngology–head Neck Surg Off J Am Acad Otolaryngology-Head Neck Surg* (2015) 153(4):569–74. doi: 10.1177/0194599815594788

8. Sentani K, Ogawa I, Uraoka N, Ikeda M, Hayashi N, Hattori T, et al. High-grade epithelial-myoepithelial carcinoma of the parotid gland with mucous cell differentiation. *Pathol Int* (2015) 65(9):490–4. doi: 10.1111/pin.12315

9. Sunami K, Yamane H, Konishi K, Iguchi H, Takayama M, Nakai Y, et al. Epithelial-myoepithelial carcinoma: An unusual tumor of the paranasal sinus. *ORL J Oto-Rhino-Laryngology Its Related Specialties* (1999) 61(2):113–6. doi: 10.1159/000027652

10. Lee Y, Ha S, Paik S, Yang H, Jeon H, Park D, et al. Epithelial-myoepithelial carcinoma originating from a minor salivary gland in the nasal septum: A case report and literature review. *Medicine* (2020) 99(5):e19072. doi: 10.1097/md.0000000000019072

11. Wang F, Li B, Wang Y, Shen Y, Yang H. Clinical and pathological analysis of 10 cases of salivary gland epithelial-myoepithelial carcinoma. *Medicine* (2020) 99 (41):e22671. doi: 10.1097/md.0000000000022671

12. Okuyama K, Michi Y, Kashima Y, Tomioka H, Hirai H, Yokokawa M, et al. Epithelial-myoepithelial carcinoma of the minor salivary glands: Case series with comprehensive review. *Diagnostics (Basel Switzerland)* (2021) 11(11):2124. doi: 10.3390/diagnostics11112124

13. Chen P, Chen C, Nicastri A, Wait R. Myoepithelial carcinoma of the breast with distant metastasis and accompanied by adenomyoepitheliomas. *Histopathology* (1994) 24(6):543–8. doi: 10.1111/j.1365-2559.1994.tb00573.x

14. Kakkar A, Jangra K, Kumar N, Sharma M, Mathur S, Deo S. Epithelial-myoepithelial carcinoma of the breast: A rare type of malignant adenomyoepithelioma. *Breast J* (2019) 25(6):1273–5. doi: 10.1111/tbj.13463

15. Baum J, Sung K, Tran H, Song W, Ginter P. Mammary epithelial-myoepithelial carcinoma: Report of a case with HRAS and PIK3CA mutations by next-generation sequencing. *Int J Surg Pathol* (2019) 27(4):441–5. doi: 10.1177/1066896918821182

16. Lavin V, Callipo F, Donofrio C, Ellwood-Thompson R, Metcalf R, Djoukhadar I, et al. Primary epithelial-myoepithelial carcinoma of the pituitary gland. *Neuropathology Off J Japanese Soc Neuropathology* (2020) 40(3):261–7. doi: 10.1111/neup.12628

17. Patra S, Panda N, Saikia U. Epithelial-myoepithelial carcinoma of the maxillary sinus: a rare case. *Laryngoscope* (2012) 122(7):1579–81. doi: 10.1002/lary.23310

18. Kuran G, Sagıt M, Akın I, Hucumenoglu S, Ocal B, Celık S. Bilateral epithelial-myoepithelial carcinoma: an extraordinary tumor of the paranasal sinuses. *Skull base Off J North Am Skull Base Soc [et al]* (2008) 18(2):145–50. doi: 10.1055/s-2007-1016955

19. Anjum S, Modaboyina S, Sen S, Sharma M, Meel R. Epithelial-myoepithelial carcinoma of the lacrimal gland: Case report of youngest patient. *Ophthalmic Plast Reconstructive Surg* (2020) 36(6):e141–e4. doi: 10.1097/iop.0000000000001663

20. Gonçalves A, de Lima P, Monteiro M. Epithelial-myoepithelial carcinoma of the lacrimal gland 14 years after en bloc resection of a pleomorphic lacrimal gland adenoma. *Ophthalmic Plast Reconstructive Surg* (2016) 32(2):e42–4. doi: 10.1097/iop.0000000000000225

21. Singh G, Sharma M, Agarwal S, Prasad G, Mishra S, Singh M, et al. Epithelial-myoepithelial carcinoma of the lacrimal gland: a rare case. *Ann Diagn Pathol* (2012) 16(4):292–7. doi: 10.1016/j.anndiagpath.2011.02.004

22. Sharma D, Neiweem A, Davis K, Prendes M, Chundury R, Illing E. Epithelial-myoepithelial carcinoma of the lacrimal sac and literature review of the lacrimal system. *Allergy Rhinology (Providence RI)* (2020) 11:2152656720920600. doi: 10.1177/2152656720920600

23. Nguyen S, Perron M, Nadeau S, Odashiro A, Corriveau M. Epithelial myoepithelial carcinoma of the nasal cavity: Clinical, histopathological, and immunohistochemical distinction of a case report. *Int J Surg Pathol* (2018) 26 (4):342–6. doi: 10.1177/1066896917747732

24. Lee H, Kim A, Lee S. Epithelial-myoepithelial carcinoma of the nasal cavity. *Eur Arch oto-rhino-laryngology Off J Eur Fed Oto-Rhino-Laryngological Societies (EUFOS) Affiliated German Soc Oto-Rhino-Laryngology - Head Neck Surg* (2000) 257(7):376–8. doi: 10.1007/s004050000250

25. Harada H, Kashiwagi S, Fujiura H, Kusukawa J, Morimatsu M. Epithelial-myoepithelial carcinoma–report of a case arising in the nasal cavity. *J Laryngology Otology* (1996) 110(4):397–400. doi: 10.1017/s0022215100133754

26. Konoglou M, Cheva A, Zarogoulidis P, Porpodis K, Pataka A, Mpaliaka A, et al. Epithelial-myoepithelial carcinoma of the trachea-a rare entity case report. *J Thorac Dis* (2014) 6(S1):S194–9. doi: 10.3978/j.issn.2072-1439.2013.11.17

27. Song D, Choi I, Ha S, Han K, Han J, Kim T, et al. Epithelial-myoepthelial carcinoma of the tracheobronchial tree: the prognostic role of myoepithelial cells. *Lung Cancer (Amsterdam Netherlands)* (2014) 83(3):416–9. doi: 10.1016/j.lungcan.2014.01.005

28. Mori M, Hanagiri T, Nakanishi R, Ashikari S, Yasuda M, Tanaka F. Primary epithelial-myoepithelial carcinoma of the lung with cavitary lesion: A case report. *Mol Clin Oncol* (2018) 9(3):315–7. doi: 10.3892/mco.2018.1678

29. Hagmeyer L, Tharun L, Schäfer S, Hekmat K, Büttner R, Randerath W. First case report of a curative wedge resection in epithelial-myoepithelial carcinoma of the lung. *Gen Thorac Cardiovasc Surg* (2017) 65(9):535–8. doi: 10.1007/s11748-017-0796-7

30. Tajima S, Aki M, Yajima K, Takahashi T, Neyatani H, Koda K. Primary epithelial-myoepithelial carcinoma of the lung: A case report demonstrating high-grade transformation-like changes. *Oncol Lett* (2015) 10(1):175–81. doi: 10.3892/ol.2015.3169

31. Shen C, Wang X, Che G. A rare case of primary peripheral epithelial myoepithelial carcinoma of lung: Case report and literature review. *Medicine* (2016) 95(35):e4371. doi: 10.1097/md.0000000000004371

32. Kim C, Jeong J, Kim S, Lee Y. Endobronchial epithelial-myoepithelial carcinoma of the lung. *Thorax* (2018) 73(6):593–4. doi: 10.1136/thoraxjnl-2017-211155

33. Rosenfeld A, Schwartz D, Garzon S, Chaleff S. Epithelial-myoepithelial carcinoma of the lung: a case report and review of the literature. *J Pediatr Hematology/Oncology* (2009) 31(3):206–8. doi: 10.1097/MPH.0b013e3181978e62

34. Nguyen C, Suster S, Moran C. Pulmonary epithelial-myoepithelial carcinoma: a clinicopathologic and immunohistochemical study of 5 cases. *Hum Pathol* (2009) 40(3):366–73. doi: 10.1016/j.humpath.2008.08.009

35. Weissferdt A, Kalhor N, Moran C. Pleuromediastinal epithelial-myoepithelial carcinomas: A clinicopathologic and immunohistochemical study of two cases. *Am J Clin Pathol* (2016) 146(6):736–40. doi: 10.1093/ajcp/aqw199

36. Donath K, Seifert G, Schmitz R. [Diagnosis and ultrastructure of the tubular carcinoma of salivary gland ducts. *Epithelial-myoepithelial carcinoma intercalated ducts] Virchows Archiv A Pathol Pathologische Anatomie* (1972) 356(1):16–31.

37. Angiero F, Sozzi D, Seramondi R, Valente M. Epithelial-myoepithelial carcinoma of the minor salivary glands: immunohistochemical and morphological features. *Anticancer Res* (2009) 29(11):4703–9.

38. Shinozaki A, Nagao T, Endo H, Kato N, Hirokawa M, Mizobuchi K, et al. Sebaceous epithelial-myoepithelial carcinoma of the salivary gland: clinicopathologic and immunohistochemical analysis of 6 cases of a new histologic variant. *Am J Surg Pathol* (2008) 32(6):913–23. doi: 10.1097/PAS.0b013e318160852a

39. Amin MB, Edge SB, Greene FL, Byrd DR, Brookland RK, Washington MK, et al. *AJCC cancer staging manual. 8th ed*. New York: Springer (2017). doi: 10.1007/978-3-319-40618-3

40. Lee A, Ng W, Pan J, Poh S, Ahn Y, AlHussain H, et al. International guideline for the delineation of the clinical target volumes (CTV) for nasopharyngeal carcinoma. *Radiotherapy Oncol J Eur Soc Ther Radiol Oncol* (2018) 126(1):25–36. doi: 10.1016/j.radonc.2017.10.032

41. Arora S, Sharma N, Bhardwaj M. Epithelial myoepithelial carcinoma of head and neck region. *Indian J Otolaryngol Head Neck Surg Off Publ Assoc Otolaryngologists India* (2013) 65:163–6. doi: 10.1007/s12070-011-0414-4

42. Cho K, el-Naggar A, Ordonez N, Luna M, Austin J, Batsakis J. Epithelial-myoepithelial carcinoma of salivary glands. a clinicopathologic, DNA flow cytometric, and immunohistochemical study of ki-67 and HER-2/neu oncogene. *Am J Clin Pathol* (1995) 103(4):432–7. doi: 10.1093/ajcp/103.4.432

43. Wakasaki T, Kubota M, Nakashima Y, Tomonobe E, Mihara T, Fukushima J. Invasive myoepithelial carcinoma ex pleomorphic adenoma of the major salivary gland: two case reports. *BMC Cancer* (2016) 16(1):827. doi: 10.1186/s12885-016-2871-3

44. Witte H, Gebauer N, Lappöhn D, Umathum V, Riecke A, Arndt A, et al. Prognostic impact of PD-L1 expression in malignant salivary gland tumors as assessed by established scoring criteria: Tumor proportion score (TPS), combined positivity score (CPS), and immune cell (IC) infiltrate. *Cancers* (2020) 12(4):873. doi: 10.3390/cancers12040873

45. Foschini M, Scarpellini F, Gown A, Eusebi V. Differential expression of myoepithelial markers in salivary, sweat and mammary glands. *Int J Surg Pathol* (2000) 8(1):29–37. doi: 10.1177/106689690000800108

46. Alos L, Carrillo R, Ramos J, Baez J, Mallofre C, Fernandez P, et al. High-grade carcinoma component in epithelial-myoepithelial carcinoma of salivary glands clinicopathological, immunohistochemical and flow-cytometric study of three cases. *Virchows Archiv an Int J Pathol* (1999) 434(4):291–9. doi: 10.1007/s004280050344

47. Teixeira L, Janner É, Teixeira T, Passador-Santos F, Martinez E, Demasi A, et al. Comparison of p63/p40 expression with myoepithelial markers in minor salivary gland tumors. *Int J Surg Pathol* (2019) 27(4):360–71. doi: 10.1177/1066896918813678

48. Kawahara A, Harada H, Yokoyama T, Kage M. p63 expression of clear myoepithelial cells in epithelial-myoepithelial carcinoma of the salivary gland: a useful marker for naked myoepithelial cells in cytology. *Cancer* (2005) 105(4):240–5. doi: 10.1002/cncr.21095

49. Hornick J, Fletcher C. Myoepithelial tumors of soft tissue: a clinicopathologic and immunohistochemical study of 101 cases with evaluation of prognostic parameters. *Am J Surg Pathol* (2003) 27(9):1183–96. doi: 10.1097/00000478-200309000-00001

50. el-Naggar A, Batsakis J, Luna M, Goepfert H, Tortoledo M. DNA Content and proliferative activity of myoepitheliomas. *J laryngology otology* (1989) 103 (12):1192–7. doi: 10.1017/s0022215100111326

51. Mikaelian D, Contrucci R, Batsakis J. Epithelial-myoepithelial carcinoma of the subglottic region: a case presentation and review of the literature. *Otolaryngology–head Neck Surg Off J Am Acad Otolaryngology-Head Neck Surg* (1986) 95(1):104–6. doi: 10.1177/019459988609500120

52. Deere H, Hore I, McDermott N, Levine T. Epithelial-myoepithelial carcinoma of the parotid gland: a case report and review of the cytological and histological features. *J Laryngology Otology* (2001) 115(5):434–6. doi: 10.1258/0022215011907875

frontiers | Frontiers in Oncology

TYPE Case Report
PUBLISHED 12 August 2022
DOI 10.3389/fonc.2022.895189

OPEN ACCESS

EDITED BY
Xi Yang,
Fudan University, China

REVIEWED BY
Yongsheng Yu,
Chinese Academy of Sciences (CAS), China
Jingjing Hou,
Xiamen University, China

*CORRESPONDENCE
Yuanyuan Cai
caiyy830819@126.com

SPECIALTY SECTION
This article was submitted to Radiation Oncology, a section of the journal Frontiers in Oncology

RECEIVED 13 March 2022
ACCEPTED 25 July 2022
PUBLISHED 12 August 2022

CITATION
Geng X, Liu J, Sun H, Song Z, Qin S, Li Y, Zhang Y, Hao F and Cai Y (2022) Subcutaneous soft tissue metastases from esophageal squamous cell carcinoma with neuroendocrine differentiation: Case report and literature review.
Front. Oncol. 12:895189.
doi: 10.3389/fonc.2022.895189

Subcutaneous soft tissue metastases from esophageal squamous cell carcinoma with neuroendocrine differentiation: Case report and literature review

Xiaotao Geng[1], Jie Liu[1], Huimin Sun[2], Zhenguo Song[3], Shaoyong Qin[4], Yang Li[1], Yanan Zhang[1], Furong Hao[1] and Yuanyuan Cai[1]*

[1]Department of Radiation Oncology, Weifang People's Hospital, Weifang, China, [2]Department of Pathology, Weifang People's Hospital, Weifang, China, [3]Department of Nuclear Medicine, Weifang People's Hospital, Weifang, China, [4]Department of Ultrasound, Weifang People's Hospital, Weifang, China

Background: Esophageal squamous cell carcinoma is the predominant subtype of esophageal cancer in China and so differs from presentations in Western countries. Common metastatic locations of esophageal cancer include the liver, lung, bone, and brain. In contrast, metastases in subcutaneous soft tissue are exceedingly rare.

Case presentation: We present the experience of a 57-year-old man with a complaint of hand and leg dysfunction on the right side. He had a past medical history of esophageal squamous cell carcinoma. Further imaging workup revealed a solitary brain metastasis, thickening of the esophageal wall, swollen lymph nodes in the mediastinum, and right adrenal gland metastasis. Gamma knife radiosurgery of the brain metastasis and intensity-modulated radiotherapy of the esophagus and lymph nodes were administered. After 1.5 months, he was admitted to our hospital again, and nodules were identified in the anterior abdominal wall and left posterior chest wall. Ultrasound, CT, and radical excision of the abdominal wall mass were undertaken and revealed metastatic squamous cell carcinoma with neuroendocrine differentiation. We administered immunotherapy followed by targeted therapy. A PET/CT scan was performed to identify other organ metastases; the scan revealed multiple areas of fluorodeoxyglucose uptake and foci in the esophagus, lung, liver, bone, and right adrenal gland; and in various lymph nodes. In addition, an intensely hypermetabolic lesion was localized in the left posterior thorax.

10.3389/fonc.2022.895189

Conclusion: This case highlights the diagnosis and treatment of uncommon metastases of esophageal squamous cell carcinoma. We hope that our clinical experience provides insights into these uncommon metastases.

KEYWORDS

esophagus, esophageal carcinoma, squamous cell carcinoma, subcutaneous soft tissue metastasis, soft tissue metastasis, radiotherapy, chemotherapy, immunotherapy

Introduction

Esophageal cancer (EC) is the eighth most common cancer and the sixth most common cause of cancer-related mortality worldwide; in 2020, 604,100 new cases and 544,076 new deaths were recorded (1). The incidence and mortality of ES are more severe in China, where it is the sixth most common cancer and the fourth leading cause of cancer-related death, than in Western countries (2). Esophageal squamous cell carcinoma (ESCC) is the major type of EC in Asia; it accounts for 90% of ECs in the Asian population and differs from the presentation in Western countries (3). Although improvements in treatment *via* immunotherapy and targeted therapy have been achieved in recent years, the 5-year survival rate of EC remains poor (4). Locoregional recurrence and distant metastases remain the main failure patterns of ESCC after treatment (5, 6). According to a population-based study of EC, the liver is the most common metastatic organ, followed by the lung, bone, and brain (7). Here, we report one patient with subcutaneous soft tissue metastases after initial treatment.

Case presentation

A 57-year-old Chinese man with a past medical history of ESCC presented to our hospital with right side dysfunction of the hand and leg on December 28, 2020. After obtaining a detailed clinical history and reviewing the patient's medical records, we learned that he was initially admitted to the hospital on May 11, 2019, and diagnosed with ESCC and right adrenal gland metastasis (cT3N1M1, stage IVB, according to the American Joint Committee on Cancer, 8th edition) (8). After that diagnosis, the patient was treated with multiple cycles of chemotherapy alone or combined with immunotherapy; treatments included docetaxel and cisplatin, gemcitabine, and cisplatin combined with nivolumab, and docetaxel and nedaplatin. During these treatment periods, the patient never underwent radiotherapy. After his presentation to our team, he underwent an MRI, which revealed a solitary brain metastasis located in the left side of the parietal lobe; subsequently, gamma knife radiosurgery was performed. Then, a CT scan was performed and showed thickening of the middle esophageal wall (maximum diameter of ~5 cm), swollen lymph nodes in the mediastinum, and a swollen nodule in the right adrenal gland. Laboratory tests showed an alanine aminotransferase level of 233 U/L and an aspartate aminotransferase level of 95 U/L. To exclude liver metastases, an abdominal MRI was performed; the imaging confirmed right adrenal metastasis. The diagnosis was updated to ESCC with mediastinal lymph node, brain, and right adrenal metastases (rT4bN1M1, stage IVB, according to the American Joint Committee on Cancer, 8th edition) (8). Because of the sizeable esophageal tumor and the abnormal liver function, we first administered local therapy instead of systemic therapy. The patient received intensity-modulated radiotherapy (IMRT) of the esophagus and lymph nodes with planning dose fractionation of 60 Gy in 30 fractions, five days a week. After the 26th treatment, however, the patient refused any additional radiotherapy.

On February 16, 2021, he was admitted to our hospital again. On physical examination, the patient was noted to have a painless 2-cm anterior abdominal wall swelling and a 2-cm swelling of the left posterior chest wall. The swollen skin did not have an abnormal color. An ultrasound scan demonstrated a 1.8×1.0×1.3 cm lesion along the left upper quadrant of the abdomen and a 1.9×1.2×1.5 cm lesion in the left posterior thorax (Figures 1A, B). All the lesions were within the superficial fascia and without dermal involvement. A CT scan confirmed the ultrasound diagnosis (Figures 1C, D) and showed a new finding of multiple lung metastases. On excision biopsy, the subcutaneous mass of the left abdomen proved to be metastatic ESCC (Figure 2A). The tumor cells were immunohistochemically positive for CK5/6 and P40, compatible with squamous cell carcinoma (Figures 2B, C). Moreover, the tumor cells were also positive for synaptophysin, which indicated neuroendocrine differentiation (Figure 2D). Because the MRI showed progression of the brain metastases, the patient again underwent gamma knife radiosurgery. The patient had previously received docetaxel combined with cisplatin and gemcitabine combined with cisplatin, so he was treated at this time with camrelizumab (200 mg on day 1) and anlotinib (12 mg on days 2–15). Because of progressive backache, a PET/CT scan was performed in March 10, 2021, to confirm whether other organ metastases had occurred;

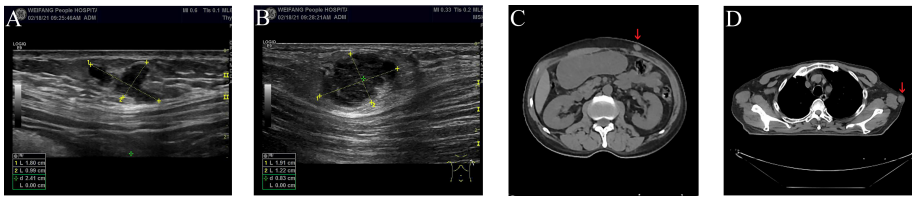

FIGURE 1
Ultrasound and CT scan of subcutaneous soft tissue metastases **(A–D)**. **(A)** Ultrasound scan of subcutaneous soft tissue metastasis in the left upper quadrant of the abdomen. **(B)** Ultrasound scan of subcutaneous soft tissue metastasis in the left posterior thorax. **(C)** CT scan of subcutaneous soft tissue metastasis in the left upper quadrant of the abdomen (red arrow). **(D)** CT scan of subcutaneous soft tissue metastasis in the left posterior thorax (red arrow).

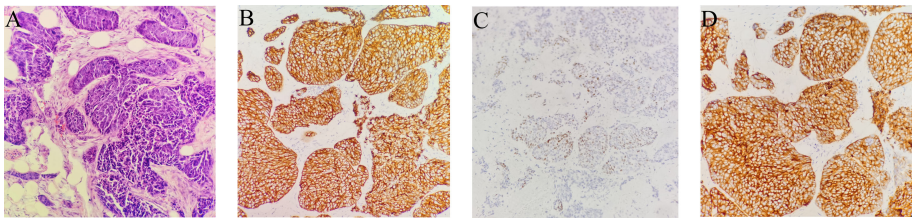

FIGURE 2
Biopsy of subcutaneous soft tissue metastasis in the left upper quadrant of the abdomen. **(A–D)**. **(A)** Squamous cell carcinoma is observed, which infiltrates the adipose tissue. Atypical epithelioid cells are observed in fibro tissue, muscle tissue and adipose tissue. (hematoxylin and eosin, original magnification × 200). **(B)** Positive CK5/6 immunohistochemical staining in a membranous distribution on the tumor cells (brown) (hematoxylin and eosin, original magnification × 200). **(C)** Positive P40 immunohistochemical staining (brown) (hematoxylin and eosin, original magnification × 200). **(D)** Positive synaptophysin immunohistochemical staining in a membranous distribution on the tumor cells (brown) (hematoxylin and eosin, original magnification × 200).

the scan revealed multiple areas of fluorodeoxyglucose uptake and foci in the esophagus, lung, liver, bone, and right adrenal gland, and in the lymph nodes in the mediastinum, abdomen, and bilateral axillary areas. In addition, an intensely hypermetabolic lesion was localized in the left posterior thorax (SUV_{max}=20.3) (Figures 3A, B). The last time the patient presented to our outpatient service was March 11, 2021, to obtain oxycodone hydrochloride sustained-release tablets; after this time, he was lost to follow-up.

Discussion

The liver, lungs, bone, and brain are the top four locations for distant metastases of EC (7). Dissemination to subcutaneous soft tissue is a conspicuous rarity. According to a large, retrospective study of 1341 patients with EC, only 25 (1.9%) had metastases to soft tissue, including skeletal muscles and/or subcutaneous fat, among whom seven patients harbored subcutaneous fat metastases (9).

A PubMed search of the English-language literature that reported subcutaneous soft tissue metastases is summarized in Table 1. Most patients in these reports had subcutaneous soft tissue metastases located in the chest wall or abdominal wall, which is in accordance with our case report. A large, retrospective study also confirmed this conclusion and suggested that the top four soft tissue metastases are the abdominal wall followed by the back, thigh, and chest wall (16). Soft tissue metastases are rare because of local soft tissue pH, temperature, and metabolite accumulation (9). We speculate that a specific microenvironment probably existed to facilitate the EC cell settlement into the soft tissue; however, the mechanisms driving this process remain uncertain and require clinical and experimental research to determine. Other questions remain unanswered as well. For example, does the overall incidence of subcutaneous soft tissue metastases among ESCC and esophageal adenocarcinoma (EA) differ? A retrospective study showed different overall incidences of soft tissue metastases among the two subtypes, and the incidence of EA was higher. However, this study concentrated on soft tissue metastases instead of subcutaneous soft tissue metastasis specifically; in addition, the incidence of EA is greater than that of ESCC in Western countries, where this study was conducted. Thus, the study may not accurately reflect the

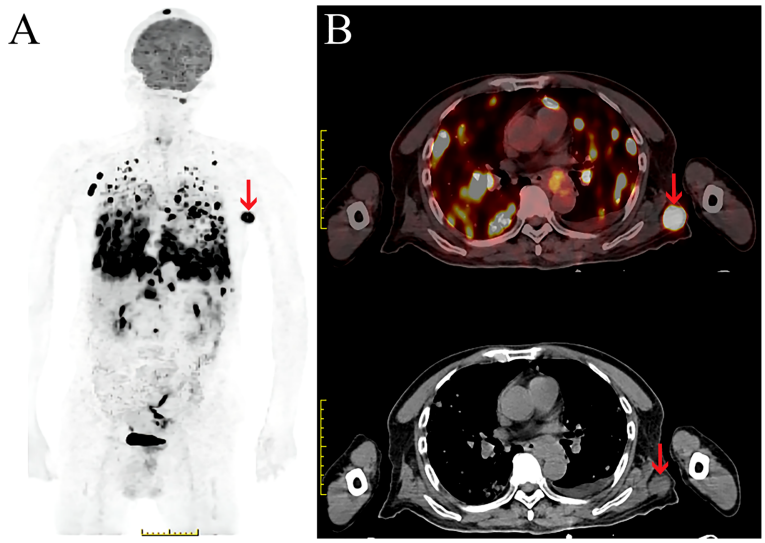

FIGURE 3
PET/CT scan of subcutaneous soft tissue metastasis in the left posterior thorax. **(A, B)**. **(A)** Maximum intensity projection (MIP) image of the whole body demonstrates a large FDG avid nodule in the left thorax (red arrow). **(B)** Fused PET/CT and CT axial image demonstrates a large FDG avid nodule in the left posterior thorax (SUVmax=20.3) (red arrow).

TABLE 1 Summary of previous studies reporting subcutaneous soft tissue metastases of ESCC.

Authors	Year	Gender/age	Methods of detection	Location	Systemic metastases	Treatment
Smyth et al. (10)	2009	Male/50	CT biopsy	Left buttock	Lung	Radiotherapy
Kapoor et al. (11)	2009	Male/72	PET/CT biopsy	Right posterior chest wall	Lung, bone	NM
Chand et al. (12)	2010	Female/73	US CT biopsy	Left anterior abdomen	Lung, liver, kidneys, and omentum	NM
Balukrishna et al. (13)	2011	Male/56	CT biopsy	Right posterior chest wall	No	Chemotherapy
de Oliveira et al. (14)	2019	Male/41	CT biopsy	Right hemithorax, flank, and armpit	Lymph node of multiple regions, retroperitoneal and pleural nodules	Chemotherapy
Puri et al. (15)	2019	Male/69	CT biopsy	Posterior neck, left index finger, and left abdomen	Lung, liver, and brain	Radiotherapy +chemotherapy

ESCC, esophageal squamous cell carcinoma; NM, not mentioned.

global differences between metastases associated with ESCC versus EA.

EC does not always contain only one histological component; EC sometimes comprises two or more components and has multidirectional differentiation abilities (17). One hypothesis about ESCC formation is that the subtype develops from totipotential cells at an early age and then transforms with multidirectional differentiation (18). The patient in our case also exhibited neuroendocrine differentiation. We speculate that ESCC with neuroendocrine differentiation has a unique biologic behavior that may facilitate multiple metastases more easily than ESCC without neuroendocrine differentiation.

The treatment of patients with subcutaneous soft tissue metastases must consider oligometastatic or systemic metastases. Patients with oligometastatic EC could benefit from local radiotherapy (19). If the subcutaneous soft tissue metastasis is solitary and no other organs are involved, radical excision may be considered. However, if the soft tissue involvement is combined with systemic metastases, chemotherapy, immunotherapy, and targeted therapy may play more important roles. To our knowledge, available case reports have not discussed immunotherapy in such patients. In recent years, immunotherapy has played a more critical role in the treatment of ESCC and has offered clinicians an alternative when patients develop resistance to chemotherapy (20). According to the ESCORT study, second-line camrelizumab significantly improved overall survival in patients with advanced or metastatic ESCC compared with chemotherapy (21). ALTER1102 showed that the use of anlotinib

significantly improved PFS in previously treated, recurrent, or metastatic ESCC patients, who had received one line, two or more lines chemotherapy compared with placebo (22). Recently, a single arm study of anlotinib in combination with PD-1 inhibitors as second-line or later therapy for advanced or metastatic ESCC have obtained a promising result with an objective response rate (ORR) of 30.0% and a disease control rate (DCR) of 87.5% (23). As such, camrelizumab with or without anlotinib may be considered for patients with subcutaneous soft tissue metastasis of ESCC after first-line or later therapy.

Conclusions

Subcutaneous soft tissue metastases from ESCC are rare. This report highlights the experience of a patient with ESCC that progressed to subcutaneous soft tissue metastases. Clinicians should pay attention to patient symptomatology and administer PET/CT to assist with diagnosis. PD-1 inhibiters with or without anlotinib could be considered as an alternative treatment when metachronous subcutaneous soft tissue metastases occur after first-line chemotherapy or later therapy. Additional study is warranted to investigate the epidemiology, mechanisms, and differences among ESCC and EA with subcutaneous soft tissue metastases. ESCC with neuroendocrine differentiation is a unique subtype of ESCC that warrants more attention from clinicians.

Data availability statement

The raw data supporting the conclusions of this article will be made available by the authors, without undue reservation.

Ethics statement

The studies involving human participants were reviewed and approved by Ethics Committee of Weifang People's Hospital. Written informed consent for participation was not required for this study in accordance with the national legislation and the institutional requirements.

Author contributions

XG retrieved clinical data, wrote and edited the manuscript. JL and FH supervised the article. HS captured biopsy images and assisted with figure development. ZS captured PET/CT images and assisted with figure development. SQ captured Ultrasound images and assisted with figure development. YL captured CT images and assisted with figure development. YZ assisted with clinical data collection. YC conceive this article, retrieved clinical data, and assisted with editing the manuscript. All authors contributed to the article and approved the submitted version.

Funding

This work was supported by the Science and Technology Development Project of Weifang City (Grant No. 2020YX008) and the Scientific Research Project of Weifang Municipal Health Commission (Grant No.WFWSJK-2021-163, Grant No.WFWSJK-2021-005).

Conflict of interest

The authors declare that the research was conducted in the absence of any commercial or financial relationships that could be construed as a potential conflict of interest.

Publisher's note

References

1. Sung H, Ferlay J, Siegel RL, Laversanne M, Soerjomataram I, Jemal A, et al. Global cancer statistics 2020: GLOBOCAN estimates of incidence and mortality worldwide for 36 cancers in 185 countries. *CA Cancer J Clin* (2021) 71(3):209–49. doi: 10.3322/caac.21660

2. Chen WQ, Li H, Sun KX, Zheng RS, Zhang SW, Zeng HM, et al. [Report of cancer incidence and mortality in China, 2014]. *Zhonghua Zhong Liu Za Zhi* (2018) 40(1):5–13. doi: 10.3760/cma.j.issn.0253-3766.2018.01.002

3. Zhang H-Z, Jin G-F, Shen H-B. Epidemiologic differences in esophageal cancer between Asian and Western populations. *Chin J Cancer* (2012) 31(6):281–6. doi: 10.5732/cjc.011.10390

4. Allemani C, Matsuda T, Di Carlo V, Harewood R, Matz M, Nikšić M, et al. Global surveillance of trends in cancer survival 2000-14 (CONCORD-3): Analysis of individual records for 37 513 025 patients diagnosed with one of 18 cancers from 322 population-based registries in 71 countries. *Lancet* (2018) 391 (10125):1023–75. doi: 10.1016/S0140-6736(17)33326-3

5. Zhao Z, Zhang Y, Wang X, Geng X, Zhu L, Li M. Clinical response to chemoradiotherapy in esophageal carcinoma is associated with survival and benefit of consolidation chemotherapy. *Cancer Med* (2020) 9(16):5881–8. doi: 10.1002/cam4.3273

6. Huang T-T, Li S-H, Chen Y-H, Lu H-I, Lo C-M, Fang F-M, et al. Definitive chemoradiotherapy for clinical T4b esophageal cancer - treatment outcomes,

failure patterns, and prognostic factors. *Radiother Oncol* (2021) 157:56–62. doi: 10.1016/j.radonc.2021.01.007

7. Ai D, Zhu H, Ren W, Chen Y, Liu Q, Deng J, et al. Patterns of distant organ metastases in esophageal cancer: A population-based study. *J Thorac Dis* (2017) 9 (9):3023–30. doi: 10.21037/jtd.2017.08.72

8. Rice TW, Ishwaran H, Ferguson MK, Blackstone EH, Goldstraw P. Cancer of the esophagus and esophagogastric junction: An eighth edition staging primer. *J Thorac Oncol* (2017) 12(1):36–42. doi: 10.1016/j.jtho.2016.10.016

9. El Abiad JM, Hales RK, Levin AS, Morris CD. Soft-tissue metastases from esophageal cancer. *J Gastrointest Surg* (2019) 23(9):1721–8. doi: 10.1007/s11605-019-04160-w

10. Smyth S, O'Donnell ME, Kumar S, Hussain A, Cranley B. Atypical presentation of an oesophageal carcinoma with metastases to the left buttock: A case report. *Cases J* (2009) 2:6691. doi: 10.1186/1757-1626-2-6691

11. Kapoor J, Basu S, Menon S. Subcutaneous metastasis in esophageal carcinoma detected by FDG-PET imaging. *Indian J Cancer* (2009) 46(4):354–5. doi: 10.4103/0019-509X.55565

12. Chand M, Thomas RJ, Dabbas N, Bateman AC, Royle GT. Soft tissue metastases as the first clinical manifestation of squamous cell carcinoma of the esophagus: Case report. *World J Oncol* (2010) 1(3):135–7. doi: 10.4021/wjon2010.05.209w

13. Balukrishna S, Jennifer P, Viswanathan PN. Solitary subcutaneous metastasis from squamous cell carcinoma of the esophagus: A case report and brief review of literature. *J Gastrointest Cancer* (2011) 42(4):269–71. doi: 10.1007/s12029-010-9239-8

14. de Oliveira RAM, da Silva T, Piovesana MM, Stecca CE, Lopes GA, Liutti VT. Advanced esophageal neoplasm with subcutaneous metastasis. *Case Rep Oncol Med* (2019) 2019:9103137. doi: 10.1155/2019/9103137

15. Puri S, Holle LM, Forouhar FA, Clement JM. Subcutaneous metastasis from recurrent basaloid squamous cell carcinoma of the esophagus. *J Oncol Pharm Pract* (2019) 25(2):492–6. doi: 10.1177/1078155217736920

16. Plaza JA, Perez-Montiel D, Mayerson J, Morrison C, Suster S. Metastases to soft tissue: a review of 118 cases over a 30-year period. *Cancer* (2008) 112(1):193–203. doi: 10.1002/cncr.23151

17. Yamasaki T, Ishii N, Okuno T, Suekane T, Inoue T, Nebiki H. A case of esophageal squamous cell carcinoma with neuroendocrine, basaloid, and ciliated glandular differentiation. *Clin J Gastroenterol* (2021) 14(1):32–8. doi: 10.1007/s12328-020-01267-5

18. Nishimaki T, Nakagawa S, Aizawa K, Suzuki T, Hatakeyama K, Watanabe H. Composite tumor of the esophagus with tripartite differentiation. *Dig Dis Sci* (1997) 42(5):1041–6. doi: 10.1023/A:1018897321851

19. Li B, Wang R, Zhang T, Sun X, Jiang C, Li W, et al. Development and validation of a nomogram prognostic model for esophageal cancer patients with oligometastases. *Sci Rep* (2020) 10(1):11259. doi: 10.1038/s41598-020-68160-6

20. Yang J, Liu X, Cao S, Dong X, Rao S, Cai K. Understanding esophageal cancer: The challenges and opportunities for the next decade. *Front Oncol* (2020) 10:1727. doi: 10.3389/fonc.2020.01727

21. Huang J, Xu J, Chen Y, Zhuang W, Zhang Y, Chen Z, et al. Camrelizumab versus investigator's choice of chemotherapy as second-line therapy for advanced or metastatic oesophageal squamous cell carcinoma (ESCORT): A multicentre, randomised, open-label, phase 3 study. *Lancet Oncol* (2020) 21(6):832–42. doi: 10.1016/S1470-2045(20)30110-8

22. Huang J, Xiao J, Fang W, Lu P, Fan Q, Shu Y, et al. Anlotinib for previously treated advanced or metastatic esophageal squamous cell carcinoma: A double-blind randomized phase 2 trial. *Cancer Med* (2021) 10(5):1681–9. doi: 10.1002/cam4.3771

23. Hong Y, Wu T, Lu P, Chang Z, Liang W, Zhang G, et al. Real-world effectiveness of anlotinib in combination with PD-1 inhibitors as second-line or later therapy for advanced or metastatic esophageal squamous cell carcinoma. *J Clin Oncol* (2022) 40(4_suppl):320. doi: 10.1200/JCO.2022.40.4_suppl.320

frontiers | Frontiers in Oncology

TYPE Case Report
PUBLISHED 24 August 2022
DOI 10.3389/fonc.2022.948463

OPEN ACCESS

EDITED BY
Ahmed Eleojo Musa,
Dalhousie University, Canada

REVIEWED BY
Dheyauldeen Shabeeb Almirtah,
University of Technology, Iraq
Yaping Xu,
Tongji University, China

*CORRESPONDENCE
Kenneth D. Westover
Kenneth.Westover@UTSouthwestern.edu

SPECIALTY SECTION
This article was submitted to Radiation Oncology, a section of the journal Frontiers in Oncology

RECEIVED 19 May 2022
ACCEPTED 18 July 2022
PUBLISHED 24 August 2022

CITATION
Yen A and Westover KD (2022) Case Report: Resolution of radiation pneumonitis with androgens and growth hormone.
Front. Oncol. 12:948463.
doi: 10.3389/fonc.2022.948463

Case Report: Resolution of radiation pneumonitis with androgens and growth hormone

Allen Yen and Kenneth D. Westover*

Department of Radiation Oncology, University of Texas Southwestern Medical Center, Dallas, TX, United States

Radiation pneumonitis (RP) occurs in some patients treated with thoracic radiation therapy. RP often self-resolves, but when severe it is most commonly treated with corticosteroids because of their anti-inflammatory properties. Androgens and human growth hormone (HGH) also have anti-inflammatory and healing properties in the lung, but have not been studied as a remedy for RP. Here we present a case of corticosteroid-refractory RP that resolved with androgen and HGH-based therapy.

Case Presentation: A 62 year old male body builder with excellent performance status presented with locally advanced non-small cell lung cancer characterized by a 7 cm mass in the right lower lobe and associated right hilar and subcarinal lymph node involvement. He was treated with chemoradiation and an excellent tumor response was observed. However, 2 months post-treatment he developed severe shortness of breath and imaging was consistent with RP. His RP was refractory to prednisone and antibiotic therapy, despite various regimens over a 9 month period. The patient self-treated with an androgen and HGH-based regimen and the RP promptly resolved.

Conclusion: The anti-inflammatory properties of androgens and HGH have prompted an exploration of their potential role in therapeutic strategies to treat pro-inflammatory conditions such as sepsis, infections and interstitial lung disease. This case study suggests a potential role for the use of androgens for the treatment of steroid-refractory RP after radiation therapy. However, the applicability of this strategy to general populations should be weighed carefully against secondary effects of these agents, especially in the setting of cancer survivorship.

KEYWORDS

radiation pneumonitis, lung cancer, androgen, growth hormone, steroids anabolics, case report

Introduction

Chemoradiation is a common treatment for inoperable locally advanced non-small cell lung cancers (1). The treatment involves radiation over 6-7 weeks with concurrent chemotherapy. Side effects can include fatigue, esophagitis, and radiation pneumonitis (RP), with the risk being roughly proportional to the extent of normal tissue exposure (2, 3). In the clinical trials that established chemoradiation as the standard of care, RP was observed in 5-20% of patients and was associated with advanced age or pre-existing lung conditions including chronic obstructive pulmonary lung disease or interstitial lung disease (3–8). At a cellular level, radiation causes several effects including edema, epithelial changes, disruption of the microvasculature, and atelectasis that lead to inflammatory changes resulting in RP (3, 4). Clinically, RP presents weeks to months following treatment, manifesting as fever, cough, shortness of breath, and ground-glass opacities (3, 4). RP can have significant negative impacts on quality of life (4, 9, 10). Severe RP is often treatable with corticosteroids with symptom improvement in 75-93% of patients, but some patients are refractory (3, 11, 12). Androgens are also well known to have anti-inflammatory properties, but have not been studied as a remedy for RP. Older studies have shown that androgen therapy can reduce the risk of exacerbations of asthma and COPD, but given the potential risks of androgen therapy including adverse cardiovascular events and increased risks of malignancy, these medications have not been implemented. In this case report, we present a patient with corticosteroid-refractory RP that responded favorably to androgen-based therapy.

Case description

A 62-year-old male body builder with a 20-pack year smoking history and surgical history of repaired inguinal hernia and appendectomy presented to his PCP with cough, fatigue, and weight loss. CT of the chest showed a 7 cm mass in the right lower lobe of the lung with enlarged subcarinal lymph nodes (Figure 1A). Subsequent PET/CT showed FDG uptake in the lung mass and right hilar and subcarinal lymph nodes (Figure 2), but no evidence of metastatic disease. Pre-treatment pulmonary function tests revealed a FVC of 66% and FEV1 of 59%. Biopsy of the right lung mass confirmed poorly-differentiated squamous cell carcinoma of pulmonary origin. Nodal involvement was confirmed by endobronchial ultrasound guided sampling of mediastinal lymph nodes. He was treated with chemoradiation to a dose of 6000 cGy in 30 fractions (Figure 3) with 6 cycles of carboplatin and paclitaxel given weekly. Of note, the lung V20 for his radiation plan was 31%. Two cycles of consolidative carboplatin and paclitaxel were also given.

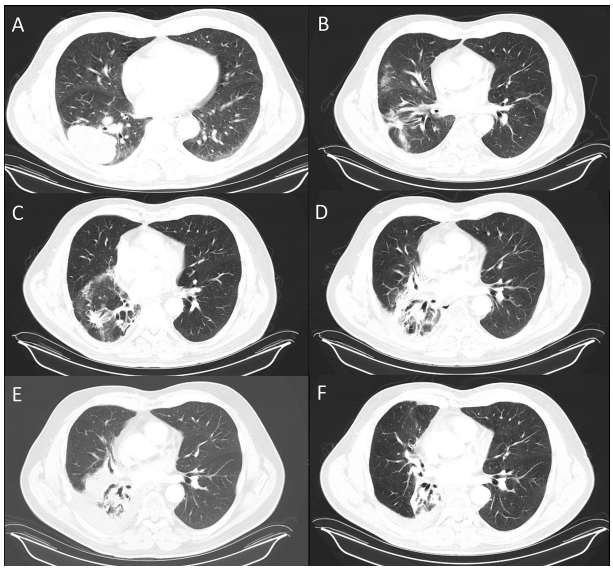

FIGURE 1
Serial CT's of the chest shows resolution of lung pneumonitis with anabolic steroids. **(A)** Lung disease at presentation and after completion of definitive chemoRT at **(B)**, 2 months **(C)**, 5 months **(D)**, 8 months **(E)**, 11 months **(F)**, 17 months. The androgen-HGH regimen was initiated after the 12 month scan, **(E)**.

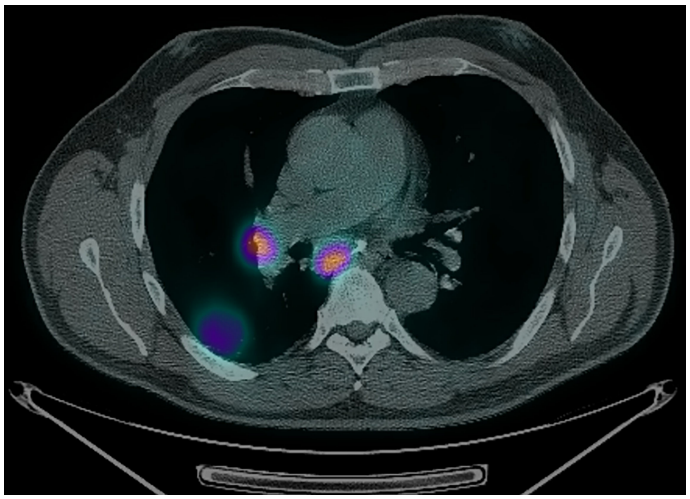

FIGURE 2
PET/CT showing FDG-avid R hilar and subcarinal lymph nodes.

CT Chest 2 months post radiation completion showed shrinkage of the primary mass to 4.4 cm, reduction in the size of involved lymph nodes and associated radiation changes in the surrounding lung (Figure 1B). However, by 3 months, he developed malaise and a persistent cough, so an empiric 1 week course of azithromycin and prednisone were prescribed for pneumonia. His symptoms persisted despite therapy and repeat imaging 3 months later showed opacities within the high and intermediate areas of radiation dose consistent with pneumonitis (Figure 1C). A 5 week prednisone taper with a starting dose of 25 mg was prescribed. Symptoms improved with therapy but returned as he tapered to 5 mg so the dose was

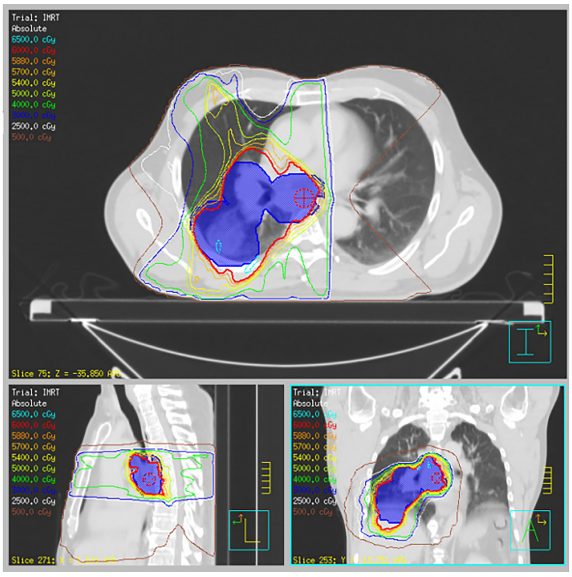

FIGURE 3
Radiation treatment plan. Representative axial, sagittal, and coronal slices for R lung lesion and mediastinal disease treated to 60 Gy in 30 fractions with concurrent carboplatin and paclitaxel.

increased to 20 mg and additional course of azithromycin was prescribed. Repeat pulmonary function tests showed had slightly worsened with a FVC of 57% and FEV1 of 63%. Further attempts over the next 4 months to wean from prednisone failed. After 9 months of collective prednisone therapy, he noted abdominal fullness and was found to have elevated ALT and AST of 114 and 53, respectively. On CT imaging he was noted to have hepatic steatosis. Evaluation with colonoscopy, abdominal US, and CT enterography were unremarkable leading to the conclusion that his liver dysfunction was a sequela of steroid therapy. Based on his understanding that androgens can have anti-inflammatory effects, the patient elected to taper prednisone and self-prescribed the androgen-based regimen shown in Table 1.

Within two weeks of initiating therapy, the patient experienced a reduction in abdominal fullness, resolution of cough and improved energy. By eight weeks, he felt fully recovered and was able to return to full workouts lifting weights. During androgen therapy, no other significant changes in medical therapy, diet or lifestyle were noted that could be linked to his improvement. CT of the chest 17 months post radiation therapy showed consolidation of the treated lobe and resolution of pneumonitis elsewhere in the lung (Figure 1F). As of most recent follow up, 5 years post treatment, the patient had no clinically significant deficits related to cancer therapy and no evidence of active disease. The patient's treatment course is summarized as as e timeline in the supplementary materials.

Discussion and conclusions

To our knowledge, this is the first case report of using androgen and HGH-based therapy to treat radiation pneumonitis. However, the concept of treating inflammatory pulmonary disease with androgen or HGH therapy has substantial precedent. The idea that androgens are important regulators of pulmonary inflammation originated with a number of clinical observations. It is well documented that men and women show differences in lung pathology. For example, female neonates produce surfactants earlier in development when compared to male neonates and are at lower risk for respiratory distress syndrome or asthma (13, 14). Also, patients with Klinefelter syndrome, the most common cause of hypogonadism, are 69% more likely to be hospitalized with

TABLE 1 Anabolic steroid and HGH regimen; CDMT = Chlorodehydromethyltestosterone, QAD = every other day, BID = twice daily, TID = three times daily.

Week 1-8			
Medication Name	**Medication Class**	**Dose**	**Dosage**
Testosterone propionate	AR agonist	250 mg	QAD
Mesterolone	AR agonist	50 mg	BID
Stanozolol	AR agonist	10 mg	TID
Anastrazole	Aromatase inhibitor	0.5 mg	QAD
CDMT	AR agonist	50 mg	BID
Human Growth Hormone	GHR agonist	0.08 mg	Biweekly (Mon and Thurs)
Week 8-16			
Medication Name	**Medication Class**	**Dose**	**Dosage**
Testosterone isocaproate	AR agonist	150 mg	Biweekly (Mon and Thurs)
Nandrolone	AR agonist	400 mg	Biweekly (Mon and Thurs)
Boldenone	AR agonist	300 mg	Biweekly (Mon and Thurs)
Anastrazole	Aromatase inhibitor	0.5 mg	QAD
Metandienone	AR agonist	50 mg	BID
Human Growth Hormone	GHR agonist	0.08 mg	Biweekly (Mon and Thurs)
Week 16-20			
Medication Name	**Medication Class**	**Dose**	**Dosage**
Testosterone propionate	AR agonist	250 mg	QAD
Drostanolone propionate	AR agonist	100 mg	Biweekly (Mon and Thurs)
Oxandrolone	AR agonist	50 mg	BID
Stanozolol	AR agonist	10 mg	TID
Mesterolone	AR agonist	50 mg	BID
Fluoxymesterone	AR agonist	10 mg	BID
Human Growth Hormone	GHR agonist	0.08 mg	Biweekly (Mon and Thurs)

pulmonary diseases like COPD or pneumonia (15). Additionally, men treated with anti-androgens experience a higher rate of interstitial lung disease with a reported odds ratio up to 6.6 (16). There is also rationale for using HGH to address lung injury. Laboratory studies have shown that HGH may participate in lung development, growth, and repair (17). Additionally, several studies on animal models of acute lung injury have shown dramatic attenuation of lung injury by recombinant HGH (18, 19).

Collectively, these observations have led to prospective studies of androgen therapy and HGH. A study on women with asthma showed that administration of testosterone decreased risks of hospitalizations from asthma attacks by 9.1% in older patients (20).. A meta-analysis from China found that androgens improved body weight, fat-free mass, and symptoms in patients with chronic obstructive pulmonary disease. These changes, however, did not translate into changes in pulmonary function or muscle strength (21). Similarly, another retrospective study of middle-aged men with COPD who received testosterone replacement therapy showed lower rates of respiratory-related hospitalizations (22). A study of HGH in patients with COPD showed improvements in pulmonary function of 27% (23).

The regimen used by the patient in this case report is complex, making it difficult to interpret which agents provided the benefits observed. Nevertheless, the dosages used can be placed into context. The testosterone regimen of 600 mg of testosterone weekly is substantially higher than doses typically used in testosterone replacement therapy (100-200 mg weekly), and has been shown to improve strength and muscle size in healthy men (24). Similarly, doses of nandrolone around 200 mg weekly improved body mass and fat-free mass over the course of 8 weeks (25). This dose was significantly lower than the dose our patient used. The HGH dose of 0.08 mg biweekly is lower than the dose used in the previously cited COPD trial where 0.05 mg/kg was given daily (23). The mesterolone dose of 50 mg BID is similar to the dose used in men with oligospermia and improved sperm counts and mobility who received 100 – 150 mg daily (26). The stanozolol dose of 10 mg TID is lower than the doses used in a recently published trial (2 mg TID) that found improved progression-free survival for patients with high-risk myelodysplastic syndrome (27). In mouse studies, anastrazole was delivered to mice and showed decrease radiation induced lung fibrosis. These mice were given doses equivalent to 1 mg given to an adult daily (28). Although our patients regimen varies from doses reported in literature, there are clear connections between anabolic steroids and beneficial clinical outcomes (29).

In this case, androgen and HGH therapy provided a clear benefit for RP and did not cause cancer recurrence. However, extending this regimen, or a portion of this regimen, to other patients would entail risks, especially within the cancer population. Testosterone or androgen precursors can also increase cardiovascular events, produce neuropsychiatric problems and alter reproductive capacity. Additionally, testosterone has been shown to increase the risk of prostate and testicular cancer and linked to increased risks of breast and liver cancer (30–33). HGH can induce tumor formation in animal models and is associated with increased risk of thyroid and colorectal cancer in patients with acromegaly. However, studies of children and adult cancer survivors who received HGH have not shown an increased risk of cancer progression (34, 35). Clearly, additional prospective studies would be necessary to establish efficacy, dosing and other guidelines for HGH or androgen therapies for RP.

Data availability statement

The original contributions presented in the study are included in the article/Supplementary Material. Further inquiries can be directed to the corresponding author.

Ethics statement

Written informed consent was obtained from the individual (s) for the publication of any potentially identifiable images or data included in this article.

Author contributions

AY and KW were responsible for the concept of the case report. AY drafted the manuscript and KW critically revised the manuscript. All authors contributed to the article and approved the submitted version.

Funding

This work was funded by the Department of Radiation Oncology at UT Southwestern.

Acknowledgments

We would like to acknowledge the patient presented in this case report for his willingness to assist us with this manuscript.

Conflict of interest

The authors declare that the research was conducted in the absence of any commercial or financial relationships that could be construed as a potential conflict of interest.

Publisher's note

All claims expressed in this article are solely those of the authors and do not necessarily represent those of their affiliated organizations, or those of the publisher, the editors and the reviewers. Any product that may be evaluated in this article, or claim that may be made by its manufacturer, is not guaranteed or endorsed by the publisher.

Supplementary material

The Supplementary Material for this article can be found online at: https://www.frontiersin.org/articles/10.3389/fonc.2022.948463/full#supplementary-material

References

1. Ettinger DSWood DEAisner DLAkerley WBauman JRBharat A, et alNon–small cell lung cancer, version 3.2022, NCCN Clinical practice guidelines in oncology. .*Journal of the National Comprehensive Cancer Network* (2022) 20 (5):497–530.

2. Rodrigues G, Lock M, D'Souza D, Yu E, Van Dyk J. Prediction of radiation pneumonitis by dose - volume histogram parameters in lung cancer–a systematic review. *Radiother Oncol* (2004) 71(2):127–38. doi: 10.1016/j.radonc.2004.02.015

3. Bledsoe TJ, Nath SK, Decker RH. Radiation pneumonitis. *Clin Chest Med* (2017) 38(2):201–8. doi: 10.1016/j.ccm.2016.12.004

4. Jain V, Berman AT. Radiation pneumonitis: Old problem, new tricks. *Cancers (Basel)* (2018) 10(7):222. doi: 10.3390/cancers10070222

5. Vogelius IR, Bentzen SM. A literature-based meta-analysis of clinical risk factors for development of radiation induced pneumonitis. *Acta Oncol* (2012) 51 (8):975–83. doi: 10.3109/0284186X.2012.718093

6. Bradley JD, Paulus R, Komaki R, Masters G, Blumenschein G, Schild S, et al. Standard-dose versus high-dose conformal radiotherapy with concurrent and consolidation carboplatin plus paclitaxel with or without cetuximab for patients with stage IIIA or IIIB non-small-cell lung cancer (RTOG 0617): A randomised, two-by-two factorial phase 3 study. *Lancet Oncol* (2015) 16(2):187–99. doi: 10.1016/S1470-2045(14)71207-0

7. Curran WJJr., Paulus R, Langer CJ, Komaki R, Lee JS, Hauser S, et al. Sequential vs. concurrent chemoradiation for stage III non-small cell lung cancer: randomized phase III trial RTOG 9410. *J Natl Cancer Inst* (2011) 103(19):1452–60. doi: 10.1093/jnci/djr325

8. Socinski MA, Zhang C, Herndon JE2nd, Dillman RO, Clamon G, Vokes E, et al. Combined modality trials of the cancer and leukemia group b in stage III non-small-cell lung cancer: Analysis of factors influencing survival and toxicity. *Ann Oncol* (2004) 15(7):1033–41. doi: 10.1093/annonc/mdh282

9. Trott KR, Herrmann T, Kasper M. Target cells in radiation pneumopathy. *Int J Radiat Oncol Biol Phys* (2004) 58(2):463–9. doi: 10.1016/j.ijrobp.2003.09.045

10. Kanemoto A, Matsumoto Y, Sugita T. Timing and characteristics of radiation pneumonitis after stereotactic body radiotherapy for peripherally located stage I lung cancer. *Int J Clin Oncol* (2015) 20(4):680–5. doi: 10.1007/s10147-014-0766-3

11. Henkenberens C, Janssen S, Lavae-Mokhtari M, Leni K, Meyer A, Christiansen H, et al. Inhalative steroids as an individual treatment in symptomatic lung cancer patients with radiation pneumonitis grade II after radiotherapy – a single-centre experience. *Radiat Oncol* (2016) 11(1):12. doi: 10.1186/s13014-016-0580-3

12. Sekine I, Sumi M, Ito Y, Nokihara H, Yamamoto N, Kunitoh H, et al. Retrospective analysis of steroid therapy for radiation-induced lung injury in lung cancer patients. *Radiother Oncol* (2006) 80(1):93–7. doi: 10.1016/j.radonc.2006.06.007

13. Farrell PM, Wood RE. Epidemiology of hyaline membrane disease in the united states: Analysis of national mortality statistics. *Pediatrics* (1976) 58(2):167–76.

14. Myers T. Pediatric asthma epidemiology: incidence, morbidity, and mortality. *Respir Care Clinics North America* (2000) 6:1–14. doi: 10.1016/S1078-5337(05)70054-X

15. Bojesen A, Juul S, Birkebaek NH, Gravholt CH. Morbidity in klinefelter syndrome: a Danish register study based on hospital discharge diagnoses. *J Clin Endocrinol Metab* (2006) 91(4):1254–60. doi: 10.1210/jc.2005-0697

16. Nawa H, Niimura T, Hamano H, Yagi K, Goda M, Zamami Y, et al. Evaluation of potential complications of interstitial lung disease associated with antiandrogens using data from databases reporting spontaneous adverse effects. *Front Pharmacol* (2021) 12:655605. doi: 10.3389/fphar.2021.655605

17. Zhang C, Cai R, Lazerson A, Delcroix G, Wangpaichitr M, Mirsaeidi M, et al. Growth hormone-releasing hormone receptor antagonist modulates lung inflammation and fibrosis due to bleomycin. *Lung* (2019) 197(5):541–9. doi: 10.1007/s00408-019-00257-w

18. Yi C, Cao Y, Mao SH, Liu H, Ji LL, Xu SY, et al. Recombinant human growth hormone improves survival and protects against acute lung injury in murine staphylococcus aureus sepsis. *Inflamma Res* (2009) 58(12):855–62. doi: 10.1007/s00011-009-0056-0

19. Yi C, Wang SR, Zhang SY, Yu SJ, Jiang CX, Zhi MH, et al. Effects of recombinant human growth hormone on acute lung injury in endotoxemic rats. *Inflammation Res* (2006) 55(11):491–7. doi: 10.1007/s00011-006-6011-4

20. Wulfsohn NL, Politzer WM, Henrico JS. TESTOSTERONE THERAPY IN BRONCHIAL ASTHMA. *S Afr Med J* (1964) 38:170–2.

21. Pan L, Wang M, Xie X, Du C, Guo Y. Effects of anabolic steroids on chronic obstructive pulmonary disease: a meta-analysis of randomised controlled trials. *PloS One* (2014) 9(1):e84855. doi: 10.1371/journal.pone.0084855

22. Baillargeon J, Urban RJ, Zhang W, Zaiden MF, Javed Z, Sheffield-Moore M, et al. Testosterone replacement therapy and hospitalization rates in men with COPD. *Chron Respir Dis* (2019) 16:1479972318793004. doi: 10.1177/1479972318793004

23. Pape GS, Friedman M, Underwood LE, Clemmons DR. The effect of growth hormone on weight gain and pulmonary function in patients with chronic obstructive lung disease. *Chest* (1991) 99(6):1495–500. doi: 10.1378/chest.99.6.1495

24. van Amsterdam J, Opperhuizen A, Hartgens F. Adverse health effects of anabolic–androgenic steroids. *Regul Toxicol Pharmacol* (2010) 57(1):117–23. doi: 10.1016/j.yrtph.2010.02.001

25. van Marken Lichtenbelt WD, Hartgens F, Vollaard NB, Ebbing S, Kuipers H. Bodybuilders' body composition: effect of nandrolone decanoate. *Med Sci Sports Exerc* (2004) 36(3):484–9. doi: 10.1249/01.MSS.0000117157.06455.B0

26. Varma TR, Patel RH. The effect of mesterolone on sperm count, on serum follicle stimulating hormone, luteinizing hormone, plasma testosterone and outcome in idiopathic oligospermic men. *Int J Gynaecol Obstet* (1988) 26 (1):121–8. doi: 10.1016/0020-7292(88)90206-8

27. Liu Y, Yang C, Xue H, Ye F, Sun W, Wang J, et al. Stanozolol improves the progression-free survival of patients with high-risk myelodysplastic syndrome after decitabine treatment. *Int J Hematol* (2021) 113(6):807–14. doi: 10.1007/s12185-021-03115-9

28. Bese NS, Altinok AY, Ozsahin EM, Yildirim S, Sut N, Altug T, et al. Aromatase inhibitors and radiation-induced lung fibrosis. *J Clin Oncol* (2008) 26 (15_suppl):614. doi: 10.1200/jco.2008.26.15_suppl.614

29. McCullough D, Webb R, Enright KJ, Lane KE, McVeigh J, Stewart CE, et al. How the love of muscle can break a heart: Impact of anabolic androgenic steroids

on skeletal muscle hypertrophy, metabolic and cardiovascular health. *Rev Endocr Metab Disord* (2021) 22(2):389–405. doi: 10.1007/s11154-020-09616-y

30. Synder P. *Use of androgens and other hormones by athletes* (2020) (Accessed November 19, 2021).

31. Bianchi VE. The anti-inflammatory effects of testosterone. *J Endocr Soc* (2018) 3(1):91–107. doi: 10.1210/js.2018-00186

32. Mohamad NV, Wong SK, Wan Hasan WN, Jolly JJ, Nur-Farhana MF, Ima-Nirwana S, et al. The relationship between circulating testosterone and inflammatory cytokines in men. *Aging Male* (2019) 22(2):129–40. doi: 10.1080/13685538.2018.1482487

33. Salerno M, Cascio O, Bertozzi G, Sessa F, Messina A, Monda V, et al. Anabolic androgenic steroids and carcinogenicity focusing on leydig cell: a literature review. *Oncotarget* (2018) 9(27):19415–26. doi: 10.18632/oncotarget.24767

34. Clayton PE, Banerjee I, Murray PG, Renehan AG. Growth hormone, the insulin-like growth factor axis, insulin and cancer risk. *Nat Rev Endocrinol* (2011) 7 (1):11–24. doi: 10.1038/nrendo.2010.171

35. Jenkins PJ, Mukherjee A, Shalet SM. Does growth hormone cause cancer? *Clin Endocrinol (Oxf)* (2006) 64(2):115–21. doi: 10.1111/j.1365-2265.2005.02404.x

frontiers | Frontiers in Oncology

TYPE Case Report
PUBLISHED 16 September 2022
DOI 10.3389/fonc.2022.919644

OPEN ACCESS

EDITED BY
Stefano Pergolizzi,
University of Messina, Italy

REVIEWED BY
Nergiz Dagoglu,
Istanbul University, Turkey
Vishal G Shelat,
Tan Tock Seng Hospital, Singapore

*CORRESPONDENCE
Jian Dong
dong.jian@zs-hospital.sh.cn
Ting Chen
13611659996@139.com

SPECIALTY SECTION
This article was submitted to Radiation Oncology, a section of the journal Frontiers in Oncology

RECEIVED 13 April 2022
ACCEPTED 23 August 2022
PUBLISHED 16 September 2022

CITATION
Hu A, Chen T and Dong J (2022) Promising clinical outcome after body gamma knife radiotherapy for mediastinal follicular dendritic cell sarcoma with thoracic spine invasion and iliac metastasis: A case report and literature review.
Front. Oncol. 12:919644.
doi: 10.3389/fonc.2022.919644

Promising clinical outcome after body gamma knife radiotherapy for mediastinal follicular dendritic cell sarcoma with thoracic spine invasion and iliac metastasis: A case report and literature review

Annan Hu[1], Ting Chen[2*] and Jian Dong[1*]

[1]Department of Orthopaedic Surgery, Zhongshan Hospital, Fudan University, Shanghai, China, [2]Department of Radiotherapy, People's Liberation Army of China (PLA) Naval Medical Center, Naval Medical University, Shanghai, China

Background: Follicular dendritic cell sarcoma (FDCS) is a rare type of intermediate grade tumor. Mediastinal FDCS with spinal invasion has not been well described. The treatment options include surgical resection and radiation therapy. The body gamma knife is a stereotactic body radiotherapy (SBRT) technology that is widely used in China. The pathological evaluation of a bone lesion after a body gamma knife procedure has not been reported. Here, we report a case of a patient with FDCS with thoracic spine invasion and iliac metastasis treated with surgery and body gamma knife.

Case summary: A 36-year-old male patient was hospitalized at Zhongshan Hospital, Fudan University, due to a gradually aggravated pain on the lateral side of the left scapula for 6 months. Imaging examination showed neoplastic lesions on the left side of C7-T2 invading the vertebral body of T1, T2, and caput costae of the second rib and suspected metastasis in the left ilium. FDCS was diagnosed after performing a computed tomography (CT)-guided core needle biopsy, and the thoracic lesion was surgically resected. The body gamma knife was used as an adjuvant radiotherapy for the thoracic lesion and a primary therapy for the left ilium lesion. Iliac bone lesion resection was performed at Zhongshan Hospital, Fudan University, 10 weeks after RT. Compared with the biopsy report, the body gamma knife treatment resulted in a pathological complete response (PCR). The magnetic resonance imaging (MRI) examinations showed stable disease of the thoracic lesion after body gamma knife radiosurgery.

Conclusion: This case report describes the treatment of mediastinal FDCS with thoracic spinal invasion and iliac metastasis. The promising outcome suggests that separation surgery is an effective treatment option for mediastinal FDCS

with spinal column invasion. It also demonstrates the application prospects of the body gamma knife treatment in malignant lesions of the axial bones.

KEYWORDS

body gamma knife, stereotactic body radiotherapy, follicular dendritic cell sarcoma, pathological complete response, separation surgery

Introduction

Follicular dendritic cell sarcoma (FDCS) was first described by Monda et al. in 1986 (1). FDCS most commonly presents as a slow-growing mass in the cervical and axillary lymph nodes (2, 3). Some studies reported more extranodal cases, which may be due to referral bias (4, 5). Among all the reported FDCS cases that occurred at the extranodal sites, only a few involved the mediastinum, and none of these case reports adequately described spinal column involvement and concurrent metastasis (4, 6). There is no standard treatment for FDCS. A combined modality approach consisting of surgery, radiotherapy (RT), and/or chemotherapy is most commonly used (6, 7). Jain et al. analyzed 66 cases and concluded that aggressive local treatment with surgery and adjuvant RT improved local control (5). A few studies have also reported the effectiveness of targeted therapy and immunotherapy (8, 9).

As one of the stereotactic body radiotherapy (SBRT) systems, the body gamma knife uses 30 or 18 Co^{60} as the radiation source to release high-dose gamma rays that focus on a target area (10). It has sharp dose gradients such that the normal tissue around the target area receives a very low dose of radiation (11). The body gamma knife has been used in the treatment of several types of solid tumors, including lung cancer, pancreatic carcinoma, and liver cancer, in China (10, 12, 13). No study has reported the application of a body gamma knife treatment in FDSC or in axial bones. After body gamma knife RT, patients generally no longer undergo surgical resection of the target area; thus, it is difficult to perform a pathological evaluation for the body gamma knife treatment. Herein, we report a case of a patient with mediastinal FDCS with thoracic spinal invasion and iliac metastasis. The thoracic lesion was successfully treated by decompression surgery and postoperative adjuvant body gamma knife RT. Iliac metastasis demonstrated a pathological complete response (PCR) after body gamma knife RT.

Case description

A 36-year-old male patient was hospitalized due to complaints of a gradually aggravated pain on the lateral side of the left scapula for 6 months. Imaging examination showed that the neoplastic lesions on the left side of C7-T2 invaded the vertebral body of T1, T2, and caput costae of the second rib (Figures 1A–C). Tumor metastasis in the left ilium was suspected (Figures 1D–F). A computed tomography (CT)-guided core needle biopsy was performed to obtain the tissue samples of the paravertebral lesion in T2 and the lesion in the left ilium. The pathological results confirmed the diagnosis of FDCS. Diffuse small spindle cells were found in the hematoxylin and eosin (H&E) staining of both paravertebral (Figures 2A, B) and iliac (Figures 2D, E) lesions. Immunohistochemical staining of the paravertebral sample was positive for cytokeratin (CK){pan} and vimentin; partially positive for cluster of differentiation 68 (CD68){KP1} and epithelial membrane antigen (EMA); slightly positive for S100 and CD34; and negative for SRY-box transcription factor 10 (Sox10), Langerin, thyroid transcription factor 1 (TTF-1), and prostatic specific acid phosphatase (PSAP) (Figure 2C). Immunohistochemical staining of the iliac sample was positive for CK{pan}, vimentin, CD68{KP1}, and epidermal growth factor receptor (EGFR); partially positive for Clusterin; slightly positive for S100, CD35, and CD20; and negative for CD21, Sox10, Langerin, and CXC chemokine ligand 13 (CXCL13) (Figure 2F).

Tumor resection and nerve root decompression were performed as treatment for thoracic disease. A midline incision was made, and the lamina and facet joints of T1–T3 were exposed. Four pedicle screws were implanted in T1 and T3 (Figures 3A1, 2). The left lamina and facet joint of T1 and T2 were resected (Figures 3A3, 4). The left second costovertebral joint and the second rib head were also resected. Transpedicular curettage was performed to ensure sufficient neural decompression of the tumor, providing a safe target volume for radiation.

The body gamma knife was used as a radical treatment for iliac tumor and as an adjuvant treatment for thoracic disease. Body gamma knife planning and delivery were similar to those reported in previous studies (10, 12, 13). The patient was placed in a supine position and immobilized using a vacuum negative pressure bag and a body frame bed, allowing to breathe naturally. Markings were made on the four areas of the body that will receive the radiation to ensure reproducible body position. The CT images were transferred to the OPEN body

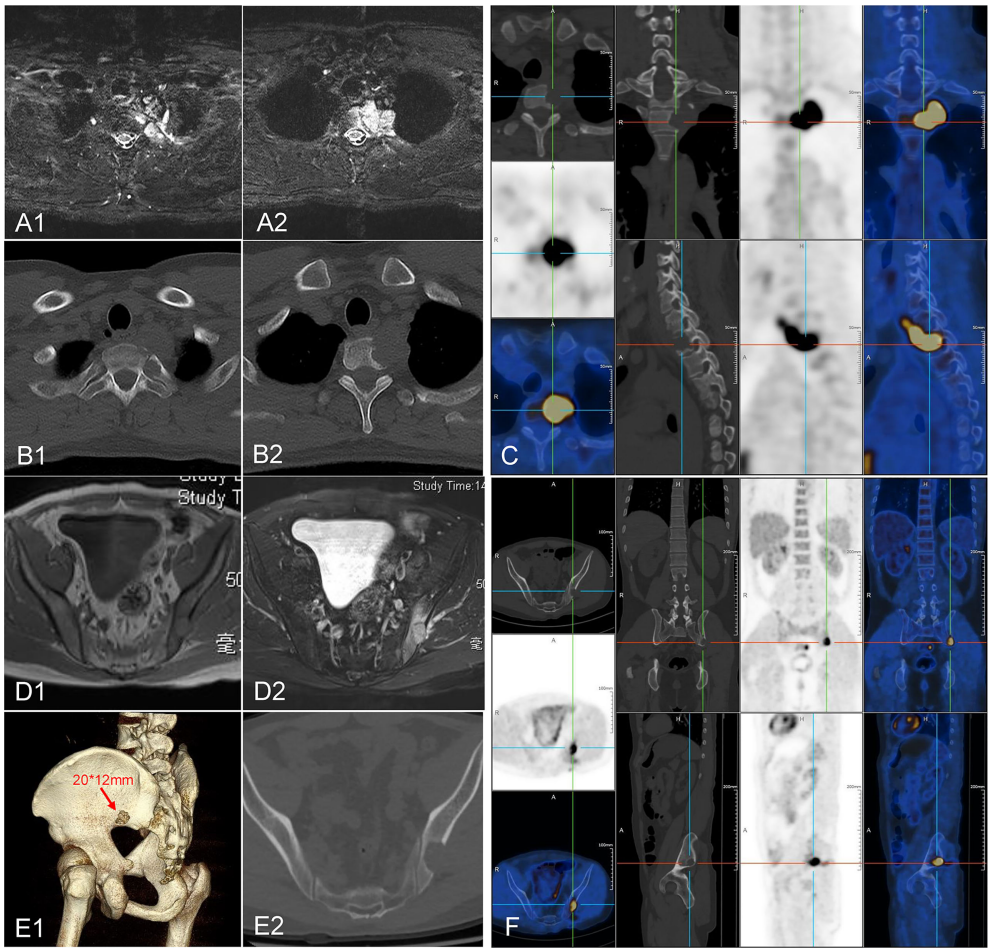

FIGURE 1
Image of the neoplastic lesions. **(A–C)** Neoplastic lesions found on the left side of C7-T2 invading the vertebrae body of T1, T2, and caput costae of the second rib. **(D–F)** A suspected metastasis was found in the left ilium.

gamma knife treatment planning system. A local bone destruction lesion was found at the posterior lower edge of the left ilium (near the sacroiliac joint) with clear boundaries and soft tissue density. The treatment target area was determined in the bone window on the CT image using the body gamma knife treatment planning system (window width, 1,000 HU; window level, 300 HU). The gross target volume (GTV) was delineated according to the lesion identified in the bone window. The clinical target volume (CTV) was generated by extending the GTV by 5 mm in all directions. The planning target volume (PTV) was generated by extending the CTV by 5 mm in all directions. The 50% radiation dose covered 100% of the PTV, the 60% dose covered 100% of the CTV, and the 70% dose covered 100% of the GTV. For the iliac lesion, the prescription dose for the PTV, CTV, and GTV margins were 40, 48, and 56 Gy in 10 fractions, respectively. The highest physical dose delivered at the center of the target area was 80 Gy. The biological effective dose (BED) of the RT was calculated using a linear quadratic (LQ) model, assuming an α/β ratio of 10. The BEDs at the margins of PTV, CTV, and GTV were 56, 71.04, and 87.36 Gy, respectively, and the highest BED delivered at the center of the target area was 144 Gy. For the thoracic lesion, the prescription doses for PTV, CTV, and GTV margins were 36, 43.2, and 50.4 Gy in 12 fractions, respectively. The highest physical dose delivered at the center of the target area was 72 Gy. The BEDs delivered to the margins of the PTV, CTV, and GTV were 46.8, 58.752, and 71.568 Gy, respectively, and the highest BED delivered at the center of the target area was 115.2 Gy. Radiotherapy target planning of thoracic and iliac lesions was presented in Supplementary Figures 1, 2. The treatment process proceeded smoothly, the patient had no complaints, and no abnormal findings were found on blood tests after RT.

The patient did not receive systemic treatment or other local control treatments after the body gamma knife treatment. CT examination of the iliac bone showed that the lesion size was slightly larger than that before the 2-month postoperative

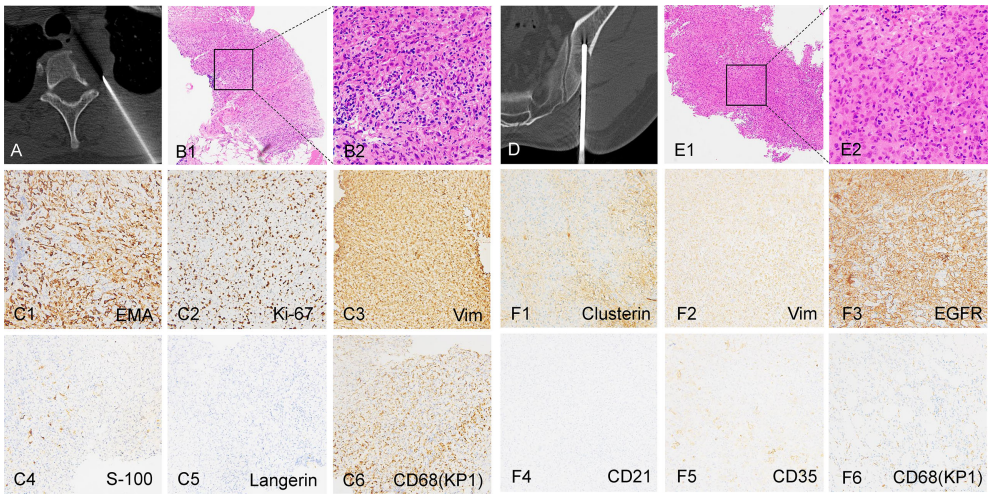

FIGURE 2
Biopsy and staining images of the tumors. **(A, B)** CT-guided core needle biopsy and the H&E staining images of the thoracic lesion. (C1-C6) Immunohistochemical staining of the thoracic lesion. **(D, E)** CT-guided core needle biopsy and the H&E staining images of the left ilium lesion. (F1-F6) Immunohistochemical staining of the left ilium lesion. B1, E1: 100×; B2, E2: 400×; **(C, F)**: 200×.

follow-up (Figures 3B1–3). Thus, iliac bone lesion resection was performed 10 weeks after RT. The pathological examination of the left iliac bone tumor suggested a small amount of bone tissue, fibrous tissue hyperplasia and hemorrhage, myofibroblast reaction, lymphocyte and plasma cell infiltration, a small amount of necrosis, and tissue cell deposition, while no tumor tissue was observed (Figures 3C1, 2). Thus, the body gamma knife treatment resulted in PCR. The patient was followed up for 1 year, and the VAS score for back pain reduced from 8 at preoperatively to 1 at the last follow-up. Thoracic and pelvic magnetic resonance imaging (MRI) examinations showed no significant enlargement or recurrence of the tumors after 15 months of follow-up (Figures 3D, E). The timeline of major clinical events during treatment and follow-up is shown in Figure 4.

Discussion

FDCS is a type of intermediate grade tumors originating from follicular dendritic cells in the germinal center of lymph nodes. It was first reported by Monda et al. (1) in 1986. The biological behavior of FDCS is similar to that of intermediate-grade soft-tissue sarcomas. The head, neck, and mediastinal FDCS cases have good prognosis, whereas a minority of cases develop local recurrence (12.5%–28.1%) and metastases (13.2%–27.2%) (7, 14, 15). The most common metastatic sites are the lung and liver; other metastatic sites include the adrenal gland, rib, vertebral body, and iliac bone (14). Metastasis of the iliac bone was observed in the present case. The reported age of onset is 9–79 years (average: 46 years) (14). FDCS tends to grow slowly and is usually asymptomatic (16). The lesions usually are hypermetabolic and present as avid spots on positron emission tomography (PET) images (3, 17). There is a subtype of FDCS that almost exclusively occurs in the liver and spleen. It is different from the FDCS that occurs in other parts. The World Health Organization (WHO) has recognized a distinct entity named inflammatory pseudotumor (IPT) like FDCS (18). It is speculated that IPT like FDCS is related to the Epstein–Barr virus (EBV) infection and is more common in women (19). The immunohistochemical results support the diagnosis of FDCS to a large extent. Normal FDC-associated markers, such as CD21, CD23, CD35, and CXCL13, are widely used. Multiple markers are often used owing to the frequent loss of antigens (20, 21). Clusterin is a sensitive and specific marker for FDCS (22). In addition, vimentin, EGFR, EMA, S-100, and CD68 were used to confirm the diagnosis (20). Immunohistochemical staining was not typical in the present case. CD35 was slightly positive and CD21 was negative. Morphologically, the nuclei appeared to be short fusiform to oval, some of the nuclei showed vacuolar-like changes, some showed small nucleoli, the cytoplasm was lightly stained, and the interstitium was scattered with lymphocytic infiltration. Based on the morphological and immunohistochemical findings, the diagnosis of FDCS was made.

To date, there is no standard therapeutic protocol for FDCS, and different approaches have been applied, including surgery, radiotherapy, and chemotherapy. Surgical resection is the primary treatment for FDCS, and the incidence of recurrence is relatively high (23). Although adjuvant radiotherapy or systemic therapy has not caused a significant improvement in

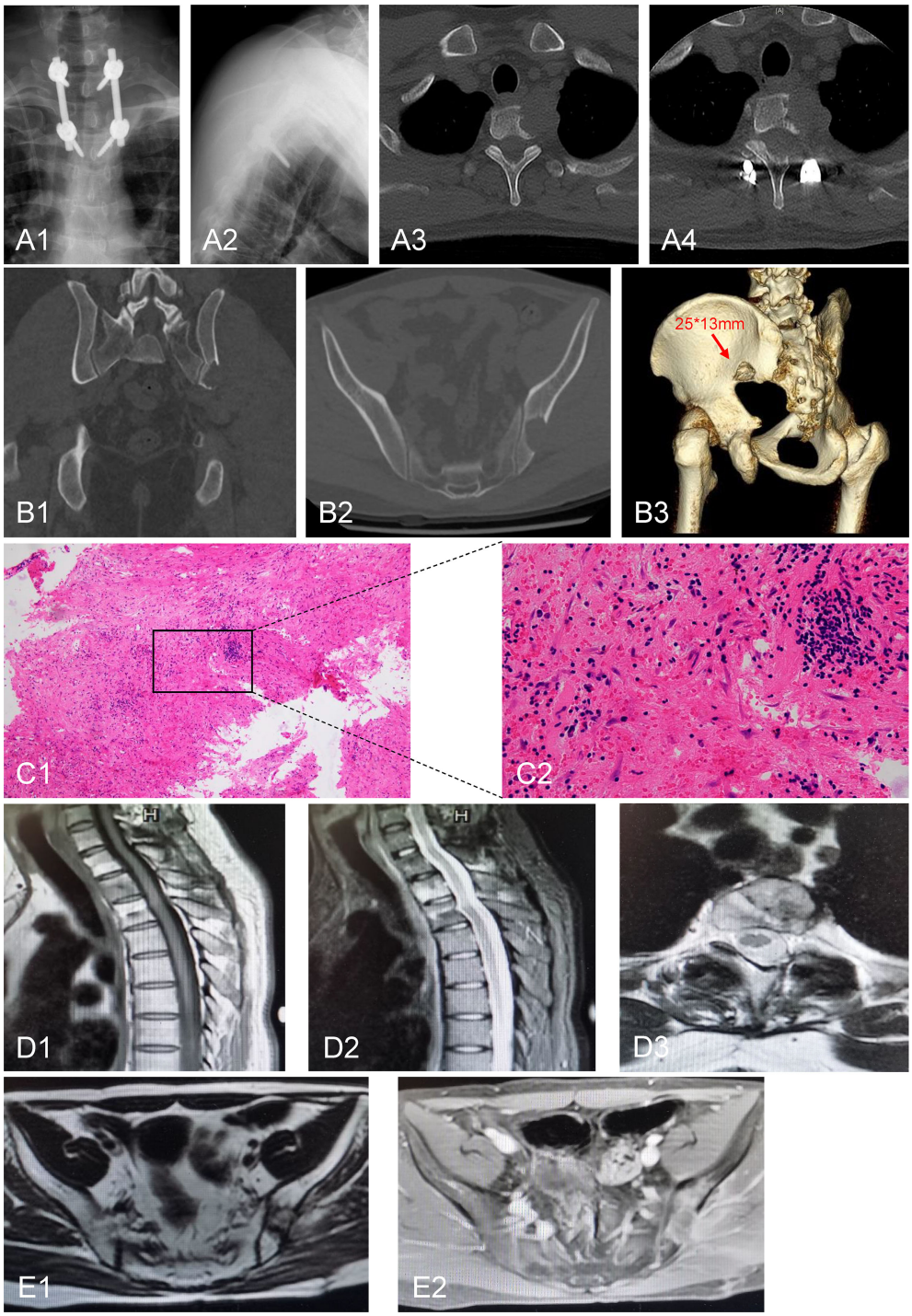

FIGURE 3
Postoperative radiological and pathological images. **(A1, 2)** Pedicle screw internal fixation was performed at the level of T1-T3. **(A3, 4)** Postoperative CT scan showed that the left lamina and the facet joint of T1 and T2 were resected. **(B1-3)** CT examination of the iliac bone showed that the lesion size was slightly larger than that before the 2-month postoperative follow-up. **(C1, 2)** H&E staining of iliac bone lesion. **(D1-3)** Thoracic MRI examination showed no significant enlargement of the lesion after 15 months of follow-up. **(E1, 2)** Pelvic MRI examination showed absence of recurrence of the iliac lesion after 15 months of follow-up. C1: 100×; C2: 400×.

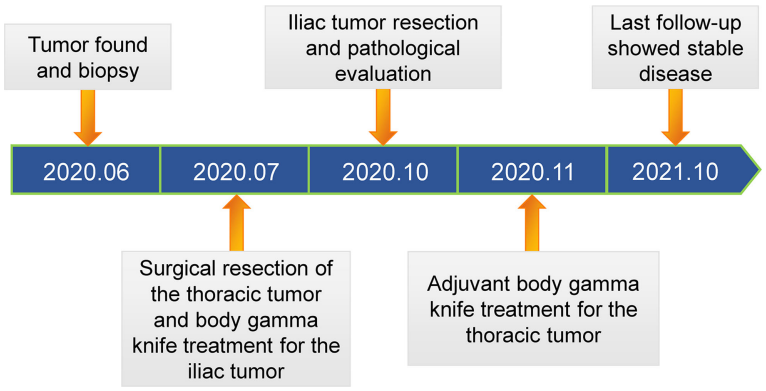

FIGURE 4
Timeline of the occurrence of major clinical events during the treatment and follow-up.

survival (24), it can be applied in patients with advanced cases (7). Patients with extranodal disease experience poor outcomes and often require combined therapy (5). Conry and Gupta reported cases in which gemcitabine and docetaxel were used as treatment for metastatic FDCS, which showed promising outcomes (25, 26). FDCS also responded to some commonly used targeted agents and immune checkpoint inhibitors. Several FDCS case reports have shown that patients may benefit from kinase inhibitors, including pazopanib, sorafenib, and sirolimus (6, 9). The programmed cell death protein 1 (PD-1) antibody is a potential therapeutic option for patients with refractory FDCS (8, 27). Localized tumors are associated with better prognosis (6). Young age, large tumor size, high mitotic index, abdominal involvement, coagulative necrosis, and significant cellular atypia were associated with poor prognosis (7).

Considering that adjuvant radiotherapy and/or chemotherapy are often used for advanced FDCS, we introduced the concept of hybrid therapy in the treatment of this patient. Hybrid therapy consists of separation surgery and postoperative SBRT, which represents the evolution of treatment for spinal metastases (28). Separation surgery focuses on decompressing the spinal cord or nerves to achieve a safe margin for RT. This was an innovative attempt to this patient. Residual paraspinal tumors can be effectively treated with SBRT. SBRT involves the delivery of a high radiation dose within a shorter course, has obvious radiobiological advantages, lessens the risk of damage to the surrounding organs, and has less complications (29). Body gamma knife SBRT can be applied in a wide range of conditions and is widely used in China. It delivers a high radiation dose to the tumor focus and skin and generates an effect similar to that of scalpel resection, which is suitable for the treatment of patients in different positions. This highly focused SBRT technique has demonstrated satisfactory local control, reduced toxicity, and cost effectiveness in the treatment of non-small cell lung cancer (10, 30). Other initiatives have been carried out to explore the efficacy of the body gamma knife in other malignancies, such as pancreatic cancer (12). In this case, the 50% dose line was used as the prescribed dose line. The unique dose distribution and treatment pattern escalate the focused dose administered to the target area, that is, from the margin to the center, while the normal tissue outside the margin receives an extremely low dose, which is reasonable in radiobiology. Cao et al. (11) reported the dose distributions of five stereotactic body radiotherapies for pancreatic cancer. Gamma knife provided the highest mean and maximum dose to the PTV, excellent gradient index, and rapid dose fall-off. In addition, the body gamma knife is less expensive compared with other SBRT technologies, which is appealing especially in developing and underdeveloped countries (10). This patient did not receive adjuvant chemotherapy or targeted therapy. This is partly because there is no consensus on the optimal treatment recommendations for FDCS. On the other hand, adjuvant systemic therapy was not associated with improvement in the median or 5-year overall survival (OS) when compared to surgery alone (3, 6). In addition, performing the separation surgery has helped us to accumulate relatively more experience in SBRT, and thoracic and pelvic MRI showed stable disease after 15 months of follow-up. Based on the above considerations, this patient was treated with RT as adjuvant therapy for the thoracic lesion and as the primary treatment for the iliac metastasis. Values of α/β ratios in human individuals are rarely known, and there is no predictive assay for α/β for individual tumors. The use of $\alpha/\beta = 5$, 10 and 15 Gy was recommended in most situations (31). An α/β ratio of 10 was applied in the calculation of BED in the present study.

In most cases, the effectiveness of RT is assessed though clinical evaluation, such as imaging and OS assessment, other than the gold standard histopathological examination. Biopsies may be used in a few cases to verify the treatment effect. A reliable pathological evaluation of malignant tumors of the body

after gamma knife treatment has not yet been reported. In this case, mild edema was found in the target area, which was slightly enlarged on CT imaging at 2 months' follow-up. Although this may be a reaction after RT, resection was performed as requested by the patient, and the whole tissue was obtained for evaluation. Pathological diagnoses before and after treatment were performed at the same hospital. After careful consultation with skilled experts, the consistency and authority of the diagnosis were ensured. This unique case showed that body gamma knife treatment can achieve not only CR but also PCR.

Some limitations of the body gamma knife should be recognized and improved. This procedure is insufficient in image guidance and localization for repeated patient positioning and the assessment for radiation dose assessment of the target area. The rapid development of medical imaging technique in recent years has enhanced the precision and efficiency of the body gamma knife.

Conclusion

This case report describes the treatment of mediastinal FDCS with thoracic spinal invasion and iliac metastasis. The promising outcome suggests that separation surgery is an effective treatment option for mediastinal FDCS with spinal column invasion. It also demonstrates the application prospects of the body gamma knife treatment in malignant lesions of the axial bones.

Data availability statement

The original contributions presented in the study are included in the article/Supplementary Material. Further inquiries can be directed to the corresponding authors.

Ethics statement

This study was reviewed and approved by Ethics Committee of Zhongshan Hospital, Fudan University (CR2022-018). The patients/participants provided their written informed consent to participate in this study. Written informed consent was obtained from the individual(s) for the publication of any potentially identifiable images or data included in this article.

Author contributions

JD and TC treated the patient. AH wrote the manuscript. JD and TC reviewed the manuscript. All authors have contributed to the manuscript and approved the submitted version.

Funding

This study was supported by the National Natural Science Foundation of China (Grant Number: 81972508).

Conflict of interest

The authors declare that the research was conducted in the absence of any commercial or financial relationships that could be construed as a potential conflict of interest.

Publisher's note

Supplementary material

The Supplementary Material for this article can be found online at: https://www.frontiersin.org/articles/10.3389/fonc.2022.919644/full#supplementary-material

References

1. Monda L, Warnke R, Rosai J. A primary lymph node malignancy with features suggestive of dendritic reticulum cell differentiation. A report of 4 cases. *Am J Pathol* (1986) 122(3):562–72.

2. Chen T, Gopal P. Follicular dendritic cell sarcoma. *Arch Pathol Lab Med* (2017) 141(4):596–9. doi: 10.5858/arpa.2016-0126-RS

3. Pang J, Mydlarz WK, Gooi Z, Waters KM, Bishop J, Sciubba JJ, et al. Follicular dendritic cell sarcoma of the head and neck: Case report, literature review, and pooled analysis of 97 cases. *Head Neck* (2016) 38 Suppl 1:E2241–9. doi: 10.1002/hed.24115

4. Kaur R, Mehta J, Borges A. Extranodal follicular dendritic cell sarcoma-a review: "What the mind does not know the eye does not see". *Adv Anat Pathol* (2021) 28(1):21–9. doi: 10.1097/PAP.0000000000000281

5. Jain P, Milgrom SA, Patel KP, Nastoupil L, Fayad L, Wang M, et al. Characteristics, management, and outcomes of patients with follicular dendritic cell sarcoma. *Br J Haematol* (2017) 178(3):403–12. doi: 10.1111/bjh.14672

6. Gounder M, Desai V, Kuk D, Agaram N, Arcila M, Durham B, et al. Impact of surgery, radiation and systemic therapy on the outcomes of patients with dendritic

cell and histiocytic sarcomas. *Eur J Cancer* (2015) 51(16):2413–22. doi: 10.1016/j.ejca.2015.06.109

7. Saygin C, Uzunaslan D, Ozguroglu M, Senocak M, Tuzuner N. Dendritic cell sarcoma: A pooled analysis including 462 cases with presentation of our case series. *Crit Rev Oncol Hematol* (2013) 88(2):253–71. doi: 10.1016/j.critrevonc.2013.05.006

8. Lee MY, Bernabe-Ramirez C, Ramirez DC, Maki RG. Follicular dendritic cell sarcoma and its response to immune checkpoint inhibitors nivolumab and ipilimumab. *BMJ Case Rep* (2020) 13(4):e234363. doi: 10.1136/bcr-2020-234363

9. Shah P, Shah S, Agostino N. Disease response to pazopanib in follicular dendritic cell sarcoma. *Case Rep Oncol* (2020) 13(3):1131–5. doi: 10.1159/000509771

10. Li H, Li J, Wang X, Pang H, Di Y, Ren G, et al. Promising clinical outcome with long term follow-up after body gamma knife stereotactic radiosurgery for patients with early stage non-small cell lung cancer. *Front Oncol* (2018) 8:618. doi: 10.3389/fonc.2018.00618

11. Cao Y, Zhang J, Li T, Qiu J, Zhang L, Zhuang Y, et al. Comparison of dose distributions among five radiotherapy apparatuses in stereotactic body radiation therapy for pancreatic cancer. *Chin J Radiat Oncol* (2021) 30(2):156–63. doi: 10.3760/cma.j.cn113030-20190606-00214

12. Wei J, Dong X, Du F, Tang S, Wei H. Successful gamma knife radiosurgery combined with s-1 in an elderly man with local recurrent pancreatic cancer: A case report. *Med (Baltimore)* (2017) 96(51):e9338. doi: 10.1097/MD.0000000000009338

13. Yu W, Tang L, Lin F, Li D, Wang J, Yang Y, et al. Stereotactic radiosurgery, a potential alternative treatment for pulmonary metastases from osteosarcoma. *Int J Oncol* (2014) 44(4):1091–8. doi: 10.3892/ijo.2014.2295

14. Li J, Zhou ML, Zhou SH. Clinical and pathological features of head and neck follicular dendritic cell sarcoma. *Hematology* (2015) 20(10):571–83. doi: 10.1179/1607845415Y.0000000008

15. Wu YL, Wu F, Xu CP, Chen GL, Zhang Y, Chen W, et al. Mediastinal follicular dendritic cell sarcoma: A rare, potentially under-recognized, and often misdiagnosed disease. *Diagn Pathol* (2019) 14(1):5. doi: 10.1186/s13000-019-0779-3

16. Lopez-Hisijos N, Omman R, Pambuccian S, Mirza K. Follicular dendritic cell sarcoma or not? a series of 5 diagnostically challenging cases. *Clin Med Insights Oncol* (2019) 13:2013427021. doi: 10.1177/1179554919844531

17. Ang WW, Bundele MM, Shelat VG. Follicular dendritic cell sarcoma: Rare presentation of incidental large hepatic mass. *Ann Hepatobiliary Pancreat Surg* (2019) 23(1):74–6. doi: 10.14701/ahbps.2019.23.1.74

18. Sabattini E, Bacci F, Sagramoso C, Pileri SA. WHO classification of tumours of haematopoietic and lymphoid tissues in 2008: An overview. *Pathologica* (2010) 102(3):83–7.

19. Bai LY, Kwang WK, Chiang IP, Chen PM. Follicular dendritic cell tumor of the liver associated with Epstein-Barr virus. *Jpn J Clin Oncol* (2006) 36(4):249–53. doi: 10.1093/jjco/hyl001

20. Chan JK, Fletcher CD, Nayler SJ, Cooper K. Follicular dendritic cell sarcoma. Clinicopathologic analysis of 17 cases suggesting a malignant potential higher than currently recognized. *Cancer-Am Cancer Soc* (1997) 79(2):294–313.

21. Vermi W, Lonardi S, Bosisio D, Uguccioni M, Danelon G, Pileri S, et al. Identification of CXCL13 as a new marker for follicular dendritic cell sarcoma. *J Pathol* (2008) 216(3):356–64. doi: 10.1002/path.2420

22. Grogg KL, Macon WR, Kurtin PJ, Nascimento AG. A survey of clusterin and fascin expression in sarcomas and spindle cell neoplasms: Strong clusterin immunostaining is highly specific for follicular dendritic cell tumor. *Mod Pathol* (2005) 18(2):260–6. doi: 10.1038/modpathol.3800294

23. De Pas T, Spitaleri G, Pruneri G, Curigliano G, Noberasco C, Luini A, et al. Dendritic cell sarcoma: An analytic overview of the literature and presentation of original five cases. *Crit Rev Oncol Hematol* (2008) 65(1):1–7. doi: 10.1016/j.critrevonc.2007.06.003

24. Facchetti F, Lorenzi L. Follicular dendritic cells and related sarcoma. *Semin Diagn Pathol* (2016) 33(5):262–76. doi: 10.1053/j.semdp.2016.05.002

25. Conry RM. Response of follicular dendritic cell sarcoma to gemcitabine and docetaxel: report of two cases and literature review. *Clin Sarcoma Res* (2014) 4:6. doi: 10.1186/2045-3329-4-6

26. Gupta AM, Goel M, Sahay A, Janjal SP, Patkar S. Role of adjuvant chemotherapy in extranodal follicular dendritic cell sarcoma. *ACG Case Rep J* (2019) 6(3):1–4. doi: 10.14309/crj.0000000000000008

27. Lei Y, Zhao S, Jiang M. Unexpected favorable outcome to PD-1 antibody plus lenvatinib in a patient with recurrent intestinal follicular dendritic cell sarcoma: A case report and literature review. *Front Immunol* (2021) 12:653319. doi: 10.3389/fimmu.2021.653319

28. Rothrock R, Pennington Z, Ehresman J, Bilsky MH, Barzilai O, Szerlip NJ, et al. Hybrid therapy for spinal metastases. *Neurosurg Clin N Am* (2020) 31(2):191–200. doi: 10.1016/j.nec.2019.11.001

29. Jaffray DA. Image-guided radiotherapy: From current concept to future perspectives. *Nat Rev Clin Oncol* (2012) 9(12):688–99. doi: 10.1038/nrclinonc.2012.194

30. Xia T, Li H, Sun Q, Wang Y, Fan N, Yu Y, et al. Promising clinical outcome of stereotactic body radiation therapy for patients with inoperable stage I/II non-small-cell lung cancer. *Int J Radiat Oncol Biol Phys* (2006) 66(1):117–25. doi: 10.1016/j.ijrobp.2006.04.013

31. Jones B, Dale RG, Deehan C, Hopkins KI, Morgan DA. The role of biologically effective dose (BED) in clinical oncology. *Clin Oncol (R Coll Radiol)* (2001) 13(2):71–81. doi: 10.1053/clon.2001.9221

frontiers | Frontiers in Oncology

TYPE Original Research
PUBLISHED 30 September 2022
DOI 10.3389/fonc.2022.986123

OPEN ACCESS

EDITED BY
Ianik Plante,
KBRwyle, United States

REVIEWED BY
Luigi Corti,
Abano Terme Hospital, Italy
Angel Montero,
HM Madrid Hospital, Spain

*CORRESPONDENCE
Sabino Russi
sabino.russi@crob.it

†These authors have contributed equally to this work and share first authorship

SPECIALTY SECTION
This article was submitted to Radiation Oncology, a section of the journal Frontiers in Oncology

RECEIVED 04 July 2022
ACCEPTED 09 September 2022
PUBLISHED 30 September 2022

CITATION
Laurino S, Omer LC, Albano F, Marino G, Bianculli A, Solazzo AP, Sgambato A, Falco G, Russi S and Bochicchio AM (2022) Radiation-induced sarcomas: A single referral cancer center experience and literature review.
Front. Oncol. 12:986123.
doi: 10.3389/fonc.2022.986123

Radiation-induced sarcomas: A single referral cancer center experience and literature review

Simona Laurino[1†], Ludmila Carmen Omer[2†], Francesco Albano[1], Graziella Marino[3], Antonella Bianculli[4], Angela Pia Solazzo[4], Alessandro Sgambato[1], Geppino Falco[5], Sabino Russi[1*] and Anna Maria Bochicchio[6]

[1]Laboratory of Preclinical and Translational Research, Istituto di Ricovero e Cura a Carattere Scientifico (IRCCS) CROB Centro di Riferimento Oncologico della Basilicata, Rionero in Vulture, Italy, [2]Trial Office, Istituto di Ricovero e Cura a Carattere Scientifico (IRCCS) CROB Centro di Riferimento Oncologico della Basilicata, Rionero in Vulture, Italy, [3]Department of Breast Surgery, Istituto di Ricovero e Cura a Carattere Scientifico (IRCCS) CROB Centro di Riferimento Oncologico della Basilicata, Rionero in Vulture, Italy, [4]Radiotherapy Unit, Istituto di Ricovero e Cura a Carattere Scientifico (IRCCS) CROB Centro di Riferimento Oncologico della Basilicata, Rionero in Vulture, Italy, [5]Department of Biology, University of Naples Federico II, Naples, Italy, [6]Multispecialty Tumor Board, Istituto di Ricovero e Cura a Carattere Scientifico (IRCCS) CROB Centro di Riferimento Oncologico della Basilicata, Rionero in Vulture, Italy

Background and objective: The oncogenic effect of ionizing radiation is widely known. Sarcomas developing after radiation therapy (RT), termed "iatrogenic disease of success", represent a growing problem, since the advancements in cancer management and screening programs have increased the number of long-term cancer survivors. Although many patients have been treated with radiation therapy, only few data are available on radiation-induced sarcomas (RIS).

Methods: We examined the medical and radiological records of 186 patients with histologically proven soft tissue and bone sarcomas, which referred to IRCCS CROB Centro di Riferimento Oncologico della Basilicata from January 2009 to May 2022. Among them, seven patients received a histological diagnosis of secondary RIS, according to Cahan's criteria. Clinicopathological features and treatment follow-up data of RIS patients were retrospectively analyzed.

Results: Among these secondary RIS, five arose in irradiated breast cancer (5/2,570, 0.19%) and two in irradiated head and neck cancer (2/1,986, 0.10%) patients, with a mean onset latency time of 7.3 years. The histology of RIS was one desmoid tumor, two angiosarcomas, one chondrosarcoma, two leiomyosarcomas, and one undifferentiated pleomorphic sarcoma. Out of the seven RIS, one received radiotherapy, one received electrochemotherapy (ECT), one received a second-line chemotherapy, three were subjected to three lines of chemotherapy, and one underwent radiofrequency ablation, chemotherapy, and ECT. Median survival time is 36 months. No significant survival differences were found stratifying patients for age at RT, latency time, and age at RIS diagnosis.

Conclusions: RIS represents a possible complication for long-survivor cancer patients. Therefore, adherence to a strict follow-up after the radiation treatment is recommended to allow early diagnosis and optimal management of RIS patients. After the planned follow-up period, considering the long-term risk to develop a RIS, a specific multispecialty survivorship care plan could be of benefit for patients.

KEYWORDS

breast cancer, head and neck cancer, radiation-induced sarcoma, radiotherapy, long-term radiation effects

Introduction

Radiation therapy (RT) represents the main treatment strategy for more than half of cancer patients (1–3), since it entails improvement of the survival rates and long-term overall survival in many types of cancer. Therefore, the employment of this treatment option is growing. Indeed, as an example, a Korean study reported a 65% increase in cancer patients who underwent RT from 2006 to 2013 (4). Despite these undoubted benefits, RT is found to be associated with the onset of a rare iatrogenic malignancy, known as "radiation-induced sarcoma" (RIS), which represents about 3% of all soft tissue sarcomas (5). This adverse event is characterized by poor 5-year overall survival, ranging from 10% to 36% in relation to disease stage at diagnosis (1). Therefore, RIS is considered an arduous challenge for physicians. It also represents a growing clinical problem, likely associated with the increasing number of long-term cancer survivors determined by the advancements in cancer screening programs and patient management (6, 7).

The first cases of sarcoma following RT were observed in 1922 by Beck and Marsch in patients irradiated to treat tuberculous bone disease (8, 9). Subsequently, in 1936, Warren and Sommer described complications after irradiation of breast carcinoma in 81 patients (9). In 1948, based on 11 cases of post-radiation osteosarcoma (PRS), Cahan and Woodard defined the following criteria for RIS diagnosis (10):

a) No evidence of the new tumor at RT time;
b) Sarcoma arises in the irradiated field;
c) Relatively long latency period before sarcoma onset; and
d) Histologically proven sarcoma.

A large analysis of the Surveillance, Epidemiology, and End Results (SEER) registries found a 257% increased risk of secondary bone sarcoma in patients who received radiotherapy compared to the general population (11). Recently, these data were examined by Snow et al., who reported that, after cervical cancer, breast cancer has the highest risk of RIS (88.2% and 78.3%, respectively) (12). RIS after breast cancer RT shows a wide range of histopathologic subtypes, among which malignant fibrous histiocytoma is the most common. Less frequent findings include leiomyosarcoma, liposarcoma, fibrosarcoma, and angiosarcoma, and rarely chondrosarcoma and osteosarcoma. These secondary RIS are usually high-grade tumors variable in size, whose histological features include presence of spindle-shaped tumor cells, hemorrhagic tumor nodules, abundant mitotic figures, and necrosis (13).

RIS of the head and neck also represents a relevant problem since, although rare, they are a lethal consequence of RT. Its average frequency was about 0.15% with a mean latency period, the interval between RT on the primary lesion and the onset of secondary sarcoma, of about 11 years. Histologically, RIS of the head and neck are mainly ascribable to osteosarcoma and fibrosarcoma (14).

Here, we performed a retrospective study on patients' records to investigate the clinical and pathological features of RIS cases that accessed IRCCS CROB Centro di Riferimento Oncologico della Basilicata from 2009 to 2022.

Materials and methods

Patient cohort and data collection

We examined the medical record of all histologically diagnosed sarcoma in patients managed from 2009 to 2022, included in both the Basilicata Cancer Registry and the Institutional Electronic Health Dossier. The latter also comprises patients from nearby regions. All data were retrieved from patients who gave their informed consent at the first access or afterwards on request.

Overall, there were 186 cases (85 male and 101 female patients) of sarcomas with a mean age of 59.7 years (range: 15–91 years). At the time of writing (June 2022), patients are followed up in an outpatient setting. The mean time of follow-up

is 58.5 months (range: 0.6–380.7 months). Their geographical origin is mainly Basilicata (121), Campania (38), and Puglia (16) (Table 1).

Diagnosis and treatments

The first diagnosis was made at CROB for 116 patients. Seventy-two patients underwent radical surgical excision. Metastases were detected in 74 patients through total body computed tomography (CT) examination at first diagnosis, whereas in 73 cases, new metastatic lesions appeared during follow-up. All patients were treated at our center, except one osteosarcoma patient who was managed at Rizzoli Orthopedic Hospital in Bologna. Several treatment regimens were administered as summarized in Table 1. Ninety patients received chemotherapy, 33 of whom received only the first-line setting, 50 patients also received a second-line treatment schedule, and 29 patients received three chemotherapy lines. Notably, off-label and/or targeted therapy regimens were tried. One patient diagnosed with carcinosarcoma (MMMT) received FOLFIRI regimen. In three cases, olaratumab was the first-line treatment. One patient with a myofibroblastic inflammatory tumor of sclera-conjunctiva, positive for anaplastic lymphoma

TABLE 1 General characteristics and management information of the enrolled sarcoma patients.

Sarcoma patients (from 2009 to 2022)	***N* = 186**
On follow-up	52
Sex (M/F)	85/101
Age, mean (range)	59.7 (15–91)
Patient territorial distribution	
• **Basilicata**	121
• **Puglia**	16
• **Campania**	38
• **Other**	11
Center of diagnosis/surgery	
• **IRCCS CROB**	116
• **Other**	70
Metastasis at diagnosis (Yes/No)	74/112
Disease progression	73
Surgical excision	72
Chemotherapy	90
• **Neoadjuvant**	7
• **1st line**	83 (33 patients only one line)
• **2nd line**	50 (I+II)
• **3rd line**	29 (I+II+III)
• **4th line**	15 (I+II+III+IV)
• **5th line**	9 (I+II+II+IV+V)
• **6th line**	3 (I+II+II+IV+V+VI)
Eribulina	2
Olaratumab	3
Crizotinib	1
Imatinib (Cordoma)	1
FOLFIRI/FUFA (carcinosarcoma-MMMT)	1
Pomalidomide (Kaposi sarcoma)	1
Protocol ISG/SSG (Ewing sarcoma)	1
Proton therapy	1
Autologous transplant	1
Brachytherapy	2
Electrochemotherapy	13
Radiotherapy	40
Palliative	6
Adjuvant	34
Months of follow-up, mean (range)	58.5 (0.6–380.7)

kinase mutation (ALK+), was treated with crizotinib. One patient received imatinib to treat cordoma.

Among the 186 patients, 40 patients received external radiotherapy, 2 cases received brachytherapy, and for 13 patients, electrochemotherapy was employed as local therapy.

Selection criteria of radiation-induced sarcoma

Criteria by Cahan et al. were used to identify RIS patients (10). For further evaluations, detailed epidemiological, clinical, pathological, and treatment history and survival information were collected.

Statistical analysis

The association of patients' overall survival with age at RT, at RIS, or latency time was estimated by log-rank test, after categorization of time in classes and using the *survminer* R package (15). In a similar way, association between RIS risk and age at RT, based on latency time, was explored. Survival curves were then plotted using the Kaplan–Meier method. Hazard ratios were also estimated for each variable by Cox proportional hazards regression model included in the *survival* package (16).

Results

Among 186 sarcoma patients, we identified seven (3.8%) cases fulfilling Cahan's criteria. In particular, five RIS arose in the irradiated field of breast cancer patients and two in that of head and neck cancer patients. To better define RIS incidence, we retrospectively analyzed all breast and head and neck primary tumors that underwent radiation therapy. Overall, we found 0.15% (7/4,556) of RIS incidence, in which breast cancer accounts for 0.19% (5/2,570), whereas head and neck cancer accounts for 0.10% (2/1,986). Histological evaluation of RIS found one desmoid tumor, two angiosarcomas, one chondrosarcoma, two leiomyosarcomas, and one undifferentiated pleomorphic sarcoma (Table 2). Out of the seven RIS patients, one received radiotherapy, one was treated with electrochemotherapy (ECT), one received a second-line chemotherapy, three underwent three lines of chemotherapy, and one was treated with radiofrequency ablation, chemotherapy, and ECT.

Mean latency time was 7.3 years, ranging from 2 to 14 years. The overall median survival is 36 months (Figure 1A). No significant survival differences, likely due to the limited number of RIS cases, were found by stratifying patients for age at RT (36 *vs.* 28 months, ≤60 *vs.* >60 years), latency time (32 *vs.* 45 months, ≤7 *vs.* >7 years), and age at RIS occurrence (32.0 *vs.* 30.5 months, ≤67 *vs.* >67 years) (Figures 1B–D). Cox hazard ratio analysis also did not show any association with these variables (Figure 1E). Similarly, RIS risk and latency time are not associated with age at RT (7 *vs.* 8 years, ≤60 *vs.* >60 years, respectively) (Figure 1F). A detailed case presentation of clinical and pathological findings, including treatments administered and outcomes, is reported below.

Case 1

A 40-year-old man, in July 2014, had a diagnosis of primary epidermoid carcinoma in the right vocal cord and left lung, stage pT4aN2cM0 and grade G3. In January 2015, both masses were radically excised after neoadjuvant radiotherapy with 66 Gy in 33 fractions on intensity-modulated radiation therapy (IMRT) mode. The patient was free of disease for 15 months until, in March 2016, he received a diagnosis of desmoid tumor in the nuchal area, external to the hot spot of the previously irradiated field. Histological evaluation on a core biopsy described a group of spindle cells included in a collagen matrix arranged as parallel fibers; less than 1/10 HPF (high-power field) mitoses were detected, leading to a diagnosis of extra-abdominal fibromatosis-desmoid tumor. Immunohistochemical staining highlighted cells positive for desmine, SMA (smooth muscle actin), negative for S100, and a Ki67 index of 4%. Angio- and neural invasion was also depicted. After case evaluation by the Institutional Multidisciplinary Tumor Board and its discussion with experts from a rare tumor Comprehensive Cancer Center, the case was considered unsuitable for surgical excision due to the presence of a locally advanced disease infiltrating vascular and nervous structures. The patient was asymptomatic and, considering the poor chemosensitivity of desmoid tumors, he entered on a follow-up care program. In April 2018, due to lesion size increase and localized pain, the patient started a chemotherapy regimen with a combination of two oral drugs, vinorelbine and methotrexate, for 15 weekly cycles. After four months of treatment, due to clinical and radiological disease progression (DP), the patient was treated with second-line chemotherapy consisting of six cycles of a 3-week doxorubicin and dacarbazine regimen. In January 2019, at disease status assessment, the patient had a partial response (PR) and then was addressed to follow-up (every 3 months for the first 2 years, and then every 6 months). At the last follow-up (September 2021), according to RECIST criteria, a further reduction of tumor size was noticed.

Case 2

The patient is a 46-year-old woman diagnosed in 2006 with nasopharyngeal carcinoma. She was treated with radiotherapy

TABLE 2 Histological features, therapeutic management, and follow-up information of radiation-induced sarcomas.

PN	Gender	Primary cancer TNM	Radiotherapy mode/dose	CCRT	Age at RT	Age at RIS	Latency (years)	Location of RIS	Pathology subtypes	Treatment of RIS	Resection Result	Outcome
1	M	pT4aN2cM0	IMRT/66 Gy	Y	40	42	2	Nuchal region	Desmoid tumor	CHT	N/A	AWD 08.09.2021 67 months
2	F	T2bN3	3D CRT/ 70 Gy	Y	46	53	7	Left sternocleidomastoid muscle	Leiomyosarcoma + pleomorphic areas	S + CHT	R0	DOD 23.08.2016 36 months
3	F	pT1N1(10/19) pT1N0	3D CRT photons/ 50 + 10 Gy	Y	63	75	12	Left breast	Chondrosarcoma	S + CHT	R0	DOD 28.09.2018 45 months
4	F	pT1cN0	3D CRT photons/ 50 Gy 3D CRT electrons 9 MeV/10 Gy	Y	75	77	2	Left scapulo-humeral	Leiomyosarcoma + undifferentiated high grade pleomorphic sarcoma	RT	R1	DOD 04.01.2014 16 months
5	F	pT1cN0	3D CRT photons/ 50 + 10 Gy	Y	61	67	6	Left breast	High grade angiosarcoma	ECT	N/A	DOD 29.10.2019 28 months
6	F	pT2N1(8/24)	3D CRT photons/ 50 + 10 Gy	Y	53	67	14	Left armpit + left thoracic wall	High-grade undifferentiated pleomorphic sarcoma (myofibroblastic sarcoma)	CHT	N/A	DOD 15.02.2021 5 months
7	F	pT1N1(1/18)	3D CRT photons/ 50 +10 Gy	Y	63	73	10	Left breast	High-grade angiosarcoma	Radiofrequency ablation + CHT + ECT	R0	AWD Last FU 01.03.2022 14 months

TNM stage according to the American Joint Committee of Cancer (AJCC) staging system (7th edition). PN, Patient number; M, Male; F, Female; CCRT, Concurrent Chemoradiotherapy; S + CHT, Surgery + Chemotherapy; RT, Radiotherapy, CHT, Chemotherapy; ECT, Electrochemotherapy; IMRT, Intensity-modulated radiotherapy; 3D CRT, three-dimensional conformal radiation therapy; DOD, Dead of disease; AWD, Alive with disease; N/A, not applicable.

10.3389/fonc.2022.986123

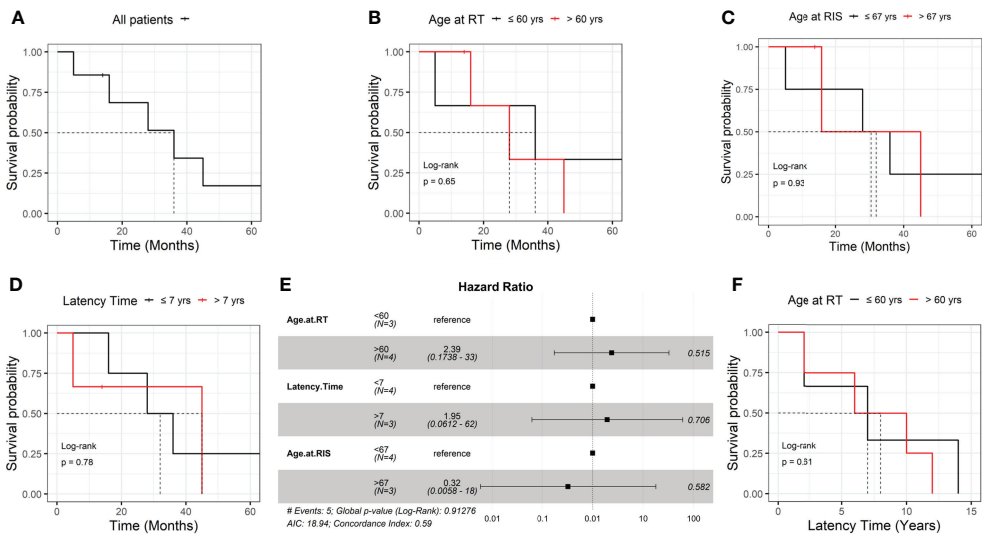

FIGURE 1
Association of radiation-induced sarcoma patients' overall survival with different parameters **(A–E)**. Association of radiation-induced sarcoma onset and age at radiation therapy **(F)**. RT, radiation therapy; RIS, radiation-induced sarcoma.

(70 Gy in 35 fractions) combined with weekly cisplatin infusions (five of six cycles regularly administered; the last cycle was suspended due to a suspect of cisplatin-induced grade 4 pancytopenia). The patient's clinical history included essential hypertension, hysterectomy for fibromyomas (in 1997), and family history of cancer (a 50-year-old brother with stage III colon cancer). A bilateral hypoacusis as a consequence of radiotherapy was recorded.

After 7 years (September 2013), during routine follow-up, clinical and radiological diagnosis of a mass on the left side of the neck (sternocleidomastoid muscle), referred to as RIS, was made. The patient underwent radical surgery of the left sternocleidomastoid muscle. Histology showed a high-grade mesenchymal neoplasia, consisting of atypical cellular elements, partly fused, with moderate-severe atypia and myogenic differentiation, partly round and oval, sometimes pleomorphic, arranged mostly in bundles and fascicles. Numerous mitotic figures and necrosis areas were observed (Grade 3). Immunohistochemical characterization showed positivity for vimentin, CD34, SMA, and negativity for CD30, CD68, CD31, desmin, and S100. Ki67 index was equal to 70%. Six months later, a local relapse was excised from the left anterior chest wall. After further 6 months, in December 2014, computed tomography (CT) scan showed multiple bilateral lung metastases and the patient received six cycles of first-line chemotherapy based on the combination of gemcitabine and docetaxel. During disease evaluation in April 2015, a strong DP with sternal relapse and pulmonary metastases accompanied by stable lymph nodes was noticed.

Starting from May 2015, six cycles of high-dose ifosfamide continuous infusion were administered as second-line chemotherapy. A minimal partial regression of disease was recorded under CT scan in January 2016. Three months later, an additional CT scan showed lung metastases progression, and dacarbazine, as third-line chemotherapy, was administered for three cycles. In August 2016, the patient was referred to the emergency room for stroke and she died. No necropsy was made and pulmonary embolism was assumed as the causal event.

Case 3

The case is a 63-year-old woman with a history of hormone-sensitive bilateral breast cancer (stage II) treated with a bilateral quadrantectomy and axillary lymph node dissection. The patient reported a family history of cancer, a brother and sister with gastric cancer, and a nephew with breast neoplasm.

The patient received a combination of adjuvant radiotherapy (50 Gy by photons in 25 fractions + 10 Gy by two 6-MeV tangential electrons beams in 5 fractions) and chemotherapy (epirubicin plus paclitaxel for four cycles and cyclophosphamide plus methotrexate plus fluorouracil for four cycles), hormone therapy with tamoxifen for 1 year, and anastrozole for 5 years to avoid endometrial hyperplasia.

After 11 years of follow-up, clinical examination of breast documented a mass in the residual of excised left breast and the patient was then subjected to left radical mastectomy. Histologically, it was referred to as poorly differentiated (G3)

metaplastic carcinoma of the breast with mesenchymal differentiation (MCMD), score 8 according to Elston and Ellis criteria. Areas of high-grade chondrosarcoma, which constitute 30% of the neoplasm, were present. Immunohistochemical characterization revealed positivity for Vimentin and S100, whereas tissue sections were negative for cytokeratin AE1/AE3 and 34beta E12, and p63. Tissue specimens were also estrogen receptor (ER) and progesterone receptor (PR) negative, and slightly positive for HER2. Ki67^{+} cells were 20%. No vascular and neural invasion were observed. TNM staging was rpT2pNx. After surgery, the patient entered a clinical and radiological follow-up program, as she refused adjuvant therapy. Nine months later, a follow-up chest x-ray showed multiple secondary lung lesions unsuitable for surgical excision. After a multispecialty evaluation, based on the absence of symptoms and the palliative intent of treatment, the patient underwent 3 days of ifosfamide continuous infusion; cycles were repeated every 3 weeks. After six cycles, the patient had partial response and she was asymptomatic during the subsequent follow-up period. Thirteen months later, a CT scan showed lung disease progression that required a systemic therapy consisting of 1,000 mg/mq gemcitabine on days 1 and 8, every 3 weeks. The patient did not improve after four cycles of treatment (June 2017). Since then, the patient chose a 1-month rest period from chemotherapy, until a further progression of lung lesions was documented. A third-line chemotherapy regimen, based on continuous infusion of high-dose ifosfamide, was administered for seven consecutive days over 14 days for eight cycles. In July 2018, pulmonary disease further progressed and, after 2 months, the patient died due to respiratory failure.

Case 4

A 75-year-old woman underwent right quadrantectomy surgery for a pT1cN0, estrogen receptor positive breast cancer. The patient was treated with CMF (cyclophosphamide plus methotrexate plus 5-fluorouracil) in an adjuvant chemotherapy setting and RT of the right breast (50 Gy by photons in 25 fractions + 10 Gy by single direct 9-MeV electron field in 5 fractions), followed by 5 years of anastrozole therapy. Two years later, during a follow-up visit, a left parascapular mass was noticed. Biopsy and radical excision showed moderately differentiated leiomyosarcoma (G2) showing giant cells with morphologically recognizable smooth muscle differentiation, histological grade 6 according to the French Federation of Cancer Centers Sarcoma Group, and pT2a according to TNM staging (7th ed.). Histologically, it was described as a malignant mesenchymal neoplasm composed of spindle cells with a marked cyto-nuclear atypia and eosinophilic poorly defined cytoplasm, organized in parallel bundles. The immunophenotypic profile was as follows: positive for vimentin, SMA, EMA (epithelial membrane antigen), and actin (clone HHF-35), and negative for CK-pan, Melan A, desmin, CD34, and S-100. The patient underwent post-surgery radiotherapy with 200 cGy for 30 fractions. After 14 months of follow-up, a local relapse in the left humerus-scapular region was observed and excised. Histological evaluation defined a high-grade pleomorphic sarcoma with skin ulcerative lesions, infiltrating subcutaneous tissue and showing vascular embolization. Due to the patient's poor general condition and comorbidities, she was not suitable for further systemic chemotherapy, and, after a period of palliative care, she died.

Case 5

The patient is a 61-year-old woman with a diagnosis of left breast infiltrating ductal carcinoma, pT1cN0, grade G2, ER 98%, PGR 20%, HER2+, who underwent quadrantectomy and axillary lymph node dissection followed by adjuvant chemotherapy, radiotherapy (50 Gy in 25 fractions + 10 Gy in 5 fractions by photons), and letrozole administration for 5 years. After 6 years of follow-up, the patient was diagnosed with a left breast locally advanced angiosarcoma, for which she received neo-adjuvant chemotherapy. One year later, the patient underwent a left mastectomy. After one month, a new mass was noticed. Nine months onward, the patient had right breast mammography and bilateral ultrasound examination, which showed a new lesion on the right breast along with an ulceration on the left thoracic wall. The patient met with our plastic surgery team and she was then subjected to surgical excision and electrochemotherapy for both lesions. Histological examination documented a high-grade angiosarcoma (G3), positive for Factor VIII and CD31, with extensive areas of necrosis and ulceration. During the last follow-up record, 3 months after surgery, she showed local condition improvement but soon after she died.

Case 6

The patient is a 53-year-old woman with a left breast triple-negative infiltrating ductal carcinoma, pT2N1 (N+8/24), G3, surgically excised through left radical mastectomy and axillary lymph node dissection. Following the decision of the Multispecialty Tumor Board, adjuvant antracycline–paclitaxel combination regimen was administered. After 12 years, a local relapse (grade 3 invasive adenocarcinoma) infiltrating dermis and muscle tissue and extending to the thoracic wall was diagnosed. The pathologist described a triple-negative breast cancer with Ki67 index at 50%. The patient underwent surgical excision of pectoral muscle and further chemotherapy treatment with CMF was administered. Seven months onward, radicalization surgery was performed. The patient was then subjected to chemotherapy with epirubicin and paclitaxel, and local radiotherapy plus CWB (chest wall boost) (50 Gy in 25 fractions + 10 Gy in 5 fractions by photons).

The patient had regular clinical and radiological follow-up for 14 years until a left axillar mass and enlarged lymph nodes

were detected. Biopsies of the left chest wall showed neoplasm from globose cells with highly pleomorphic nuclei immersed in large necrosis areas. The immunophenotypic profile was found to be positive for CD10, desmin, muscle actin HHF-35, and CD68 (occasionally), and negative for Myo D1, SMA, S-100, CK-pan, CD31, CD34, and Factor VIII; Ki67 proliferation index was 50%. On these bases, it was referred to as a high-grade phyllodes tumor or sarcoma with myofibroblastic/pleomorphic differentiation. Disease evaluation with magnetic resonance imaging (MRI) and CT showed an extensive mass with lymph node metastases. The patient received chemotherapy based on epirubicin and ifosfamide. After two cycles, the patient's conditions deteriorated with massive pleural effusion and chest invasion, which led to the patient's death.

Case 7

The case concerns a 63-year-old woman who, in 2011, underwent left breast quadrantectomy and axillary lymph node dissection for infiltrating ductal breast cancer [pT1cN1 (1/18), G2, ER: 90%, PGR: 60%, Ki67 index at 15%, and HER2 negative]. Thereafter, the patient received chemotherapy with six cycles of FEC regimen (5-fluorouracil, epidoxorubicin, and cyclophosphamide), radiotherapy (50 Gy in 25 fractions + 10 Gy in 5 fractions by photons), and letrozole for 5 years. During the follow-up, 9 years later, there was evidence of an ulcerated and bleeding left breast lump, 7 cm in diameter, adherent to the chest wall, and a suspect of bilateral secondary pulmonary lesions through total body CT. A biopsy of the lesion documented a morphological picture showing fibrotic tissue and atypical epithelioid cell aggregates that sometimes optically border empty spaces. The absence of Pan-cytokeratin and positivity for vascular markers was reported. Ki67 was positive in 60% of neoplastic cells. The overall picture was traceable to angiosarcoma. The patient received a single radiofrequency thermoablation session on the breast lesion, resulting in suspension of bleeding, and a first-line chemotherapy for radio-induced angiosarcoma based on three cycles of gemcitabine and docetaxel but without benefit. In July 2021, after internal collegial discussion and sharing the case with a Cancer Center specialized in sarcomas, the patient received one electrochemotherapy session and then a second-line chemotherapy based on weekly doxorubicin administration. A new disease evaluation was made after nine chemotherapy cycles; CT images showed stable pulmonary nodes and no new mass onset. The patient was subjected to another session of electrochemotherapy after 6 months. Biopsy showed chronic and acute inflammation with ascending characters and giant cells from foreign body, marked fibrosis, and epidermal atrophy but no evidence of neoplasm. The patient received 15 cycles of chemotherapy. During the last follow up, in March 2022, she has shown stable disease.

Discussion

Although radiotherapy represents one of the cornerstones in cancer treatment, it has been assessed that RIS could be a complication. Since the interval between the RT and RIS occurrence is long, it is a key point to perform a strict and continuous follow-up to make an early and accurate diagnosis in order to guarantee an adequate treatment. Overall, RIS represented less than 4% of all sarcoma patients, and arose in 0.19% and 0.10% of RT-treated breast and head and neck cancers, respectively. These results are in line with previous reports (5, 12, 17–20). Our cohort of patients showed clinicopathological features similar to those in existing literature (13, 14). In our study, female patients with RIS were about 85% (6/7), according to the high prevalence of primary breast cancer in women (21). In previous studies, a median age of primary tumor diagnosis ranging from 41 to 46 years, a median latency period to RIS from 8 to 14 years, and a median age at RIS presentation ranging from 52 to 59 years have been reported (21). In slight contrast, we found that our patients were older at primary cancer diagnosis (57.3 years) and that they were characterized by a shorter RIS latency period (7.6 years), which also delayed the median age at RIS diagnosis (64.8 years) (14). This shorter latency time might be in part associated with concurrent chemotherapy administered to treat primary tumor, as previously described by Zhang et al. (22). However, the median survival time, 36 months, was found to be quite comparable to that from other reports (14, 23).

Despite their low incidence, RIS is characterized by high aggressiveness from both local and systemic points of view, which results in high mortality rates. Recent reports highlighted the non-inferiority of the hypofractionated radiation regimen as compared with the conventional one (24, 25). Notably, although long-term real-life data on the RIS risk associated with hypofractionated irradiation are lacking, some reports highlight the possible occurrence of secondary cancers in the irradiated field (26, 27). R0 resection is widely considered the only curative chance for these patients (28), although all RIS patients in our case series had tumor relapse after surgical resection. Moreover, our patients received scarce benefits from multiple lines of chemotherapy. However, the poor prognosis of RIS patients did not discourage the employment of radiotherapy, an indispensable therapeutic approach for cancer treatment, since its benefits undoubtedly outweigh the risks.

Conclusions

RIS is a possible complication of long-survivor cancer patients; thus, much attention has to be paid to early diagnose these cancers to employ optimal lifesaving therapies. Adherence to a strict follow-up regimen after the radiation treatment to assess and mitigate the risk of post-radiation tumor onset is recommended. After the

planned follow-up period, considering the long-term risk to develop a RIS, it is also necessary to apply a specific survivorship care plan. Our center is working to organize a multispecialty survivorship program that will include hospital physicians, general practitioners, and outsource experts specialized in supportive discipline, including nutritional support.

Data availability statement

The raw data supporting the conclusions of this article will be made available by the authors, without undue reservation.

Ethics statement

Ethical review and approval was not required for the study on human participants in accordance with the local legislation and institutional requirements. The patients/participants provided their written informed consent to participate in this study.

Author contributions

SR and AMB designed the work. LCO, SL, AB, APS collected data. SL, FA, and SR analysed data. GM and AMB interpreted data. LCO, SL, and SR drafted the work. AS, GF, and AMB substantially revised the work. All authors contributed to the article and approved the submitted version.

Funding

This study has been funded by Ministero della Salute, Ricerca Corrente 2022.

Conflict of interest

The authors declare that the research was conducted in the absence of any commercial or financial relationships that could be construed as a potential conflict of interest.

Publisher's note

References

1. Mirjolet C, Merlin JL, Truc G, Noël G, Thariat J, Domont J, et al. RILA blood biomarker as a predictor of radiation-induced sarcoma in a matched cohort study. *EBioMedicine* (2019) 41:420–6. doi: 10.1016/j.ebiom.2019.02.031

2. Baskar R, Lee KA, Yeo R, Yeoh K-W. Cancer and radiation therapy: Current advances and future directions. *Int J Med Sci* (2012) 9:193–9. doi: 10.7150/ijms.3635

3. Abshire D, Lang MK. The evolution of radiation therapy in treating cancer. *Semin Oncol Nurs* (2018) 34:151–7. doi: 10.1016/j.soncn.2018.03.006

4. Joo MW, Kang YK, Ogura K, Iwata S, Kim JH, Jeong WJ, et al. Post-radiation sarcoma: A study by the Eastern Asian musculoskeletal oncology group. *PLoS One* (2018) 13:e0204927. doi: 10.1371/journal.pone.0204927

5. Pradniwat K, Ong KW, Sittampalam K, Bay BH, Tan PH. Sarcoma of the breast and chest wall after radiation treatment for bilateral breast carcinoma. *J Clin Pathol* (2015) 68:491–5. doi: 10.1136/jclinpath-2015-202963

6. Tubiana M. Can we reduce the incidence of second primary malignancies occurring after radiotherapy? a critical review. *Radiother Oncol* (2009) 91:4–15. doi: 10.1016/j.radonc.2008.12.016

7. O'Regan K, Hall M, Jagannathan J, Giardino A, Kelly PJ, Butrynski J, et al. Imaging of radiation-associated sarcoma. *AJR Am J Roentgenol* (2011) 197(1): W30–6. doi: 10.2214/AJR.10.5558

8. Phillips TL, Sheline GE. Bone sarcomas following radiation therapy. *Radiology* (1963) 81:992–6. doi: 10.1148/81.6.992

9. Pendlebury SC, Bilous M, Langlands AO. Sarcomas followig radiation therapy for breast cancer: A report of three cases and a review of the literature. *Int J Radiat OncologyBiologyPhysics* (1995) 31:405–10. doi: 10.1016/0360-3016(95)93157-3

10. Cahan WG, Woodard HQ. Sarcoma arising in irradiated bone; report of 11 cases. *Cancer* (1948) 1:3–29. doi: 10.1002/(sici)1097-0142(19980101)82:1<8::aid-cncr3>3.0.co;2-w

11. Wu LC, Kleinerman RA, Curtis RE, Savage SA, Berrington de González A. Patterns of bone sarcomas as a second malignancy in relation to radiotherapy in adulthood and histologic type. *Cancer Epidemiol Biomarkers Prev* (2012) 21:1993–9. doi: 10.1158/1055-9965.EPI-12-0810

12. Snow A, Ring A, Struycken L, Mack W, Koç M, Lang JE. Incidence of radiation induced sarcoma attributable to radiotherapy in adults: A retrospective cohort study in the SEER cancer registries across 17 primary tumor sites. *Cancer Epidemiol* (2021) 70:101857. doi: 10.1016/j.canep.2020.101857

13. Sheth GR, Cranmer LD, Smith BD, Grasso-Lebeau L, Lang JE. Radiation-induced sarcoma of the breast: a systematic review. *Oncologist* (2012) 17:405–18. doi: 10.1634/theoncologist.2011-0282

14. Lou J, Jiang L, Dai X, Wang H, Yang J, Guo L, et al. Radiation-induced sarcoma of the head and neck following radiotherapy for nasopharyngeal carcinoma: A single institutional experience and literature review. *Front Oncol* (2020) 10:526360. doi: 10.3389/fonc.2020.526360

15. Hothorn T, Lausen B. On the exact distribution of maximally selected rank statistics. *Comput Stat Data Anal* (2003) 43:121–37. doi: 10.1016/S0167-9473(02)00225-6

16. Therneau TM. *A package for survival analysis in r* (2022). Available at: https://CRAN.R-project.org/package=survival (Accessed May 31, 2022).

17. Bjerkehagen B, Smeland S, Walberg L, Skjeldal S, Hall KS, Nesland JM, et al. Radiation-induced sarcoma: 25-year experience from the Norwegian radium hospital. *Acta Oncol* (2008) 47:1475–82. doi: 10.1080/02841860802047387

18. Taghian A, de Vathaire F, Terrier P, Le M, Auquier A, Mouriesse H, et al. Long-term risk of sarcoma following radiation treatment for breast cancer. *Int J Radiat Oncol Biol Phys* (1991) 21:361–7. doi: 10.1016/0360-3016(91)90783-z

19. Kirova YM, Feuilhade F, Calitchi E, Otmezguine Y, Le Bourgeois JP. Radiation-induced sarcomas following radiotherapy for breast cancer: Six case reports and a review of the literature. *Breast* (1998) 7:277–82. doi: 10.1016/S0960-9776(98)90096-0

20. Garcia M, Hernandez DL, Mendoza S, Buelvas N, Alvarez A, Esguerra J, et al. Tumors associated with radiotherapy: A case series. *J Med Case Rep* (2020) 14:179. doi: 10.1186/s13256-020-02482-x

21. Callesen LB, Safwat A, Rose HK, Sørensen FB, Baad-Hansen T, Aggerholm-Pedersen N. Radiation-induced sarcoma: A retrospective population-based study over 34 years in a single institution. *Clin Oncol (R Coll Radiol)* (2021) 33:e232–8. doi: 10.1016/j.clon.2020.12.009

22. Zhang AY, Judson I, Benson C, Wunder JS, Ray-Coquard I, Grimer RJ, et al. Chemotherapy with radiotherapy influences time-to-development of radiation-induced sarcomas: A multicenter study. *Br J Cancer* (2017) 117:326–31. doi: 10.1038/bjc.2017.198

23. Cha C, Antonescu CR, Quan ML, Maru S, Brennan MF. Long-term results with resection of radiation-induced soft tissue sarcomas. *Ann Surg* (2004) 239:903–9. doi: 10.1097/01.sla.0000128686.51815.8b

24. Lertbutsayanukul C, Pitak M, Nantavithya C. Long-term oncological outcomes of hypofractionated versus conventional fractionated whole breast irradiation with simultaneous integrated boost in early-stage breast cancer. *Radiat Oncol J* (2022) 40:141–50. doi: 10.3857/roj.2021.00927

25. Piras A, Boldrini L, Menna S, Venuti V, Pernice G, Franzese C, et al. Hypofractionated radiotherapy in head and neck cancer elderly patients: A feasibility and safety systematic review for the clinician. *Front Oncol* (2021) 11:761393. doi: 10.3389/fonc.2021.761393

26. Cook MR, Martinez MP, Fenger JM, Desai NC. Radiation-induced sarcoma in a cat following hypofractionated, palliative intent radiation therapy for large-cell lymphoma. *JFMS Open Rep* (2019) 5(2):2055116919889159. doi: 10.1177/2055116919889159

27. Zwahlen DR, Bischoff LI, Gruber G, Sumila M, Schneider U. Estimation of second cancer risk after radiotherapy for rectal cancer: comparison of 3D conformal radiotherapy and volumetric modulated arc therapy using different high dose fractionation schemes. *Radiat Oncol* (2016) 11:149. doi: 10.1186/s13014-016-0723-6

28. Giannini L, Incandela F, Fiore M, Gronchi A, Stacchiotti S, Sangalli C, et al. Radiation-induced sarcoma of the head and neck: A review of the literature. *Front Oncol* (2018) 8:449. doi: 10.3389/fonc.2018.00449

frontiers | Frontiers in Oncology

TYPE Case Report
PUBLISHED 14 November 2022
DOI 10.3389/fonc.2022.1045752

OPEN ACCESS

EDITED BY
Mattia Falchetto Osti,
Sapienza University of Rome, Italy

REVIEWED BY
Vincent Vinh-Hung,
Centre Hospitalier de la Polynésie Française (CHPF), French Polynesia
Hideyuki Yoshitomi,
Dokkyo Medical University, Japan
Manuel Conson,
University of Naples Federico II, Italy
Yan Yuan,
Guangzhou Medical University Cancer Hospital, China

*CORRESPONDENCE
Hsin-Hua Lee
dr.hh.lee@gmail.com

SPECIALTY SECTION
This article was submitted to Radiation Oncology, a section of the journal Frontiers in Oncology

RECEIVED 16 September 2022
ACCEPTED 25 October 2022
PUBLISHED 14 November 2022

CITATION
Tu K-Y, Huang Y-S, Lau J and Lee H-H (2022) Adaptive Tomotherapy for locally advanced unresectable pancreatic neuroendocrine tumor: Case report and literature review. *Front. Oncol.* 12:1045752. doi: 10.3389/fonc.2022.1045752

Adaptive Tomotherapy for locally advanced unresectable pancreatic neuroendocrine tumor: Case report and literature review

Kuan-Yi Tu[1,2], Yen-Shuo Huang[3], Juntiong Lau[4] and Hsin-Hua Lee[5,6,7,8]*

[1]School of Post Baccalaureate Medicine, Kaohsiung Medical University, Kaohsiung, Taiwan, [2]College of Medicine, Kaohsiung Medical University, Kaohsiung, Taiwan, [3]Department of Pathology, Kaohsiung Medical University Hospital, Kaohsiung Medical University, Kaohsiung, Taiwan, [4]Department of Surgery, Kaohsiung Medical University Hospital, Kaohsiung Medical University, Kaohsiung, Taiwan, [5]Ph.D. Program in Environmental and Occupational Medicine, Kaohsiung Medical University and National Health Research Institutes, Kaohsiung, Taiwan, [6]Department of Radiation Oncology, Kaohsiung Medical University Hospital, Kaohsiung, Taiwan, [7]Department of Radiation Oncology, Faculty of Medicine, College of Medicine, Kaohsiung Medical University, Kaohsiung, Taiwan, [8]Center for Cancer Research, Kaohsiung Medical University, Kaohsiung, Taiwan

Background: Pancreatic neuroendocrine tumor (NET) is rare, and the majority presents late in their clinical course. Here, we present a huge locally advanced pancreatic NET having Hi-Art helical Tomotherapy that resulted in a 68% reduction in target volume during adaptive image-guided radiotherapy (IGRT).

Case summary: A 63-year-old man without any history of systemic disease developed voiding difficulty for several months. Associated symptoms included poor appetite, nausea, distended abdomen, and body weight loss. Further magnetic resonance imaging showed a large multilobulated tumor in the left upper abdomen. Tumor biopsy revealed well-differentiated, grade 2, neuroendocrine tumor. Complete resection was unattainable. Therefore, Lanreotide was prescribed initially. However, tumor progression up to the greatest diameter of 18 cm was noted on computed tomography 5 months later. Thus, he stopped Lanreotide and commenced on concurrent chemoradiotherapy (CCRT). With a total dose of 70 Gy in 35 fractions, we generated two adaptive treatment plans during the whole course. Laparoscopic subtotal pancreatectomy with spleen preservation was performed after neoadjuvant CCRT. It has been more than 3 years after IGRT, and he remains cancer free and reports no side effects during regular follow-ups.

Conclusion: Tomotherapy caused tumor size reduction and hence facilitated surgical possibility for this originally unresectable pancreatic NET. Neoadjuvant IGRT incorporated with adaptive treatment planning enhanced

10.3389/fonc.2022.1045752

delivery accuracy. In this case of pancreatic NET resistant to Lanreotide, inter-fractional tumor regression from 1910 to 605 cc (68%) was documented.

KEYWORDS

Tomotherapy, pancreas, abdomen, unresectable neuroendocrine tumor (NET), neuroendocrine neoplasm (NEN), image-guided radiotherapy (IGRT), adaptive planning, case report

Introduction

Pancreatic neuroendocrine tumor (NET) is a rare type of neuroendocrine neoplasm (NEN) that arises from endocrine cell in pancreatic tissue, accounting for only 3% of all pancreatic tumors (1). The majority of pancreatic NETs are non-functional without defined clinical syndrome or abnormal hormone profiles, and their presentation is often delayed until significant mass effect or distant metastasis (2). In this situation, curative surgical resection is often intricate. However, the role of surgical resection in the treatment of pancreatic NET is imperative. Hill et al. have investigated the impact of resection on overall survival. Resection of pancreatic NET was related to significantly improved survival in contrast with those patients who were recommended for surgery but did not undergo resection (114 *vs.* 35 month; $p<0.01$) (2).

Surgery was, however, not recommended in cases of giant size and small probability of complete resection. Combining different treatment modalities prior to definitive surgical intervention was hence applied. Radiotherapy used as a main treatment of primary pancreatic NET is novel and not often reported, although it has long been regarded as an approved treatment option in palliative symptom relief (3). Here, we present a case of locally advanced unresectable pancreatic NET who underwent neoadjuvant concurrent chemoradiation (CCRT) *via* Tomotherapy and subsequent surgical resection successfully. To the best of our knowledge, this is the first reported pancreatic NET who had 68% regression of target volume during IGRT of 70 Gy.

Case description

A 63-year-old man without any history of systemic disease developed voiding difficulty for several months prior to his presence in the hospital. Associated symptoms included poor appetite, nausea, distended abdomen, and body weight loss. Further abdominal magnetic resonance imaging (MRI) showed a large multilobulated tumor with the size of 16.1 × 14.9 × 14.5 cm in the left upper abdomen (Figure 1A). During physical examination, a very big abdominal mass was palpated in the left upper quadrant with firm texture. The mass was fixed with regular border. His laboratory data, such as alpha-fetoprotein and carcinoembryonic antigen, were within normal limits. He received tumor biopsy in which it revealed tissue fragment infiltrated by tumor cells bearing relatively uniform round nuclei and high nucleus–cytoplasm ratio arranged in sheet or rosette-like patterns. Immunohistochemical staining showed positive for chromogranin A, synaptophysin, and somatostatin receptor 2A (SSTR2A) (Figures 2A–C). Moreover, the mitotic activity was about 3 per 10 high-power fields. The Ki-67 labeling index was about 4%. Well-differentiated, grade 2, neuroendocrine tumor was diagnosed.

There was no metastasis or regional lymph node involvement under initial MRI and further contrast-enhanced computerized tomography (CT). Because the tumor size was too large to differentiate the primary affected organ and the border of the tumor was implicated with surrounding organ, complete resection was not achievable. Therefore, Lanreotide was given initially. However, marked enlargement up to the greatest diameter of 18 cm was noted on CT scan 5 months later (Figure 1B). Coinciding with this, he complained about bulging abdomen interfering with digestion. In the second-line therapeutic regimens, there are multiple anti-tumor therapy including Everolimus- or Sunitinib-based targeted therapy, chemotherapy, and even peptide receptor radionuclide therapy (PRRT). Among these therapies, PRRT was not achievable in our hospital, and reimbursement for Temozolomide for pancreatic NET was not included in the National Health Insurance of our country. Given the bulky and progressive disease status, a second-line therapeutic regimen with cytotoxic chemotherapy was taken into consideration. After offering multidisciplinary treatment options in the full discussion with the patient and his families, CCRT was chosen for strengthening local control. Thus, he began to receive capecitabine + oxaliplatin (XELOX) concurrently with image-guided radiotherapy (IGRT).

We utilized the Hi-Art helical Tomotherapy, version 2.2.4.1 (TomoTherapy, Inc., Madison, WI). The planned total dose was 70 Gy in 35 fractions. The dose statistics was provided in the supplementary material regarding doses of the various organs at risk at each of the three plans, e.g., kidneys, liver, stomach, and spinal cord. After 14 fractions, we performed adaptive treatment planning to better suit regressed tumor. The target volume has shrunk from 1,910 to 1,057 cc (Figures 3A, B). Again, after 10 more

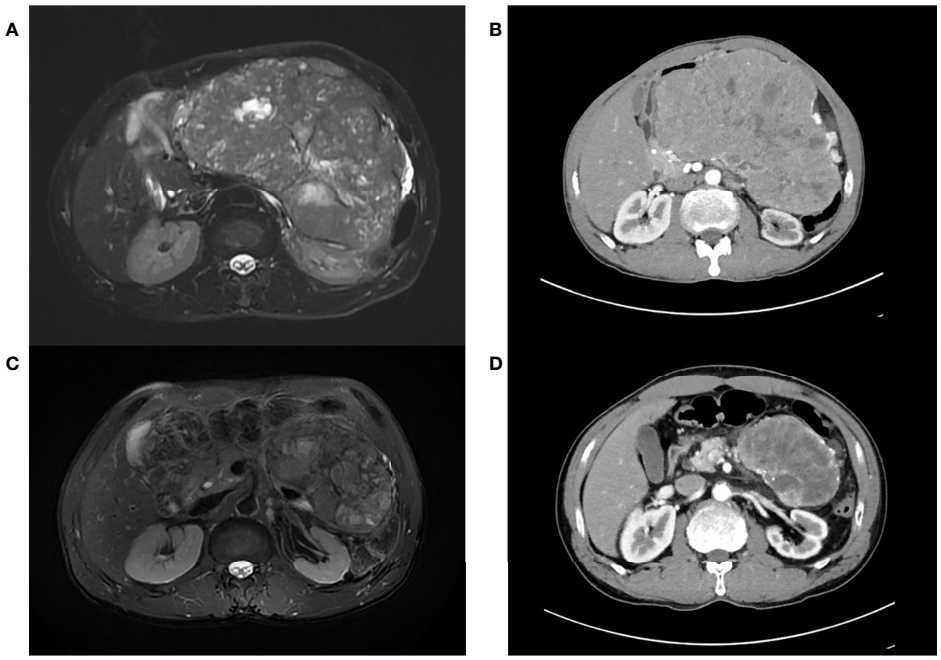

FIGURE 1
(A) Pretreatment magnetic resonance imaging (MRI) image depicting a multilobulated tumor with the size of 16.1 cm × 14.9 cm × 14.5 cm in the left upper abdomen. **(B)** Tumor progression up to the greatest diameter of 18 cm in the axial view of computerized tomography (CT) scans after treatment of Lanreotide. **(C)** Prominent tumor shrinkage after concurrent chemoradiation. **(D)** At least 50% reduction of tumor axial perpendicular diameters in preoperative CT.

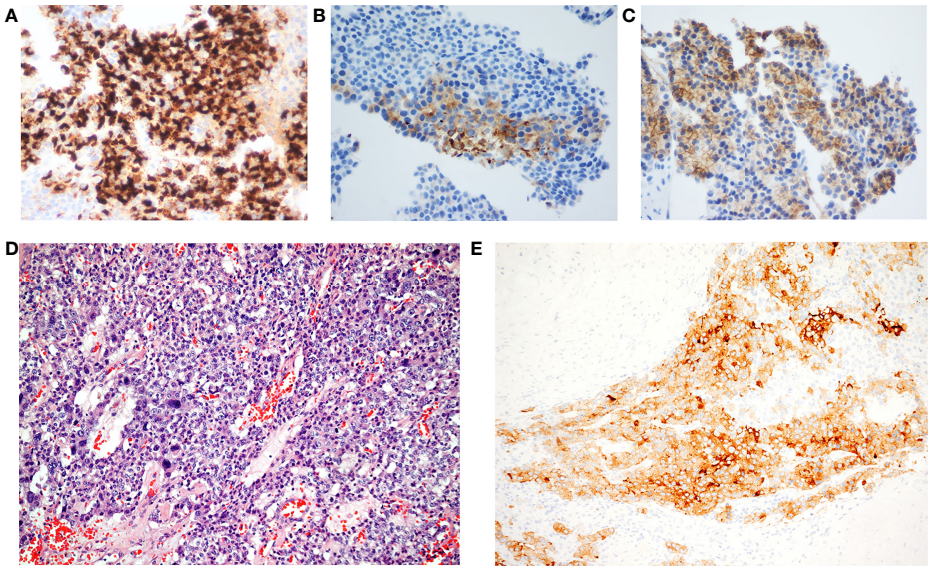

FIGURE 2
(A) Chromogranin, **(B)** synaptophysin, **(C)** somatostatin receptor 2A, and **(D)** monomorphous round to cuboidal cells arranging in solid and trabecular patterns. These cells have rich cytoplasm, and salt and pepper nuclei (hematoxylin–eosin stain; original magnification, 100×). **(E)** The immunohistochemical study reveals immunoreactivity of synaptophysin (original magnification, 100×).

fractions, IGRT revealed further shrinkage. Another new adaptive plan was administered, since the target volume has shrunk from 1,057 to 605 cc (Figures 3B, C). Corresponding with radiological response, his urinary and abdominal symptoms improved. The tumor volumes of the enhanced CT before and after radiotherapy have been calculated by the radiation oncologist utilizing a segmentation tool program. It was 2,199.35 cc before radiotherapy and 315.54 cc after radiotherapy. On the third month of CCRT, MRI showed a continuously decreased tumor dimension (Figure 1C). The axial perpendicular diameters of the tumor reduced at least 50% in preoperative CT after CCRT (Figure 1D).

His baseline performance status before CCRT was Eastern Cooperative Oncology Group (ECOG) grade 1 with only mild urinary frequency but no other complaint. There was also no acute radiation-induced nausea, diarrhea, or abdominal cramping. The radiotherapy-related toxicity was evaluated by the Common Terminology Criteria for Adverse Events (CTCAE) v4.0. Radiotherapy was well-tolerated without acute toxicities >2. In addition, his kidney function, as measured by creatinine clearance, remains mostly the same throughout the radiotherapy. He developed grade 1 radiation-induced dermatitis with mild erythema and later worsened because of a weekend trip swimming in the ocean. Grade 2 dermatitis subsided after Tomotherapy. Apart from avoiding disease progression, CCRT under current regimens resulted in tremendous tumor volume shrinkage. To achieve the best prognosis for the patient, curative surgical resection of tumor was indicated. Laparoscopic subtotal pancreatectomy with spleen preservation was performed, and the surgeons did not report any unusual difficulty. Pathology confirmed a pancreatic NET with the size of 12 × 10 × 6 cm and weighed 315.9 g with American Joint Committee on Cancer (AJCC) stage II, ypT3 (Figure 2). The surgical margin was 15 mm and uninvolved by tumor, which was confined to the pancreas.

The patient recovered well without post-operative complication. There was neither diabetes mellitus, postoperative ileus, nor surgery-related infection after subtotal pancreatectomy. Then, he was under regular surveillance in the outpatient department with abdominal CT every 3 months in the first year post-resection and every 12 months after the first year post-resection. It has been more than 46 months since his diagnosis of pancreatic NET, and he has no recurrence or distant metastasis during regular follow-ups. The overview of the clinical course of this patient is illustrated in Figure 3D.

Discussion

Surgical resection is the only treatment that can cure pancreatic NETs, and it is recommended to remove all

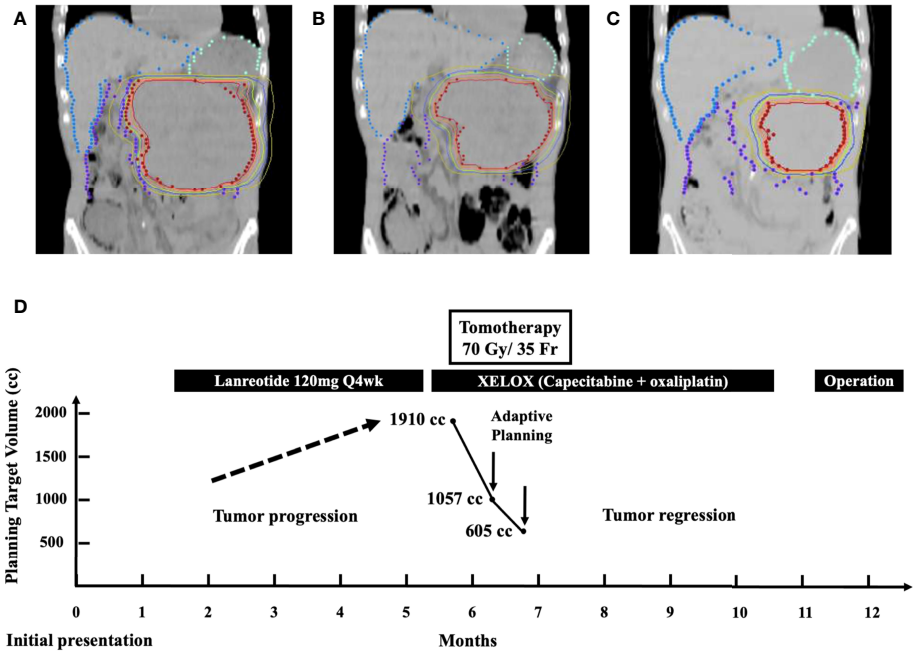

FIGURE 3
(A) Isodose curves depicting a target volume of 1,910 cc in the initial treatment plan of Tomotherapy. **(B)** Target volume reduced from 1,910 to 1,057 cc after 14 fractions. **(C)** Target volume reduced from 1,057 to 605 cc after 10 fractions. **(D)** Multidisciplinary treatment course of the patient from the day of initial presentation until definitive surgery: adaptive Tomotherapy plans were administrated twice at the timing of substantial target volume reduction from 1910 to 1,057 cc and from 1,057 to 605 cc, respectively.

localized and limited metastatic disease (4). However, for our patient who presented with a sizeable tumor burden causing high surgical risk and impossibility of complete tumor resection, other modality like somatostatin analogues was applied. Within 5 months of commencing Lanreotide, this locally advanced tumor kept progressing. We shifted to CCRT for tumor growth control and symptom alleviation. Radiotherapy acted as a bridge forward to curative surgical resection. This patient was able to receive curative operation when the tumor became smaller to less than one-third of the original size after CCRT.

Although radiotherapy is not considered a curative method as much as surgery, Iwata et al. demonstrated that radiotherapy was effective for local control in pancreatic NET. This retrospective study included 11 patients with pancreatic NET who received radiotherapy with maximum dose of 60 Gy in 30 fractions and ended up having 100% disease control rate (1). In addition, symptomatic relief owing to reduction in the physical pressure from large tumor burden was obvious after radiotherapy. However, Iwata et al. disclosed that median progression-free survival (PFS) and median overall survival for patients with pancreatic NET were 5.5 months (95% confidence interval [CI], 3.7–28.2 months) and 35.9 months (95% CI, 9.04 months—not reached), respectively (1). On the contrary, our patient had been alive without disease recurrence for 45 months. In our case, radiotherapy was delivered up to 70 Gy in 35 fractions *via* Tomotherapy with image-guided and adaptive planning ability. Nine of 11 patients in the study of Iwata et al. utilized three-dimensional conformal radiation therapy, which delivered 50–54 Gy in 25–30 fractions (1). Moreover, the fact that 8 of 11 patients were in metastasis status and only one patient underwent post-RT surgical resection was the major cause of the different prognosis between the study of Iwata et al. and our case (1).

Tomotherapy allows radiation oncologists to visualize inter-fractional radiation responses. Kupelian et al. illustrated the benefit of IGRT in head and neck tumors by comparing the severity of inter-fractional setup errors. Even if imaging guidance was performed every other day, about 10% of all fractions still had a setup error over 5 mm (5). In addition to setup errors and organ mobilization, the dimension of targeted tumor was likely to change after each fraction, which may cause daily deviation. Different anatomic sites also have various setup uncertainties. Studies have shown that inter-fractional displacement in the lung is the largest followed by that in the abdomen (6). The mean 3D displacement (average of lateral, longitudinal, vertical, and rotational direction) of inter-fractional variation in the abdomen was 4.4 mm (6). The advantage of applying IGRT to avoid daily variation before abdominal irradiation is evident.

The recent advancements in radiotherapy technologies have made the delivery of the highly conformal dose to the target volume possible. The organ at risk that needed to be considered first was the kidneys. With the aim of maximal renal parenchymal sparing, radiotherapy was delivered. We provide the dose statistics in the supplementary material regarding the doses of the various organs at risk at each of the three plans, e.g., kidneys, liver, stomach, and spinal cord. With daily IGRT *via* Tomotherapy, we have carefully prescribed 70 Gy in 35 fractions, exceeding the doses of previous reports for pancreatic NET while causing no chronic-radiation-induced side effect (7). Bresciani et al. reported minimal toxicities from 66 Gy in 30 fractions delivered *via* Tomotherapy for para-aortic lymphadenopathy in the upper abdomen (8). The majority of patients received 45–50.4 Gy in 1.8 Gy per fraction as their abdominal radiation course. Radiation-induced diarrhea or emesis is commonly seen during abdominal–pelvic radiotherapy. Wang et al. has calculated that mean dose to the small bowel is associated with radiation-induced emesis. They suggested to limit the constraint of the small bowel mean dose to <63% of the prescribed dose (median, 28.35 Gy) (9). In the present case, the mean dose of the small bowel was 26.56, 24.97, and 18.39 Gy, respectively, in all three plans.

Somatostain analogues (SSAs) have been used in advanced or grade 1 or 2 (Ki-67 <10%) enteropancreatic, somatostatin receptor-positive NET (10), and the National Comprehensive Cancer Network (NCCN) guidelines have regarded it as an appropriate drug for symptom control and prevention of tumor progression (3). However, the huge tumor remained enlarged and resistant to Lanreotide in our case. The clinically predictive factors for tumor resistance in SSA can be determined by baseline tumor growth rate, and the patients can then be stratified by disease status and documented progression status to individualized treatment protocol (11). In pathological or molecular aspect, the NCCN guideline recommended using SSA on patients with positive SSTR2A expression (3). Recent research also showed the significant correlation between SSTR2A expression and the clinical efficacy of Lanreotide (12). Increased Ki-67 index and poorly differentiated NET also had unsatisfying SSA treatment outcome (13). In addition, genetic difference had been found between poorly differentiated neuroendocrine carcinoma (NEC) and well-differentiated NET. Poorly differentiated NEC, which includes small- and large- cell NEC, has frequent loss of immunolabeling patterns in p53 and Rb (14). On the other hand, loss of nuclear death domain-associated protein (DAXX) and alpha-thalassemia X-linked intellectual disability syndrome (ATRX) immunolabeling was observed in 5 of 11 (45%) well-differentiated pancreatic NET (14). There is also more clinical value of the finding of ATRX and DAXX gene mutations. In one recent meta-analysis, altered ATRX and DAXX gene had significant correlation with the prognosis of pancreatic NET (15). Disease- and relapse-free survival significantly decreased in patients who had ATRX and DAXX mutations (15). However, the present case did not undergo genetic testing as part of the assessment. More advanced investigation on molecular characteristics of pancreatic NET can help us predict the prognosis and set individualized clinical practice.

Our patient had a huge locally advanced abdominal tumor cured without chronic treatment-related complication. We searched on PubMed and Medline databases for articles written in English from 2016 to 2022 with keywords such as "Abdominal mass," "Neuroendocrine tumor," and "locally advanced." Table 1 shows the clinicopathological characteristics of eight recent cases. The definitive treatment for NET is surgical resection, and the resectability is associated with size and location. The cases whose primary site was in the liver or duodenum or colon received surgery as primary treatment even if the tumor size was up to 20 cm × 16 cm × 11 cm (18–20, 22). Tumors with the pancreas as the primary site and with an initial tumor diameter of 4/3.8 cm were able to be resected (16), and yet, some researchers preferred chemotherapy and radiotherapy in tumors with the greatest diameter up to 9.8 cm (17). In the case of a 9.8-cm pancreatic NET, systemic therapy followed by CCRT with 54 Gy in 30 fractions was applied and reached partial response (17). Similar to our case, CCRT was used. With unprecedented 70 Gy, a 68% reduction in target volume followed by a successful conversion to resectable status was presented in our case. Quite the opposite, colorectal NET was rare and often diagnosed very late, and bowel perforation was noted in the case of Alshammari et al. (19). Namikawa et al. presented a case of gastric NET that developed hepatic metastasis (diameter up to 25 cm). Spontaneous rupture of hepatic metastasis was noted 8 months after initial treatment with everolimus plus somatostatin (21).

Further prospective studies with larger patient numbers are required to establish the role of IGRT in huge NET (7). However, it is often not expected to see one with such considerable size in the present case. It is imperative to take into consideration various treatment options for the best benefits of each individual patient. As in our case, IGRT showed its value in optimizing the therapeutic ratio by maximizing target dose safely. Most of all, the conversion of surgical suitability has extended his disease-free survival.

Conclusions

IGRT *via* Tomotherapy has eased the patients' symptoms from such 18-cm pancreatic NET in this case. Apart from complete relief of abdominal and pelvic discomfort, CCRT caused a 68% target volume reduction (1,910 to 605 cc) and facilitated further surgical resectability. To the best of our knowledge, this is the first reported case using Tomotherapy to deliver 70 Gy to a pancreatic NET with such favorable outcome. Adaptive planning helps to modify doses according to volumetric changes.

Patient perspective

I was at first disheartened with the diagnosis of an inoperable tumor. When I came to the Department of Radiotherapy, I was dismayed and yet impressed by the coordination of simulation scanning and resource intensive re-planning due to markedly shrinkage of the tumor. Following more and more fractions of Tomotherapy, I felt vigorous because of a flatter belly coinciding with the diminished tumor volume. I remember swimming at the beach during the radiation treatment course, and the belly skin became painful, which was later relieved by topical medication

TABLE 1 Clinicopathological characteristics of reported cases of locally advanced abdominal neuroendocrine tumor.

Articles	Age (year)	Sex	Location	Grade (G)	Initial size (cm)	Treatment 1	Treatment 2	Treatment 3	Outcome
Mirică et al., 2016 (16)	59	F	Pancreas	G2	4/3.8	Surgery	Somatostatin analogue	Chemotherapy	#Alive 34 months
Won et al., 2017 (17)	52	F	Pancreas	NEC	9.8	Etoposide + cisplatin	CCRT (etposide+. Cisplatin + 54 Gy/30 Fr)	Irinotecan + cisplatin	$Alive 11 months
Meng et al., 2018 (18)	56	F	Liver	G1	20×16×11	Surgery	None	None	$Alive 6 years
Alshammari et al., 2019 (19)	57	M	Colon	NEC	9×7	Surgery	None	None	N/A
Wang et al., 2021 (20)	55	F	Duodenum	G2	6.2×5.8	Surgery	None	None	$Alive 3 months
Namikawa et al., 2021 (21)	64	M	Stomach	G3	*25	Everolimus + somatostatin	None	None	*Died 8 months
Felux et al., 2022 (22)	65	F	Colon	NEC	9.8–10.5	Surgery	Carboplatin + Etoposide	None	N/A
Present case, 2022	63	M	Pancreas	G2	16.1× 14.9× 14.5	Lanreotide	CCRT (XELOX+ 70 Gy/35 Fr)	Surgery	$Alive 45 months

F, female; M, male; NEC, neuroendocrine carcinoma; CCRT, concurrent chemoradiotherapy; Gy, Gray; Fr, fraction; XELOX, Capecitabine plus oxaliplatin; N/A, not applicable.
*The case was diagnosed with hemoperitoneum due to hemorrhaging of the enormous liver metastasis with 25 cm in diameter. CT imaging revealed progression of liver metastasis, and the patient died 8 months after initial treatment.
#Alive since diagnosis.
$Alive since initial treatment.

from Dr. Lee. She advised me to be heedful of skin care. Owing to the strikingly smaller size after radiotherapy, I was able to take on surgery followed by an uneventful postoperative recovery. It has been almost 4 years, and I am energetic with my cancer-free life.

Data availability statement

The original contributions presented in the study are included in the article/Supplementary Material. Further inquiries can be directed to the corresponding author.

Ethics statement

Ethical review and approval was not required for the study on human participants in accordance with the local legislation and institutional requirements. The patients/participants provided their written informed consent to participate in this study. Written informed consent was obtained from the individual(s) for the publication of any potentially identifiable images or data included in this article.

Author contributions

K-YT and JL wrote the first draft of the manuscript and made the table. K-YT and Y-SH contributed to image review and figure legends. K-YT generated the timeline figure. H-HL treated the patient, conceived the paper layout, and revised the manuscript. All authors contributed to the article and approved the submitted version.

Conflict of interest

The authors declare that the research was conducted in the absence of any commercial or financial relationships that could be construed as a potential conflict of interest.

Publisher's note

All claims expressed in this article are solely those of the authors and do not necessarily represent those of their affiliated organizations, or those of the publisher, the editors and the reviewers. Any product that may be evaluated in this article, or claim that may be made by its manufacturer, is not guaranteed or endorsed by the publisher.

Supplementary material

The Supplementary Material for this article can be found online at: https://www.frontiersin.org/articles/10.3389/fonc.2022.1045752/full#supplementary-material

References

1. Iwata T, Ueno H, Itami J, Ito Y, Inaba K, Morizane C, et al. Efficacy of radiotherapy for primary tumor in patients with unresectable pancreatic neuroendocrine tumors. *Jpn J Clin Oncol* (2017) 47(9):826–31. doi: 10.1093/jjco/hyx081

2. Hill JS, McPhee JT, McDade TP, Zhou Z, Sullivan ME, Whalen GF, et al. Pancreatic neuroendocrine tumors: The impact of surgical resection on survival. *Cancer* (2009) 115(4):741–51. doi: 10.1002/cncr.24065

3. Shah MH, Goldner WS, Benson AB, Bergsland E, Blaszkowsky LS, Brock P, et al. Neuroendocrine and adrenal tumors, version 2. *2021 Nccn Clin Pract Guidelines Oncol J Natl Compr Canc Netw* (2021) 19(7):839–68. doi: 10.6004/jnccn.2021.0032

4. Akirov A, Larouche V, Alshehri S, Asa SL, Ezzat S. Treatment options for pancreatic neuroendocrine tumors. *Cancers (Basel)* (2019) 11(6):828. doi: 10.3390/cancers11060828

5. Kupelian P, Langen K. Helical tomotherapy: Image-guided and adaptive radiotherapy. *Front Radiat Ther Oncol* (2011) 43:165–80. doi: 10.1159/000322420

6. Zhou J, Uhl B, Dewit K, Young M, Taylor B, Fei DY, et al. Analysis of daily setup variation with tomotherapy megavoltage computed tomography. *Med Dosim* (2010) 35(1):31–7. doi: 10.1016/j.meddos.2009.01.005

7. Chan DL, Thompson R, Lam M, Pavlakis N, Hallet J, Law C, et al. External beam radiotherapy in the treatment of gastroenteropancreatic neuroendocrine tumours: A systematic review. *Clin Oncol (R Coll Radiol)* (2018) 30(7):400–8. doi: 10.1016/j.clon.2018.03.006

8. Bresciani S, Garibaldi E, Cattari G, Maggio A, Di Dia A, Delmastro E, et al. Dose to organs at risk in the upper abdomen in patients treated with extended fields by helical tomotherapy: A dosimetric and clinical preliminary study. *Radiat Oncol* (2013) 8:247. doi: 10.1186/1748-717x-8-247

9. Wang YM, Chen YF, Lee PY, Ho MW, Huang EY. Radiation-induced emesis (Rie) in extended-field radiotherapy for gynecological malignancies: Dosimetric and non-dosimetric factors. *Curr Oncol* (2021) 28(5):3602–9. doi: 10.3390/curroncol28050308

10. Caplin ME, Pavel M, Ćwikła JB, Phan AT, Raderer M, Sedláčková E, et al. Lanreotide in metastatic enteropancreatic neuroendocrine tumors. *N Engl J Med* (2014) 371(3):224–33. doi: 10.1056/NEJMoa1316158

11. Carmona-Bayonas A, Jiménez-Fonseca P, Lamarca Á, Barriuso J, Castaño Á, Benavent M, et al. Prediction of progression-free survival in patients with advanced, well-differentiated, neuroendocrine tumors being treated with a somatostatin analog: The getne-trasgu study. *J Clin Oncol* (2019) 37(28):2571–80. doi: 10.1200/jco.19.00980

12. Kasajima A, Papotti M, Ito W, Brizzi MP, La Salvia A, Rapa I, et al. High interlaboratory and interobserver agreement of somatostatin receptor immunohistochemical determination and correlation with response to somatostatin analogs. *Hum Pathol* (2018) 72:144–52. doi: 10.1016/j.humpath.2017.11.008

13. Lee L, Ramos-Alvarez I, Jensen RT. Predictive factors for resistant disease with Medical/Radiologic/Liver-directed anti-tumor treatments in patients with advanced pancreatic neuroendocrine neoplasms: Recent advances and controversies. *Cancers (Basel)* (2022) 14(5):1250. doi: 10.3390/cancers14051250

14. Yachida S, Vakiani E, White CM, Zhong Y, Saunders T, Morgan R, et al. Small cell and Large cell neuroendocrine carcinomas of the pancreas are genetically similar and distinct from well-differentiated pancreatic neuroendocrine tumors. *Am J Surg Pathol* (2012) 36(2):173–84. doi: 10.1097/PAS.0b013e3182417d36

15. Wang F, Xu X, Ye Z, Qin Y, Yu X, Ji S. Prognostic significance of altered Atrx/Daxx gene in pancreatic neuroendocrine tumors: A meta-analysis. *Front Endocrinol (Lausanne)* (2021) 12:691557. doi: 10.3389/fendo.2021.691557

16. Mirică A, Bădărău IA, Mirică R, Păun S, Păun DL. A rare case of metastasized non-functional pancreatic neuroendocrine tumor with a good long-term survival. *J Med Life* (2016) 9(4):369–72. doi: 10.22336/jml.2016.0409

17. Won YG, Seo KJ, Hyeon J, Shin OR, Chang E, Sun S, et al. Gastroenteropancreatic-origin neuroendocrine carcinomas: Three case reports

with favorable responses following localized radiotherapy and a review of literature. *Med (Baltimore)* (2017) 96(49):e9009. doi: 10.1097/md.0000000000009009

18. Meng XF, Pan YW, Wang ZB, Duan WD. Primary hepatic neuroendocrine tumor case with a preoperative course of 26 years: A case report and literature review. *World J Gastroenterol* (2018) 24(24):2640–6. doi: 10.3748/wjg.v24.i24.2640

19. Alshammari TF, Hakami RA, Alali MN, AlShammari S, Zayed MA, AlSohaibani MO, et al. A perforated colonic neuroendocrine tumor with liver metastasis: A case report and literature review. *Am J Case Rep* (2019) 20:920–5. doi: 10.12659/ajcr.916288

20. Wang X, Wu Y, Cao X, Zhang X, Cheng Y, Kong L. Duodenal neuroendocrine tumor: A rare case report. *Med (Baltimore)* (2021) 100(6): e24635. doi: 10.1097/md.0000000000024635

21. Namikawa T, Yokota K, Yamaguchi S, Fukudome I, Munekage M, Uemura S, et al. Spontaneous intra-abdominal hemorrhage of a well-differentiated, grade 3 gastric neuroendocrine tumor during drug-based treatment. *Clin J Gastroenterol* (2021) 14(4):1244–9. doi: 10.1007/s12328-021-01433-3

22. Felux K, McCarty B, Turner D, Gray T, Patel V. Poorly differentiated Large cell neuroendocrine carcinoma of the colon: A case report. *Cureus* (2022) 14(1): e20949. doi: 10.7759/cureus.20949

frontiers | Frontiers in Oncology

TYPE Case Report
PUBLISHED 22 November 2022
DOI 10.3389/fonc.2022.1060307

OPEN ACCESS

EDITED BY
Ianik Plante,
KBRwyle, United States

REVIEWED BY
John E. Mignano,
Tufts University, United States
Frank Paulsen,
University Hospital, Germany

*CORRESPONDENCE
Hiroto Ishikawa
ohmyeye@gmail.com

SPECIALTY SECTION
This article was submitted to Radiation Oncology, a section of the journal Frontiers in Oncology

RECEIVED 05 October 2022
ACCEPTED 07 November 2022
PUBLISHED 22 November 2022

CITATION
Zhou X, Ishikawa H and Gomi F (2022) Macular hole and vitreous hemorrhage subsequent to stereotactic hypofractionated radiotherapy for choroidal melanoma: A case report and review of the literature. *Front. Oncol.* 12:1060307. doi: 10.3389/fonc.2022.1060307

Macular hole and vitreous hemorrhage subsequent to stereotactic hypofractionated radiotherapy for choroidal melanoma: A case report and review of the literature

Xiaoyin Zhou[1], Hiroto Ishikawa[1,2]* and Fumi Gomi[1]

[1]Department of Ophthalmology, Hyogo College of Medicine, Hyogo, Japan, [2]Department of Ophthalmology, Mirai Eye & Skin Clinic, Osaka, Japan

Choroidal melanoma is the leading primary intraocular tumor with potentially fatal outcomes in adults. The coexistence of choroidal melanoma and a macular hole is extremely rare, and treatment strategies and information on the prognosis of associated complications are currently lacking. We report the first case of choroidal melanoma complicated with a macular hole and vitreous hemorrhage after stereotactic hypofractionated radiotherapy in Japan, and review the relevant literature in relation to the possible mechanisms, treatment strategies, and outcomes. An 83-year-old male with choroidal melanoma was treated with stereotactic hypofractionated radiotherapy in January 2021. Five months later, a full-thickness macular hole developed, followed by an acute massive vitreous hemorrhage about 2 weeks later. Following confirmation of tumor regression, the patient underwent a pars plana vitrectomy and internal limiting membrane peeling. The macular hole was closed postoperatively and the patient's best-corrected visual acuity improved to 20/125. There was no evidence of intraocular tumor dissemination or distant metastases during follow-up. A systematic literature search only identified 10 previous cases of choroidal melanoma with a macular hole in eight reports worldwide, mainly in females. Macular edema may be the primary cause of macular hole formation in these cases. Most patients who underwent vitrectomy for complications after tumor regression achieved a good prognosis. The development of a macular hole is a rare complication associated with choroidal melanoma. Anterior-posterior traction of posterior vitreous detachment and secondary macular edema may have contributed to the formation of the macular hole in the current case.

KEYWORDS

choroidal melanoma, stereotactic hypofractionated radiotherapy, macular hole, vitreous hemorrhage, case report, pars plana vitrectomy

Introduction

Choroidal melanoma is the leading primary intraocular malignancy among adults (1), with a low incidence of 0.6 cases per million per year in Japan (2). However, considering the high mortality rate of malignant metastases, this life-threatening disease should be diagnosed and treated promptly. Radiation therapy, including plaque brachytherapy, proton beam radiotherapy, and stereotactic radiotherapy, is an alternative to enucleation and has become the first-line treatment for choroidal melanoma (3–5). However, the tumor may be accompanied by complications, such as vitreous hemorrhage, rhegmatogenous retinal detachment, and macular hole (MH). Care is therefore needed to prevent intraocular or extraocular tumor dissemination during therapy for these complications (6).

Choroidal melanoma coexisting with a MH is extremely rare. To the best of our knowledge, only 10 previous cases have been reported worldwide (6–13), none of which occurred after stereotactic hypofractionated radiotherapy, and with limited information on the treatment of associated complications. Herein, we report on a patient who was diagnosed with asymptomatic choroidal melanoma with atypical presentation, and who developed a full-thickness MH and vitreous hemorrhage during follow-up, which was eventually repaired by pars plana vitrectomy (PPV) with internal limiting membrane (ILM) peeling. We also reviewed the relevant literature regarding the possible mechanisms of MH formation in patients with choroidal melanoma, and the corresponding treatment management and outcomes.

Case presentation

An 83-year-old man was referred to our hospital with suspected serous retinal detachment in his left eye. The patient's clinical course is presented in Figure 1. The best-corrected visual acuity (BCVA) was 20/20 in his right eye and 20/17 in his affected left eye. The intraocular pressure was normal (14 mmHg in the right eye and 13 mmHg in the left eye), and there were no appreciable findings in the anterior segments. Ultra-wide-field fundus photography (Figure 2A) of the left eye revealed an elevated choroidal mass with a central dark brown speckle in the nasal quadrant, about 4 disc diameters from the optic disc, along with concomitant posterior vitreous detachment (PVD). Fluorescein angiography showed that the choroidal mass had early diffuse hyperfluorescence with a central area of hypofluorescence (Figure 2B). Indocyanine green angiography showed blocked fluorescence due to the choroidal mass and a small hyperfluorescent area at the margin in the late stage (Figure 2C). Magnetic resonance imaging demonstrated a tumor measuring 5.9×5.7 mm in basal dimensions and 4.1 mm thick, with a hyperintense signal toward the vitreous cavity on axial T1 imaging-fast spin-echo (Figure 2D). Iodine-123 isopropyl iodoamphetamine brain single-photon emission computed tomography revealed high focal uptake in his left eye, corresponding to the choroidal tumor (Figure 2E). The patient underwent integrated positron emission tomography/computed tomography, and a transaxial section across the left eye revealed no fluorodeoxyglucose activity and no evidence of distant metastases. There were no abnormalities in the fellow eye.

The patient received a course of stereotactic hypofractionated radiotherapy (60 Gy in 5 fractions) for 5 consecutive days after the clinical diagnosis of choroidal melanoma. Five months later, the patient complained of visual deterioration with a BCVA of 20/50 and distortion in his left eye. Fundus examination and optical coherence tomography showed a full-thickness MH (stage 4) with cystic cavities (Figure 3A). Approximately 2 weeks later, his BCVA had decreased to 20/2000, attributed to an acute massive vitreous hemorrhage (Figure 3B). Repeat positron emission tomography/computed tomography examination showed no significant abnormalities or metastases. We therefore performed a vitrectomy and inverted ILM peeling. During surgery, we found

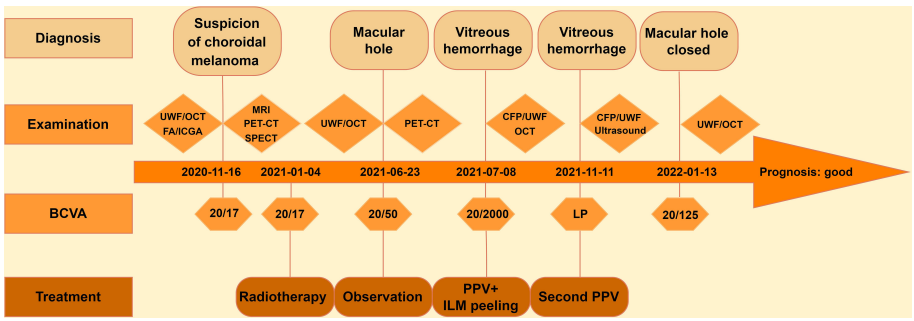

FIGURE 1
Clinical course of the patient with choroidal melanoma. UWF, ultra-wide-field fundus photography; OCT, optical coherence tomography; FA, fluorescein angiography; ICGA, indocyanine green angiography; MRI, magnetic resonance imaging; PET-CT, positron emission tomography-computed tomography; SPECT, single-photon emission computed tomography; CFP, color fundus photography; BCVA, best-corrected visual acuity; LP, light perception; PPV, pars plana vitrectomy; ILM, internal limiting membrane.

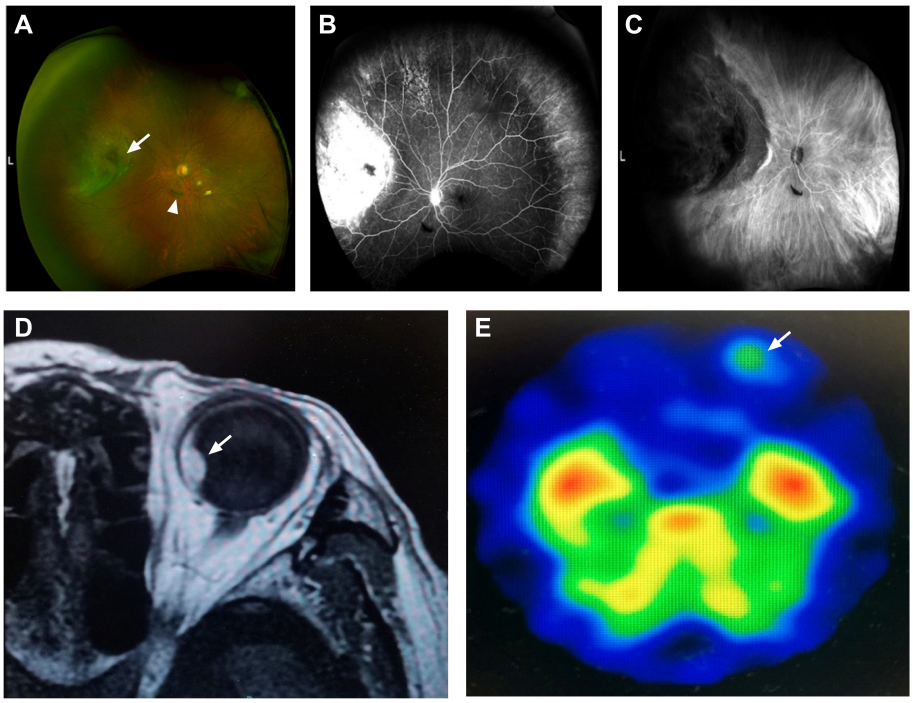

FIGURE 2
An 83-year-old man with choroidal melanoma. **(A)** Ultra-wide-field fundus photography revealed a white, elevated choroidal tumor with a central dark brown speckle (arrow) in the nasal quadrant and posterior vitreous detachment (arrowhead) inferior to the optic nerve. **(B)** Fluorescein angiography showed early hyperfluorescence corresponding to the mass. **(C)** Indocyanine green angiography showed blocked fluorescence and a small hyperfluorescent area at the edge. **(D)** Magnetic resonance imaging demonstrated a hyperintense tumor (arrow) with a smooth border on axial T1 imaging-fast spin-echo. **(E)** Iodine-123 isopropyl iodoamphetamine brain single-photon emission computed tomography showed high uptake in his left eye (arrow).

a massive subretinal hemorrhage, abundant fibrin, and retinal fragility but no obvious tears in his left eye. Gas-fluid exchange was completed at the end of surgery using 20% sulfur hexafluoride. After the first vitrectomy, the MH was closed on optical coherence tomography examination. However, the vitreous hemorrhage reappeared 2 weeks later and we performed a second vitrectomy after 4 months of observation. The MH remained closed after the two procedures (Figure 3C), the retina remained attached, the tumor displayed marked regression, and the BCVA had improved to 20/125.

Review of the literature

We conducted a literature review by searching the PubMed, Cochrane Library, and Web of Science databases using the keywords ("choroidal melanoma" OR "uveal melanoma") AND ("macular hole" OR "retinal tear"), ("uveal neoplasms" OR " choroidal neoplasms") AND ("macular hole" OR "retinal tear"), for articles published from December 1951 to March 2022. The search was limited to publications in English. We reviewed the abstracts and full texts of the identified articles and the related references. Simultaneous occurrence of choroidal melanoma and MH was reported in 10 patients in eight publications (6–13), after excluding one case with MH in which it was difficult to determine the intraocular tumor type (14) and one case in which MH was considered a post-vitrectomy complication (15). The findings of the literature review and the current case are presented in Table 1.

The total of 11 patients included four males and seven females, with an average age of 68.1 ± 13.2 years (range, 45–84 years). Five cases were reported in America, three in Europe (England, Italy, Switzerland), and two in West Asia (India, Israel). The current case was first documented in Japan (East Asia). The mean tumor-base diameter was 10.2×9.6 mm and the mean thickness was 4.9 mm. Most cases had a melanotic appearance, but the present case appeared amelanotic. Regarding the treatment of the tumor, one case underwent enucleation due to the large size of the tumor (height 13 mm) and total retinal detachment (10), one case underwent transscleral local resection (13), and the remaining cases were treated with radiotherapy, including stereotactic hypofractionated radiotherapy (the only treatment in the current case). MH developed in five cases after radiotherapy

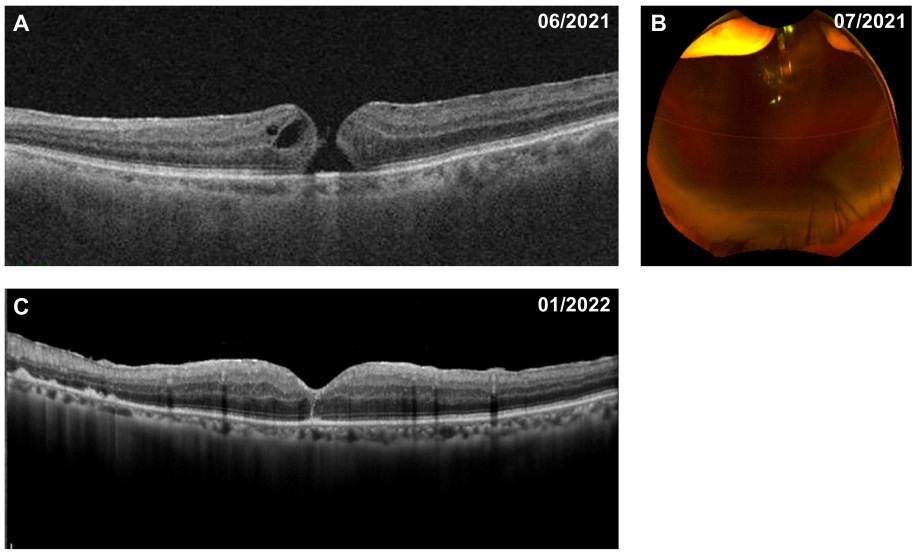

FIGURE 3
Fundus appearance in the patient with choroidal melanoma before and after vitrectomy. **(A)** Five months after radiotherapy, a full-thickness macular hole with cystic cavities was shown on optical coherence tomography. **(B)** A further 2 weeks later, a massive vitreous hemorrhage appeared on ultra-wide-field fundus photography. **(C)** The macular hole was successfully closed after pars plana vitrectomy with internal limiting membrane peeling.

and in one case after resection, and was observed in four cases at melanoma diagnosis. The most common concomitant manifestations during the follow-up period were retinal detachment and macular edema; the present case was the only one in which PVD and massive vitreous hemorrhage were observed. Five cases with MH were repaired with PPV and ILM peeling and achieved good results, except for the absence of detailed information on the macular prognosis in one case (6) and one case that was unsuccessfully repaired by PPV and eventually underwent enucleation (13). Two cases that underwent observation (7) and subtenon triamcinolone acetonide injection (11), respectively, ended in failure of macular closure. One case reported by Gold et al. died of suspected metastatic disease (7), but no recurrence or metastases were reported in the remaining cases.

Discussion

Uveal melanoma is a severe intraocular malignancy with an elevated gray or gray-brown appearance, which predominantly occurs in Caucasians and is generally complicated with exudative retinal detachment and occasional vitreous hemorrhage (1, 16). Rarely, MH can develop, and appropriate procedures must be followed to avoid metastasis (7). We presented a case with an atypical manifestation of choroidal melanoma with MH and subsequent vitreous hemorrhage in a patient who achieved a good prognosis after treatment.

Full-thickness MH represents an anatomical defect in the fovea involving interruption of all the retinal layers from the ILM to the retinal pigment epithelium (17). Notably, MH is more prevalent in women over the age of 60 years, due to hormonal influences (18), which may explain the high proportion of women in the above case series. There are several hypotheses regarding the co-occurrence of melanoma and MH. Typically, the development of MH in the retina has been attributed to anterior-posterior traction, commonly induced by PVD (19). In our case, PVD was detected by fundus observation at the first diagnosis, with no obvious retinal break. Although the specific etiology was unclear, we presumed that the PVD might have been caused by chronic tumor-related vitreous inflammation or floating blood cells, which could induce vitreous condensation, liquefaction, and final separation from the retina. In elderly patients, PVD may be caused by an inevitable, complex series of events such as synchysis and syneresis in the vitreous (17). It is therefore also possible that normal age-related PVD with secondary MH may have occurred coincidentally with melanoma in our case. In addition, tangential traction possibly resulting from an epiretinal membrane or increasing tumor height/thickness causing a lateral shift of vitreomacular traction may also play an important role in the pathogenesis of MH (20), as in a prior case report (7).

However, degenerative etiologies such as cystoid macular edema (CME) and secondary rupture of cysts may be responsible for the formation of MH, as seen in four previous

TABLE 1 Review of previously reported cases of choroidal melanoma with macular hole and the current case.

	Country	Age/ Sex/ Eye	Initial visual acuity	Tumor location to the optic disc	Tumor base (mm)	Tumor thickness (mm)	Tumor color	Tumor treatment	Time of macular hole	Macular hole diameter (μm)	Other manifestations	Procedure	Macular hole/Metastases
Zhou XY	Japan	83/M/ OS	20/17	Nasal	5.9 × 5.7	4.1	Amelanotic	Stereotactic hypofractionated radiotherapy	5M after radiotherapy	232	PVD; VH	PPV+ILMP	Closed/No
Foster WJ (6)	America	84/M/ OS	NA	Anterior to the equator	7 × 6	3.5	NA	Plaque	After Plaque	NA	NA	PPV+ILMP	NA/No
Gold AS (7)	America	65/F/ OS	20/400	Temporal	16 × 14	2.4	Melanotic	Plaque	Concurrence	NA	RD	PPV+ILMP	Closed/No
Gold AS (7)	America	77/F/ OS	20/200	Nasal	14 × 13	2.3	Melanotic	Plaque	Concurrence	NA	CME	No	Unclosed/No
Gold AS (7)	America	70/F/ OD	20/200	Inferonasal	16 × 14	5.8	Melanotic	Plaque	NA	NA	CME	No	NA/Yes
Narang S (8)	India	45/F/ OS	20/1200	Temporal	10.2 × 9.1	4.7	Orangeish-yellow	TTT	Concurrence	500	RD; CME	No	NA/No
Balestrazzi A (9)	Italy	62/F/ OS	20/20	Superior	8.2 × 7.7	2.5	Pigmented	TTT	3M after TTT	NA	RD	PPV+ILMP	Closed/No
Uffer S (10)	Switzerland	71/M/ OS	HM	Temporal	NA	13.0	Pigmented	Enucleation	Concurrence	NA	RD; CME; PVD	No	NA/No
Shields CL (11)	America	75/F/ OD	20/100	Superonasal	NA	NA	Melanotic	Plaque	26M after Plaque	NA	DH; CME	STTA	Unclosed/NA
Beykin G (12)	Israel	72/F/ OS	FC 30cm	NA	6.4 × 7.2	2.6	NA	Plaque	After Plaque	NA	RD	PPV+ILMP	Closed/No
Damato B (13)	England	45/M/ OS	NA	Nasal	8 × NA	8	NA	Local resection	After resection	NA	RD	PPV	Unclosed/NA

OD, right eye; OS, left eye; HM, hand motion; FC, finger counting; TTT, transpupillary thermotherapy; Plaque: iodine-125 plaque brachytherapy; PVD, posterior vitreous detachment; VH, vitreous hemorrhage; RD, retinal detachment; CME, cystoid macular edema; DH, disk hemorrhage; PPV, pars plana vitrectomy; ILMP, internal limiting membrane peeling; STTA, subtenon triamcinolone acetonide injection; NA, not available.

10.3389/fonc.2022.1060307

reports (7, 8, 10, 11). Retinal degeneration overlying the tumor, intraretinal edema secondary to chronic exudative retinal detachment, or an inflammatory cellular reaction to the necrotic tumor in the vitreous may lead to the development of CME in patients with melanoma (21). In one case in which peripheral melanoma was associated with CME, trypsin digest preparation of the intraretinal space demonstrated abnormal capillary architecture, which was thought to account for vascular leakage (22). CME may have been caused by an increase in capillary permeability during inflammation, resulting in MH (8). Similarly, we detected cystic cavities in the current case, suggesting that tractional forces followed by retinal tissue degeneration at the macula may have facilitated the formation of the MH.

Stereotactic hypofractionated radiotherapy, iodine-125 plaque brachytherapy, and transpupillary thermotherapy (TTT) are possible options for globe-salvaging treatment in patients with peripherally located tumors (3, 23–25). However, ocular complications such as cataract, glaucoma, maculopathy, and optic neuropathy require prompt attention (26). Mashayekhi et al. reported that most cases of atrophic retinal holes in the TTT-treated area occurred within 6 months after treatment, while retinal atrophy was much less prominent in patients treated with plaque radiotherapy or stereotactic hypofractionated radiotherapy (27, 28). Heat-induced vitreous changes in TTT may lead to vitreoretinal traction or retinal atrophy, which may in turn explain the formation of a retinal hole (27). Balestrazzi et al. described a case of MH that occurred 3 months after TTT in a patient with melanoma. However, given the distance between the tumor and the macula, TTT was considered unlikely to have caused the MH in this case (9). In another case report, Beykin et al. observed an atrophic MH in close proximity to a melanoma after plaque radiotherapy (12). More than 50% of patients in one study cohort suffered late-onset radiation retinopathy 5 years after stereotactic hypofractionated radiotherapy (28). Another study found that the distance from the fovea to the tumor was the primary determinant of maculopathy in patients undergoing radiotherapy (26). In the current case, MH was observed 5 months after stereotactic hypofractionated radiotherapy, and the melanoma site was distant from the macula, thus ruling out the possibility of radiation-induced MH. However, long-term complications still require cautious evaluation in this case.

The incidences of vitreous hemorrhage in patients with uveal melanoma treated with plaque radiotherapy were 15.1% at 5 years and 18.6% at 10 years (29). Radiation can lead to fibrosis and necrosis of tumor tissue, as well as thinning and fragility of the retina, thus increasing the risk of bleeding. Radiation-induced tumor necrosis is most commonly linked to vitreous hemorrhage in melanoma-affected eyes after radiotherapy, followed by proliferative radiation retinopathy and PVD (29). Combined with the surgical finding of bleeding from the tumor surface, we considered that the hemorrhage in the present case was a consequence of acute ischemic shrinkage of the tumor after stereotactic hypofractionated radiotherapy and vascular rupture within the tumor. However, it is important to note that the occurrence of vitreous hemorrhage before melanoma treatment should raise concerns about possible tumor invasion through Bruch's membrane and diffuse intraocular tumor dissemination (6).

Limited information is available on the treatment of MH and vitreous hemorrhage in eyes with choroidal melanoma. Hypofractionated stereotactic radiotherapy with 50–70 Gy in five fractions or plaque brachytherapy has recently proven sufficient to preserve the eyeball and achieve excellent local tumor control in patients with choroidal melanoma (28, 30). Among these 11 cases we reviewed, two cases did not explicitly state whether a metastasis occurred and one case was unclear whether the macular hole developed before or after radiation treatment, but was lost to follow-up and metastatic disease was presumed. In the remaining cases, no metastases were found during follow-up. Besides, almost all eyes with treated melanoma had a good prognosis in terms of the MH after PPV and ILM peeling treatment. Beykin et al. retrospectively evaluated six patients with radiation-treated choroidal melanoma who developed retinal detachment and one who developed MH, all of whom underwent PPV and ultimately had attached retinas (12). During a 5-year follow-up period, Bianciotto et al. revealed that the resolution rate of vitreous hemorrhage in regressed melanoma eyes was as high as 72% after vitrectomy, and PPV did not increase the risk of tumor recurrence or distant metastasis, with low rates of 3% and 5%, respectively (29). Exceptionally, Foster et al. reported one patient with vitreous hemorrhage before tumor treatment who unfortunately developed intraocular tumor spread after PPV, while the remaining eight patients with tumor regression developed complications including vitreous hemorrhage, MH, or retinal detachment, but showed no tumor spread following PPV (6). Therefore, we consider the complication that happened before tumor treatment will increase the risk of metastasis. In contrast, metastasis is comparatively low if a complication occurs following tumor remission. The timing of vitrectomy in our case was 6 months after tumor radiotherapy and the shortest interval was 3 months in a previous case; with no evidence of tumor dissemination in either case during follow-up (9). The conservative interval for vitrectomy after tumor treatment is unclear, but definite tumor regression should be confirmed before carrying out vitrectomy or other intraocular surgery. Furthermore, direct contact with the tumor or direct instrument interaction should be minimized and all steps should be carried out carefully during surgery.

The expectation of visual improvement also needs to be considered, especially in patients with chronic MH. Two cases of choroidal melanoma still had poor vision after MH repair surgery (7, 12). Conversely, another case who developed MH 3 months after TTT had improved visual acuity from hand motion to 20/80 after timely vitrectomy (9), similar to the current case. PPV after

confirmed tumor regression thus seems to be a feasible and effective treatment in terms of anatomical and visual success, and may be more beneficial in cases with newly developed MH. A recent case report notably demonstrated extraocular extension of a brachytherapy-treated choroidal melanoma following PPV and scleral buckle for rhegmatogenous retinal detachment (31). Combined with previous reports, PPV, especially with ILM peeling, might increase the risk of tumor recurrence or migration of tumor cells, but the risks of these surgical complications in patients with regressed tumors are probably low (6). However, minimizing visual loss and preventing metastasis of malignant tumors still require careful assessment to balance the risks and benefits.

In conclusion, there have been few reports of choroidal melanoma complicated with MH and vitreous hemorrhage in the literature. Vitrectomy seems to be feasible for repairing MH in patients with regressed tumors. However, the occurrence of complications after intraocular tumor treatment and the safety of vitrectomy for these complications require longer follow-up and cautious management.

Data availability statement

The raw data supporting the conclusions of this article will be made available by the authors, without undue reservation.

Ethics statement

Ethical review and approval was not required for the study on human participants in accordance with the local legislation and institutional requirements. The patients/participants provided their written informed consent to participate in this study. Written informed consent was obtained from the individual(s) for the publication of any potentially identifiable images or data included in this article.

Author contributions

HI conceived the idea for the article. XZ performed the literature review and drafted the manuscript. HI and FG revised and approved the final version of the manuscript.

Funding

This study was supported by Hyogo Medical University Diversity Grant for Research Promotion" under MEXT Funds for the Development of Human Resources in Science and Technology, Initiative for Realizing Diversity in the Research Environment (Characteristic-Compatible Type).

Conflict of interest

The authors declare that the research was conducted in the absence of any commercial or financial relationships that could be construed as a potential conflict of interest.

Publisher's note

All claims expressed in this article are solely those of the authors and do not necessarily represent those of their affiliated organizations, or those of the publisher, the editors and the reviewers. Any product that may be evaluated in this article, or claim that may be made by its manufacturer, is not guaranteed or endorsed by the publisher.

References

1. Jager MJ, Shields CL, Cebulla CM, Abdel-Rahman MH, Grossniklaus HE, Stern MH, et al. Uveal melanoma. *Nat Rev Dis Primers* (2020) 6:18–20. doi: 10.1038/s41572-020-0158-0

2. Tomizuka T, Namikawa K, Higashi T. Characteristics of melanoma in Japan: A nationwide registry analysis 2011-2013. *Melanoma Res* (2017) 27:492–7. doi: 10.1097/CMR.0000000000000375

3. Reichstein DA, Brock AL. Radiation therapy for uveal melanoma: a review of treatment methods available in 2021. *Curr Opin Ophthalmol* (2021) 32:183–90. doi: 10.1097/ICU.0000000000000761

4. Thornton S, Coupland SE, Heimann H, Hussain R, Groenewald C, Kacperek A, et al. Effects of plaque brachytherapy and proton beam radiotherapy on prognostic testing: a comparison of uveal melanoma genotyped by microsatellite analysis. *Br J Ophthalmol* (2020) 104:1462–6. doi: 10.1136/bjophthalmol-2019-315363

5. Tsai YC, Kuo CY, Lin JW, Yang ST, Lai SC, Tsai JT. Gamma knife perfexion® radiosurgery and endo diode laser thermotherapy for choroidal melanoma with technical analysis: a case report. *Oncol Lett* (2018) 15:91–8. doi: 10.3892/ol.2017.7300

6. Foster WJ, Harbour JW, Holekamp NM, Shah GK, Thomas MA. Pars plana vitrectomy in eyes containing a treated posterior uveal melanoma. *Am J Ophthalmol* (2003) 136:471–6. doi: 10.1016/S0002-9394(03)00244-7

7. Gold AS, Bermudez E, Latiff A, Wildner AC, Ehlies FJ, Murray TG. Posterior uveal melanoma coexistent with macular hole. *Optom Vis Sci* (2013) 90:156–60. doi: 10.1097/OPX.0b013e3182924a9b

8. Narang S, Kochar S, Pannu KS, Kalra N, Gupta R, Sood S. Choroidal melanoma with macular hole. *Indian J Ophthalmol* (2004) 52:238–41. Available at: https://www.ijo.in/text.asp?2004/52/3/238/14582

9. Balestrazzi A, Blasi MA, Scupola TA, Balestrazzi TE. Retinal detachment due to macular hole after transpupillary thermotherapy of choroidal melanoma. *Retina* (2001) 21:384–5. doi: 10.1097/00006982-200108000-00019

10. Uffer S, Zografos L. Macular hole in a case of choroidal melanoma. *Eur J Ophthalmol* (1997) 7:115–8. doi: 10.1177/112067219700700121

11. Shields CL, Demirci H, Marr B, Mashayekhi A, Dai V, Materin M, et al. Intravitreal triamcinolone acetonide for acute radiation papillopathy. *Retina* (2006) 26:537–44. doi: 10.1097/00006982-200605000-00007

12. Beykin G, Pe'er J, Hemo Y, Frenkel S, Chowers I. Pars plana vitrectomy to repair retinal detachment following brachytherapy for uveal melanoma. *Br J Ophthalmol* (2013) 97:1534–7. doi: 10.1136/bjophthalmol-2013-303331

13. Damato B, Groenewald CP, McGalliard JN, Wong D. Rhegmatogenous retinal detachment after transscleral local resection of choroidal melanoma. *Ophthalmology* (2002) 109:2137–43. doi: 10.1016/S0161-6420(02)01240-X

14. Gündüz AK, Mirzayev I, Ceyhan K, Özalp Ateş FS. Transretinal biopsy *via* 23-gauge pars plana vitrectomy for retinal and choroidal tumors: cytopathological results, surgical complications, and patient outcomes. *Jpn J Ophthalmol* (2021) 65:250–60. doi: 10.1007/s10384-020-00795-4

15. McCannel TA, McCannel CA. Iodine 125 brachytherapy with vitrectomy and silicone oil in the treatment of uveal melanoma: 1-to-1 matched case-control series. *Int J Radiat Oncol Biol Phys* (2014) 89:347–52. doi: 10.1016/j.ijrobp.2014.02.021

16. Shields CL, Manalac J, Das C, Ferguson K, Shields JA. Choroidal melanoma: clinical features, classification, and top 10 pseudomelanomas. *Curr Opin Ophthalmol* (2014) 25(3):177–85. doi: 10.1097/ICU.0000000000000041

17. Duker JS, Kaiser PK, Binder S, De Smet MD, Gaudric A, Reichel E, et al. The international vitreomacular traction study group classification of vitreomacular adhesion, traction, and macular hole. *Ophthalmology* (2013) 120:2611–9. doi: 10.1016/j.ophtha.2013.07.042

18. Evans JR, Schwartz SD, McHugh JDA, Thamby-Rajah Y, Hodgson SA, Wormald RPL, et al. Systemic risk factors for idiopathic macular holes: a case control study. *Eye* (1998) 12:256–9. doi: 10.1038/eye.1998.60

19. Smiddy WE, Flynn HW. Pathogenesis of macular holes and therapeutic implications. *Am J Ophthalmol* (2004) 137:525–37. doi: 10.1016/j.ajo.2003.12.011

20. Bonnin N, Cornut P, Chaise F, Labeille E, Manificat HJ, Feldman A, et al. Spontaneous closure of macular holes secondary to posterior uveitis: case series and a literature review. *J Ophthalmic Inflammation Infect* (2013) 3:1–7. doi: 10.1186/1869-5760-3-34

21. Garoon RB, Shields CL, Kaliki S, Shields JA. Cystoid macular edema as the initial manifestation of choroidal melanoma. *Oman J Ophthalmol* (2012) 5:187–9. doi: 10.4103/0974-620X.106104

22. Michael JG, Venecia GDE. Retinal trypsin digest study of cystoid macular edema associated with peripheral choroidal melanoma. *Am J Ophthalmol* (1995) 119:152–6. doi: 10.1016/S0002-9394(14)73867-X

23. Puusaari I, Heikkonen J, Summanen P, Tarkkanen A, Kivela T. Iodine brachytherapy as an alternative to enucleation for large uveal melanomas. *Ophthalmology* (2003) 6420:2223–34. doi: 10.1016/S0161-6420(03)00661-4

24. Dunavoelgyi R, Dieckmann K, Gleiss A, Sacu S, Kircher K, Georgopoulos M, et al. Local tumor control, visual acuity, and survival after hypofractionated stereotactic photon radiotherapy of choroidal melanoma in 212 patients treated between 1997 and 2007. *Int J Radiat Oncol Biol Phys* (2011) 81:199–205. doi: 10.1016/j.ijrobp.2010.04.035

25. Jouhi S, Al-Jamal RT, Täll M, Eskelin S, Kivelä TT. Presumed incipient choroidal melanoma: Proposed diagnostic criteria and management. *Br J Ophthalmol* (2021) 1–6. doi: 10.1136/bjophthalmol-2020-318658

26. Puusaari I, Heikkonen J, Kivelä T. Ocular complications after iodine brachytherapy for large uveal melanomas. *Ophthalmology* (2004) 111:1768–77. doi: 10.1016/j.ophtha.2004.03.027

27. Mashayekhi A, Shields CL, Lee SC, Marr BP, Shields JA. Retinal break and rhegmatogenous retinal detachment after transpupillary thermotherapy as primary or adjunct treatment of choroidal melanoma. *Retina* (2008) 28:274–81. doi: 10.1097/IAE.0b013e318145abe8

28. Eibenberger K, Dunavoelgyi R, Gleiss A, Sedova A, Georg D, Poetter R, et al. Hypofractionated stereotactic photon radiotherapy of choroidal melanoma: 20-year experience. *Acta Oncol* (2021) 60:207–14. doi: 10.1080/0284186X.2020.1820572

29. Bianciotto C, Shields CL, Pirondini C, Mashayekhi A, Furuta M, Shields JA. Vitreous hemorrhage after plaque radiotherapy for uveal melanoma. *Retina* (2012) 32:1156–64. doi: 10.1097/IAE.0b013e3182340cc1

30. Relimpio-López I, Garrido-Hermosilla AM, Espejo F, Gessa-Sorroche M, Coca L, Domínguez B, et al. Clinical outcomes after surgical resection combined with brachytherapy for uveal melanomas. *J Clin Med* (2022) 11:1616. doi: 10.3390/jcm11061616

31. Shabto JM, Bergstrom CS, Wells JR. Extraocular extension of a regressed choroidal melanoma after vitrectomy and scleral buckle for rhegmatogenous retinal detachment. *Ophthalmology* (2022) 129:275. doi: 10.1016/j.ophtha.2021.07.029

frontiers | Frontiers in Oncology

TYPE Case Report
PUBLISHED 06 December 2022
DOI 10.3389/fonc.2022.1066191

OPEN ACCESS

EDITED BY
Ianik Plante,
KBRwyle, United States

REVIEWED BY
Mattia Falchetto Osti,
Sapienza University of Rome, Italy
Hidekazu Tanaka,
Yamaguchi University Graduate School of Medicine, Japan

*CORRESPONDENCE
Kathleen M. Schmainda
kathleen@mcw.edu

†These authors have contributed equally to this work

SPECIALTY SECTION
This article was submitted to Radiation Oncology, a section of the journal Frontiers in Oncology

RECEIVED 10 October 2022
ACCEPTED 21 November 2022
PUBLISHED 06 December 2022

CITATION
Amidon RF, Santos-Pinheiro F, Straza M, Prah MA, Mueller WM, Krucoff MO, Connelly JM, Kleefisch CJ, Coss DJ, Cochran EJ, Bovi JA, Schultz CJ and Schmainda KM (2022) Case report: Fractional brain tumor burden magnetic resonance mapping to assess response to pulsed low-dose-rate radiotherapy in newly-diagnosed glioblastoma. *Front. Oncol.* 12:1066191. doi: 10.3389/fonc.2022.1066191

Case report: Fractional brain tumor burden magnetic resonance mapping to assess response to pulsed low-dose-rate radiotherapy in newly-diagnosed glioblastoma

Ryan F. Amidon[1†], Fernando Santos-Pinheiro[2†], Michael Straza[3], Melissa A. Prah[4], Wade M. Mueller[5], Max O. Krucoff[5,6], Jennifer M. Connelly[2], Christopher J. Kleefisch[7], Dylan J. Coss[8], Elizabeth J. Cochran[8], Joseph A. Bovi[3,5], Christopher J. Schultz[3] and Kathleen M. Schmainda[4,7*]

[1]School of Medicine, Medical College of Wisconsin, Milwaukee, WI, United States, [2]Department of Neurology, Medical College of Wisconsin, Milwaukee, WI, United States, [3]Department of Radiation Oncology, Medical College of Wisconsin, Milwaukee, WI, United States, [4]Department of Biophysics, Medical College of Wisconsin, Milwaukee, WI, United States, [5]Department of Neurosurgery, Medical College of Wisconsin, Milwaukee, WI, United States, [6]Department of Biomedical Engineering, Marquette University and Medical College of Wisconsin, Milwaukee, WI, United States, [7]Department of Radiology, Medical College of Wisconsin, Milwaukee, WI, United States, [8]Department of Pathology, Medical College of Wisconsin, Milwaukee, WI, United States

Background: Pulsed low-dose-rate radiotherapy (pLDR) is a commonly used reirradiation technique for recurrent glioma, but its upfront use with temozolomide (TMZ) following primary resection of glioblastoma is currently under investigation. Because standard magnetic resonance imaging (MRI) has limitations in differentiating treatment effect from tumor progression in such applications, perfusion-weighted MRI (PWI) can be used to create fractional tumor burden (FTB) maps to spatially distinguish active tumor from treatment-related effect.

Methods: We performed PWI prior to re-resection in four patients with glioblastoma who had undergone upfront pLDR concurrent with TMZ who had radiographic suspicion for tumor progression at a median of 3 months (0-5 months or 0-143 days) post-pLDR. The pathologic diagnosis was compared to retrospectively-generated FTB maps.

Results: The median patient age was 55.5 years (50-60 years). All were male with IDH-wild type (n=4) and O^6-methylguanine-DNA methyltransferase (MGMT) hypermethylated (n=1) molecular markers. Pathologic diagnosis revealed treatment effect (n=2), a mixture of viable tumor and treatment effect (n=1), or viable tumor (n=1). In 3 of 4 cases, FTB maps were indicative of lesion volumes being comprised predominantly of treatment effect with

10.3389/fonc.2022.1066191

enhancing tumor volumes comprised of a median of 6.8% vascular tumor (6.4-16.4%).

Conclusion: This case series provides insight into the radiographic response to upfront pLDR and TMZ and the role for FTB mapping to distinguish tumor progression from treatment effect prior to redo-surgery and within 20 weeks post-radiation.

KEYWORDS

glioblastoma, pulsed low-dose-rate radiotherapy (pLDR), MRI, fractional tumor burden (FTB), relative cerebral blood volume (rCBV), pseudoprogression, treatment effect, tumor progression

Introduction

Glioblastoma is a primary central nervous system glioma designated as World Health Organization (WHO) grade 4 with wildtype isocitrate dehydrogenase (IDH-wt) (1). Patients with glioblastoma have a median overall survival of 12-15 months following diagnosis, with a five-year survival between 3 and 5.5% (2–5). The standard of care for glioblastoma includes surgical resection, chemoradiotherapy with temozolomide (TMZ) followed by adjuvant TMZ and tumor-treating fields (TTF) (5–9). Response to treatment is routinely assessed by magnetic resonance imaging (MRI). Pulsed low-dose-rate radiotherapy (pLDR) is a commonly used reirradiation technique for recurrent high-grade gliomas, but its upfront use with concurrent TMZ is currently under investigation (10–13). While other salvage therapies for recurrent high-grade glioma exist, including stereotactic radiosurgery, conformal external beam radiation, and brachytherapy, pLDR delivers radiation in subfractions at specific time intervals, taking advantage of the hyper-radiosensitivity of proliferating tumor cells to low doses of radiation, as well as the reduced toxicity to normal brain tissue (12, 14). Currently, there is limited data on the radiographic response to pLDR.

Distinguishing between treatment effect and tumor progression is challenging on standard imaging, with a definitive diagnosis only possible with pathologic confirmation. Radiotherapy may induce an inflammatory intraparenchymal response with subsequent necrosis and/or edema that is indistinguishable from, or intermingled with, tumor progression on MRI (15). Specifically, postcontrast MRI highlights blood-brain barrier disruption, which can be observed with both non-tumor and viable tumor tissue (15). Therefore, a new contrast-enhancing lesion arising within the radiation field of a treated glioblastoma can neither confirm nor refute progression of disease (16). A recent meta-analysis identified treatment effect in 36% of high-grade glioma cases (17). More recently, certain tumor and treatment factors have correlated with increased observation of treatment effect on MRI, including O^6-methylguanine-DNA methyltransferase (MGMT) promoter methylation, radiation dose, dose per fraction, treatment duration, irradiated brain volume, and concurrent use of TMZ (18–22).

Fractional tumor burden (FTB) mapping is a novel radiographic biomarker that spatially distinguishes viable high-grade tumor from treatment effect within postcontrast T1-weighted enhancement on MRI (23). These maps are generated from dynamic susceptibility contrast (DSC) MR perfusion, which allows for the visualization of regional cerebral blood volume (RCBV) to identify neovascularization. FTB maps use tissue-validated standardized regional cerebral blood volume (sRCBV) thresholds (23, 24) and assign primary colors to different perfusion patterns: treatment effect (blue; sRCBV < 1.0), tumor/treatment effect admixture (yellow; 1.0 > sRCBV < 1.6), and viable tumor (red; sRCBV > 1.6). Standardized thresholds are advantageous in that they require minimal user input compared to thresholds normalized based on user-defined reference tissues (25). It was demonstrated that regions of high-grade vascular tumor (yellow + red) could be distinguished from regions of treatment effect (blue) with a sensitivity/specificity of 79.4%/90% and an accuracy of 85% (23). Hoxworth et al. prospectively validated FTB maps with tissue, observing an 85% accuracy of identifying voxels with at least 50% viable tumor (25). Of note, Iv et al. determined that either the red or blue regions were best at distinguishing tumor from treatment effect, using a different sRCBV threshold of 1.75 (26).

In this case series, we present four patients with glioblastoma treated with upfront pLDR with concurrent TMZ following maximal safe resection. Treatment response was assessed by 3 Tesla (3T) MRI with and without contrast, FTB maps, and radiographic findings were confirmed by pathology.

10.3389/fonc.2022.1066191

Case descriptions

Case 1

A 50-year-old male presented with a progressive cognitive decline, expressive aphasia, and personality changes. Brain MRI revealed a non-enhancing small region of increased T2-weighted signal in the right frontal lobe; a follow-up MRI 25 weeks later revealed an avidly enhancing mass exhibiting significant mass effect. He was eventually submitted for craniotomy and gross-total resection of the enhancing lesion. Integrated diagnosis was consistent with glioblastoma, WHO grade 4, IDH-wt, and MGMT hypermethylated. At four-weeks post-surgery, there was improvement in cognitive performance although personality changes persisted. He was treated with pLDR as part of a prospective phase II study (NCT04747145) to a total dose of 60 Gray (Gy) in 30 fractions with concurrent TMZ, which he tolerated with anticipated side effects. This was followed by adjuvant TMZ and TTF.

The patient completed a total of four cycles of TMZ and TTF before MRI of the brain, obtained at 20 weeks post-pLDR, which raised concerns for tumor progression. Increased nodular enhancement around the resection cavity (Figure 1A) was observed in the setting of the patient experiencing neurocognitive decline. FTB maps revealed predominantly treatment effect with 70.3% non-tumor, 22.9% tumor admixture, and 6.8% tumor tissue (Figures 1B, D).

At 23 weeks post-pLDR, the patient was submitted for redo-craniotomy in the absence of FTB-guidance. Near-total resection

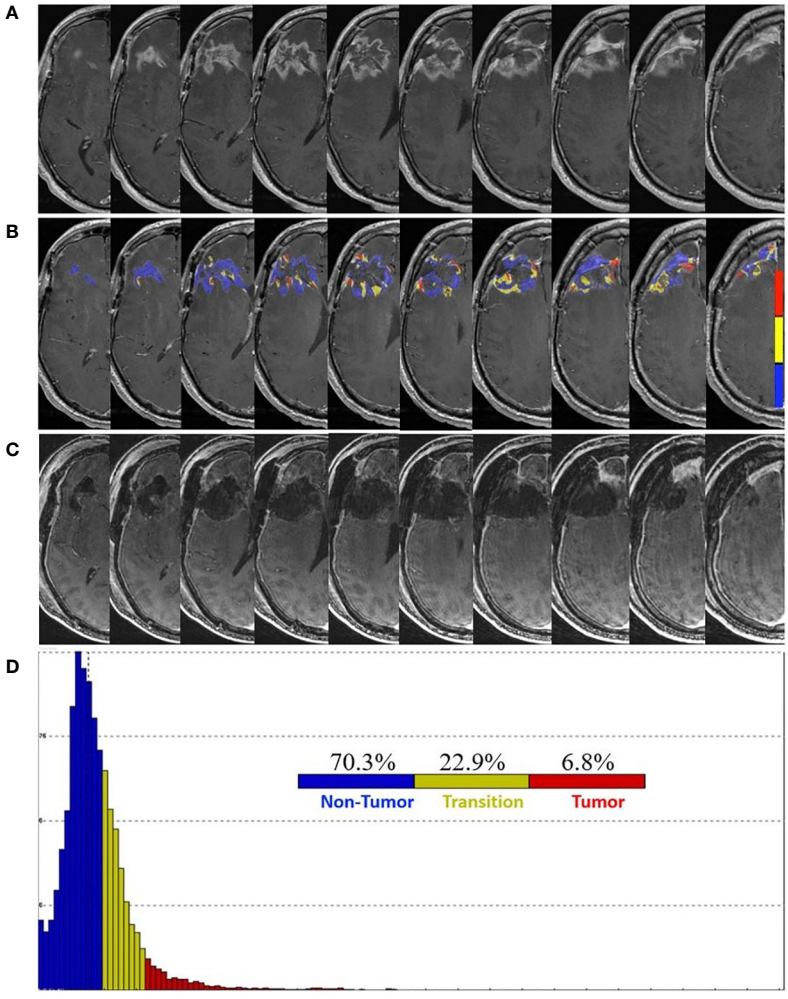

FIGURE 1
Pre- and post-surgery MRI. **(A)** Postcontrast T1-weighted MRI obtained 20 weeks following the completion of pLDR and two weeks before redo-surgery. **(B)** Corresponding maps of FTB superimposed on the postcontrast T1-weighted MRI images. The FTB maps show areas of active tumor (red), treatment effect (blue), and transitional zone (yellow). **(C)** Immediate post-operative postcontrast T1-weighted MRI demonstrating extent of resection. **(D)** Distribution of T1-weighted enhancement volume based on vascularization as measured by FTB maps.

of the enhancing lesion was later confirmed by postoperative MRI (Figure 1C). Microscopy of the five tissue specimens revealed a combination of necrosis, hyalinized and necrotic blood vessels, chronic inflammation, foamy macrophages, mineralization, and reactive gliosis, consistent with treatment effect. Therefore, the patient resumed adjuvant treatment with TMZ and TTF. Of note, compliance with TTF averaged 90% of "ON" time throughout the treatment period. At four weeks post-redo surgery, the patient remained clinically stable.

Case 2

A 56-year-old male presented with a history of seizure and expressive aphasia. Brain MRI revealed a left parietal mass with surrounding vasogenic edema and mass effect. Craniotomy and gross-total resection were performed, and integrated diagnosis was consistent with glioblastoma WHO grade 4, IDH-wt, and MGMT unmethylated. The patient was treated with pLDR as a part of a prospective phase II study (NCT04747145) to a total dose of 60 Gy in 30 fractions with concurrent TMZ followed by adjuvant TMZ and TTF.

At one week post-pLDR, there was clinical decline with MRI demonstrating significant vasogenic edema for which a bevacizumab infusion was provided every two weeks at 10 mg/kg. It was discontinued after two infusions due to a poor response and continued clinical decline. At five weeks post-pLDR, MRI demonstrated an increase in the left parietal peripherally enhancing lesion size (Figure 2A). FTB maps revealed predominantly treatment effect within the contrast enhancement surrounding the resection cavity with 84.0% non-tumor, 9.6% tumor admixture, and 6.4% tumor (Figures 2B, D).

At eight weeks post-pLDR, redo-craniotomy was performed in the absence of FTB-guidance. Reduced vasogenic edema and regions of enhancement around the resection cavity were later confirmed by MRI performed four weeks post-surgery (Figure 2C). Three tissue specimens were evaluated, two of which showed necrosis and hyalinized vessels, consistent with treatment effect, while the last sample revealed hypercellular high-grade glioma. The patient continued adjuvant treatment with TMZ and TTF. At nine weeks post-redo surgery, the patient's neurological symptoms included fatigue, right hemiparesis, and global aphasia. At 10 weeks post-redo surgery, he was restarted on bevacizumab at 10 mg/kg every 2 weeks, completing two infusions. Ultimately, he experienced a traumatic fall complicated by intraparenchymal hemorrhage and was transitioned to hospice.

Case 3

A 55-year-old male presented with a seizure, visual impairment and personality changes. Brain MRI revealed an enhancing left occipital mass surrounded by diffuse FLAIR hyperintensity signal. Craniotomy and gross-total resection were performed and integrated diagnosis was consistent with glioblastoma WHO grade 4, IDH-wt, and MGMT unmethylated. Following surgery, his symptoms included right hemiparesis, global aphasia, and a right homonymous hemianopsia. The patient was enrolled in a prospective phase II study (NCT04747145) to be treated with pLDR to a total dose of 60 Gy in 30 fractions with concurrent TMZ followed by adjuvant TMZ and TTF.

Near completion of pLDR (fraction 24) and 8 weeks post-surgery, he was admitted for worsening symptoms of gait dysfunction, nausea and vomiting, and dysphagia. MRI revealed increased enhancement around the resection cavity with increased mass effect and left ventricular trapping (Figure 3A). FTB maps revealed predominantly treatment effect within the contrast enhancement surrounding the resection cavity with 64.6% non-tumor, 19.1% tumor admixture, and 16.4% tumor (Figures 3B, D). Radiation was withheld and redo-craniotomy was performed in the absence of FTB-guidance. Five tissue specimens revealed necrotic tissue and sparse reactive brain tissue, consistent with treatment effect. Neurologically, the patient improved in memory and speech with residual comprehensive aphasia and right visual field defect. Bevacizumab was subsequently started at 10 mg/kg every 2 weeks.

The patient continued adjuvant treatment with bevacizumab, TMZ, and TTF. Of note, compliance with TTF averaged 75-90% of "ON" time throughout the treatment period. At one week post-surgery, brain MRI demonstrated retraction of the resection cavity and decreased peripheral enhancement along the surgical margins (Figure 3C). At 29 weeks post-redo surgery, the patient was transitioned to hospice, experienced respiratory failure caused by aspiration from worsening dysphagia and expired.

Case 4

A 60-year-old male presented with progressive left hemiparesis and memory decline. Brain MRI revealed an enhancing mass within the right frontal lobe that was resected. Integrated diagnosis was consistent with glioblastoma WHO grade 4, IDH-wt, and MGMT unmethylated. There was significant postoperative improvement in symptoms. The patient was treated with pLDR as a part of a prospective phase II study (NCT04747145) to a total dose of 60 Gy in 30 fractions with concurrent TMZ followed by adjuvant TMZ. Adjuvant TTF were declined.

Follow-up brain MRI studies demonstrated progressively increasing enhancement around the resection cavity. At 13 weeks post-pLDR, FTB maps revealed 47.9% non-tumor, 19.2% tumor admixture, and 32.9% tumor within the contrast-

10.3389/fonc.2022.1066191

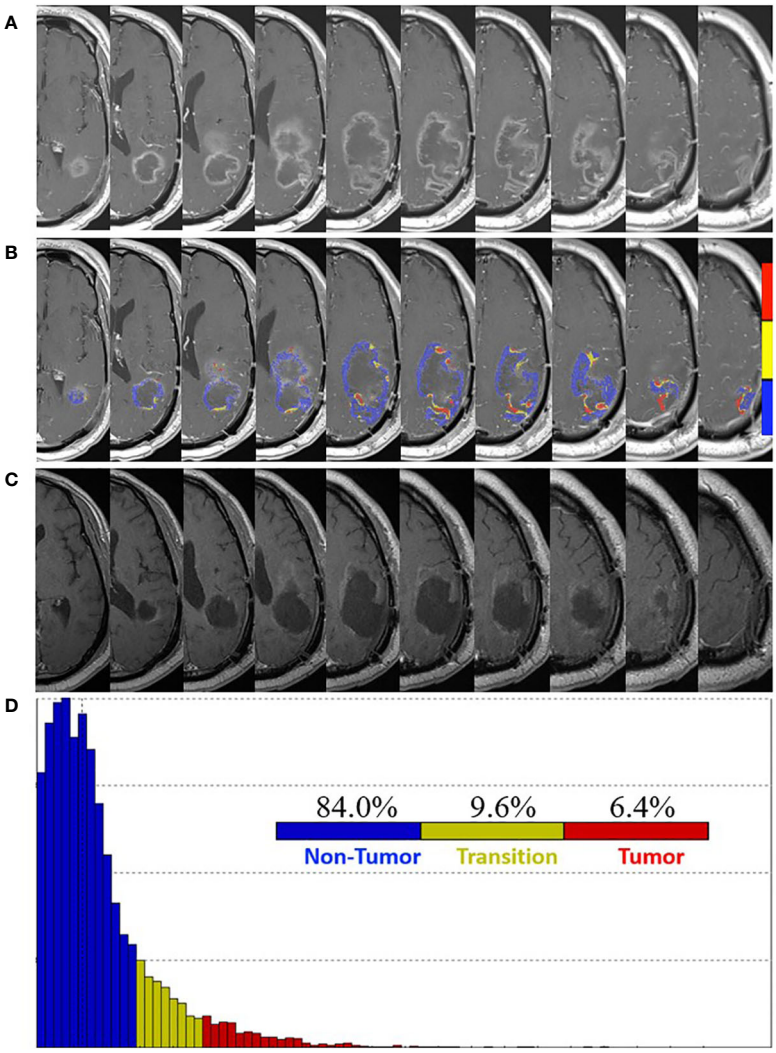

FIGURE 2
Pre- and post-surgery MRI. **(A)** Postcontrast T1-weighted MRI obtained five weeks post-pLDR and two weeks before redo-surgery. **(B)** Corresponding maps of FTB superimposed on the postcontrast T1-weighted MRI images. The FTB maps show areas of active tumor (red), treatment effect (blue), and transitional zone (yellow). **(C)** Post-surgery (four weeks) postcontrast T1-weighted MRI demonstrating extent of resection. **(D)** Distribution of T1-weighted enhancement volume based on vascularization as measured by FTB maps.

enhancing tissue. Seven weeks later, brain MRI demonstrated increased enhancement, particularly at the superomedial resection cavity margin (Figure 4A). FTB maps were again obtained with increasing proportions of vascular tumor tissue suggesting progression: 42.9% non-tumor, 13.5% tumor admixture, and 43.6% tumor (Figures 4B, D).

At 30 weeks post-pLDR, redo-craniotomy was performed in the absence of FTB-guidance. Significant debulking was later confirmed by MRI (Figure 4C). Two tissue specimens revealed moderately cellular atypical glial proliferation, supportive of active tumor. At three weeks post-redo surgery, the patient progressed with gait dysfunction, dysphagia, expressive aphasia, and left facial droop.

Discussion

This case series describes examples of how FTB can improve radiologic accuracy when used as a biomarker to assess treated glioblastoma. In one study, participating physicians determined that they would change treatment in 93% of cases where the tumor fraction was predominant and not change treatment in 75% of cases where treatment effect was predominant, based on their interpretation of FTB maps (26). The authors suggested the potential use of FTB for providing guidance in deciding which patients need an operation (26). In all four of the cases presented here, there were concerns about tumor progression based on standard 3T MRI. Pathologic examination revealed treatment

10.3389/fonc.2022.1066191

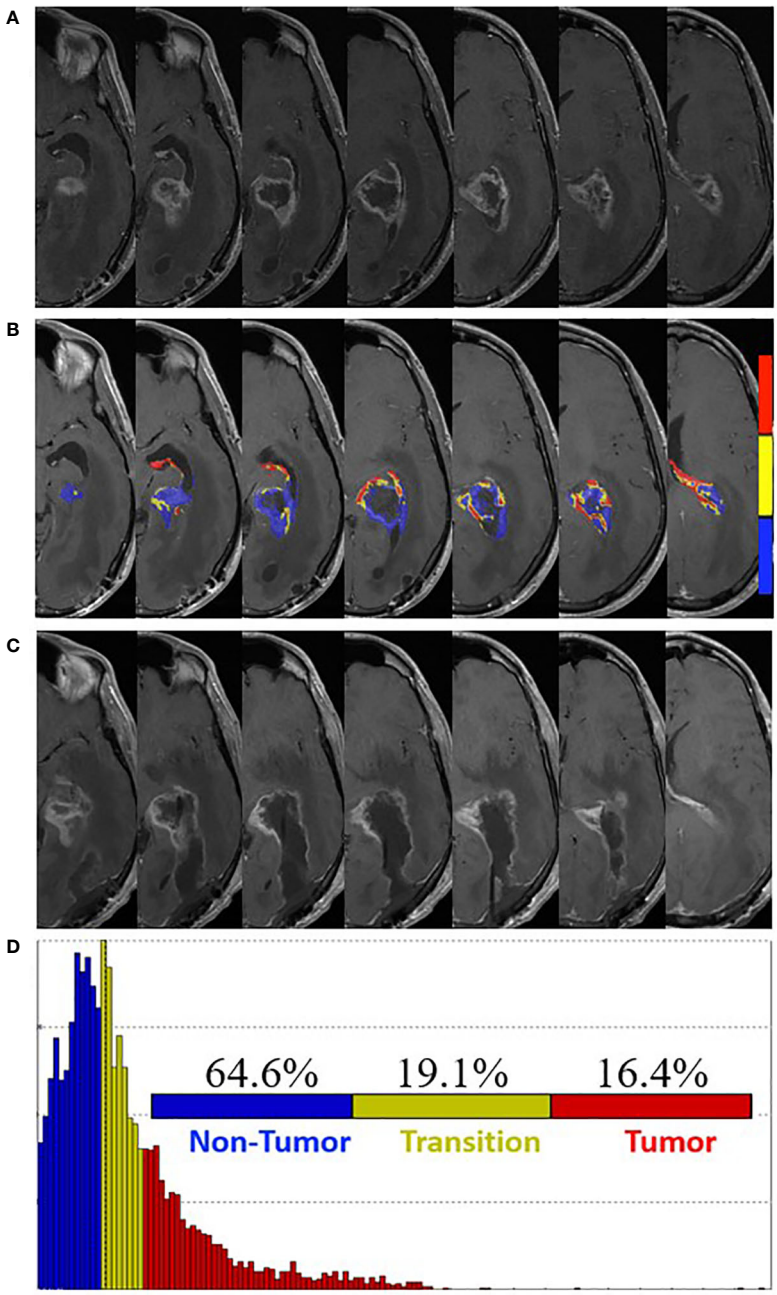

FIGURE 3
Pre- and post-surgery MRI. **(A)** Postcontrast T1-weighted MRI obtained four weeks post-pLDR treatment and one week before redo-surgery. **(B)** Corresponding maps of FTB superimposed on the postcontrast T1-weighted MRI images. The FTB maps show areas of active tumor (red), treatment effect (blue), and transitional zone (yellow). **(C)** Post-surgery (one week) postcontrast T1-weighted MRI demonstrating extent of resection. **(D)** Distribution of T1-weighted enhancement volume based on vascularization as measured by FTB maps.

effect in two cases and viable tumor in the other two cases. FTB maps were indicative of lesion volumes being comprised of predominantly treatment effect in three cases and predominantly viable tumor in one case. From the three FTB maps in the former category, the median fraction of the enhancing tumor volume comprised of vascular tumor was 6.8% (range 6.4-16.4%).

Radiologic assessment of treated glioblastoma remains a challenge as an indistinguishable MRI pattern between treatment effect and viable tumor may develop in about 36% of

10.3389/fonc.2022.1066191

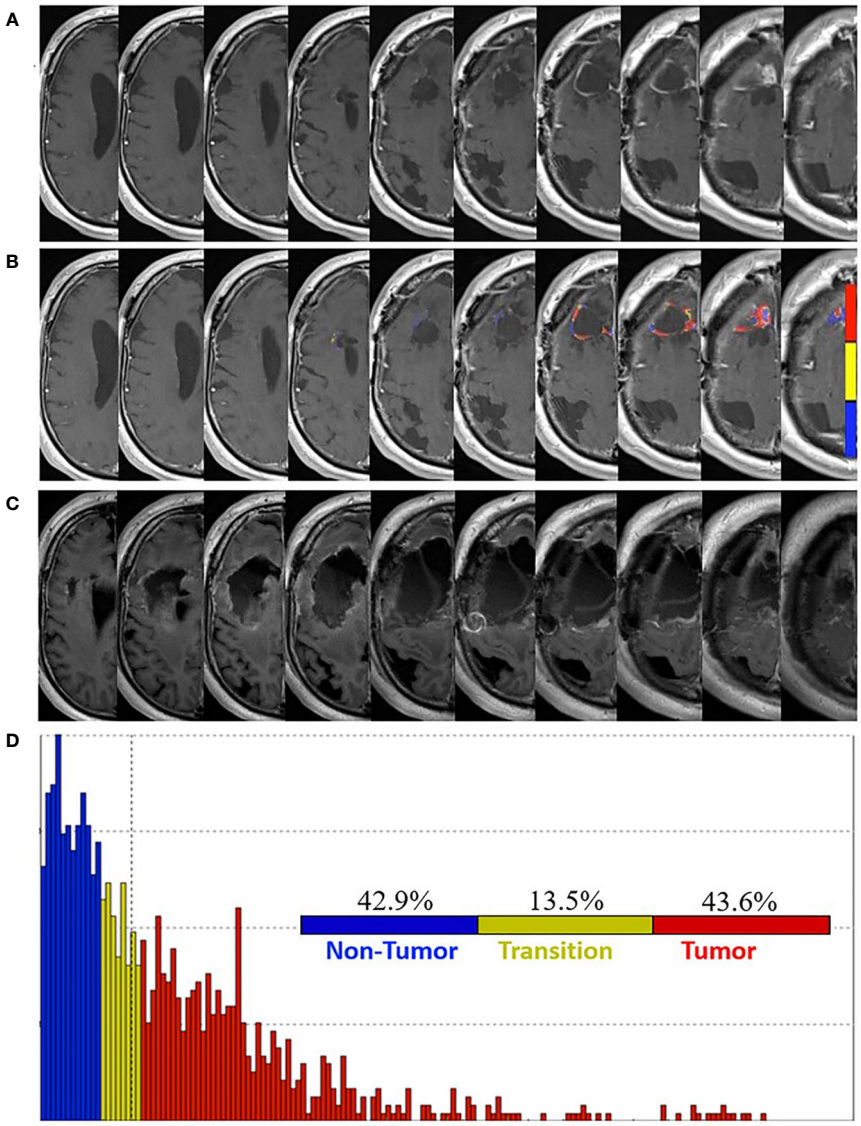

FIGURE 4
Pre- and post-surgery MRI. **(A)** Postcontrast T1-weighted MRI obtained 20 weeks post-pLDR and 10 weeks before redo-surgery. **(B)** Corresponding maps of FTB superimposed on the postcontrast T1-weighted MRI images. The FTB maps show areas of active tumor (red), treatment effect (blue), and transitional zone (yellow). **(C)** Immediate post-operative postcontrast T1-weighted MRI with FLAIR demonstrating extent of resection, which encompasses regions of tumor identified in the FTB maps. **(D)** Distribution of T1-weighted enhancement volume based on vascularization as measured by FTB maps.

these cases (17). Often, with no other options, biopsy or surgery is pursued for diagnostic confirmation, posing potentially unnecessary risks. This common scenario highlights the need for more accurate radiologic biomarkers that not only guide treatment but also prevent unnecessary surgical intervention. This is of particular importance with heterogenous tumors such as glioblastoma that are more prone to sampling error. FTB maps provide meaningful information regarding the spatial distribution of tumor and treatment effect within enhancing lesions and may be able to fill that gap.

There are several limitations to this study. FTB maps were generated retrospectively and therefore not used for surgical guidance or tissue confirmation in none of the four cases. It also does not provide information about the clinical course of the disease. Monitoring FTB over time may provide additional information to evaluate this, as demonstrated in Case 4. We also assume that the pathology reports are always accurate, when sampling bias may occur. For instance, it is unknown whether an active tumor is in the process of dying or may die in the near future, especially if it is sampled too soon following radiation. In

parallel, bevacizumab as a treatment for symptomatic radiation necrosis in Cases 2 and 3 may have confounded their respective radiologic responses to pLDR, as it may reduce the area of enhancing necrosis by decreasing vascular permeability and inflammation (27). Finally, the small sample size from our single institution limits generalizability.

This case series provides insight into response to upfront pLDR concurrent with TMZ following resection of newly diagnosed glioblastoma. It also highlights the capacity of FTB maps to accurately distinguish tumor progression from treatment effect. Therefore, full validation of FTB mapping as a biomarker should be pursued as a prospective study with larger sample size.

Data availability statement

The original contributions presented in the study are included in the article/supplementary material. Further inquiries can be directed to the corresponding author.

Ethics statement

The studies involving human participants were reviewed and approved by Medical College of Wisconsin Institutional Review Board. The patients/participants provided their written informed consent to participate in this study. Written informed consent was obtained from the individual(s) for the publication of any potentially identifiable images or data included in this article.

Author contributions

FS-P, MS, WM, and MK treated the patients. DC and EC analyzed tissue samples and generated pathology reports for the patients. RA wrote the first draft of the manuscript and generated figures. MP and KS performed image processing and generated the FTB maps. MP, MS, FS, WM, MK, CK, DC, EC, JB, CS, and KS edited the paper. All authors contributed to the article and approved the submitted version.

Funding

Funding support was provided by NIH/NCI U01CA176110, NIH/NCI R01CA255123 and NIH/NCI R01CA264992.

Acknowledgments

Cathy Marszalkowski and Jaimy Pettit research coordinators, for obtaining consents from patients and managing the extensive brain tumor database.

Conflict of interest

KS has ownership interest in IQ-AI Ltd, and financial interest in Imaging Biometrics LLC. Processing software from Imaging Biometrics LLC was used for processing the MRI images. WM is a member of the medical advisory board for Prism Clinical Imaging Inc. KS also has ownership interest in Prism Clinical Imaging Inc.

The remaining authors declare that the research was conducted in the absence of any commercial or financial relationships that could be construed as a potential conflict of interest.

Publisher's note

References

1. Louis DN, Perry A, Wesseling P, Brat DJ, Cree IA, Figarella-Branger D, et al. The 2021 WHO classification of tumors of the central nervous system: A summary. *Neuro Oncol* (2021) 23:1231–51. doi: 10.1093/neuonc/noab106

2. Ostrom QT, Gittleman H, Xu J, Kromer C, Wolinsky Y, Kruchko C, et al. CBTRUS statistical report: Primary brain and other central nervous system tumors diagnosed in the united states in 2009-2013. *Neuro Oncol* (2016) 18(suppl_5):v1–v75. doi: 10.1093/neuonc/now207

3. Korja M, Raj R, Seppä K, Luostarinen T, Malila N, Seppälä M, et al. Glioblastoma survival is improving despite increasing incidence rates: A nationwide study between 2000 and 2013 in Finland. *Neuro Oncol* (2019) 21:370–9. doi: 10.1093/neuonc/noy164

4. Chien LN, Gittleman H, Ostrom QT, Hung KS, Sloan AE, Hsieh YC, et al. Comparative brain and central nervous system tumor incidence and survival between the united states and Taiwan based on population-based registry. *Front Public Health* (2016) 4:151. doi: 10.3389/fpubh.2016.00151

5. Stupp R, Mason WP, van den Bent MJ, Weller M, Fisher B, Taphoorn MJ, et al. Radiotherapy plus concomitant and adjuvant temozolomide for glioblastoma. *N Engl J Med* (2005) 352:987–96. doi: 10.1056/NEJMoa043330

6. Stupp R, Hegi ME, Mason WP, van den Bent MJ, Taphoorn MJ, Janzer RC, et al. Effects of radiotherapy with concomitant and adjuvant temozolomide versus radiotherapy alone on survival in glioblastoma in a randomised phase III study: 5-

year analysis of the EORTC-NCIC trial. *Lancet Oncol* (2009) 10:459–66. doi: 10.1016/S1470-2045(09)70025-7

7. Herrlinger U, Tzaridis T, Mack F, Steinbach JP, Schlegel U, Sabel M, et al. Lomustine-temozolomide combination therapy versus standard temozolomide therapy in patients with newly diagnosed glioblastoma with methylated MGMT promoter (CeTeG/NOA-09): a randomised, open-label, phase 3 trial. *Lancet* (2019) 393:678–88. doi: 10.1016/S0140-6736(18)31791-4

8. Stupp R, Taillibert S, Kanner AA, Kesari S, Steinberg DM, Toms SA, et al. Maintenance therapy with tumor-treating fields plus temozolomide vs temozolomide alone for glioblastoma: A randomized clinical trial. *JAMA* (2015) 314:2535–43. doi: 10.1001/jama.2015.16669

9. Stupp R, Taillibert S, Kanner A, Read W, Steinberg D, Lhermitte B, et al. Effect of tumor-treating fields plus maintenance temozolomide vs maintenance temozolomide alone on survival in patients with glioblastoma: A randomized clinical trial. *JAMA* (2017) 318:2306–16. doi: 10.1001/jama.2017.18718

10. Cannon GM, Tomé WA, Robins HI, Howard SP. Pulsed reduced dose-rate radiotherapy: Case report: a novel re-treatment strategy in the management of recurrent glioblastoma multiforme. *J Neurooncol* (2007) 83:307–11. doi: 10.1007/s11060-007-9329-z

11. Murphy ES, Rogacki K, Godley A, Qi P, Reddy CA, Ahluwalia MS, et al. Intensity modulated radiation therapy with pulsed reduced dose rate as a reirradiation strategy for recurrent central nervous system tumors: An institutional series and literature review. *Pract Radiat Oncol* (2017) 7:e391–9. doi: 10.1016/j.prro.2017.04.003

12. Bovi JA, Prah MA, Retzlaff AA, Schmainda KM, Connelly JM, Rand SD, et al. Pulsed reduced dose rate radiotherapy in conjunction with bevacizumab or bevacizumab alone in recurrent high-grade glioma: Survival outcomes. *Int J Radiat Oncol Biol Phys* (2020) 108(4):979–86. doi: 10.1016/j.ijrobp.2020.06.020

13. Prabhu AV, Lee M, Galhardo E, Newkirk M, Rodriguez A, Xia F. Pulsed reduced dose-rate radiotherapy for previously irradiated tumors in the brain and spine. *Surg Neurol Int* (2021) 12:280. doi: 10.25259/SNI_589_2020

14. Ma CMC. Pulsed low dose-rate radiotherapy: Radiobiology and dosimetry. *Phys Med Biol* (2022) 67:03TR01. doi: 10.1088/1361-6560/ac4c2f

15. Nichelli L, Casagranda S. Current emerging MRI tools for radionecrosis and pseudoprogression diagnosis. *Curr Opin Oncol* (2021) 33:597–607. doi: 10.1097/CCO.0000000000000793

16. Raimbault A, Cazals X, Lauvin MA, Destrieux C, Chapet S, Cottier JP. Radionecrosis of malignant glioma and cerebral metastasis: A diagnostic challenge in MRI. *Diagn Interv Imaging* (2014) 95:985–1000. doi: 10.1016/j.diii.2014.06.013

17. Abbasi AW, Westerlaan HE, Holtman GA, Aden KM, van Laar PJ, van der Hoorn A. Incidence of tumour progression and pseudoprogression in high-grade gliomas: A systematic review and meta-analysis. *Clin Neuroradiol* (2018) 28:401–11. doi: 10.1007/s00062-017-0584-x

18. Brandes AA, Franceschi E, Tosoni A, Blatt V, Pession A, Tallini G, et al. MGMT promoter methylation status can predict the incidence and outcome of pseudoprogression after concomitant radiochemotherapy in newly diagnosed glioblastoma patients. *J Clin Oncol* (2008) 26:2192–7. doi: 10.1200/JCO.2007.14.8163

19. Verma N, Cowperthwaite MC, Burnett MG, Markey MK. Differentiating tumor recurrence from treatment necrosis: A review of neuro-oncologic imaging strategies. *Neuro Oncol* (2013) 15:515–34. doi: 10.1093/neuonc/nos307

20. Donovan EK, Parpia S, Greenspoon JN. Incidence of radionecrosis in single-fraction radiosurgery compared with fractionated radiotherapy in the treatment of brain metastasis. *Curr Oncol* (2019) 26:e328–33. doi: 10.3747/co.26.4749

21. Lee AW, Kwong DL, Leung SF, Tung SY, Sze WM, Sham JS, et al. Factors affecting risk of symptomatic temporal lobe necrosis: Significance of fractional dose and treatment time. *Int J Radiat Oncol Biol Phys* (2002) 53:75–85. doi: 10.1016/s0360-3016(02)02711-6

22. Brandsma D, Stalpers L, Taal W, Sminia P, van den Bent MJ. Clinical features, mechanisms, and management of pseudoprogression in malignant gliomas. *Lancet Oncol* (2008) 9:453–61. doi: 10.1016/S1470-2045(08)70125-6

23. Prah MA, Al-Gizawiy MM, Mueller WM, Cochran EJ, Hoffmann RG, Connelly JM, et al. Spatial discrimination of glioblastoma and treatment effect with histologically-validated perfusion and diffusion magnetic resonance imaging metrics. *J Neurooncol* (2018) 136:13–21. doi: 10.1007/s11060-017-2617-3

24. Hu LS, Eschbacher JM, Heiserman JE, Dueck AC, Shapiro WR, Liu S, et al. Reevaluating the imaging definition of tumor progression: Perfusion MRI quantifies recurrent glioblastoma tumor fraction, pseudoprogression, and radiation necrosis to predict survival. *Neuro Oncol* (2012) 14:919–30. doi: 10.1093/neuonc/nos112

25. Hoxworth JM, Eschbacher JM, Gonzales AC, Singleton KW, Leon GD, Smith KA, et al. Performance of standardized relative CBV for quantifying regional histologic tumor burden in recurrent high-grade glioma: Comparison against normalized relative CBV using image-localized stereotactic biopsies. *AJNR Am J Neuroradiol* (2020) 41:408–15. doi: 10.3174/ajnr.A6486

26. Iv M, Liu X, Lavezo J, Gentles AJ, Ghanem R, Lummus S, et al. Perfusion MRI-based fractional tumor burden differentiates between tumor and treatment effect in recurrent glioblastomas and informs clinical decision-making. *AJNR Am J Neuroradiol* (2019) 40:1649–57. doi: 10.3174/ajnr.A6211

27. Yonezawa S, Miwa K, Shinoda J, Nomura Y, Asano Y, Nakayama N, et al. Bevacizumab treatment leads to observable morphological and metabolic changes in brain radiation necrosis. *J Neurooncol* (2014) 119:101–9. doi: 10.1007/s11060-014-1453-y

frontiers | Frontiers in Oncology

TYPE Case Report
PUBLISHED 05 January 2023
DOI 10.3389/fonc.2022.995376

OPEN ACCESS

EDITED BY
Ianik Plante,
KBRwyle, United States

REVIEWED BY
Romain Natale,
Clinique Saint Jean, France
Florent Vilotte,
Institut Bergonié, France

*CORRESPONDENCE
Rémy Kinj
remy.kinj@chuv.ch

SPECIALTY SECTION
This article was submitted to Radiation Oncology, a section of the journal Frontiers in Oncology

RECEIVED 26 July 2022
ACCEPTED 09 December 2022
PUBLISHED 05 January 2023

CITATION
Bentahila R, Kinj R, Huck C, El Houat Y, Mampuya A, Tuleasca C, Ozsahin M, Bourhis J and Schiappacasse L (2023) Re-irradiation of recurrent vertebral metastasis after two previous spinal cord irradiation: A case report. *Front. Oncol.* 12:995376. doi: 10.3389/fonc.2022.995376

Re-irradiation of recurrent vertebral metastasis after two previous spinal cord irradiation: A case report

Rita Bentahila[1], Rémy Kinj[1]*, Constance Huck[1], Yasmine El Houat[1], Ange Mampuya[1], Constantin Tuleasca[2], Mahmut Ozsahin[1], Jean Bourhis[1] and Luis Schiappacasse[1]

[1]Department of Radiation Oncology, Lausanne University Hospital (CHUV), Lausanne, Switzerland, [2]Department of Neurosurgery, Lausanne University Hospital (CHUV), Lausanne, Switzerland

Background: Management of a recurrent vertebral metastasis in a situation of previously irradiated spinal cord is a challenging clinical dilemma.

Case presentation: We report a first case of second retreatment of a spinal metastasis initially irradiated with standard radiotherapy and stereotactic body radiation therapy (SBRT), who subsequently progressed with imaging-confirmed local tumor progression at the same level. After a third course of irradiation with SBRT, a complete response was achieved. After 8 months of follow-up, the patients remain free of local recurrence.

Conclusion: A third course of vertebral irradiation for a recurrent vertebral metastasis failing to two previous irradiations, in this particular case, have shown the feasibility and efficacy of the technique as a salvage treatment option. This approach could be used in a selected group of patient if an adequate dose is delivered to the target while observing critical tissue tolerance limits.

KEYWORDS

retreatment, spine, stereotactic radiation, vertebral metastases, radiosurgery

Introduction

In recent years, the development of Stereotactic Body Radiotherapy (SBRT) for spinal metastases is emerging as a safe and effective ablative treatment for recurrent tumors. Modern prospective series and randomized trials have shown promising results on local control and pain relief of bone metastases (1, 2).

However, in the particular case of vertebral reirradiation, there have been concerns about spinal cord toxicity when treating recurrent metastases after conventional palliative radiotherapy or a first course of SBRT.

There are some reports about the safety and efficacy of SBRT in previously irradiated vertebral metastases (3–7), but to our knowledge, no report have been published for a patient treated several times.

In this report, we describe our experience with a single patient receiving a third irradiation for a T8 vertebral metastasis secondary to an invasive ductal carcinoma 15 years after the first conventional (2D) irradiation and 3 years after a first SBRT over the same lesion.

Case presentation

We herein report the case of a women born in 1962 who was diagnosed with an invasive ductal carcinoma pT1b (0.9 cm) pN1a (2/17) cM0, grade 2, ER-positive and HER-2 positive in 1998. She underwent a right breast-conserving surgery and axillary lymph nodes dissection. After surgery, she received adjuvant treatment including chemotherapy, whole breast radiotherapy (including internal mammary chain (IMC) irradiation) and endocrine therapy by tamoxifen.

During the follow-up in 2006, a Fluoro-2-deoxy-D-glucose (FDG) PET-CT scan revealed an oligoprogression in the form of a regional submammary nodule and two bone metastases (T8 and left iliac wing). A biopsy confirmed the diagnosis of invasive ductal carcinoma grade 2, ER-positive and HER-2 positive.

Spine MRI showed a large lytic metastasis of the T8 vertebra with wedge compression (Bilsky grade 1a with epidural impingement) (Figure 1A) (8).

The patient received a conventional (2D) radiotherapy to the T7-T9 spine delivering a dose 30 Gy in 12 fractions of 2.5 Gy in April 2006, using a Siemens Primus linear accelerator system (Siemens, Concord CA, US). Patients planning images with dose distribution are shown in Figure 2A.

She started a systemic therapy with Leuprorelin acetate, Letrozole, and Ibandronate until January 2014.

In July 2014, evaluation with MRI and (FDG) PET-CT imaging revealed an osteolytic lesion of the anterior portion of the T8 vertebra body, in the previous treated field, suspect of local progression (Figure 1B).

A new biopsy of the T8 vertebra confirmed the recurrence of invasive ductal carcinoma. This was followed by a vertebral body cementoplasty on September 2014.

Spine surgery evaluation was not performed because, as shown by the radiotherapy scheme chosen in 2006, at that time the patient was considered a strictly palliative case, being managed as such outside from our institution.

A re-irradiation of the previously described T8 lesion using SBRT with a dose of 18 Gy in 3 fractions at isodose 80% was performed; the irradiation volume only included hypercaptation on PET-CT (Figure 2B). A CyberKnife robotic stereotactic radiotherapy system (Accuray, Sunnyvale, Concord CA, US) was used. This treatment was delivered using the Xsight spine tracking system, which co-relates imaging using bony anatomy for continuous imaging, repositioning, and tracking without fiducials, allowing a tracking of the target in real time. Doses

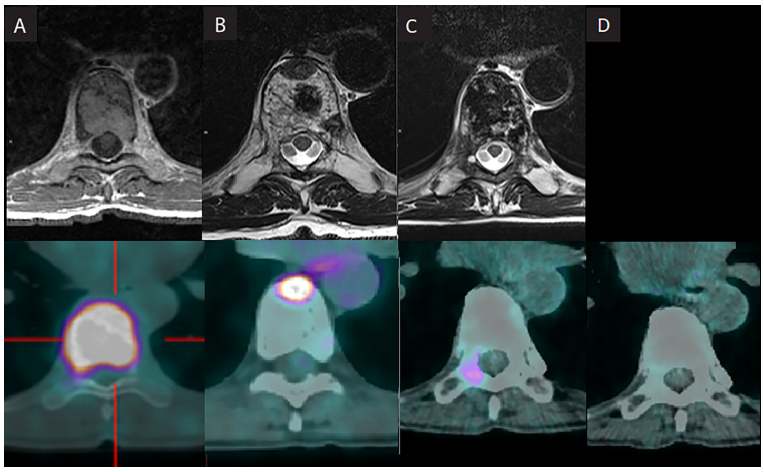

FIGURE 1
(A–C) T8 metastasis evolution after iterative irradiation. **(A)** 2006: First presentation: large deposit in the D8 vertebra with wedge compression (Bilsky grade 1a with epidural impingement). **(B)** 2014: First recurrence: osseous lysis lesion of the anterior portion of the T8 vertebra body **(C)**. 2021: Further recurrence: right transverse pedicle of D8 vertebra **(D)**. 2022: Recent follow-up (April 2022) showing complete response.

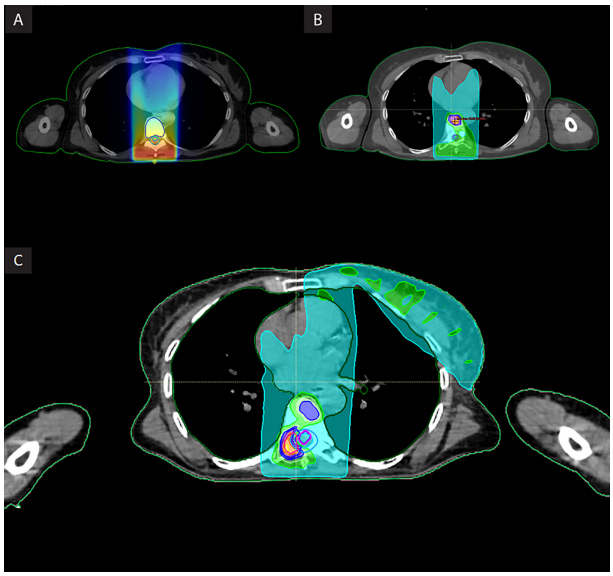

FIGURE 2
(A–C) Patient's planning image with cumulative dose distribution. **(A)**. First course of 2D radiotherapy (30 Gy in 12 fractions) **(B)**. First re-irradiation vertebral SBRT (18 Gy in 3 fractions) **(C)**. Composite dose including vertebral after second SBRT (30 Gy in 5 fractions).

were calculated using Precision Treatment Planning system (Accuray, Sunnyvale, Concord CA, US).

Following SBRT, the patient resumed systemic therapy with Trastuzumab and endocrine therapy until July 2015.

From July 2015 to January 2021, evaluation with FDG PET-CT imaging revealed oligoprogressive disease with bone lesions (C1, T6 and T8 vertebra, right acetabulum, left clavicle and left iliac wing), confirmed by biopsy. These lesions were treated with several lines of systemic therapy and SBRT over all lesions (with good metabolic response) except T8.

The T8 vertebra metastasis relapsed on right transverse pedicle and was treated using radiofrequency ablation in April 2018 (with complete response) and three more times in 2021, after new recurrences, obtaining only partial responses.

In October 2021, despite iterative radiofrequency treatments follow up with (FDG) PET-CT scan showed a new local progression on the right transverse pedicle of T8 vertebra (Figure 1C).

Spine surgery team evaluated the patient, and confirmed that surgery was not an option due to the technical challenge and the important risks inherent to this procedure.

Considering the short time between local recurrences after radiofrequency ablation, and after a dosimetric evaluation considering all radiation treatments impacting T8, a new SBRT was decided.

Before the last SBRT was performed, it was explained to the patient that there was a risk of radiculitis at the D9 level, due to the impossibility of respecting the tolerance dose of this nerve root, because of the previous delivered radiation.

A dose of 30 Gy in 5 fractions at isodose 80% (maximum dose in the PTV: 37.5 Gy.) was planned for the second course of SBRT (third course of irradiation) using a CyberKnife system (Figure 2C). This scheme is based on the one used at MD Anderson Cancer Center and published by Chang et al. in 2007.

Dose limits to the critical neural tissues (CNT) was determined using Sahgal et al. re-irradiation recommendations (9), and the report of the AAPM Task Group 101 on SBRT. For the calculations considering the spinal cord we used an α/β of 2; for the rest of OAR, an α/β of 3. Velocity AI software (Varian Medical Systems, Inc., Palo Alto, CA, US) was used to convert the different schemes and different fractionations to the equivalent in EQD2, giving an α/β ratio for the spinal cord of 2. We then performed a summation of all recalculated schemes in EQD2, using a rigid fusion and a ROI involving the region of the spine to be reirradiated. Then we calculated the residual safety margin (or dose limit) at the spinal cord level and other OARs, which we used to plan the treatment without exceeding the previously described constraints.

Technical characteristics of plans and dose parameters for all radiation treatments are shown in Table 1.

After calculation of a composite dose in equivalent total doses in 2-Gy fractions (EQD_2) of all the previous described treatments (including the IMC field dose contribution) spinal cord received a maximum dose (Dmax, 0.035 cc) of 42.78 Gy.

Patient completed re-irradiation SBRT without any side effect.

Following this treatment with SBRT re-irradiation, the patient resumed systemic treatment with Trastuzumab and Emtansine.

TABLE 1 Technical characteristics of plans and dose parameters for all radiation treatments.

Parameters	2D-conventional radiotherapy (1rst course)*	Re-irradiation SBRT (2nd course)	Re-irradiation SBRT (3rd course)	Cumulative dose
Dose fractionation [Gy]	30 Gy in 12 fractions	18 Gy in 3 fractions	30 Gy in 5 fractions	
Technique	2D radiotherapy	SBRT	SBRT	2D + SBRT
PTV volume [cm^3]	N/A	2.76	5.87	
PTV D95%	N/A	19.02 Gy	23.43 Gy	
PTV D50%	N/A	20.16 Gy	33.88 Gy	
Organs at risk (OARs) Spinal cord D_{max} EQD_2 [Gy]	34.7	2.89	3.94	42.78

Gy — Gray; cm^3 — cubic centimetre; D_x cm^3 — dose received by × cm^3 of volume; D_{max} — maximum dose; EQD_2 — equivalent dose in 2 Gy.
*We have included the dose delivered during the IMC irradiation (Dmax 5.46 Gy, corresponding to an EQD_2 of 3.05 Gy).
NA, not available.

At 8 months of follow-up after the third course of irradiation, most recent assessment with (FDG) PET-CT scan shows complete response of the T8 vertebra metastasis (Figure 1D).

No evidence of toxicity secondary to the third course of irradiation according to CTCAE v.5 scale has been observed.

Discussion

Treating vertebral metastases in the context of a previously irradiated spinal cord is a challenging clinical dilemma. Vertebras are a complex site for SBRT due to the proximity of the spinal cord. Risk of myelopathy and potential toxicity of progressive tumors must be carefully balanced by the radiation oncologist when evaluating the feasibility of a radiotherapeutic approach.

The most common site of distant breast metastases, occurring in around 40 to 51% of metastatic patients, is bone (10). An increment in the use of new imaging technologies and (FDG) PET-CT during the follow-up might be responsible for the increased incidence in diagnosis of isolated bone metastasis.

Moreover, in a context of prolonged survival due to new systemic and focal treatments, vertebral recurrences incidence tend to increase and their management becomes more challenging.

For a second course irradiation, often with 30 Gy in 5 fractions, most retrospective studies exhibited consistent results in terms of pain relief and sustained local control (3–7).

In a cohort of 59 patients, Garg et al. conducted a study on a single re-irradiation after spinal SBRT. The 1-year radiographic local control and overall survival for all patients was 76% (4). In a retrospective study, Thibault et al. concluded that a salvage second-course vertebral SBRT is feasible and efficacious after in-field failure of the first course of SBRT for spinal metastases. The median time to failure after the first course of SBRT was 11.7 months (7).

We report a first case of reirradiation of a vertebral recurrence after two previous courses of radiotherapy.

Time between the first irradiation and the second was 15 years, and 3 years between the second and third irradiation over the same lesion.

The time interval between two courses of radiation is not yet validated as a protective factor for toxicity. Therefore, the time-dependent recovery of neurological function and cumulative spinal cord dose limits remains largely hypothetical. Sahgal et al. suggests that SBRT given at least 5 months after conventional palliative radiotherapy appears to be safe, if several conditions are met (9).

At the time of last T8 progression, the patient presented a low burden volume of metastatic disease.

The recurrences were located in different parts of the T8 vertebra. Failure might be cause by insufficient extension of the radiation field beyond the visible tumor (not including pedicles and posteriors elements) or underdosed epidural space in order to limit spinal cord dose (11–13).

Dmax over the spinal cord was still not reached during two previous irradiations (conventional radiotherapy and SBRT) and distance between the targeted lesion (T8) and the spinal cord allowed us to avoid this critical organ, delivering radiation safely and respecting spinal cord constraints.

Following the previous described data, and on the basis of the published literature by Nieder et al. that described reirradiation spinal cord tolerances (14), a third course of radiation was decided.

With the support of our spinal surgery team, we have decided to accept the risk of radiculitis at the D9 level in order to avoid potential spinal cord threat due to the lack of control of this metastatic lesion. In the event of this complication, a surgical procedure would allow desensitization of this root, with only sensory consequences at the level of this dermatome for the patient.

A local complete response was achieved. After 6 months of follow-up, the patient remains without local recurrence and asymptomatic.

The benefits of SBRT, besides of local control, extend to the possibility of delaying the start of a new line of systemic treatment.

This case is the first case report on re-irradiating a vertebra after a conventional radiotherapy and SBRT previous courses of radiotherapy.

Conclusion

Re-irradiation after standard irradiation and vertebral SBRT appears to be feasible with an acceptable level of toxicity, and can be considered as an efficacious salvage treatment option if delivered to a selected group of patients with an adequate dose delivered to the target while observing critical neural tissue tolerance limits.

Even if previously described retrospective series suggest the efficacy and safety of vertebral re-irradiation using SBRT, further evidence is needed before spreading the use of this technique in an extreme situation like ours.

Data availability statement

The raw data supporting the conclusions of this article will be made available by the authors, without undue reservation.

Ethics statement

Ethical review and approval was not required for the study on human participants in accordance with the local legislation and institutional requirements. The patients/participants provided their written informed consent to participate in this study. Written informed consent was obtained from the individual(s) for the publication of any potentially identifiable images or data included in this article.

Author contributions

Conceptualization, RB and LS; methodology, RB and LS; validation, RK, AM, CT, MO, JB and LS; data curation, RB, CH and YH; writing—original draft preparation, RB, RK, CH, YH, and LS; writing—review and editing, RB, RK, CH, YH, AM, CT, MO, JB and LS; supervision, LS; project administration, LS. All authors contributed to the article and approved the submitted version.

Funding

Open access funding was provided by the University of Lausanne.

Conflict of interest

The authors declare that the research was conducted in the absence of any commercial or financial relationships that could be construed as a potential conflict of interest.

Publisher's note

All claims expressed in this article are solely those of the authors and do not necessarily represent those of their affiliated organizations, or those of the publisher, the editors and the reviewers. Any product that may be evaluated in this article, or claim that may be made by its manufacturer, is not guaranteed or endorsed by the publisher.

References

1. Tseng CL, Soliman H, Myrehaug S, Lee YK, Ruschin M, Atenafu EG, et al. Imaging-based outcomes for 24 gy in 2 daily fractions for patients with de Novo spinal metastases treated with spine stereotactic body radiation therapy (SBRT). *Int J Radiat Oncol Biol Phys* (2018) 102(3):499–507. doi: 10.1016/j.ijrobp.2018.06.047

2. Palma DA, Olson R, Harrow S, Gaede S, Louie AV, Haasbeek C, et al. Stereotactic ablative radiotherapy for the comprehensive treatment of oligometastatic cancers: Long-term results of the SABR-COMET phase II randomized trial. *J Clin Oncol* (2020) 38(25):2830–8. doi: 10.1200/JCO.20.00818

3. Chang UK, Cho WI, Kim MS, Cho CK, Lee DH, Rhee CH. Local tumor control after retreatment of spinal metastasis using stereotactic body radiotherapy; comparison with initial treatment group. *Acta Oncol* (2012) 51(5):589–95. doi: 10.3109/0284186X.2012.666637

4. Garg AK, Wang XS, Shiu AS, Allen P, Yang J, McAleer MF, et al. Prospective evaluation of spinal reirradiation by using stereotactic body radiation therapy: The university of Texas MD Anderson cancer center experience. *Cancer.* (2011) 117 (15):3509–16. doi: 10.1002/cncr.25918

5. Myrehaug S, Sahgal A, Hayashi M, Levivier M, Ma L, Martinez R, et al. Reirradiation spine stereotactic body radiation therapy for spinal metastases: Systematic review. *J Neurosurg Spine.* (2017) 27(4):428–35. doi: 10.3171/2017.2.SPINE16976

6. Navarria P, Mancosu P, Alongi F, Pentimalli S, Tozzi A, Reggiori G, et al. Vertebral metastases reirradiation with volumetric-modulated arc radiotherapy. *Radiother Oncol* (2012) 102(3):416–20. doi: 10.1016/j.radonc.2011.11.005

7. Thibault I, Campbell M, Tseng CL, Atenafu EG, Letourneau D, Yu E, et al. Salvage stereotactic body radiotherapy (SBRT) following in-field failure of initial SBRT for spinal metastases. *Int J Radiat Oncol Biol Phys* (2015) 93(2):353–60. doi: 10.1016/j.ijrobp.2015.03.029

8. Bilsky MH, Boakye M, Collignon F, Kraus D, Boland P. Operative management of metastatic and malignant primary subaxial cervical tumors. *J Neurosurg Spine.* (2005) 2(3):256–64. doi: 10.3171/spi.2005.2.3.0256

9. Sahgal A, Ma L, Weinberg V, Gibbs IC, Chao S, Chang UK, et al. Reirradiation human spinal cord tolerance for stereotactic body radiotherapy. *Int J Radiat Oncol Biol Phys* (2012) 82(1):107–16. doi: 10.1016/j.ijrobp.2010.08.021

10. Witzel I, Oliveira-Ferrer L, Pantel K, Muller V, Wikman H. Breast cancer brain metastases: Biology and new clinical perspectives. *Breast Cancer Res* (2016) 18(1):8. doi: 10.1186/s13058-015-0665-1

11. Chang EL, Shiu AS, Mendel E, Mathews LA, Mahajan A, Allen PK, et al. Phase I/II study of stereotactic body radiotherapy for spinal metastasis and its pattern of failure. *J Neurosurg Spine.* (2007) 7(2):151–60. doi: 10.3171/SPI-07/08/151

12. Cox BW, Spratt DE, Lovelock M, Bilsky MH, Lis E, Ryu S, et al. International spine radiosurgery consortium consensus guidelines for target volume definition in spinal stereotactic radiosurgery. *Int J Radiat Oncol Biol Phys* (2012) 83(5):e597–605. doi: 10.1016/j.ijrobp.2012.03.009

13. Ryu S, Rock J, Rosenblum M, Kim JH. Patterns of failure after single-dose radiosurgery for spinal metastasis. *J Neurosurg* (2004) 101 Suppl 3:402–5. doi: 10.3171/sup.1991.75.1s.0s21

14. Nieder C, Grosu AL, Andratschke NH, Molls M. Proposal of human spinal cord reirradiation dose based on collection of data from 40 patients. *Int J Radiat Oncol Biol Phys* (2005) 61(3):851–5. doi: 10.1016/j.ijrobp.2004.06.016

frontiers | Frontiers in Oncology

TYPE Case Report
PUBLISHED 06 January 2023
DOI 10.3389/fonc.2022.1033084

OPEN ACCESS

EDITED BY
Ianik Plante,
KBRwyle, United States

REVIEWED BY
Xinyu Zheng,
The First Affiliated Hospital of China Medical University, China
Bilgin Kadri Aribas,
Bülent Ecevit University, Turkey

*CORRESPONDENCE
Yongchun Zhang
zyc18661805058@163.com

SPECIALTY SECTION
This article was submitted to Radiation Oncology, a section of the journal Frontiers in Oncology

RECEIVED 31 August 2022
ACCEPTED 15 December 2022
PUBLISHED 06 January 2023

CITATION
Wu Y, Chen Z, Li W, Wang F and Zhang Y (2023) Primary squamous cell carcinoma of the breast: A case report and review of the literature. *Front. Oncol.* 12:1033084. doi: 10.3389/fonc.2022.1033084

Primary squamous cell carcinoma of the breast: A case report and review of the literature

Yaping Wu, Zhiying Chen, Wei Li, Fengguang Wang and Yongchun Zhang*

Department of Radiation Oncology, The Affiliated Hospital of Qingdao University, Qingdao, China

Primary squamous cell carcinoma (PSCC) of the breast, as a rare metaplastic breast cancer, currently has limited clinical data on its biological behavior, treatment and prognosis. At present, the optimal treatment of this tumor is still controversial. We reported a case of a 56-year-old woman with a mass on the right breast. She underwent a modified radical mastectomy and lymph node biopsy, which revealed that the tumor was a metaplastic squamous cell carcinoma with axillary lymph node metastasis, followed by traditional adjuvant chemotherapy and radiotherapy. The patient re-examined by PET/CT after two years in May 2017 and found a recurrence in the right chest wall, so resection of the recurring lesion was resected, then she was given postoperative adjuvant radiotherapy and chemotherapy. In August 2019, the patient re-examined by PET/CT, and there were pulmonary and mediastinal lymph node metastases. After 4 cycles of albumin paclitaxel plus cisplatin chemotherapy combined with nivolumab immunotherapy, the patient achieved complete response (CR), and then switched to nivolumab immune maintenance therapy. So far, no obvious metastasis has been seen. We believe that surgical treatment is necessary for PSCC of the breast;paclitaxel and cisplatin chemotherapy regimens and adjuvant radiotherapy are effective, but it may be resistant to radiotherapy; and immunotherapy may prolong the survival of patients with PSCC of the breast.

KEYWORDS

breast squamous cell carcinoma (BSqCC), breast metaplastic carcinoma, treatment, recurrence, case report

Introduction

Primary squamous cell carcinoma (PSCC) of the breast is an extremely rare tumor, accounting for less than 0.1% of all invasive breast cancers (1, 2), and in 2012, the World Health Organization classified PSCC as metaplastic breast cancer. There are no standard treatment guidelines for PSCC of the breast, and most patients are treated with surgery,

radiotherapy and chemotherapy, like breast ductal carcinoma. However, it is considered that breast PSCC is more malignant and aggressive than invasive ductal carcinoma of the breast (3). It is reported that the recurrence and metastasis of breast PSCC are common after treatment, and the prognosis is poor (4, 5). Here we present a case of a breast PSCC patient who had recurrences after radical mastectomy and adjuvant chemotherapy and radiotherapy. She had a long-term benefit from the use of immunotherapy combined with taxane and platinum-based chemotherapy.

Case presentation

A 56-year-old postmenopausal woman went to the hospital because she found a lump on her right breast. She had no other clinical symptoms such as pain, skin change, nipple retraction, or nipple discharge. She denied family history of breast cancer and other tumors.

On physical examination, there was a 2 × 1.5 cm mass at 12 o'clock in the right breast, 0.5 cm away from the nipple. The lump was firm, movable and irregular. The rest of the physical examination showed no obvious abnormalities.

The patient underwent diagnostic mammography and ultrasound to evaluate the right breast mass. The breast mammography showed (Figures 1A, B) abnormal density and calcification behind the right breast papilla, and bilateral axillary lymph nodes were slightly enlarged. Ultrasound of the breast showed (Figures 1C, D) insulting hypoechoic nodules. The patient underwent ultrasound-guided needle biopsy of the mass in the right breast, which revealed low-grade ductal carcinoma *in situ* with suspicious microinvasion.

The patient underwent a systemic examination to rule out distant metastases and other primary tumors. Then she underwent a modified radical resection of the right breast and a right axillary lymph node dissection on May 25, 2015. The final pathology showed (Figures 2A, B): (Right) Metaplastic carcinoma-squamous cell carcinoma (histological grade III, size 2.5*2.5*1.5cm) is seen in the upper and middle quadrant of the breast, interstitial vascular tumor thrombus (+);cancer metastasis can be seen in axillary lymph nodes (3/21); immunohistochemical showed (Figures 2F–I) estrogen

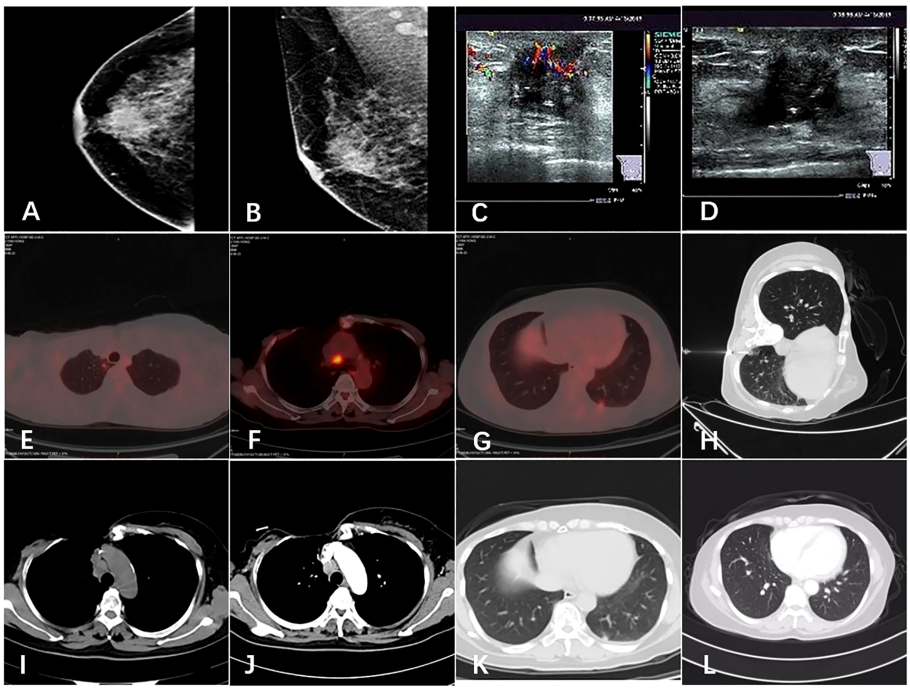

FIGURE 1
Imaging of the tumor. **(A, B)** Mammogram showed an irregular high-density shadow posterior to the nipple of the right breast and bilateral axillary lymph nodes were slightly enlarged. **(C, D)** Ultrasound showed a hypoechoic nodule on the right breast, 0.3 cm from the nipple at 12 o 'clock, 1.7 × 1.4 cm in size. **(E, F, G)** The patient's PET-CT results in 2019. Hypermetabolic lesions were found in the subpleura of the apical segment of the right upper lobe of the lung, the mediastinal anterior tracheal posterior vena cava lymph nodes and the subpleura of the basal segment of the left lower lobe. **(H)** Chest computed tomography guided needle biopsy of the left pulmonary nodule was performed. **(I, J, K, L)** Comparison of pulmonary nodules and mediastinal metastatic lymph nodes before and after the treatment.

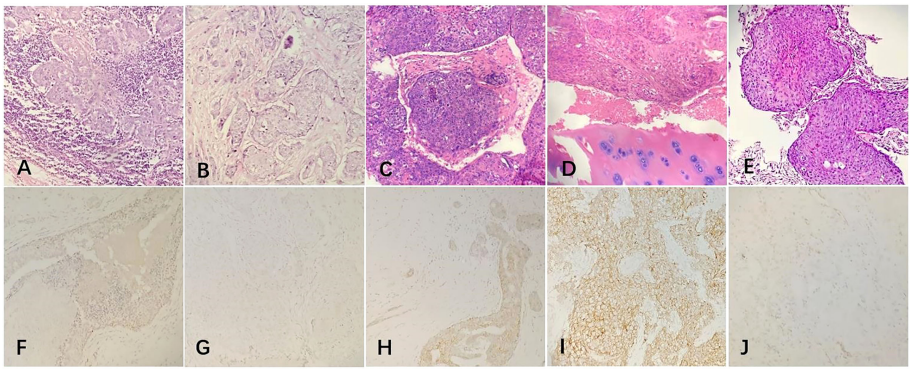

FIGURE 2
The postoperative pathological examination with hematoxylin and eosin (HE) staining and immunohistochemical (IHC) staining of the tumor. **(A, B)** Microscopically, the ductal cells in the mammary tumor area showed squamous degeneration and the lymph nodes were invaded by tumor cells (20x). **(C, D)** Histological findings with HE staining showed that the chest wall tumor was a moderately differentiated squamous cell carcinoma and the bone tissue was invaded by tumor cells(20x). **(E)** Histological findings with HE staining showed that the lung tumor was a metaplastic squamous cell carcinoma(20x). **(F–I)** IHC staining of the primary tumor in 2015. **(F)** ER negativity (20×). **(G)** PR negativity (20×). **(H)** HER2 receptor negativity (20×). **(I)** EGFR positive expression (20×). **(J)** IHC staining of the lung tumor showed that the PD-L1 positive.

receptor (ER) (-), progesterone receptor (PR) (-), human epidermal growth factor receptor 2 (HER2) (-), CK5/6 diffuse (+), CK14 diffuse (+), Ki67 positive rate 80%, P53 positive rate 90%,epidermal growth factor receptor(EGFR)(+), E-cadherin (-), P63 (+), D2-40 (+).After the operation, the patient received further adjuvant chemotherapy and radiation therapy. The specific chemotherapy regimen was a 4-cycle epirubicin combined with cyclophosphamide, followed by a 4-cycle docetaxel. After chemotherapy, radiotherapy was given. The scope of radiotherapy was the chest wall combined with the supraclavicular area; the dose was: 50Gy/25f, and the 95% isodose line was around the target area.

The patients received regular follow-up after the radiotherapy and chemotherapy. The PET/CT review on 2017-05-19 showed that: 1. There was a soft tissue mass on the right anterior chest wall (the inner side of the second anterior rib on the right), and the boundary between some layers and the right side of the sternum was not clear. Increased metabolism, standard uptake value (SUV)max was 4.0, considered chest wall metastasis and sternum invasion. The patient underwent a rib lesion resection under general anesthesia on May 26, 2017. Postoperative pathology showed (Figures 2C, D): (chest wall tumor) moderately differentiated squamous cell carcinoma. Combined with the medical history, the opinion was that the breast-derived metaplastic carcinoma (squamous cell carcinoma), nerve invasion (+), vascular invasion (+), estrogen receptor (ER) (-), progesterone receptor (PR) (-), human epidermal growth factor receptor 2 (HER2) (-), CK5/6 diffuse (+), Ki67 positive rate 60%, P40(+), P63 (+), the surrounding bone tissue was invaded, and the severed end was not involved. After the operation, 6 cycles of liposomal paclitaxel combined with carboplatin were given as chemotherapy. After chemotherapy, single-field electron irradiation was given. The irradiation range was ribs and sternum area. The dose was 54Gy/18f.

The patient's PET/CT on August 23, 2019 showed (Figures 1E–G): 1. There were subpleural nodules in the posterior basal segment of the left lower lobe, and the metabolism was increased, the SUVmax was about 2.1; 2. There were small subpleural nodules in the apical segment of the right upper lobe, with increased metabolism, and the SUVmax was about 2.0; compared with the previous PET/CT examination, above lesions were new lesions, and metastasis was considered. 3. In the mediastinum, the anterior tracheal and retrocaval lymph nodes were slightly enlarged with increased metabolism, and the SUVmax was about 7.3, which was considered as lymph node metastasis. The patient underwent needle biopsy of the left pulmonary nodule (Figure 1H). The left lung nodule puncture pathology showed(Figures 2E, J) that the lung tissue had moderately differentiated squamous cell carcinoma infiltration, PD-L1(SP263) positive rate 2%,which was considered to be derived from breast cancer. We gave the patient an albumin paclitaxel plus cisplatin regimen for 4 cycles of chemotherapy combined with immunotherapy with nivolumab. After 4 cycles, the left and right lung nodules and mediastinal lymph nodes were basically invisible, and the curative effect was evaluated as CR (Figures 1I–L). Subsequently, the patient underwent nivolumab immune maintenance therapy for a year. So far, no obvious recurrence or metastasis has been found (Figure 3).

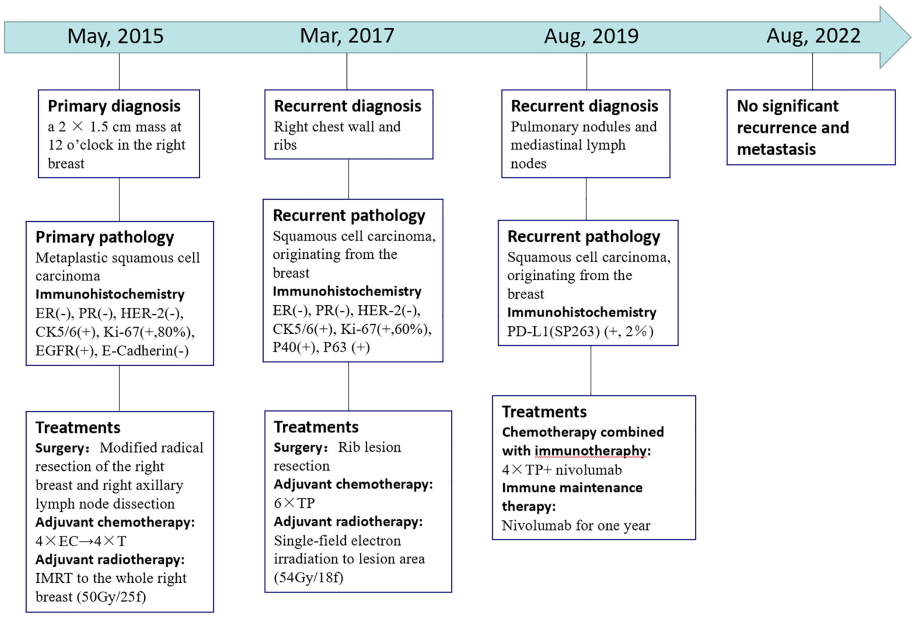

FIGURE 3
Timeline showcasing relevant data from the episode of care. (–): Negative expression; (+): Positive expression. 4 × EC→ 4 × T: four cycles chemotherapy of epirubicin and cyclophosphamide followed by four cycles of docetaxel. IMRT: intensity modulated radiotherapy. 6 × TP: Six cycles chemotherapy of liposomal paclitaxel and carboplatin. 4 x TP + nivolumab: four cycles chemotherapy of albumin paclitaxel plus cisplatin combined with nivolumab.

Discussion

At present, there are few studies on PSCC of the breast. Its pathogenesis is still unclear, and there is a lack of standardized management of its molecular pathological characteristics, treatment and prognosis (6–8).

As a rare pathological type of breast cancer, some authors believe that it arises from benign breast disease (1, 9) and is seen in cystic epithelium, fibroadenoma, phyllodes tumor, papilloma, or chronic abscess. There are also some who suggest that phenotypic changes in breast cancer are the result of malignant transformation of breast cancer stem cells (histogenesis) or mutations in specific genes occurring early or late in carcinogenesis (dedifferentiation) (10). According to reports, radiotherapy can increase the occurrence of breast PSCC (11); in addition, implantation of prosthesis may be related to the occurrence of PSCC (12).

It is particularly important to make a correct diagnosis of PSCC of the breast. The current diagnosis of the disease believes that: the breast tumor cannot be derived from the skin of the breast or the skin of the nipple, or other attachments to the skin; the squamous cell carcinoma component in the tumor tissue accounts for more than 90%; excluding breast tumors derived from other primary tumors metastasized (13, 14). Metastatic breast cancer may be similar to primary breast cancer. Therefore, metastasis from other tumors should be excluded at the time of diagnosis. Testing for expression of CK7 and CK20 is considered to be the most beneficial. The great majority of primary breast cancers are CK7-positive and CK20-negative, whereas other metastases, such as colorectal cancers, are usually CK7-negative and CK20-positive. Aribas et al. similarly confirmed the diagnosis of breast metastases from colorectal cancer by immunohistochemistry (15).

A number of studies have found that the molecular expression of breast PSCC is significantly different from that of invasive ductal carcinoma. Most breast squamous cell carcinomas are ER-negative, PR-negative HER2-negative, CK5/6-positive, EGFR-positive, and highly proliferative (16).This "basal-like" phenotype can explain the poor prognosis of PSCC, even more aggressive than triple-negative breast cancer (17). The hormone receptors-negative and HER2-negative means that hormone therapy and HER-2 targeted therapy may not be effective in this tumor. In the future, the expression of high EGFR may bring new drugs to the treatment of PSCC of the breast (18).

It is reported that breast PSCC has a lower axillary lymph node metastasis rate (19). Previous studies have found that 10%-30% of breast PSCC cases have axillary lymph node metastasis, but blood spread and distant metastasis are more common (1, 13, 19). Also in other studies, compared with traditional breast cancer, the PSCC mass is larger, and part of it is a cystic mass of the breast (20, 21). The larger tumor size and less axillary lymph

node metastasis suggest that PSCC may be suitable for modified radical mastectomy rather than breast-conserving surgery and sentinel lymph node resection is feasible for axillary lymph nodes.

For common breast cancer, if there are high-risk factors, adjuvant radiotherapy and chemotherapy are required after surgery. Our previous study showed that radiotherapy could reduce the local recurrence rate of breast PSCC, but the extent and dose of radiotherapy needed to be further confirmed (22). In a single institute series, in adjuvant radiotherapy for breast cancer, 6 out of 19 (32%) PSCC patients had local recurrences, and 4 of them had local recurrences in the irradiation field (3). In Mami Ogita's multi-center study (23), 7 of 25 PSCC patients (28%) had local recurrence, of which 6 occurred at the irradiated site. It was found that a higher proportion of recurrences occurred in the irradiated area, concluded that breast PSCC may be radiation resistant. Therefore, increasing the radiation dose may be an option. Studies on chemotherapy regimens for PSCC lack large-scale clinical data. Some researchers have found that PSCC can benefit from platinum-based drug treatment, but is resistant to traditional breast cancer chemotherapy drugs such as anthracyclines and fluorouracils (24). Dejager et al. reported that cisplatin-based chemotherapy regiments normally used for squamous cell carcinoma in major organs other than the breast were also effective for squamous cell carcinoma of the breast (25). Rokutanda et al. and Murialdo et al. also reported the effectiveness of cisplatin-based chemotherapy in breast PSCC. After the patient relapsed after surgery, she chose to use paclitaxel combined with platinum-based chemotherapy, and both achieved good results (26, 27). Considering that breast PSCC may be the same as squamous cell carcinoma from other organs, we speculate that it is sensitive to taxans and platinum. Like the new drug albumin paclitaxel, whether it can further improve the efficacy remains to be studied on a large scale.

Currently, programmed cell death 1 (PDCD1, also known as PD-1)/programmed cell death 1 ligand 1 (PDCD1LG1, Pd-l1 (also known as PD-L1) immune checkpoint inhibitors for immunotherapy of breast cancer have gradually become a hot spot in clinical research, but there is a relative lack of research on the immunotherapy of primary squamous cell carcinoma. Using different antibodies and scoring systems, Muenst et al. found that PD-L1 was expressed in 152 of 650 breast cancer specimens (23.4%) (28). Doğukan et al. used immunohistochemistry to detect the expression of PD-L1 in 61 patients with triple negative breast cancer (TNBC), and the results showed that the positive expression rates of PD-L1 in tumor and tumor microenvironment were 37.7% and 47.5%, respectively (29). Sabatier et al. found that PD-L1 expression was associated with more aggressive subtypes (basal and erb-B2-rich), and in basal tumors, higher PD-L1 expression is associated with better PFS and OS and better response to chemotherapy (30). Studies have found that chemotherapy may enhance the release of tumor antigens, thereby enhancing the anti-cancer activity of immune checkpoint inhibitors. In particular, paclitaxel drugs can additionally activate the activity of toll-like receptors and promote the activity of dendritic cells (29). There have been several clinical trials of PD-1/PD-L1 inhibitors combined with chemotherapy in breast cancer, particularly in triple-negative breast cancer. In the Phase III clinical study of IMpassion130, patients with untreated metastatic triple-negative breast cancer were randomly assigned (in a 1:1 ratio) to receive atezolizumab plus albumin-bound paclitaxel or placebo plus albumin-bound paclitaxel treatment (31). The results showed that atezolizumab combined with albumin paclitaxel could further prolong the PFS and OS of triple-negative breast cancer, and the benefit was more obvious in the PD-L1 positive subgroup, and the adverse reactions of immunity and chemotherapy could be tolerated. After this patient developed lung and mediastinal lymph nodes metastases, we used nivolumab combined with albumin-bound paclitaxel and carboplatin. The lung and mediastinal lymph nodes metastases have achieved CR. Subsequently, immune maintenance therapy with nivolumab was administered for a year, and so far, the patient has not developed significant recurrence or metastasis. Most breast PSCC have a "basal-like" phenotype and the molecular phenotype is partially similar to triple-negative breast cancer, we speculate that breast PSCC may have a relatively high PD-L1 expression rate. Based on the efficacy of immunotherapy combined with chemotherapy in this patient and previous studies of immunotherapy in breast cancer, we believe that immunotherapy may also benefit patients with breast PSCC.

In conclusion, through the treatment of this patient, combined with previous studies, we believe that paclitaxel combined with platinum is a suitable chemotherapy regimen for breast PSCC. Adjuvant radiotherapy is beneficial, but it may be resistant, and increasing the dose of radiotherapy may further reduce the local recurrence rate. For advanced patients, chemotherapy combined with PD-1/PD-L1 inhibitors immunotherapy and immune maintenance therapy can further extend the patient's survival, but it needs to be confirmed by large-scale clinical studies.

Data availability statement

The original contributions presented in the study are included in the article/supplementary material. Further inquiries can be directed to the corresponding author.

Ethics statement

The studies involving human participants were reviewed and approved by Medical Ethic committee of Affiliated Hospital of

Qingdao University. The patients/participants provided their written informed consent to participate in this study. Written informed consent was obtained from the individual(s) for the publication of any potentially identifiable images or data included in this article.

Author contributions

YW, ZC, WL, FW and YZ collected the patient's data. YW and ZC finished the original manuscript and YW revised it. WL and FW provided the figures. YZ provided final approval for the version to be published. All authors contributed to the article and approved the submitted version.

Conflict of interest

The authors declare that the research was conducted in the absence of any commercial or financial relationships that could be construed as a potential conflict of interest.

Publisher's note

References

1. Behranwala KA, Nasiri N, Abdullah N, Trott PA, Gui GP. Squamous cell carcinoma of the breast: clinico-pathologic implications and outcome. *Eur J Surg Oncol J Eur Soc Surg Oncol Br Assoc Surg Oncol* (2003) 29:386–9. doi: 10.1053/ejso.2002.1422

2. Weigel RJ, Ikeda DM, Nowels KW. Primary squamous cell carcinoma of the breast. *South Med J* (1996) 89:511–5. doi: 10.1097/00007611-199605000-00013

3. Hennessy BT, Krishnamurthy S, Giordano S, Buchholz TA, Kau SW, Duan Z, et al. Squamous cell carcinoma of the breast. *J Clin Oncol Off J Am Soc Clin Oncol* (2005) 23:7827–35. doi: 10.1200/jco.2004.00.9589

4. Flikweert ER, Hofstee M, Liem MS. Squamous cell carcinoma of the breast: a case report. *World J Surg Oncol* (2008) 6:135. doi: 10.1186/1477-7819-6-135

5. Carbone S, Lobo Alvarez R, Lamacchia A, Almenar Gil A, Martin Hernandez R, Lopez Guerra JL, et al. Primary squamous cell carcinoma of the breast: A rare case report. *Rep Pract Oncol radiotherapy J Greatpoland Cancer Center Poznan Polish Soc Radiat Oncol* (2012) 17:363–6. doi: 10.1016/j.rpor.2012.07.004

6. Darlington CD, Anitha GFS. Squamous cell carcinoma of the breast mimicking chronic breast abscess. *Nigerian J Surg Off Publ Nigerian Surg Res Soc* (2019) 25:101–3. doi: 10.4103/njs.NJS_22_18

7. Jakubowska K, Kańczuga-Koda L, Kisielewski W, Koda M, Famulski W. Squamous cell carcinoma of the breast as a clinical diagnostic challenge. *Mol Clin Oncol* (2018) 8:587–91. doi: 10.3892/mco.2018.1581

8. Bhatt L, Fernando I. Primary squamous cell carcinoma of the breast: achieving long-term control with cisplatin-based chemotherapy. *Clin Breast Cancer* (2009) 9:187–8. doi: 10.3816/CBC.2009.n.031

9. Gupta C, Malani AK, Weigand RT, Rangineni G. Pure primary squamous cell carcinoma of the breast: a rare presentation and clinicopathologic comparison with usual ductal carcinoma of the breast. *Pathology Res Pract* (2006) 202:465–9. doi: 10.1016/j.prp.2006.01.006

10. van Deurzen CH, Lee AH, Gill MS, Menke-Pluijmers MB, Jager A, Ellis IO, et al. Metaplastic breast carcinoma: tumour histogenesis or dedifferentiation? *J Pathol* (2011) 224:434–7. doi: 10.1002/path.2872

11. Singh H, Williams SP, Kinsella V, Lynch GR. Postradiation squamous cell cancer of the breast. *Cancer Invest* (2000) 18:343–6. doi: 10.3109/07357900009012177

12. Zhou YM, Chaudhry HE, Shah A, Andrews J. Breast squamous cell carcinoma following breast augmentation. *Cureus* (2018) 10:e3405. doi: 10.7759/cureus.3405

13. Aparicio I, Martínez A, Hernández G, Hardisson D, De Santiago J. Squamous cell carcinoma of the breast. *Eur J obstetrics gynecology Reprod Biol* (2008) 137:222–6. doi: 10.1016/j.ejogrb.2007.03.021

14. Ribeiro-Silva A, Luzzatto F, Chang D, Zucoloto S. Limitations of fine-needle aspiration cytology to diagnose metaplastic carcinoma of the breast. *Pathol Oncol Res POR* (2001) 7:298–300. doi: 10.1007/bf03032387

15. Aribas BK, Onursever A, Kiziltepe TT, Aydin H, Cosar S, Uzun H. Breast metastasis from rectal adenocarcinoma: a case report with US and CT findings. *Imaging Med* (2016) 8:89–92.

16. Siegelmann-Danieli N, Murphy TJ, Meschter SC, Stein ME, Prichard J. Primary pure squamous cell carcinoma of the breast. *Clin Breast Cancer* (2005) 6:270–2. doi: 10.3816/CBC.2005.n.030

17. El Zein D, Hughes M, Kumar S, Peng X, Oyasiji T, Jabbour H, et al. Metaplastic carcinoma of the breast is more aggressive than triple-negative breast cancer: A study from a single institution and review of literature. *Clin Breast Cancer* (2017) 17:382–91. doi: 10.1016/j.clbc.2017.04.009

18. Badge SA, Gangane NM, Shivkumar VB, Sharma SM. Primary squamous cell carcinoma of the breast. *Int J Appl basic Med Res* (2014) 4:53–5. doi: 10.4103/2229-516x.125697

19. Menes T, Schachter J, Morgenstern S, Fenig E, Lurie H, Gutman H. Primary squamous cell carcinoma (SqCC) of the breast. *Am J Clin Oncol* (2003) 26:571–3. doi: 10.1097/01.coc.0000045809.85995.3B

20. Anne N, Sulger E, Pallapothu R. Primary squamous cell carcinoma of the breast: a case report and review of the literature. *J Surg Case Rep* (2019) 2019:rjz182. doi: 10.1093/jscr/rjz182

21. Stevenson JT, Graham DJ, Khiyami A, Mansour EG. Squamous cell carcinoma of the breast: a clinical approach. *Ann Surg Oncol* (1996) 3:367–74. doi: 10.1007/bf02305666

22. Chen Z, An N, Zhang L, Cui H, Jiang Y, Zhang Y. Clinicopathological and therapeutic analysis of primary breast squamous cell carcinoma. *Gland Surg* (2022) 11:125–35. doi: 10.21037/gs-21-810

23. Ogita M, Shiraishi K, Karasawa K, Tokumasu K, Nakajima N, Chang T, et al. Clinical outcome of adjuvant radiotherapy for squamous cell carcinoma of the breast; a multicenter retrospective cohort study. *Breast (Edinburgh Scotland)* (2020) 52:88–94. doi: 10.1016/j.breast.2020.05.003

24. Tsung SH. Primary pure squamous cell carcinoma of the breast might be sensitive to cisplatin-based chemotherapy. *Case Rep Oncol* (2012) 5:561–5. doi: 10.1159/000343745

25. Dejager D, Redlich PN, Dayer AM, Davis HL, Komorowski RA. Primary squamous cell carcinoma of the breast: sensitivity to cisplatinum-based chemotherapy. *J Surg Oncol* (1995) 59:199–203. doi: 10.1002/jso.2930590313

26. Rokutanda N, Iino Y, Yokoe T, Maemura M, Horiguchi J, Takei H, et al. Primary squamous cell carcinoma of the breast during lactation: a case report. *Japanese J Clin Oncol* (2000) 30:279–82. doi: 10.1093/jjco/hyd069

27. Murialdo R, Boy D, Musizzano Y, Tixi L, Murelli F, Ballestrero A. Squamous cell carcinoma of the breast: a case report. *cases J* (2009) 2:7336. doi: 10.4076/1757-1627-2-7336

28. Muenst S, Schaerli AR, Gao F, Däster S, Trella E, Droeser RA, et al. Expression of programmed death ligand 1 (PD-L1) is associated with poor prognosis in human breast cancer. *Breast Cancer Res Treat* (2014) 146:15–24. doi: 10.1007/s10549-014-2988-5

29. Emens LA, Middleton G. The interplay of immunotherapy and chemotherapy: harnessing potential synergies. *Cancer Immunol Res* (2015) 3:436–43. doi: 10.1158/2326-6066.Cir-15-0064

30. Sabatier R, Finetti P, Mamessier E, Adelaide J, Chaffanet M, Ali HR, et al. Prognostic and predictive value of PDL1 expression in breast cancer. *Oncotarget* (2015) 6:5449–64. doi: 10.18632/oncotarget.3216

31. Emens LA, Molinero L, Loi S, Rugo HS, Schneeweiss A, Diéras V, et al. Atezolizumab and nab-paclitaxel in advanced triple-negative breast cancer: Biomarker evaluation of the IMpassion130 study. *J Natl Cancer Institute* (2021) 113:1005–16. doi: 10.1093/jnci/djab004

frontiers | Frontiers in Oncology

TYPE Case Report
PUBLISHED 27 January 2023
DOI 10.3389/fonc.2023.925233

OPEN ACCESS

EDITED BY
Wenyin Shi,
Thomas Jefferson University, United States

REVIEWED BY
Guido Scoccianti,
Careggi University Hospital, Italy
Sarat Chander,
Peter MacCallum Cancer Centre, Australia

*CORRESPONDENCE
Yuhong Zhou
zhou.yuhong@zs-hospital.sh.cn
Weiqi Lu
lu.weiqi@zs-hospital.sh.cn

†These authors share first authorship

SPECIALTY SECTION
This article was submitted to Radiation Oncology, a section of the journal Frontiers in Oncology

RECEIVED 21 April 2022
ACCEPTED 09 January 2023
PUBLISHED 27 January 2023

CITATION
Zhang C, Liu W, Wang B, Zhu N, Guo X, Wang Z, Zhuang R, You Y, Zhang Y, Tong H, Lu W and Zhou Y (2023) Case report: Pathological complete response to perioperative treatment of radiotherapy combined with angiogenesis inhibitor in a patient with pleomorphic liposarcoma. *Front. Oncol.* 13:925233. doi: 10.3389/fonc.2023.925233

Case report: Pathological complete response to perioperative treatment of radiotherapy combined with angiogenesis inhibitor in a patient with pleomorphic liposarcoma

Chenlu Zhang[1†], Wenshuai Liu[2†], Binliang Wang[3], Na Zhu[4], Xi Guo[1], Zhiming Wang[1], Rongyuan Zhuang[1], Yang You[1], Yong Zhang[2], Hanxing Tong[2], Weiqi Lu[2*] and Yuhong Zhou[1*]

[1]Department of Medical Oncology, Zhongshan Hospital, Fudan University, Shanghai, China, [2]Department of General Surgery, Zhongshan Hospital, Fudan University, Shanghai, China, [3]Department of Radiation, Zhongshan Hospital, Fudan University, Shanghai, China, [4]Department of Pathology, Zhongshan Hospital, Fudan University, Shanghai, China

Background: Liposarcomas (LPS) are mesenchymal malignancies with four principal subtypes presenting distinct molecular and clinical features. Pleomorphic liposarcoma (PLPS) is one of the rarest and most aggressive subtypes of LPS. Surgical resection is currently a preferred curative approach for localized PLPS. However, the prognosis of unresectable PLPS is extremely poor, and there is no standard treatment.

Case presentation: A 59-year-old Chinese woman was diagnosed with unresectable PLPS. The case was discussed and managed by specialists from a multidisciplinary team at Fudan Zhongshan Hospital. Preoperative radiotherapy (RT) of intensity-modulated radiation therapy (IMRT) at 50 Gy/25 Fx concurrently with the angiogenesis inhibitor anlotinib (8 mg, days 1–14, every 3 weeks) was prescribed to the patient. The dosage of anlotinib was increased to 10 mg after RT. After 6 months of treatment, the tumor had significantly shrunk and was successfully resected. Examination of the surgical specimens showed a pathological complete response (pCR). Until the latest follow-up (April 2022), no recurrence was observed, and disease-free survival has exceeded 14 months.

Conclusion: This case sheds light on the probability that perioperative RT combined with an angiogenesis inhibitor can be effectively used in PLPS, which is resistant to chemotherapy and usually considered to have a poor prognosis. Further studies with randomized controlled clinical trials will improve our knowledge of this preoperative treatment strategy.

KEYWORDS

pleomorphic liposarcoma, preoperative radiotherapy, angiogenesis inhibitor, pathological complete response, case report

Introduction

Liposarcoma (LPS) is a heterogeneous soft tissue sarcoma. LPS is among the most common soft tissue sarcomas (STS) and accounts for approximately 15% to 20% of all STS (1). Pleomorphic liposarcoma (PLPS), a less frequent but more aggressive subtype with a 5-year survival rate of 57%, which is closer to that of other high-grade STS, accounts for only 5%–10% of LPS (2).

The LPS arising in the retroperitoneum and intra-abdomen is recommended to be evaluated and managed by a multidisciplinary team (MDT) according to the latest NCCN guideline. Surgery is currently the mainstay, but patients with unresectable disease—defined as tumors affecting important structures or causing unacceptable morbidity after excision—should consider perioperative treatment. Perioperative radiotherapy (RT) is one option, as it reduces tumor size and facilitates tumor resection (3). However, evidence regarding perioperative RT is limited. To date, the STRASS trial (NCT01344018) is the first randomized, phase III clinical trial to value the role of preoperative RT for localized retroperitoneal STS (RPS) (4). Unfortunately, this trial showed a negative result in that preoperative RT did not improve recurrence-free survival. A subgroup analysis of patients with LPS suggested a 10% increase in recurrence-free survival in the RT plus surgery group.

Angiogenesis inhibitors such as anlotinib have recently been proven to be effective in advanced and metastatic STS (5). Although angiogenesis inhibitors are not recommended as perioperative treatment in the guidelines, some recent early-phase clinical trials have explored the safety and efficacy of angiogenesis inhibitors in STS, mostly in combination with perioperative RT (6). These trials showed that the combination of antiangiogenesis therapy with perioperative RT is worth trying in individually selected patients.

Owing to the low incidence of PLPS and the lack of related investigations, the optimal perioperative treatment regimen is challenging. Here, we report a case of PLPS with a pathological complete response (pCR) after RT combined with an antiangiogenesis drug as perioperative therapy.

Case description

The case management is described below, and Figure 1A provides a detailed timeline. A 59-year-old Chinese woman presented with abdominal distension. The results of the blood test were normal, and the patient did not have a family history of malignancies. The performance status measured by the ECOG score was one. Computed tomography (CT) was performed in June 2020 and

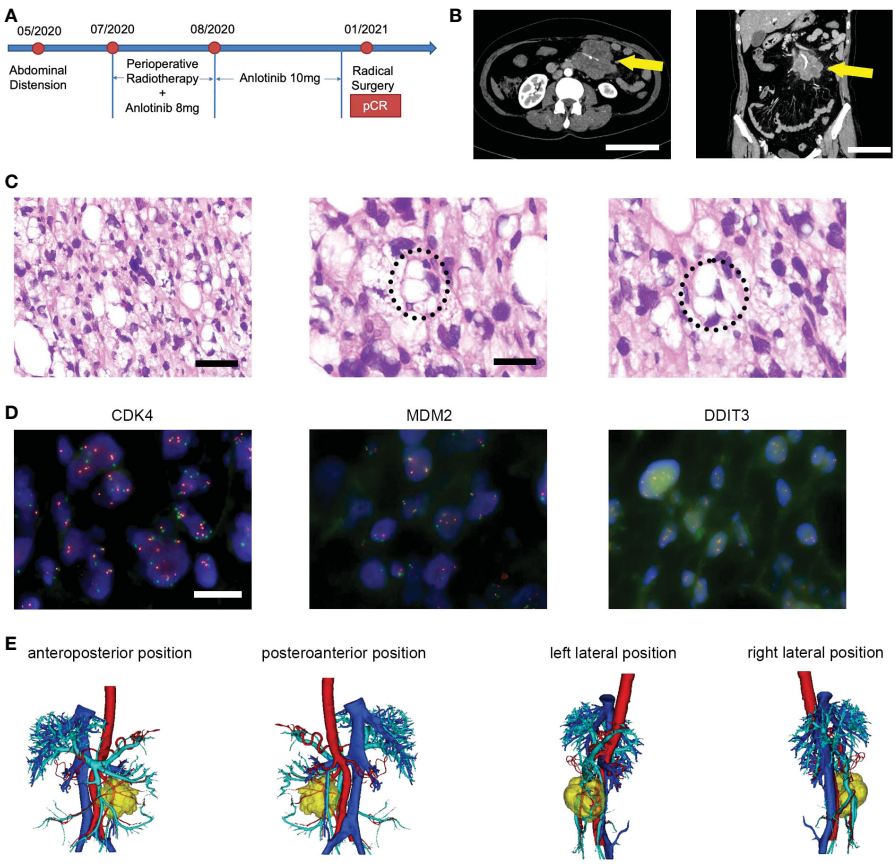

FIGURE 1
(A) Timeline of therapy in a patient with unresectable PLPS who received preoperative RT plus anlotinib and achieved pCR after the surgery. **(B)** The initial CT scan revealed a soft tissue mass in the left abdominal cavity with the superior mesenteric artery passing through, measuring 7.4 cm × 6.2 cm × 7.2 cm in diameter. Scale bar = 10 cm. **(C)** Micrographs of hematoxylin and eosin (HE) staining. Scale bar = 50 μm. The latter two images showed the lip blasts in a circle. Scale bar = 25 μm. **(D)** The FISH image showed negative results labeled by CDK4, MDM3, and DDIT3 probes, respectively. Scale bar = 10 μm. **(E)** 3D reconstruction imaging displayed the relationship between tumors and vessels. Yellow, tumor; red, artery; blue, vein.

showed a soft tissue mass, sized 7.4 cm × 6.2 cm ×7.2 cm, in the left abdominal cavity with the superior mesenteric artery passing through (Figure 1B). A biopsy was performed, and histopathology revealed undifferentiated pleomorphic epithelioid or spindled cells, admixed with some cells presenting lipid vacuoles (Figure 1C). Lipoblasts could be found in the biopsy sections. The immunohistochemistry reading was ERG (−), CD34 (vessels+), CD117 (−), Fli-1 (−), OCT4 (−), SMA (−), Ki67 (20%+), CD31 (−), DOG1 (−), S100 (−), Des (−), and MDM2 (100%++). Fluorescence *in situ* hybridization (FISH) revealed no amplification of MDM2 and CDK4 and no rearrangement of DDIT3 (Figure 1D). The diagnosis was pleomorphic liposarcoma, staging cT2N0M0G2, IIIA based on the above information and pathological evaluation of the biopsy. Furthermore, 3D reconstruction imaging confirmed that the first branch of the superior mesenteric artery was surrounded by the tumor (Figure 1E). The careful preoperative imaging helped the MDT to comprehensively evaluate the case. At that time, immediate surgery would necessitate a resection of the entire small bowel to completely remove the tumor, and the patient would need lifelong parenteral nutrition afterward. Consequently, preoperative RT combined with an antiangiogenesis drug was suggested, and the patient agreed with it. From July 2020 to August 2020, the patient received intensity-modulated radiation therapy (IMRT) of 50 Gy/25 Fx concurrently with anlotinib (8 mg, days 1–14, every 3 weeks). The anlotinib dosage was increased to 10 mg after RT. The therapy was well tolerated, and the main adverse event was G1 fatigue. Follow-up CT scans were performed in October and December 2020, indicating notable tumor shrinkage to 2.8 cm × 1.9 cm (Figure 2A). On 29 January 2021, the patient underwent radical resection of the lesion and partial resection of the superior mesenteric artery and small intestines (Figure 2B). The surgical margins showed no evidence of tumor involvement. The pathology of surgical specimens displayed adipose tissue composed of large areas of hyperplastic collagen tissue, scattered small blood vessels, histocytes, and chronic inflammatory cells (Figure 2C). The diagnosis results revealed a pCR. After surgery, the patient underwent CT and blood tests every 3 months. At the last follow-up in April 2022, 14 months postsurgery, the patient was in good condition, and no suspicious recurrence was detected.

Discussion

PLPS is the rarest and most aggressive subtype of LPS, and there is currently no standardized treatment yet. Complete resection with clear surgical margins is the preferred curative option for localized PLPS (7). However, local recurrence of PLPS is approximately 30%–50% (8), which is the reason for the predominant failure of surgical treatment. Perioperative treatment may resolve this issue by reducing local recurrence. In this case, although the follow-up of 14 months was rather short, the patient did not develop a local or distant recurrence during this time.

The results of a systematic review and meta-analysis indicated that external beam radiation therapy could reduce local recurrence in RPS (odds ratio (OR) = 0.47, p <0.0001), which was less frequent in the preoperative RT group than the postoperative group (OR = 0.03, p = 0.02) (9). Another study showed that patients with intermediate or high-grade RPS could benefit from the treatment with preoperative RT plus complete resection, with 5-year local recurrence-free survival (RFS) of 60%, disease-free survival (DFS) of 46%, and overall survival (OS) rates of 61% (10). Additionally, retrospective studies have revealed that using perioperative RT in combination with surgery for RPS could also improve OS. The analysis showed that the median OS was significantly improved in the perioperative RT plus surgery group compared to the surgery-only group, which were 110 and 66 months, respectively (hazard ratio = 0·70, 95% confidence interval = 0·59–0·82; p < 0.0001) (11).

However, in contrast to extremity STS (3, 12), the role of preoperative RT in RPS still lacks relevant high-grade clinical evidence. The STRASS trial is a prominent randomized clinical trial that aimed to evaluate the effect of preoperative RT on RPS (4). There was no improvement in abdominal recurrence-free survival (ARFS) in patients receiving preoperative RT plus surgery compared to surgery alone. This study was hobbled by several key limitations, as ARFS was a complex primary endpoint and the trial was not histotype-specific. Nevertheless, the STRASS trial provided some suggestive evidence regarding the possible benefit of preoperative RT in specific RPS histologic subtypes, including LPS and low-grade sarcoma subgroups. Further histotype-specific investigations are still required.

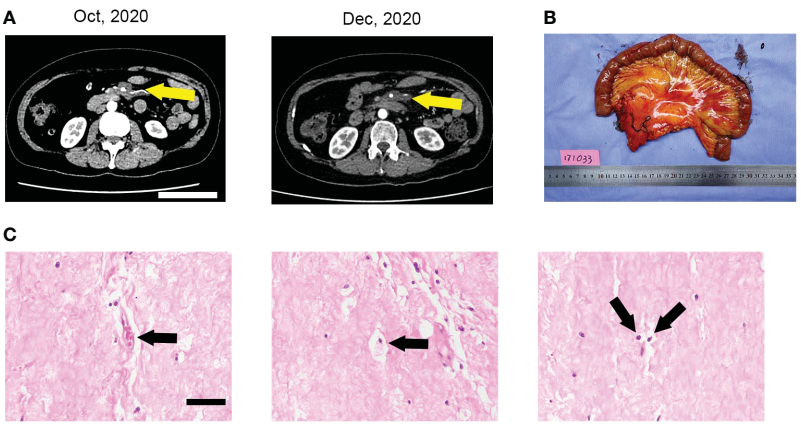

FIGURE 2
(A) The CT scan showed that the tumor shrank remarkably after the treatment of perioperative RT plus anlotinib, measuring 2.8 cm × 1.9 cm. **(B)** The surgical specimens of the tumor, partial small intestines, mesentery, and superior mesenteric artery. **(C)** Micrographs of HE staining showed collagen tissue with no viable tumor cells. The images displayed blood vessels, histiocytes, and chronic inflammatory cells, which were pointed with arrowheads.

Conventional chemotherapy shows a low response in PLPS; therefore, new target therapies are urgently needed. Vascular endothelial growth factor (VEGF) expression was observed in 68% of PLS specimens, which is an excellent sign of the potential benefit of angiogenesis inhibitors (13). Angiogenesis inhibitors, including pazopanib, anlotinib, and regorafenib, have been approved for use in advanced and metastatic STS (5, 14, 15). Anlotinib is a multi-targeted tyrosine kinase inhibitor that selectively targets VEGFR-2, VEGFR-3, and VEGFR-4; FGFR-1, FGFR-2, FGFR-3, and FGFR-4; PDGFR; and c-Kit, contributing to reduced tumor growth and vasculature (16). A phase II clinical trial showed that anlotinib was the first TKI with antitumor activity in LPS patients that progressed after standard first-line therapy. The progression-free rate $(PFR)_{12\ weeks}$ and the objective response rate (ORR) was 63% and 7.7% in LPS (17). However, there is no clear recommendation for locally advanced PLPS and whether angiogenesis inhibitors can be used in perioperative treatment.

A combination of RT and angiogenesis inhibitors has been demonstrated to be an effective therapy that enhances the sensitivity of tumor cells to radiation (6, 18). This effect can be explained by the fact that anti-VEGF normalizes tumor vasculature, resulting in increased tumor oxygenation and cytotoxicity to radiation (19). Combination treatment has been proven to increase the efficacy of RT in different malignancies. Several trials have evaluated the addition of bevacizumab, a humanized anti-VEGF monoclonal antibody, in the treatment of rectal cancer along with preoperative chemoradiotherapy (20–22). Higher pCR rates were observed in the bevacizumab group, ranging from 23.8% to 39.5%. Early clinical studies have also been conducted on STS. Sunitinib or bevacizumab was administered concurrently with preoperative RT in patients with STS originating from the extremities, retroperitoneum, and trunk (23–25). Remarkably, the pathological examination of tumor specimens revealed less than 10% viable tumor cells in approximately one-third of the patients after the combination treatment. Moreover, combination treatment did not lead to severe adverse events or affect the dose of RT. This implied that the addition of angiogenesis inhibitors to RT could increase RT efficacy without increasing toxicity.

In summary, to the best of our knowledge, this is the first case report of a pathologically complete response to the combination of perioperative RT and antiangiogenic agents in a patient with primary unresectable PLPS. Combined therapy provides a practical therapeutic approach to overcome the obstacles in PLPS that have no standard treatment. Further studies will help us better understand the underlying molecular mechanisms of PLPS and establish an optimal treatment strategy.

Data availability statement

The original contributions presented in the study are included in the article/Supplementary Material. Further inquiries can be directed to the corresponding authors.

Ethics statement

The studies involving human participants were reviewed and approved by Ethics Committee of Zhongshan Hospital, Fudan University. The patients/participants provided their written informed consent to participate in this study. Written informed consent was obtained from the individual(s) for the publication of any potentially identifiable images or data included in this article.

Author contributions

CZ and WSL collected the clinical information, diagnostic information, therapeutic information, and images of the patients. BW provided the radiotherapy information. YZ and HT provided the surgical information and images. NZ reviewed the pathological sections and took pathological photos. CZ wrote the manuscript. CZ and WSL revised the manuscript. YHZ proofread the manuscript. YHZ and WQL were responsible for the study's conception and design. XG, ZW, RZ, and YY took part in the management and follow-up of the patient. All authors contributed to the article and approved the submitted version.

Funding

This study was supported by the Shanghai Sailing Program (19YF1407100).

Acknowledgments

We appreciate our patient and her family, as well as the colleagues at Shanghai Zhongshan Hospital who supported us in the preparation of this manuscript.

Conflict of interest

The authors declare that the research was conducted in the absence of any commercial or financial relationships that could be construed as a potential conflict of interest.

Publisher's note

References

1. Lee ATJ, Thway K, Huang PH, Jones RL. Clinical and molecular spectrum of liposarcoma. *J Clin Oncol* (2018) 36(2):151–9. doi: 10.1200/JCO.2017.74.9598

2. Gebhard S, Coindre JM, Michels JJ, Terrier P, Bertrand G, Trassard M, et al. Pleomorphic liposarcoma: Clinicopathologic, immunohistochemical, and follow-up analysis of 63 cases: A study from the French federation of cancer centers sarcoma group. *Am J Surg Pathol* (2002) 26(5):601–16. doi: 10.1097/00000478-200205000-00006

3. Baldini EH, Wang D, Haas RL, Catton CN, Indelicato DJ, Kirsch DG, et al. Treatment guidelines for preoperative radiation therapy for retroperitoneal sarcoma: Preliminary consensus of an international expert panel. *Int J Radiat Oncol Biol Phys* (2015) 92(3):602–12. doi: 10.1016/j.ijrobp.2015.02.013

4. Bonvalot S, Gronchi A, Le Pechoux C, Swallow CJ, Strauss D, Meeus P, et al. Preoperative radiotherapy plus surgery versus surgery alone for patients with primary retroperitoneal sarcoma (Eortc-62092: Strass): A multicentre, open-label, randomised, phase 3 trial. *Lancet Oncol* (2020) 21(10):1366–77. doi: 10.1016/S1470-2045(20)30446-0

5. Chi Y, Fang Z, Hong X, Yao Y, Sun P, Wang G, et al. Safety and efficacy of anlotinib, a multikinase angiogenesis inhibitor, in patients with refractory metastatic soft-tissue sarcoma. *Clin Cancer Res* (2018) 24(21):5233–8. doi: 10.1158/1078-0432.CCR-17-3766

6. Spalek MJ, Kozak K, Czarnecka AM, Bartnik E, Borkowska A, Rutkowski P. Neoadjuvant treatment options in soft tissue sarcomas. *Cancers (Basel)* (2020) 12 (8):2061. doi: 10.3390/cancers12082061

7. Anderson WJ, Jo VY. Pleomorphic liposarcoma: Updates and current differential diagnosis. *Semin Diagn Pathol* (2019) 36(2):122–8. doi: 10.1053/j.semdp.2019.02.007

8. Hornick JL, Bosenberg MW, Mentzel T, McMenamin ME, Oliveira AM, Fletcher CD. Pleomorphic liposarcoma: Clinicopathologic analysis of 57 cases. *Am J Surg Pathol* (2004) 28(10):1257–67. doi: 10.1097/01.pas.0000135524.73447.4a

9. Albertsmeier M, Rauch A, Roeder F, Hasenhutl S, Pratschke S, Kirschneck M, et al. External beam radiation therapy for resectable soft tissue sarcoma: A systematic review and meta-analysis. *Ann Surg Oncol* (2018) 25(3):754–67. doi: 10.1245/s10434-017-6081-2

10. Pawlik TM, Pisters PW, Mikula L, Feig BW, Hunt KK, Cormier JN, et al. Long-term results of two prospective trials of preoperative external beam radiotherapy for localized intermediate- or high-grade retroperitoneal soft tissue sarcoma. *Ann Surg Oncol* (2006) 13(4):508–17. doi: 10.1245/ASO.2006.05.035

11. Nussbaum DP, Rushing CN, Lane WO, Cardona DM, Kirsch DG, Peterson BL, et al. Preoperative or postoperative radiotherapy versus surgery alone for retroperitoneal sarcoma: A case-control, propensity score-matched analysis of a nationwide clinical oncology database. *Lancet Oncol* (2016) 17(7):966–75. doi: 10.1016/S1470-2045(16)30050-X

12. O'Sullivan B, Davis AM, Turcotte R, Bell R, Catton C, Chabot P, et al. Preoperative versus postoperative radiotherapy in soft-tissue sarcoma of the limbs: A randomised trial. *Lancet* (2002) 359(9325):2235–41. doi: 10.1016/S0140-6736(02)09292-9

13. Ghadimi MP, Liu P, Peng T, Bolshakov S, Young ED, Torres KE, et al. Pleomorphic liposarcoma: Clinical observations and molecular variables. *Cancer* (2011) 117(23):5359–69. doi: 10.1002/cncr.26195

14. van der Graaf WT, Blay JY, Chawla SP, Kim DW, Bui-Nguyen B, Casali PG, et al. Pazopanib for metastatic soft-tissue sarcoma (Palette): A randomised, double-blind, placebo-controlled phase 3 trial. *Lancet* (2012) 379(9829):1879–86. doi: 10.1016/S0140-6736(12)60651-5

15. Berry V, Basson L, Bogart E, Mir O, Blay JY, Italiano A, et al. Regosarc: Regorafenib versus placebo in doxorubicin-refractory soft-tissue sarcoma-a quality-adjusted time without symptoms of progression or toxicity analysis. *Cancer* (2017) 123(12):2294–302. doi: 10.1002/cncr.30661

16. Sun Y, Niu W, Du F, Du C, Li S, Wang J, et al. Safety, pharmacokinetics, and antitumor properties of anlotinib, an oral multi-target tyrosine kinase inhibitor, in patients with advanced refractory solid tumors. *J Hematol Oncol* (2016) 9(1):105. doi: 10.1186/s13045-016-0332-8

17. Sleijfer S, Ray-Coquard I, Papai Z, Le Cesne A, Scurr M, Schoffski P, et al. Pazopanib, a multikinase angiogenesis inhibitor, in patients with relapsed or refractory advanced soft tissue sarcoma: A phase ii study from the European organisation for research and treatment of cancer-soft tissue and bone sarcoma group (Eortc study 62043). *J Clin Oncol* (2009) 27(19):3126–32. doi: 10.1200/JCO.2008.21.3223

18. Rani V, Prabhu A. Combining angiogenesis inhibitors with radiation: Advances and challenges in cancer treatment. *Curr Pharm Des* (2021) 27(7):919–31. doi: 10.2174/1381612826666201002145454

19. Mazeron R, Azria D, Deutsch E. [Angiogenesis inhibitors and radiation therapy: From biology to clinical practice]. *Cancer Radiother* (2009) 13(6-7):568–73. doi: 10.1016/j.canrad.2009.06.015

20. Borg C, Mantion G, Boudghene F, Mornex F, Ghiringhelli F, Adenis A, et al. Efficacy and safety of two neoadjuvant strategies with bevacizumab in mri-defined locally advanced T3 resectable rectal cancer: Final results of a randomized, noncomparative phase 2 inova study. *Clin Colorectal Cancer* (2019) 18(3):200–8.e1. doi: 10.1016/j.clcc.2019.04.006

21. Yu X, Wang QX, Xiao WW, Chang H, Zeng ZF, Lu ZH, et al. Neoadjuvant oxaliplatin and capecitabine combined with bevacizumab plus radiotherapy for locally advanced rectal cancer: Results of a single-institute phase ii study. *Cancer Commun (Lond)* (2018) 38(1):24. doi: 10.1186/s40880-018-0294-z

22. Nogue M, Salud A, Vicente P, Arrivi A, Roca JM, Losa F, et al. Addition of bevacizumab to xelox induction therapy plus concomitant capecitabine-based chemoradiotherapy in magnetic resonance imaging-defined poor-prognosis locally advanced rectal cancer: The avacross study. *Oncologist* (2011) 16(5):614–20. doi: 10.1634/theoncologist.2010-0285

23. Jakob J, Simeonova A, Kasper B, Ronellenfitsch U, Rauch G, Wenz F, et al. Combined sunitinib and radiation therapy for preoperative treatment of soft tissue sarcoma: Results of a phase I trial of the German interdisciplinary sarcoma group (Gisg-03). *Radiat Oncol* (2016) 11:77. doi: 10.1186/s13014-016-0654-2

24. Jakob J, Simeonova A, Kasper B, Ronellenfitsch U, Wenz F, Hohenberger P. Combined radiation therapy and sunitinib for preoperative treatment of soft tissue sarcoma. *Ann Surg Oncol* (2015) 22(9):2839–45. doi: 10.1245/s10434-015-4680-3

25. Yoon SS, Duda DG, Karl DL, Kim TM, Kambadakone AR, Chen YL, et al. Phase ii study of neoadjuvant bevacizumab and radiotherapy for resectable soft tissue sarcomas. *Int J Radiat Oncol Biol Phys* (2011) 81(4):1081–90. doi: 10.1016/j.ijrobp.2010.07.024

frontiers | Frontiers in Oncology

TYPE Case Report
PUBLISHED 28 March 2023
DOI 10.3389/fonc.2023.837394

OPEN ACCESS

EDITED BY
Benjamin Clasie,
Massachusetts General Hospital, Harvard Medical School, United States

REVIEWED BY
Fiori Alite,
Geisinger Commonwealth School of Medicine, United States
Bilgin Kadri Aribas,
Bülent Ecevit University, Türkiye

*CORRESPONDENCE
Xuemei Wu
wuxuemei72@163.com
Shuyuan Chu
emilyyuanchu@163.com

SPECIALTY SECTION
This article was submitted to Radiation Oncology, a section of the journal Frontiers in Oncology

RECEIVED 01 March 2022
ACCEPTED 15 March 2023
PUBLISHED 28 March 2023

CITATION
Ke M, Zeng J, Chen Z, Huang R, Wu X and Chu S (2023) Stent loaded with radioactive Iodine-125 seeds for adenoid cystic carcinoma of central airway: A case report of innovative brachytherapy. *Front. Oncol.* 13:837394. doi: 10.3389/fonc.2023.837394

Stent loaded with radioactive Iodine-125 seeds for adenoid cystic carcinoma of central airway: A case report of innovative brachytherapy

Mingyao Ke[1], Junli Zeng[1], Zhide Chen[1], Rui Huang[1], Xuemei Wu[1]* and Shuyuan Chu[2]*

[1]Department of Respiratory Centre, The Second Affiliated Hospital of Xiamen Medical College, Xiamen, Fujian, China, [2]Laboratory of Respiratory Disease, Affiliated Hospital of Guilin Medical University, Guilin, Guangxi, China

Adenoid cystic carcinoma (ACC) of central airway is very rare. More than half of ACCs are unresectable for tumor extension. There's rare report on local ACCs only in central airway. We present a case of ACC in central airway who underwent an innovative brachytherapy. A 44-year-old woman was diagnosed with primary ACC in central airway without regional lymphadenopathy or metastatic disease. Stenosis was observed in lower trachea and both left and right main bronchi (stenosis in lumen ≥50%) with bronchoscopy. The tumor was unresectable due to local extension. A Y-shaped and stainless-steel stent loaded with radioactive ^{125}I seeds was placed in the central airway using bronchoscope. The number and distribution of ^{125}I seeds were planed using treatment planning system. The stent was removed three months later. The patient tolerated the procedure well. She was alive without relapse three years after removing the stent with ^{125}I seeds. This case demonstrates the successful use of stent with radioactive ^{125}I seeds for unresectable ACCs in central airway. In the procedure, the stent was placed with bronchoscope and under the vision from bronchoscope. This innovative brachytherapy is well-tolerated, safe, precise and individualized designed. The patient with unresectable ACCs could get a long-term relapse-free survival. Clinical trials could be taken to validate its effectiveness and tolerability in patients with ACCs of central airway.

KEYWORDS

adenoid cystic carcinoma, central airway, brachytherapy, radioactive stent, bronchoscope

Abbreviations: ACC, Adenoid cystic carcinoma; ^{125}I, Iodine-125; PET-CT, positron emission tomography and computed tomography; CT, computerized tomography.

Introduction

Malignant obstruction in central airway is usually involved with tumors in trachea or mainstem bronchi. In general, tracheal tumors are uncommon, making up only 0.2% of all respiratory malignancies (1). Adenoid cystic carcinoma (ACC) of trachea accounts for approximately 15%-20% of primary tracheal carcinomas (2). Thus, there's rare report on local ACC only in central airway. The ACC in central airway poses a challenge to diagnosis and treatment. Here, we present a rare case of unresectable ACC in central airway, who underwent an innovative brachytherapy. She was placed a stainless-steel stent loaded with radioactive Iodine-125 (^{125}I) seeds in central airway using bronchoscope under the guidance from bronchoscope. At the most recent follow-up, she achieved a three-year relapse-free survival after removing the stent with ^{125}I seeds.

Case description

A 44-year-old woman presented with cough for one year and bloody phlegm for six months. She also presented with shortness of breath after walking on a level road for three months. The bronchoscopic biopsy confirmed a diagnosis of primary ACC in her central airway. The work-up with positron emission tomography and computed tomography (PET-CT) showed negative for regional lymphadenopathy and metastatic disease. However, the ACC was unresectable due to the extension of tumor.

She was referred to our hospital. In physical examination, the intensity of her breath sounds in both lungs was decreased. Thoracic computerized tomography (CT) scanning showed soft tissue nodules at the bifurcation of the right main bronchus (Figures 1A–G). On July 12, 2018, bronchoscopy showed swelling and congestion of mucosa in lower trachea, widened and rough carina, and stenosis in lower trachea and both left and right main bronchi (stenosis in lumen ≥50%) (Figures 2A–C). With bronchoscope, she underwent ablative therapy to remove visible tumors using high-frequency electrocautery system, as well as balloon dilation for stenosis in central airway.

On July 24, 2018, under the guidance from bronchoscope, a Y-shaped and stainless-steel stent loaded with 40 radioactive ^{125}I seeds (0.60 mCi) was placed in her lower trachea using bronchoscope (Figures 2D–F; Supplementary File 1). The number and distribution of seeds were planed using treatment planning system (TPS) (Beijing Feitianzhaoye Co., Ltd.) (Figure 3) before placement based on the thoracic CT scanning (Figures 1A–G). A dose of 120Gy was prescribed to the planning target volume (PTV). All layers of trachea and mainstem bronchi with the tumor in CT scans

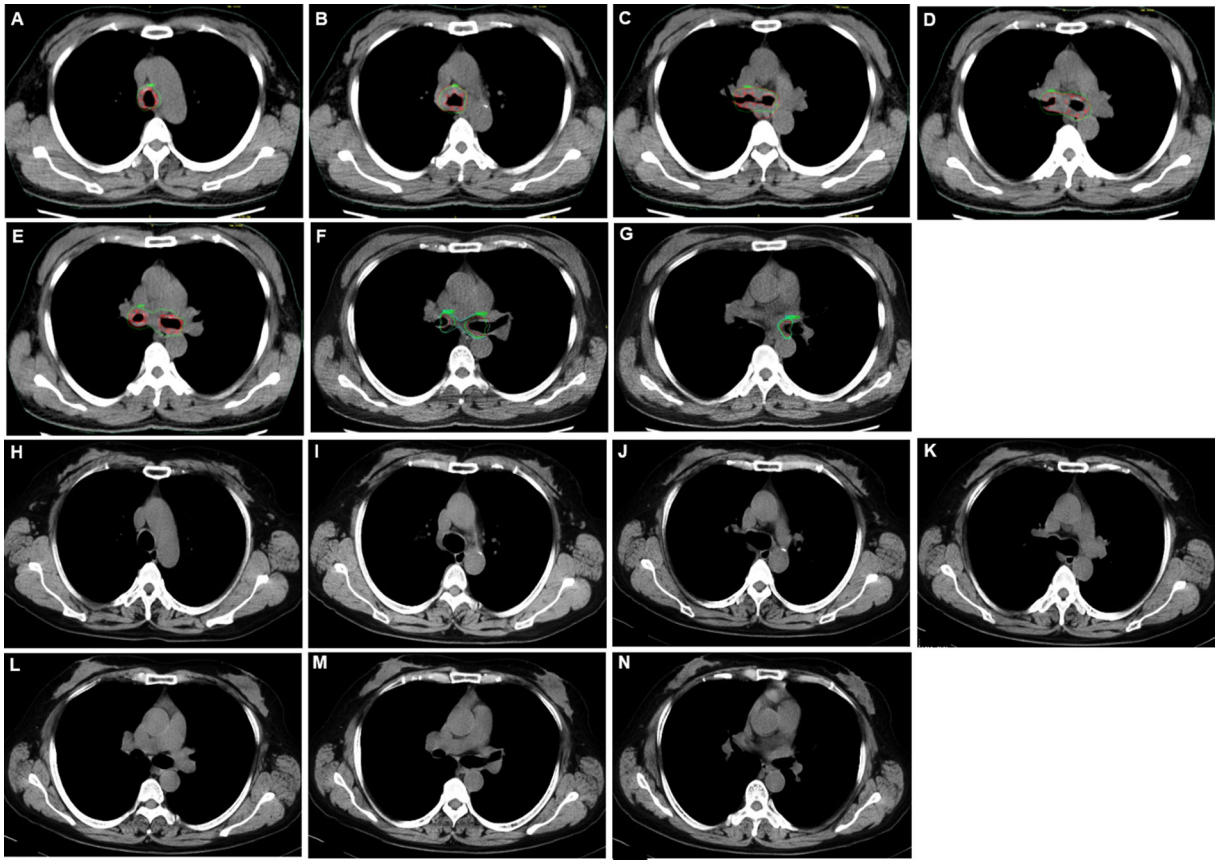

FIGURE 1
Thoracic computerized tomography (CT) scans for adenoid cystic carcinoma (ACC) in central airway. **(A–G)** Thoracic CT scans before placing the stent with ^{125}I seeds. **(H–N)** Thoracic CT scans 35 months after removing the stent with ^{125}I seeds.

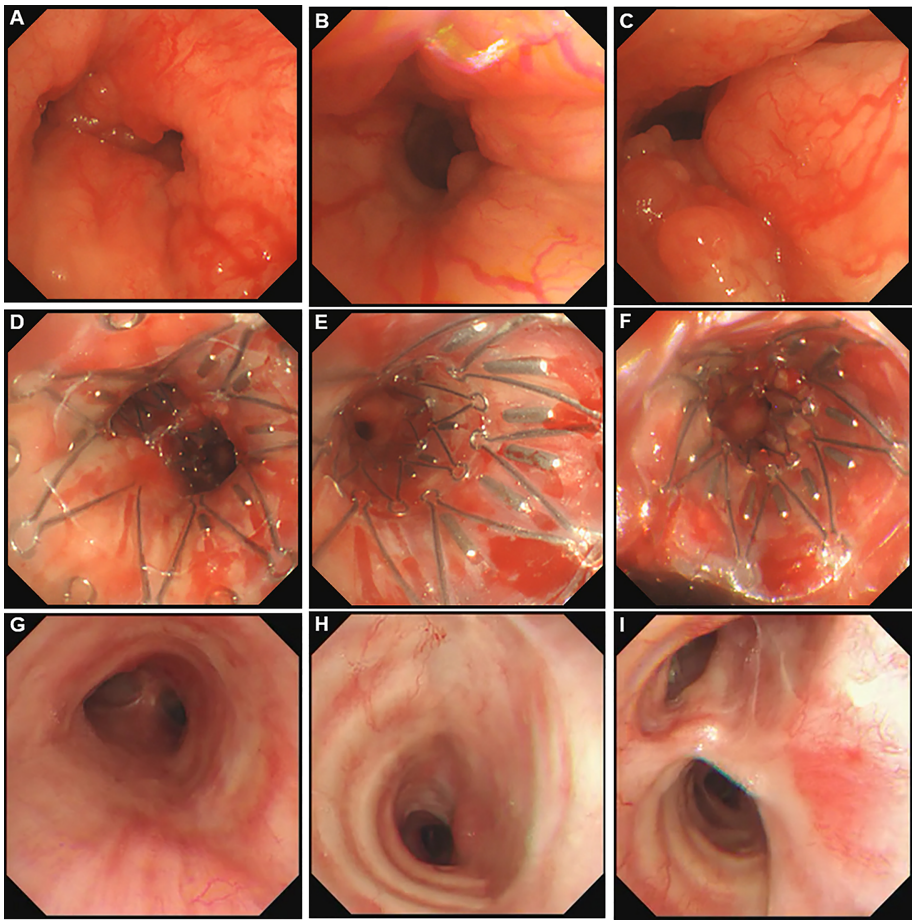

FIGURE 2
Bronchoscopy pictures in central airway. **(A)** Adenoid cystic carcinoma (ACC) in lower trachea. **(B)** ACC in left main bronchus. **(C)** ACC in right main bronchus. **(D)** Stent carrying ^{125}I seeds in lower trachea. **(E)** Stent carrying ^{125}I seeds in left main bronchus. **(F)** Stent carrying ^{125}I seeds in right main bronchus. **(G)** lower trachea 35 months after removing the stent. **(H)** Left main bronchus 35 months after removing the stent. **(I)** Right main bronchus 35 months after removing the stent.

were contoured as clinical target volume (CTV), because the depth of tumor invasion can't be determined from CT scans. Moreover, the stent with ^{125}I seeds was placed in the central airway. And the distance from tumor to the seeds remained the same even when breathing or changing body positions. Thus, PTV wasn't extended from CTV. For organs at risk, only spinal cord was contoured, but wasn't included in PTV. The dose for spinal cord at risk was constrained less than 45Gy, which was referenced from the dose of external beam radiotherapy.

For radiation protection, the patient, endoscopist and assistant wore lead apron in the procedure. The lead apron covered both front and back of the body. In a lead box with a lead-glass window, the stent was loaded with radioactive ^{125}I seeds, and then was put into a metal and radiation-resistant stent-conveyor. During this process, the endoscopist was wearing lead gloves. Thus, the endoscopist and assistant were protected from ^{125}I radiation in the procedure. The patient tolerated the procedure well without chest pain, fistula formation, pulmonary infection, pneumothorax, hemoptysis or stent displacement. No bleeding was observed at the site. When she was discharged home, the radioactive background of the patient was the same as that from the ^{125}I seeds. The background was nearly zero when she's wearing lead apron. The patient was given precaution instructions which were similar to other low-dose-rate (LDR) brachytherapy. Particularly, she had to wear the lead apron whenever she was in a room with any other person till the stent with ^{125}I seeds was removed. This lead apron covered both front and back of her body. We required her family to help her keep doing this. We also followed her every month to make sure she did it till removing the stent with ^{125}I seeds.

For this case, the stent with radioactive ^{125}I seeds was kept in the stenosis for about 1.5 half-lives of ^{125}I seeds. The reason was that the radioactive activity of ^{125}I reduces to 25% after two half-lives. While this duration was necessary to deliver the majority of the activity, there were potential side effects due to the stent, such as septum excretion. Thus, we proposed that the stent should be kept in the airway for one to two half-lives of ^{125}I seeds. On October 15, 2018, the Y-shaped stent with radioactive ^{125}I seeds was removed using bronchoscope. No visible airway stenosis was observed in bronchoscopy. Tumor cells were not found with bronchoscopic brushing. At that time, she didn't present with shortness of breath or bloody phlegm. The patient was followed with thoracic CT scanning and bronchoscopy. At the most recent follow-up on

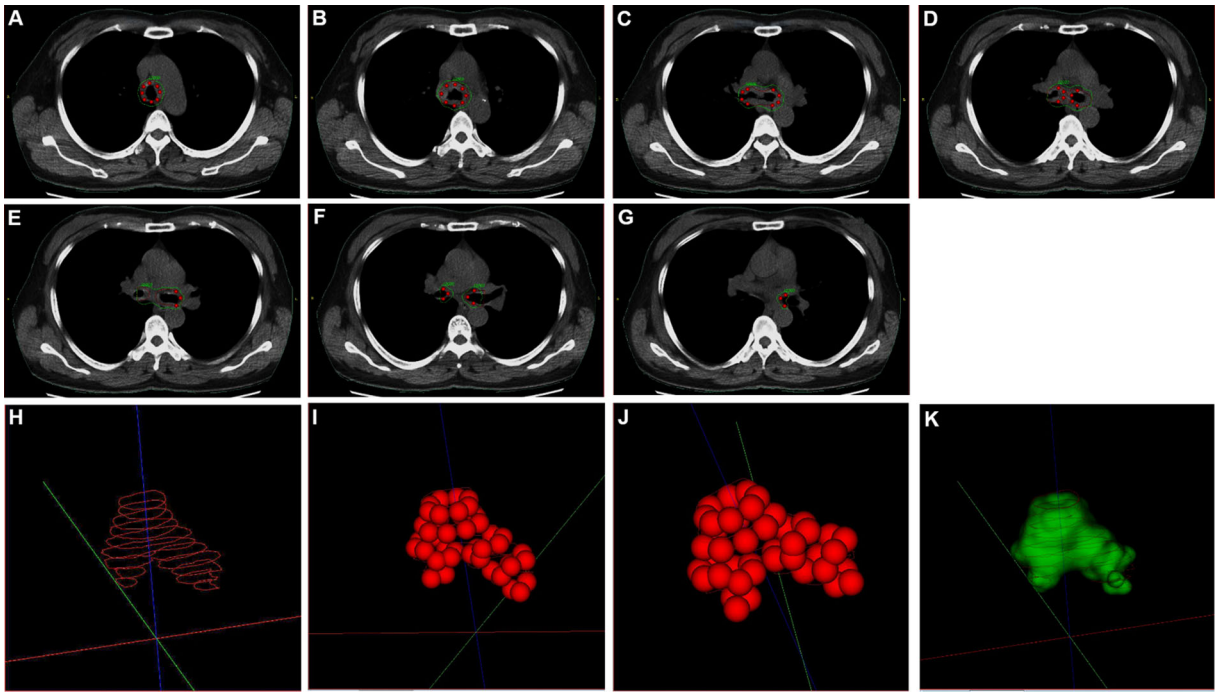

FIGURE 3
The number and distribution of seeds in plan before placement. **(A–G)** The seeds distribution and isodose distribution in thoracic computerized tomography (CT) scans. **(H)** Planning target volume (PTV) in three-dimension (3D). **(I, J)** ^{125}I seeds distribution in 3D. **(K)** Isodose cloud of 120Gy in 3D. Red seeds: ^{125}I seeds. Red curve: target area in planning. Green curve: Isodose curve of 120Gy.

September 9, 2021, the patient was alive without symptoms, and her central airway looked like normal without stenosis or tumors (Figures 1H–N, 2G–I; Supplementary File 2). To the best of our knowledge, no case of ACC in central airway has been reported to be treated with stent loaded with radioactive ^{125}I seeds using bronchoscope with the guidance of bronchoscope, and then got three-year relapse-free survival. Table 1 illustrates the timeline with the episode of care. The authors are accountable for all aspects of the work in ensuring that questions related to the accuracy or integrity of any part of the work are appropriately investigated and resolved. All procedures performed in the study involving human participant were in accordance with the ethical standards of the institutional research committee and with the Helsinki Declaration (as revised in 2013). Written informed consent was obtained from the patient for publication of this case report and accompanying images.

Discussion

ACC is a slow-growing and painless tumor, which has a potential to invade into surrounding tissues. It's preferred to remove the entire tumor by a wide surgical excision. However, ACCs usually have involved a long segment of airway before it's obstructive. Thus, most of them are unresectable when patients present symptoms. In the experience of Massachusetts General Hospital, 25% of patients with ACCs had unresectable tumor (1). As determined by bronchoscopy, tumor length was the most common reason that resection was declined in 68% of these patients (1). Our case was one of those 68% patients. Mostly, neither signs nor symptoms of ACCs are found for many months and years before they're diagnosed (1). For our case, when the ACC was diagnosed, the tumor had already been unresectable. At this time, local therapy was an effective alternative to provide

TABLE 1 The timeline with the episode of care.

Date	Episode of care
July 12, 2018	1. Bronchoscopy showed stenosis in central airway. 2. The patient underwent bronchoscopic ablative therapy and balloon dilation.
July 24, 2018	A Y-shaped and stainless-steel stent loaded with radioactive ^{125}I seeds was placed in the lower trachea with bronchoscope and under the vision from bronchoscope.
October 15, 2018	The Y-shaped stent with radioactive ^{125}I seeds was removed using bronchoscope.
September 9, 2021	In the most recent follow-up, the patient was alive without symptoms, and her central airway was almost normal without stenosis or tumors.

meaningful palliation and good life quality to the patient. Thus, brachytherapy should be an appropriate option for this patient.

Stent loaded with radioactive seeds has been widely used for malignant airway obstruction due to lung cancer or esophageal cancer (3, 4), which is under guidance of CT or C-arm angiographic unit. In contrast, we placed the stent with radioactive ^{125}I seeds under the vision from bronchoscope in this patient with ACC of central airway. This innovative brachytherapy hasn't been reported yet. Compared with CT-guided percutaneous placement, this innovative one could accurately place the stent in the stenotic segment of airway under guidance of bronchoscope, without side effect such as chest pain, fistula formation or pulmonary infection. Moreover, both patient and doctors exposed less radiation in the process of this innovative brachytherapy than in the CT-guided one. For ACC in airway, the tumor cells usually infiltrate into the wall of airway. With the innovative brachytherapy, the stent could keep the radioactive seeds exactly in the stenotic segment of airway. At the end of therapeutic period, the radioactive stent could be taken out using bronchoscope. All of those for treating ACC in airway can't be done by percutaneous CT-guided radioactive stent placement.

In addition, the innovative brachytherapy could be better than traditional brachytherapy or after-loading radiation therapy for ACCs in central airway. The reasons are as follows. First, radioactive stent in airway could keep continuous brachytherapy with a therapeutic dose for the tumor in airway stenosis. This radioactive dose is too low to cause side effects which are happened in traditional brachytherapy. The ^{125}I seed has a half-life of 59.4 days. The radioactive stent could be kept in the airway affected by tumor without displacement during the period of brachytherapy, which is one to two half-lives of ^{125}I seed (5). For our case, the stent with radioactive ^{125}I seeds was kept in the segment affected by tumor for about 1.5 half-lives of ^{125}I seed. Second, the individualized dose and distribution of radioactive seeds are planned by TPS before placing into airway. That leads to more precise dose and location of seeds for the tumor and then a better effect than traditional brachytherapy, whereas less side effects. For our case, since the ACC had infiltrated into the tracheal and bronchial wall, it's impossible to distinguish the tumor and normal tissues in airway wall even in contrast-enhanced CT scans. Thus, all layers of tracheal and bronchial wall were regarded as the PTV in our case with non-contrast CT pictures. It's reported that a case of primary tracheal ACC was treated with high dose-rate brachytherapy, who developed tracheal stenosis 22 months after brachytherapy and had to be placed a tracheal stent (6). In contrast, our case wasn't observed tracheal stenosis in the most recent follow-up, confirming the efficacy and safety of the innovative brachytherapy in the long term. Moreover, the procedure of this innovative brachytherapy is minimally invasive and well tolerated.

Tracheal ACCs were reported to be treated with a high dose of permanent Palladium-103 seed implantation under CT guidance (7). The three patients were followed for an average time of nine months, when they showed disease regression and symptom improvement. However, long-term results weren't reported. In contrast, our case achieved a three-year relapse-free survival using ^{125}I seeds in a low-dose irradiation. For our case, almost all of the ACC was eliminated by impermanently placing a stent with radioactive ^{125}I seeds under the vision from bronchoscope. The ACC in central airway hasn't been relapsed till the most recent follow-up, as long as 35 months after removing the stent with ^{125}I seeds. The efficacy of this brachytherapy for our case suggests that ACCs should be radiosensitive for endobronchial ^{125}I brachytherapy. Our finding is consistent with the previous report that tracheal tissue is radio-sensitivity (8). And radiotherapy is suggested as adjuvant therapy for primary tracheal tumors, particularly if the tumor is unresectable (8). That could support the endobronchial brachytherapy for ACCs in central airway. Moreover, it's recently reported that ACCs in eye, head or neck were all radiosensitive for ^{125}I brachytherapy (9, 10). That further confirms the radio-sensitivity of ACCs for ^{125}I seeds in our case. The ^{125}I seeds provide continuous radiation in a low dose, which could lead to a buildup of radiation damage through synchronizing tumor cells to radiosensitive G2-M phase (11). As a source of low-dose radiation, ^{125}I seeds allow normal tissue to repair the sublethal damage, whereas the tumor cells are damaged and killed (12). Therefore, ^{125}I seeds could be appropriate in brachytherapy for ACCs in airway.

For organs at risk, only spinal cord was contoured for our case. The reason is as follows. The distance from spinal cord to the nearest ^{125}I seeds was about 1cm. The radiative dose is sharply attenuated at a distance more than 1cm. Therefore, the dose of irradiation is little and safe for organs such as esophagus, heart or spinal cord in LDR brachytherapy. Even in high-dose-rate endobronchial brachytherapy or interstitial brachytherapy, the dose exposed in spinal cord, heart and esophagus is safe (13, 14), let alone LDR brachytherapy for our case. Spinal cord was contoured in our case, because it's so crucial that any overdose could lead to irreversible injury. For our case, a dose of 45Gy was the limit for spinal cord at risk, which was referenced from the dose of external beam radiotherapy using conventional fractionation with 1.8-2Gy per fraction. That's because there isn't guideline of LDR brachytherapy for endobronchial cancer (15). Actually, the dose exposed in spinal cord was far less than 45Gy in practice.

Despite a slow-growing growth pattern, the National Cancer Institute (USA) considers ACC as a high-grade malignancy (16). According to previous report, for patients with tracheal ACC, the 5-year survival ranged from 33% to 52% and the 10-year survival ranged from 10% to 29% regardless of whether ACC was resected or not (17). Considering that, our innovative technique could be an appropriate option for unresectable ACCs in central airway. This innovative technique is an impermanent implantation of radioactive seeds using bronchoscope. It could provide a high quality of life to those patients with unresectable ACCs of central airway in the long term. However, we acknowledged the limitation of this innovative technique that it's not appropriate to the tumor in peripheral lung.

In conclusion, this case demonstrates the successful use of stent loaded with radioactive ^{125}I seeds for unresectable ACCs of central

airway. In the procedure, the stent was placed with bronchoscope and under the vision from bronchoscope. This innovative brachytherapy is well-tolerated, safe and individualized designed, which could get a long-term relapse-free survival for patients with unresectable ACCs of central airway. Clinical trials could be taken to validate its effectiveness and tolerability in patients with ACCs and obstruction in central airway.

Concluding remarks

Our case is the first time to demonstrate the successful use of stent with radioactive Iodine-125 seeds in unresectable ACCs of central airway, in which the stent was placed with bronchoscope and under the vision from bronchoscope. This innovative brachytherapy is well-tolerated, safe, precise and individualized designed, which could get a long-term relapse-free survival for patients. Considering the challenge of treatment for ACC in central airway, our findings may provide an innovative brachytherapy to treat the malignant airway obstruction.

Data availability statement

The original contributions presented in the study are included in the article/Supplementary Material. Further inquiries can be directed to the corresponding authors.

Ethics statement

Ethical review and approval was not required for the study on human participants in accordance with the local legislation and institutional requirements. The patient/participant provided her written informed consent to participate in this study. Written informed consent was obtained from the individual for the publication of any potentially identifiable images or data included in this article.

Author contributions

MK, JZ, ZC, RH, and XW were responsible for the patient's treatment and collected the patient's information. SC drafted this manuscript. MK and SC revised the paper. MK, XW and SC offered constructive suggestions for this study. All authors contributed to the article and approved the submitted version.

Conflict of interest

The authors declare that the research was conducted in the absence of any commercial or financial relationships that could be construed as a potential conflict of interest.

Publisher's note

Supplementary material

The Supplementary Material for this article can be found online at: https://www.frontiersin.org/articles/10.3389/fonc.2023.837394/full#supplementary-material

SUPPLEMENTARY FILE 1
The video of bronchoscopy when the stent with Iodine-125 seeds was placed.

SUPPLEMENTARY FILE 2
The video of bronchoscopy 35 months after removing the stent with Iodine-125 seeds.

References

1. Gaissert HA, Mark EJ. Tracheobronchial gland tumors. *Cancer Control* (2006) 13:286–94. doi: 10.1177/107327480601300406

2. Urdaneta AI, Yu JB, Wilson LD. Population based cancer registry analysis of primary tracheal carcinoma. *Am J Clin Oncol* (2011) 34:32–7. doi: 10.1097/COC.0b013e3181cae8ab

3. Meng QK, Yu XY, Li W, Sun QL. Radioactive and normal stent insertion for the treatment of malignant airway stenosis: A meta-analysis. *Brachytherapy* (2021) 20:883–91. doi: 10.1016/j.brachy.2021.03.002

4. Wang Y, Lu J, Guo JH, Zhu GY, Zhu HD, Chen L, et al. A novel tracheobronchial stent loaded with ^{125}I seeds in patients with malignant airway obstruction compared to a conventional stent: A prospective randomized controlled study. *EBio Med* (2018) 33:269–75. doi: 10.1016/j.ebiom.2018.06.006

5. Tepper J. *Gunderson and Tepper's Clinical Radiation Oncology*. 5th ed. Elsevier (2019).

6. Carvalho Hde A, Figueiredo V, Pedreira WL Jr, Aisen S. High dose-rate brachytherapy as a treatment option in primary tracheal tumors. *Clinics (Sao Paulo)* (2005) 60:299–304. doi: 10.1590/S1807-59322005000400007

7. Doggett S, Chino S, Lempert T, Federhart J. Percutaneous CT-fluoroscopic-guided radioisotope seed placement for the management of adenoid cystic carcinoma of the trachea. *Brachytherapy* (2017) 16:639–45. doi: 10.1016/j.brachy.2016.11.007

8. Honings J, Gaissert HA, van der Heijden HF, Verhagen AF, Kaanders JH, Marres HA. Clinical aspects and treatment of primary tracheal malignancies. *Acta Otolaryngol* (2010) 130:763–72. doi: 10.3109/00016480903403005

9. Wang P, Ma N, Zhang S, Ning X, Guo C, Zhang Q, et al. ^{125}I interstitial brachytherapy for malignant lacrimal sac tumours: an innovative technique. *Eye (Lond)* (2021) 35:1240–7. doi: 10.1038/s41433-020-1098-3

10. Chen Y, Dai J, Jiang Y, Ji Z, Jiang P, Sun H, et al. Long-term outcomes of personalized stereotactic ablative brachytherapy for recurrent head and neck adenoid cystic carcinoma after surgery or external beam radiotherapy: A 9-year study. *J Pers Med* (2021) 26:11. doi: 10.3390/jpm11090839

11. Qu A, Wang H, Li J, Wang J, Liu J, Hou Y, et al. Biological effects of (125)I seeds radiation on A549 lung cancer cells: G2/M arrest and enhanced cell death. *Cancer Invest* (2014) 32:209–17. doi: 10.3109/07357907.2014.905585

12. Chen Z, Nath R. Biologically effective dose (BED) for interstitial seed implants containing a mixture of radionuclides with different half-lives. *Int J Radiat Oncol Biol Phys* (2003) 55:825–34. doi: 10.1016/S0360-3016(02)04282-7

13. Sawicki M, Łyczek J, Szutkowski Z. Analysis of dose distribution between contemporary and standard planning in high-dose-rate endobronchial brachytherapy based on three-dimensional imaging. *J Contemp Brachytherapy* (2019) 11(5):462–8. doi: 10.5114/jcb.2019.89194

14. Rashid A, Pinkawa M, Haddad H, Hermani H, Temming S, Schäfer A, et al. Interstitial single fraction brachytherapy for malignant pulmonary tumours. *Strahlenther Onkol* (2021) 197(5):416–22. doi: 10.1007/s00066-021-01758-5

15. Stewart A, Parashar B, Patel M, O'Farrell D, Biagioli M, Devlin P, et al. American Brachytherapy society consensus guidelines for thoracic brachytherapy for lung cancer. *Brachytherapy* (2016) 15(1):1–11. doi: 10.1016/j.brachy.2015.09.006

16. *Adenoid cystic carcinoma of trachea*. Available at: https://www.dovemed.com/diseases-conditions/adenoid-cystic-carcinoma-trachea/ (Accessed September 1, 2021).

17. Gaissert HA, Grillo HC, Shadmehr MB, Wright CD, Gokhale M, Wain JC, et al. Long-term survival after resection of primary adenoid cystic and squamous cell carcinoma of the trachea and carina. *Ann Thorac Surg* (2004) 79(6):1889–96; discussion 1896-7. doi: 10.1016/j.athoracsur.2004.05.064

frontiers | Frontiers in Oncology

TYPE Case Report
PUBLISHED 27 April 2023
DOI 10.3389/fonc.2023.965166

OPEN ACCESS

EDITED BY
Benjamin Clasie,
Massachusetts General Hospital and Harvard Medical School, United States

REVIEWED BY
Urban Emmenegger,
Sunnybrook Research Institute (SRI), Canada
Yoshihito Nomoto,
Mie University, Japan

*CORRESPONDENCE
Xiaotao Zhang
sabr@vip.163.com

RECEIVED 12 July 2022
ACCEPTED 29 March 2023
PUBLISHED 27 April 2023

CITATION
Lu L, Wang Y, Li L, Yu L, Liu L, Qu B and Zhang X (2023) ^{125}I Radiotherapy combined with metronomic chemotherapy may boost the abscopal effect, leading to complete regression of liver metastasis in an SCLC patient with a 58.5-month OS: a case report.
Front. Oncol. 13:965166.
doi: 10.3389/fonc.2023.965166

^{125}I Radiotherapy combined with metronomic chemotherapy may boost the abscopal effect, leading to complete regression of liver metastasis in an SCLC patient with a 58.5-month OS: a case report

Linlin Lu[1], Yu Wang[2], Lei Li[2], Lan Yu[2], Li Liu[2], Baozhen Qu[1] and Xiaotao Zhang[2,3]*

[1]Qingdao Cancer Prevention and Treatment Research Institute, Affiliated Qingdao Central Hospital of Qingdao University, Qingdao Cancer Hospital, Qingdao, China, [2]Department of Oncology, Affiliated Qingdao Central Hospital of Qingdao University, Qingdao Cancer Hospital, Qingdao, China, [3]Department of Oncology, Shandong Provincial Qianfoshan Hospital, Shandong University, Jinan, China

The liver is the most common and lethal metastatic site in patients with extensive-stage small-cell lung cancer (ES-SCLC), and median survival with current standard treatment is only 9–10 months from diagnosis. Clinical observations show that a complete response (CR) is extremely rare in ES-SCLC patients with liver metastasis. Moreover, to the best of our knowledge, complete regression of liver metastasis induced by the abscopal effect, boosted primarily by permanent radioactive iodine-125 seeds implantation (PRISI), combined with a low-dose metronomic temozolomide (TMZ) regimen, has not been recorded. Here, we present the case of a 54-year-old male patient who developed multiple liver metastases from ES-SCLC after multiple lines of chemotherapy. The patient was given partial PRISI therapy (two out of six tumor lesions; 38 iodine-125 seeds in one dorsal lesion and 26 seeds in one ventral lesion), which was combined with TMZ metronomic chemotherapy (50 mg/m^2/day, days 1–21, every 28 days). The abscopal effect was observed for 1 month after PRISI treatment. After about 1 year, all the liver metastases had completely disappeared, and the patient experienced no relapse. The patient eventually died of malnutrition caused by a non-tumor intestinal obstruction and had an overall survival of 58.5 months after diagnosis. PRISI combined with TMZ metronomic chemotherapy might be considered a potential therapy to trigger the abscopal effect in patients with liver metastases.

KEYWORDS

SCLC, abscopal effect, metronomic chemotherapy, permanent iodine-125 seeds implantation, liver metastases

Introduction

Small-cell lung cancer (SCLC) is marked by its exceptionally high proliferation, early metastasis, and poor prognosis. The 5-year overall survival (OS) rate remains dismal, around 7%–10%, mainly because of the high risk of distant metastasis (1, 2). Among all the common metastatic sites, such as the liver, bones, brains, lungs, and adrenal glands, the liver is the most common site of metastasis, and metastasis to the liver, alone or in combination with metastasis to other organs, is associated with the worst outcomes (3–6). There were no important therapeutic clinical advances for over three decades (7, 8); a subset of patients have derived benefit from immunotherapy in recent years, but patients with liver metastases have not (9).

Radiation is a highly effective local treatment for tumor lesions. It works primarily by damaging the DNA inside cancer tissues. Spontaneous regression of tumors outside the irradiated field (abscopal effect) is rare but has been occasionally observed (10). However, the abscopal effect, induced by permanent radioactive iodine-125 seeds implantation (PRISI), has not been reported. Metronomic chemotherapy is designed to maintain low, but active, concentrations of chemotherapeutic drugs over prolonged periods of time without causing serious toxicities (Y. L. 11). As has been reported, metronomic chemotherapy can promote tumor regression not only by inducing anti-angiogenesis but also by increasing latent antitumor immune responses (12, 13).

The aim of this report is to present the case of a patient with extensive stage- (ES-)SCLC who showed an unusual liver abscopal effect after receiving PRISI combined with temozolomide (TMZ) metronomic chemotherapy. This resulted in a sustained complete response (CR) and long-term survival. The patient died of malnutrition caused by a non-tumor intestinal obstruction 15 months after PRISI.

Case presentation

Here we present the case of a 54-year-old male patient who had previously been diagnosed with SCLC and received multiple lines of chemotherapy regimens, including etoposide and cisplatin (EP), irinotecan and cisplatin (IP), and paclitaxel and cisplatin (TP). He had also received radiotherapy of the chest wall, the right supraclavicular region, the thoracic vertebrae, and the right adrenal gland from December 2013 to August 2015 at another hospital, and was assessed as having a partial response. Unfortunately, he experienced multiple relapses, and presented to our clinic in October 2015.

Before treatment, a magnetic resonance (MR) scan was carried out, and revealed multiple metastases to the right axilla, bilateral supraclavicular lymph nodes, the right seventh rib, and the left ilium. His disease progressed and, after treatment with two cycles of EP and one cycle of single paclitaxel chemotherapy, a MR scan revealed multiple liver metastases (Figure 1A, 2016–02–16). No tumor response was observed after completion of two cycles of combined chemotherapy with albumin-bound paclitaxel and carboplatin, but a new right-side pleural metastasis was found. He then received radiotherapy to the right chest wall (50 Gy in 25 fractions) and achieved a CR. Specimens of the initial tumor were analyzed for sequencing mutations. The tumor was found to be SCLC and to contain no proven drug-sensitive gene mutations. In any event, treatment targeting the programmed cell death 1 ligand 1 (PD-1/L1) had not yet been approved in China in 2015.

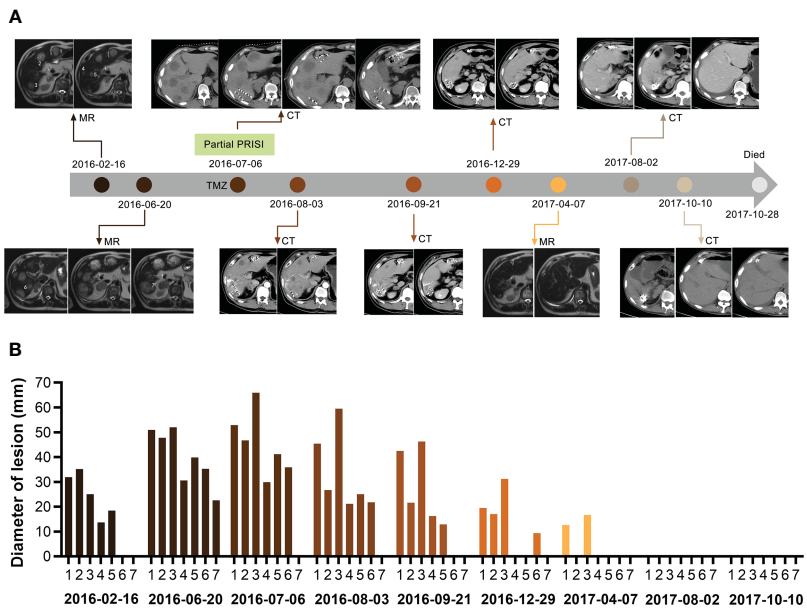

FIGURE 1
Course of the complete regression of the patient's multiple liver metastases. **(A)** MR/CT scans of the patient's liver before and after partial PRISI and treatment with the low-dose metronomic TMZ regimen. **(B)** Diagram showing the progressive change in the size of tumor lesions. Lesion numbers labeled on scans correspond to the same lesion numbers in the diagram. PRISI, permanent radioactive iodine-125 seeds implantation; TMZ, temozolomide.

The patient's liver metastases significantly progressed, with two masses measuring > 50 mm in diameter and five metastases > 20 mm in diameter: individually, 50.91mm, 47.75mm, 52mm, 30.58mm, 39.86mm, 35.26mm, 22.61mm in diameter (Figures 1A, B, 2016–06–20). The patient complained of severe pain in the upper right abdomen. After a multidisciplinary discussion, we decided to apply computer tomography- (CT-)guided PRISI as a salvage treatment. The two lesions chosen for treatment were those that would require the shortest path for the implantation surgery, aiming to minimize secondary damage to the patient's liver. In detail, the patient underwent permanent implantation of ^{125}I seeds (measuring 4.5 × 0.8 mm, half-life of 60.2 days, photon energy spectrum 27–35 keV, radioactive activity of 0.7 mCi) in two of the liver metastases (one dorsal and one ventral) in July 2016. The prescription dose at the target volume was 120 Gy. We implanted 38 seeds in the dorsal lesion and 26 seeds in the ventral lesion (Figures 1A, 2016–07–06).

In addition, a low-dose metronomic TMZ regimen (50 mg/m^2/day, days 1–21, every 28 days) was instituted before PRISI local therapy as a low-toxicity systemic therapy. This was also done to prevent secondary brain metastasis, because clinical studies have shown that 40%–50% of SCLC patients develop brain metastases after completion of palliative chemotherapy (this was not a standard of care use of TMZ in SCLC).

Follow-up CT in August and September 2016 revealed that all of the patient's liver lesions were significantly reduced, including the four liver lesions not treated with PRISI and also those outside the ^{125}I seeds radiation field, which means that abscopal regression was observed (Figures 1A, B, 2016–08–03, 2016–09–21).

CT and MR scans taken between December 2016 and April 2017, i.e., 5–9 months after implantation, showed that nearly all of the patient's metastatic nodules, whether or not treated with PRISI, had undergone CR. The remaining two lesions had achieved partial response (PR), shrinking in diameter in one case from 52.86 mm to 12.62 mm and in the other case from 65.92 mm to 16.69 mm (Figures 1A, B, 2016–12–29, 2017–04–07).

Extraordinarily, all liver nodules had achieved CR by around 1 year after PRISI therapy (Figure 1, 2017–08–02). Follow-up results 13–15 months post PRISI therapy showed continued CR of liver metastases (Figures 1A, B, 2017–08–02 and 2017–10–10).

Unfortunately, the patient died of malnutrition caused by a non-tumor intestinal obstruction on 28 October 2017.

Discussion and conclusions

Radiotherapy has traditionally been reserved for the palliation of symptoms in patients with advanced disease, including in those who have poor responses to chemotherapy. Brachytherapy has been used for the clinical treatment of malignant tumors worldwide for many years (14), including for hepatocellular carcinoma (HCC) (15, 16), lung cancer (17, 18), prostate cancer, pancreatic cancer, pulmonary carcinoma, oral and maxillofacial tumors, and head and neck malignant neoplasms (19; K. 15, 20–29). Its therapeutic efficacy has been reported to be promising.

PRISI has been used in the liver, and there are reports of PRISI increasing OS in HCC patients after curative resection and in patients with metastatic liver cancer (25; K. 15, 30). In addition, PRISI has been reported to result in a high rate of CR and PR in patients with advanced unresectable HCC (26). Li et al. (16) suggested that palliative surgery plus PRISI is an appropriate therapeutic option for patients with large (diameter >5 cm) HCC tumors. In this case, we performed partial PRISI (in only one dorsal nodule and one ventral nodule) as salvage treatment to reduce tumor-related clinical symptoms and improve the patient's quality of life. To our surprise, abscopal regression was observed in the liver metastatic lesions that were not treated with ^{125}I seeds. Normally, the abscopal effect is driven by external beam radiotherapy (EBRT), which is prescribed to control the disease (10). The median reported radiation dose is 31 Gy (range: 0.45–60.75 Gy) with a median dose of 3 Gy per fraction (range: 0.15–26 Gy) (10). In this case, the prescription dose at the target volume was 120 Gy. Brachytherapy with interstitial implantation of radioactive seeds can achieve a high dose within the target area but the irradiation is sharply attenuated with distance (radiation diameter of 1.7 cm) (30), with the original dose reduced to 1% at 5 cm from the source. However, in this patient, multiple liver metastasis nodules first shrank and then eventually exhibited CR. In fact, the four lesions not treated with PRISI, i.e., which were not located inside the ^{125}I seeds radiation field, within 1 month exhibited abscopal regression in the same way as the as two lesions implanted with ^{125}I seeds. Impressively, follow-up MR and CT scans at 5 months after treatment showed PR or CR of multiple liver metastatic lesions, and subsequent MR and CT scans at 13–15 months' follow-up showed complete resolution. The patient's quality of life, as self-reported, improved significantly.

Studies suggest that immunological mechanisms play a key role in this rare phenomenon (31, 32). When radiation damage tumor cells to liberate tumor-associated antigens (TAAs) like necrotic and apoptotic tumor cells and debris. Increasing and diversity of TAAs stimulate tumor-specific immune response, antigen-presenting cells (APCs) engulf these TAAs and then activate CD8+ T cells to attack the tumor tissue (32). Irradiated tumor cells may also release cellular danger-associated molecular patterns (DAMPs) and cytokines that enhance the migration of immune cells (33).

On the other hand, we speculate that our metronomic TMZ regime also played a crucial role in this case, combining with ^{125}I brachytherapy to boost the abscopal effect. Metronomic chemotherapy is designed to maintain low, but active, concentrations of chemotherapeutic drugs over prolonged periods of time without causing serious toxicities (Y. L. 11). Metronomic chemotherapy can promote tumor regression not only by inducing anti-angiogenesis but also by selectively depleting immunosuppressive cells such as myeloid-derived suppressor cells (MDSCs) and regulatory T cells (Tregs) and by increasing latent antitumor immune responses (C. A. 11–13, 34). Banissi et al. found that a low-dose metronomic TMZ regimen reduced the Treg/CD4$^+$ ratios in the spleen of tumor-bearing rats (35). In our case, a low-dose metronomic TMZ regimen (50 mg/m^2/day, days 1-21, every 4 weeks) was instituted before PRISI to prevent

secondary brain metastasis, as clinical studies have shown that 40%–50% of SCLC patients develop brain metastases after completion of palliative chemotherapy. As shown from the clinical results, this patient still benefited from metronomic TMZ chemotherapy even after multiline treatment, including EP, IP, and TP. Besides, without grade 3-4 adverse events and fewer incidents of treatment interruption during the whole course of treatment. In addition, metronomic chemotherapy is known to induce tumor cells to release TAAs, initiating a T-cell anti-tumor response in the same way as radiation. Moreover, signals released by killed tumor cells would have had an impact on phagocytosis and/or antigen processing, or the maturation and trafficking of dendritic cells (13, 36–38). Taken together, the liver immune microenvironment might have been changed by PRISI and metronomic TMZ treatment in this patient. Regrettably, we did not undertake pathology or laboratory studies to measure cytokines and immune cell subsets and, therefore, have no relevant laboratory data to confirm the postulated mechanisms, mentioned above, in this case.

To our knowledge, this is the first study to report that PRISI boosts the abscopal effect in an ES-SCLC patient with multiple metastases. The metronomic TMZ regime may also help to generate abscopal regression in this therapeutic process. Although more clinical and laboratory trials are needed to elucidate the mechanism, PRISI combined with metronomic chemotherapy is a potential salvage treatment and could be used to control tumor metastases with few complications.

Data availability statement

The original contributions presented in the study are included in the article/Supplementary Material. Further inquiries can be directed to the corresponding author.

Ethics statement

Written informed consent was obtained from the individual(s) for the publication of any potentially identifiable images or data included in this article.

Author contributions

Conceptualization: LLu and XZ. Treatment decision-making and discussions: XZ, LLi, YW, LY, and LLiu. Data collection and analysis: LLu, BQ, and XZ. Manuscript writing: LLu. Final approval of manuscript: XZ. All authors contributed to the article and approved the submitted version.

Acknowledgments

We would like to give our thanks to the patient and his family for their willingness to share the patient's experiences and feelings with the public.

Conflict of interest

The authors declare that the research was conducted in the absence of any commercial or financial relationships that could be construed as a potential conflict of interest.

Publisher's note

Supplementary material

The Supplementary Material for this article can be found online at: https://www.frontiersin.org/articles/10.3389/fonc.2023.965166/full#supplementary-material

References

1. Dingemans AC, Fruh M, Ardizzoni A, Besse B, Faivre-Finn C, Hendriks LE, et al. Small-cell lung cancer: ESMO clinical practice guidelines for diagnosis, treatment and follow-up(). *Ann Oncol* (2021) 32(7):839–53. doi: 10.1016/j.annonc.2021.03.207

2. Rudin CM, Brambilla E, Faivre-Finn C, Sage J. Small-cell lung cancer. *Nat Rev Dis Primers* (2021) 7(1):3. doi: 10.1038/s41572-020-00235-0

3. Nakazawa K, Kurishima K, Tamura T, Kagohashi K, Ishikawa H, Satoh H, et al. Specific organ metastases and survival in small cell lung cancer. *Oncol Lett* (2012) 4 (4):617–20. doi: 10.3892/ol.2012.792

4. Byers LA, Rudin CM. Small cell lung cancer: where do we go from here? *Cancer* (2015) 121(5):664–72. doi: 10.1002/cncr.29098

5. Cai H, Wang H, Li Z, Lin J, Yu J. The prognostic analysis of different metastatic patterns in extensive-stage small-cell lung cancer patients: a large population-based study. *Future Oncol* (2018) 14(14):1397–407. doi: 10.2217/fon-2017-0706

6. Wang X, Wang Z, Pan J, Lu ZY, Xu D, Zhang HJ, et al. Patterns of extrathoracic metastases in different histological types of lung cancer. *Front Oncol* (2020) 10:715. doi: 10.3389/fonc.2020.00715

7. Gazdar AF, Bunn PA, Minna JD. Small-cell lung cancer: what we know, what we need to know and the path forward. *Nat Rev Cancer* (2017) 17(12):765. doi: 10.1038/nrc.2017.106

8. Muppa P, Parrilha Terra SBS, Sharma A, Mansfield AS, Aubry MC, Bhinge K, et al. Immune cell infiltration may be a key determinant of long-term survival in small cell lung cancer. *J Thorac Oncol* (2019) 14(7):1286–95. doi: 10.1016/j.jtho.2019.03.028

9. Iams WT, Porter J, Horn L. Immunotherapeutic approaches for small-cell lung cancer. *Nat Rev Clin Oncol* (2020) 17(5):300–12. doi: 10.1038/s41571-019-0316-z

10. Abuodeh Y, Venkat P, Kim S. Systematic review of case reports on the abscopal effect. *Curr Probl Cancer* (2016) 40(1):25–37. doi: 10.1016/j.currproblcancer.2015.10.001

11. Chen YL, Chang MC, Cheng WF. Metronomic chemotherapy and immunotherapy in cancer treatment. *Cancer Lett* (2017) 400:282–92. doi: 10.1016/j.canlet.2017.01.040

12. Chen CA, Ho CM, Chang MC, Sun WZ, Chen YL, Chiang YC, et al. Metronomic chemotherapy enhances antitumor effects of cancer vaccine by

depleting regulatory T lymphocytes and inhibiting tumor angiogenesis. *Mol Ther* (2010) 18(6):1233–43. doi: 10.1038/mt.2010.34

13. Hao YB, Yi SY, Ruan J, Zhao L, Nan KJ. New insights into metronomic chemotherapy-induced immunoregulation. *Cancer Lett* (2014) 354(2):220–6. doi: 10.1016/j.canlet.2014.08.028

14. Aronowitz JN. Buried emanation; the development of seeds for permanent implantation. *Brachytherapy* (2002) 1(3):167–78. doi: 10.1016/s1538-4721(02)00059-4

15. Chen K, Xia Y, Wang H, Xiao F, Xiang G, Shen F. Adjuvant iodine-125 brachytherapy for hepatocellular carcinoma after complete hepatectomy: a randomized controlled trial. *PloS One* (2013) 8(2):e57397. doi: 10.1371/journal.pone.0057397

16. Li X, Lu P, Li B, Yang R, Luo K. Combination of permanent interstitial (125)I-seed brachytherapy and surgery for the treatment of Large hepatocellular carcinoma. *Technol Cancer Res Treat* (2017) 16(6):930–4. doi: 10.1177/1533034617711352

17. Hilaris BS, Martini N. Interstitial brachytherapy in cancer of the lung: a 20 year experience. *Int J Radiat Oncol Biol Phys* (1979) 5(11-12):1951–6. doi: 10.1016/0360-3016(79)90944-1

18. Heelan RT, Hilaris BS, Anderson LL, Nori D, Martini N, Watson RC, et al. Lung tumors: percutaneous implantation of I-125 sources with CT treatment planning. *Radiology* (1987) 164(3):735–40. doi: 10.1148/radiology.164.3.3615870

19. Armstrong JG, Anderson LL, Harrison LB. Treatment of liver metastases from colorectal cancer with radioactive implants. *Cancer* (1994) 73(7):1800–4. doi: 10.1002/1097-0142(19940401)73:7<1800::aid-cncr2820730705>3.0.co;2-e

20. Son YH, Ariyan S. Intraoperative adjuvant radiotherapy for advanced cancers of the head and neck. preliminary report. *Am J Surg* (1985) 150(4):480–4. doi: 10.1016/0002-9610(85)90158-8

21. Goertz SR, Ali MM, Parker GA. Local management of pancreatic carcinoma: iodine-125 implantation. *Clin Oncol (R Coll Radiol)* (1990) 2(1):22–6. doi: 10.1016/s0936-6555(05)80214-6

22. Horwitz EM, Frazier AJ, Martinez AA, Keidan RD, Clarke DH, Lacerna MD, et al. Excellent functional outcome in patients with squamous cell carcinoma of the base of tongue treated with external irradiation and interstitial iodine 125 boost. *Cancer* (1996) 78(5):948–57. doi: 10.1002/(SICI)1097-0142(19960901)78:5<948::AID-CNCR3>3.0.CO;2-8

23. Horwitz EM, Frazier AJ, Vicini FA, Clarke DH, Edmundson GK, Keidan RD, et al. The impact of temporary iodine-125 interstitial implant boost in the primary management of squamous cell carcinoma of the oropharynx. *Head Neck* (1997) 19(3):219–26. doi: 10.1002/(SICI)1097-0347(199705)19:3<219::AID-HED10>3.0.CO;2-6

24. Ragde H, Blasko JC, Grimm PD, Kenny GM, Sylvester JE, Hoak DC, et al. Interstitial iodine-125 radiation without adjuvant therapy in the treatment of clinically localized prostate carcinoma. *Cancer* (1997) 80(3):442–53. doi: 10.1002/(SICI)1097-0142(19970801)80:3<442::AID-CNCR12>3.0.CO;2-X

25. Martinez-Monge R, Nag S, Nieroda CA, Martin EW. Iodine-125 brachytherapy in the treatment of colorectal adenocarcinoma metastatic to the liver. *Cancer* (1999) 85(6):1218–25. doi: 10.1002/(SICI)1097-0142(19990315)85:6<1218::AID-CNCR2>3.0.CO;2-F

26. Nag S, DeHaan M, Scruggs G, Mayr N, Martin EW. Long-term follow-up of patients of intrahepatic malignancies treated with iodine-125 brachytherapy. *Int J Radiat Oncol Biol Phys* (2006) 64(3):736–44. doi: 10.1016/j.ijrobp.2005.08.029

27. Heysek RV. Modern brachytherapy for treatment of prostate cancer. *Cancer Control* (2007) 14(3):238–43. doi: 10.1177/107327480701400306

28. Zhang FJ, Li CX, Wu PH, Wu YX, Jiao DC, Liu J, et al. CT guided radioactive 125I seed implantation in treating localized advanced pulmonary carcinoma. *Zhonghua Yi Xue Za Zhi* (2007) 87(46):3272–5.

29. Huang K, Sneed PK, Kunwar S, Kragten A, Larson DA, Berger MS, et al. Surgical resection and permanent iodine-125 brachytherapy for brain metastases. *J Neurooncol* (2009) 91(1):83–93. doi: 10.1007/s11060-008-9686-2

30. Chuan-Xing L, Xu H, Bao-Shan H, Yong L, Pei-Jian S, Xian-Yi Y, et al. Efficacy of therapy for hepatocellular carcinoma with portal vein tumor thrombus: chemoembolization and stent combined with iodine-125 seed. *Cancer Biol Ther* (2011) 12(10):865–71. doi: 10.4161/cbt.12.10.17676

31. Demaria S, Ng B, Devitt ML, Babb JS, Kawashima N, Liebes L, et al. Ionizing radiation inhibition of distant untreated tumors (abscopal effect) is immune mediated. *Int J Radiat Oncol Biol Phys* (2004) 58(3):862–70. doi: 10.1016/j.ijrobp.2003.09.012

32. Grass GD, Krishna N, Kim S. The immune mechanisms of abscopal effect in radiation therapy. *Curr Probl Cancer* (2016) 40(1):10–24. doi: 10.1016/j.currproblcancer.2015.10.003

33. Barker HE, Paget JT, Khan AA, Harrington KJ. The tumour microenvironment after radiotherapy: mechanisms of resistance and recurrence. *Nat Rev Cancer* (2015) 15(7):409–25. doi: 10.1038/nrc3958

34. Sevko A, Michels T, Vrohlings M, Umansky L, Beckhove P, Kato M, et al. Antitumor effect of paclitaxel is mediated by inhibition of myeloid-derived suppressor cells and chronic inflammation in the spontaneous melanoma model. *J Immunol* (2013) 190(5):2464–71. doi: 10.4049/jimmunol.1202781

35. Banissi C, Ghiringhelli F, Chen L, Carpentier AF. Treg depletion with a low-dose metronomic temozolomide regimen in a rat glioma model. *Cancer Immunol Immunother* (2009) 58(10):1627–34. doi: 10.1007/s00262-009-0671-1

36. Shurin GV, Tourkova IL, Kaneno R, Shurin MR. Chemotherapeutic agents in noncytotoxic concentrations increase antigen presentation by dendritic cells *via* an IL-12-dependent mechanism. *J Immunol* (2009) 183(1):137–44. doi: 10.4049/jimmunol.0900734

37. Tanaka H, Matsushima H, Mizumoto N, Takashima A. Classification of chemotherapeutic agents based on their differential *in vitro* effects on dendritic cells. *Cancer Res* (2009) 69(17):6978–86. doi: 10.1158/0008-5472.CAN-09-1101

38. Hu J, Kinn J, Zirakzadeh AA, Sherif A, Norstedt G, Wikstrom AC, et al. The effects of chemotherapeutic drugs on human monocyte-derived dendritic cell differentiation and antigen presentation. *Clin Exp Immunol* (2013) 172(3):490–9. doi: 10.1111/cei.12060

frontiers | Frontiers in Oncology

TYPE Case Report
PUBLISHED 21 June 2023
DOI 10.3389/fonc.2023.1146041

OPEN ACCESS

EDITED BY
Vinay Sharma,
University of the Witwatersrand,
South Africa

REVIEWED BY
Francesco Cuccia,
ARNAS Ospedali Civico Di Cristina Benfratelli, Italy
Agolli Linda,
Uniklinikum Giessen und Marburg, Germany

*CORRESPONDENCE
Gianluca Ferini
gianluca.ferini@grupposamed.com

†These authors share last authorship

RECEIVED 16 January 2023
ACCEPTED 25 May 2023
PUBLISHED 21 June 2023

CITATION
Ferini G, Zagardo V, Viola A, Aiello MM, Harikar MM, Venkataram T, Palmisciano P, Illari SI, Valenti V and Umana GE (2023) Considerations on surgery invasiveness and response and toxicity patterns in classic palliative radiotherapy for acrometastases of the hand: a hint for a potential role of stereotactic body radiation therapy? A case report and literature review.
Front. Oncol. 13:1146041.
doi: 10.3389/fonc.2023.1146041

Considerations on surgery invasiveness and response and toxicity patterns in classic palliative radiotherapy for acrometastases of the hand: a hint for a potential role of stereotactic body radiation therapy? A case report and literature review

Gianluca Ferini[1]*, Valentina Zagardo[1], Anna Viola[2], Marco Maria Aiello[3], Mandara Muralidhar Harikar[4], Tejas Venkataram[4], Paolo Palmisciano[5], Salvatore Ivan Illari[2], Vito Valenti[1†] and Giuseppe Emmanuele Umana[4†]

[1]Department of Radiation Oncology, REM Radioterapia Srl, Viagrande, Italy, [2]Department of Radiation Oncology, Fondazione Istituto Oncologico del Mediterraneo (IOM), Viagrande, Italy, [3]Medical Oncology, University Hospital Policlinico San Marco, Catania, Italy, [4]Department of Neurosurgery, Trauma Center, Gamma Knife Center, Cannizzaro Hospital, Catania, Italy, [5]Department of Neurosurgery, College of Medicine, University of Cincinnati, Cincinnati, OH, United States

Background: The rarity of hand acrometastases hampers the consensus-building for their optimal management among the involved oncology professionals. In the current literature, demolitive surgery overcomes the use of palliative radiotherapy, which proved to be ineffective in more than 30% of cases treated with classic palliative dose schemes, carrying also a not negligible radiation-related adverse event rate. Against this background, stereotactic body radiation therapy (SBRT) could emerge as a well-balanced therapeutic option.

Case summary: Here we describe the methods and outcomes of a SBRT treatment of a painful and function-limiting hand acrometastasis in a patient with a history of stage IIIB lung adenocarcinoma. We delivered a total dose of 30 Gy in five daily fractions to a soft-tissue metastasis abutting the fifth metacarpal bone through the SBRT protocol generally used for intracranial treatments. A few weeks later, the patient reported a clinical complete response with acrometastasis and pain disappearance, function recovery, and no significant toxicity. The acrometastasis was the first sign of an atypical cancer progression.

Conclusions: SBRT for hand acrometastases is feasible and might have the best therapeutic profile among the currently available treatment options for this rare clinical scenario. Larger investigations are needed to confirm the present single-case experience.

KEYWORDS

acrometastases, hand metastases, stereotactic body radiotherapy (SBRT), metastatic lung adenocarcinoma, palliative radiation therapy

Introduction

Acrometastases, namely metastases located distally to the elbow and knee, represent a rare clinical scenario generally indicating a high overall tumor burden and consequently a dismal prognosis, which does not exceed six months of median survival (1). Due to their rarity and absence of pathognomonic signs, acrometastases are often misdiagnosed and confused with benign diseases (i.e. pyogenic granuloma, osteomyelitis, tuberculosis, inflammatory processes, gout, etc.), especially when presenting in the context of undiagnosed cancer (2). The most prevalent primary tumors are lung, kidney, and breast carcinoma. Acrometastases to the hands arise as hot, reddened, growing, and painful nodules swelling the soft tissues and/or destroying the bones (3). This peculiar tumor location may severely impair function and alter quality of life, thus calling for timely diagnosis and treatment. As regards the latter, surgery procedures ranging from curettage to amputation are the most used therapeutic options for local removal (4), relegating radiotherapy (RT) to mere pain control by the classic palliative radiation doses commonly employed in metastatic bone disease (i.e. 8 Gy in single fraction, 20 Gy in five daily fractions, 30 Gy in ten daily fractions) (5). However, such a dose range may be inadequate to effectively shrink any relatively large lesion that disables motor function and causes severe pain due to the over-stretching of the hand's densely innervated soft tissues (6–9). On the other side, surgery may physically eliminate the source of pain but often at the cost of crippling consequences on hand function (10). Therefore, within a non-standardized therapeutic algorithm for this rare clinical condition, stereotactic body radiation therapy (SBRT) using ablative doses could be introduced to achieve both symptom relief and function recovery, avoiding demolitive surgical procedures. SBRT uses large doses per fraction precisely delivered with specific stereotactic equipment to limit any damage to the healthy tissues surrounding the tumor target (11–14).

Here we describe the methods used for a metastatic lung cancer patient with an acrometastasis to the left hand treated with SBRT, together with the subsequent atypical clinical course.

Case report

Clinical presentation

A 57-year-old female with a history of stage IIIB lung adenocarcinoma (biopsy on 12 April 2022: KRAS-G12X, EGFR-wt, BRAF-wt, PDL1-, ALK-, ROS1-, RET-, MET- negative) submitted to concomitant chemo-radiotherapy (56 Gy in standard fractionated involved-field radiotherapy plus cisplatin-pemetrexed) in May-June 2022 needed a 30 Gy-palliative RT course to the right sacroiliac joint for the appearance of a painful gait-limiting metastasis to the corresponding sacral ala the following August, as detected by an 18F-FDG Positron Emission Tomography (PET). Almost simultaneously, the patient started complaining of moderate pain in her left hand, which rapidly developed allodynia, redness, and swelling of the hypothenar eminence and corresponding dorsal side. This greatly limited the hand function. Unfortunately, the PET scan was extended up to the proximal third of the forearms, having been performed with the arms overhead. An ultrasound exam revealed a nodular lesion measuring 3,8x3,1 cm at the palmo-lateral edge of the left hand and no other suspicious findings in the PET-unscanned forearm. A hand X-ray did not detect any macroscopic lysis of the abutting fifth metacarpal bone. The final magnetic resonance imaging (MRI) confirmed the suspicion of a soft tissue acrometastasis closely adherent to the cortical bone of the basis of the fifth metacarpal bone. The patient refused any surgical procedures and was admitted to radiotherapy care. Given the low overall tumor burden (still classifiable as oligoprogressive disease), the patient's good performance status (Karnofsky score = 80), and our concerns about classic palliative radiotherapy, we decided on SBRT before starting immunotherapy.

Intervention description

A prerequisite for high-precision SBRT is a robust immobilization system to ensure a reproducible and accurate setup as much as possible. As we chose to deliver the treatment by a Novalis TrueBeam STx (Varian, Palo Alto, CA, USA), we used the stereotactic equipment for intracranial targets: the patient was positioned prone on the simul-Computed Tomography (CT) couch with her left hand above her head and between a two-sheet stereotactic mask within the frameless extension for ExacTrac™ system (Brainlab®, Munich, Germany) at the couch top, the hand replacing the skull (Figure 1). The simulation CT scan was acquired with 1.5mm thickness slices and merged with the previous diagnostic MRI for precise delineation of the gross tumor volume (GTV). This was 1 mm-expanded to create a clinical target volume (CTV) covering any possible subclinical spread, especially in the fifth metacarpal bone. A final

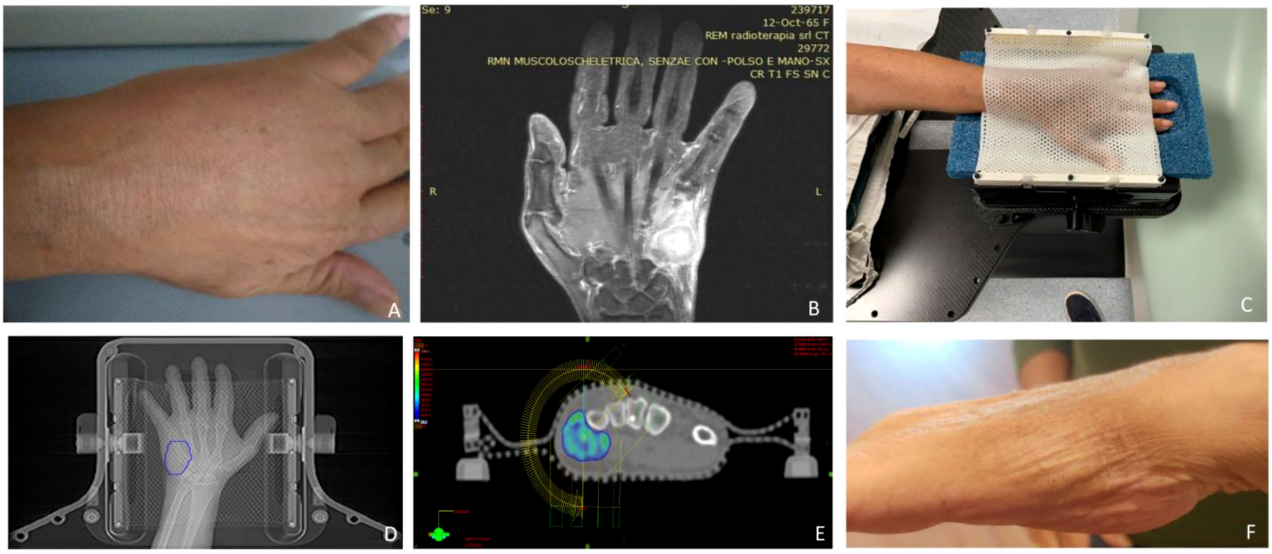

FIGURE 1
(A) Clinical presentation of the acrometastasis; **(B)** MR exam of the left hand; **(C)** set-up procedure; **(D)** contouring process on the CT-simulation; **(E)** 95% dose coverage with the two treatment coplanar arcs highlighted; **(F)** hand status one month after SBRT.

expansion of 1 mm was added to the CTV for the definition of the planning target volume (PTV) to avoid missing the target for submillimeter displacements, i.e. the largest possible per protocol. We planned a total dose of 30 Gy in five daily fractions and reported 95% of the dose prescription to the 98% of the PTV (with a 108,4% maximum point dose) by two coplanar volumetric modulated arcs (VMAT) (50°-181°CCW/CW). The treatment was delivered under both the ExacTrac- and cone beam CT-guidance in five consecutive days in September 2022 (Figure 2).

Outcomes and follow-up

The patient experienced a rapid acrometastasis shrinkage with progressive resolution of pain and recovery of hand function, which were complete four weeks after the end of RT. No significant toxicity was complained. Then, the patient started a systemic treatment with Nivolumab, which was suspended just after two cycles due to the occurrence of severe pneumonitis first and of pseudomembranous colitis later, requiring hospitalization for more than one month. Once these intercurrent events passed and before starting any further systemic treatments, the patient returned to our attention due to the painful progression of her metastatic disease at the right supraclavicular fossa (7,8 cm diameter) and at three further sites of her left arm: a large epitrochlear lymph node metastasis (2,7 cm diameter), a soft tissue metastasis inside the bicep muscle (5,5 cm diameter), and bulky matted axillary node metastases (7,7 cm diameter) causing mild arm swelling. In our opinion, the centripetal in transit-like progression of the tumor disease at this stage needed a more inclusive RT approach rather than selectively irradiating only the three metastatic sites of the left arm. Thus, in December 2022, we treated the whole left arm from the shoulder to the elbow with a dose of 20 Gy in five fractions of 4 Gy each while simultaneously boosting (simultaneous integrated boost, SIB) the gross nodal and tumor volumes to 30 Gy (6 Gy/day). The right bulky supraclavicular metastasis was concomitantly treated with a dose of 30 Gy. Just after the completion of these treatments (14 December), the patient performed a brain MRI exam to establish the brain tumor burden as the previous contrast-enhanced CT had detected two small brain metastases, eventually amenable to stereotactic radiosurgery. Unfortunately, the brain MRI revealed multiple disseminated subcentimeter metastases, for which the most appropriate treatment was deemed to be whole-brain radiotherapy. This was delivered with a dose of 20 Gy in five consecutive days to initiate a systemic treatment as early as possible. The patient started docetaxel on 2 January 2023. At the last follow-up (16 January 2023), all four extracranial metastases except the one in the biceps downsized and were nontender while the left hand still presented a sustained complete response with full functional recovery and no residual pain. The brain MRI re-evaluation is awaited in due course (Figure 3).

Discussion

To our knowledge, this is the first case of acrometastasis to the hand treated with SBRT. According to the recent systematic review by Umana et al. (2), surgery is the most common treatment for this metastatic bone site, especially in the form of digital or ray amputation (15). Obviously, such a demolitive surgery has an adverse aesthetic and functional impact and represents a physical and psychological trauma worsening the patient's daily living (10).

Radiotherapy is a historical therapeutic option for the palliative treatment of painful or complicated bone metastases (5), being able to be also integrated with new systemic anticancer therapies (16). With advancing technology and awareness of the oligometastatic or oligoprogressive status, which deserve dose-escalation aimed at

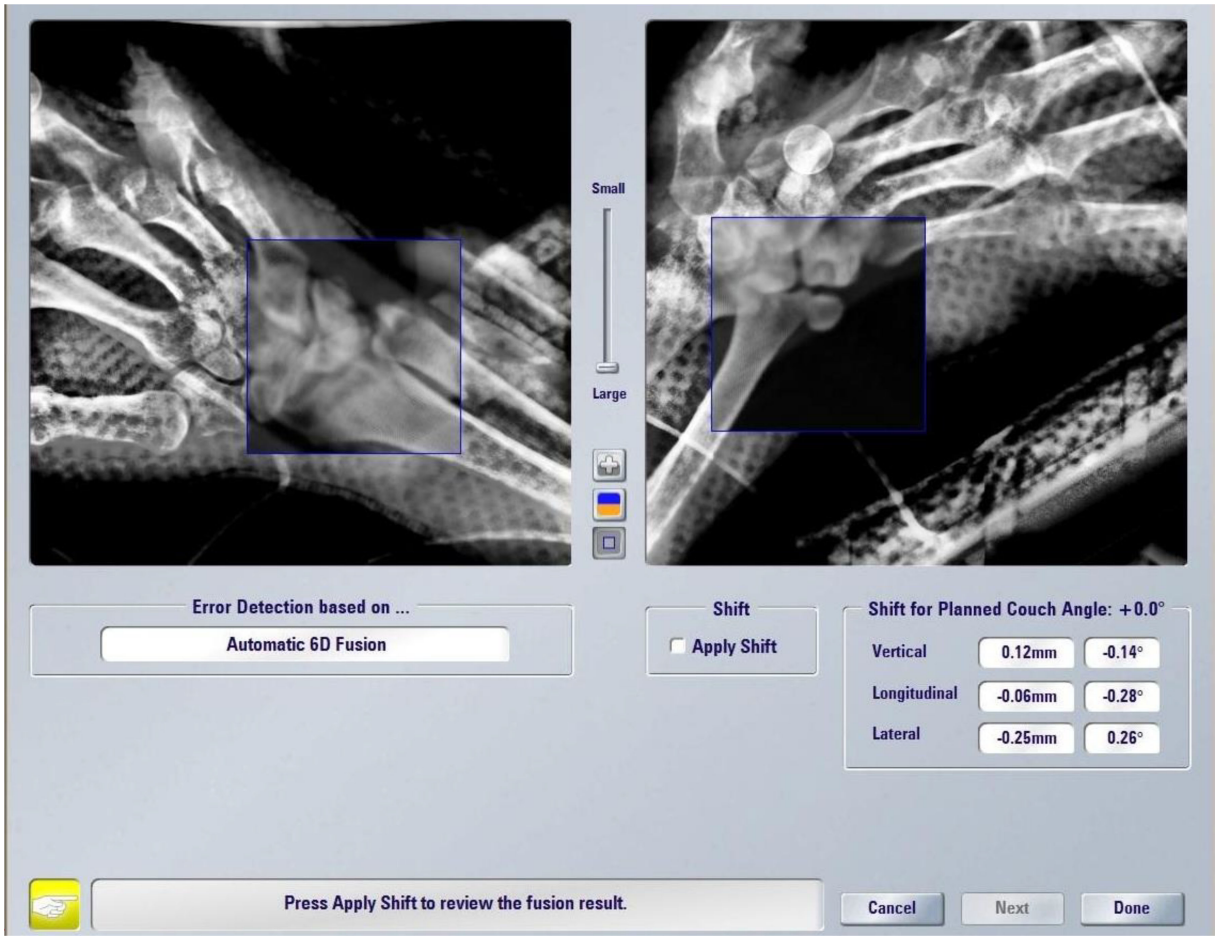

FIGURE 2
Treatment setup verification by the ExacTrac system.

better local control (17, 18), the SBRT use for bone metastases is enormously increased in recent years, being currently tested also for polymetastatic setting (19). Compared to classic palliative RT using low biologically effective doses, SBRT adopts larger doses, which fall steeply off the tumor target, drastically reducing the risk of damage to surrounding healthy tissues exposed to radiation (20–22). In metastatic bone disease, this technique demonstrated to improve the complete pain response rate while reducing the local progression one (23).

Reviewing the literature on hand acrometastases shows that the response to classic palliative RT doses is variable. For example, the clinical results achieved through 30 Gy in 10 fractions ranged from good symptom palliation in three cases (two metacarpal, one phalangeal), modest pain control in another report with metastatic involvement of a distal phalanx, and to no significant benefit with even worsening of swelling in another patient with bilateral carpal bone metastases (6, 24–27). In another case of thumb metastasis, a 30 Gy dose produced a symptomatic improvement, along with soft tissue edema as a collateral event (28). Longer dose fractionation schemes (54 Gy in 27 fractions and 40 Gy in 20 fractions) were equally effective, but more treatment sessions could potentially discomfort patients in terms of compliance with the RT schedule (27, 29). A total dose of 27 Gy, whose fractionation scheme was omitted, resulted in the complete disappearance of both pain and swelling in a patient with a metacarpal bone metastasis (30). Pain and motion complaints resolved after 8 Gy-single fraction administration in other two cases of metacarpal metastases (3). Two further patients benefitted from an 8 Gy-single fraction (31, 32). A dose of 15 Gy in 3 fractions produced only transient pain relief lasting a few weeks (7). Lastly, 20 Gy in 5 fractions produced no response in two patients (8, 9) and complete pain relief and regaining of the full range of motion in another one (33). No indication about the dose used in another mostly ineffective RT treatment for a distal phalanx metastasis was provided by the authors (34). This inconsistency of results motivated us to test an escalation of radiation dose in our case. Indeed, from this pooled cohort, there is evidence of a treatment failure rate and radiation-related adverse event rate equal to 31,6% (6/19) and 10,5% (2/19), respectively. The above findings are summarized in Table 1.

Given the excellent performance of easier ultra-hypofractionated RT protocols (without the support of any stereotactic technology) even among frail patients (35, 36), one may question the need for SBRT in the scenario described here. However, it is worth noting that an expanded target volume (i.e. PTV to take into account any positional uncertainties) at this body site may provoke excessive

10.3389/fonc.2023.1146041

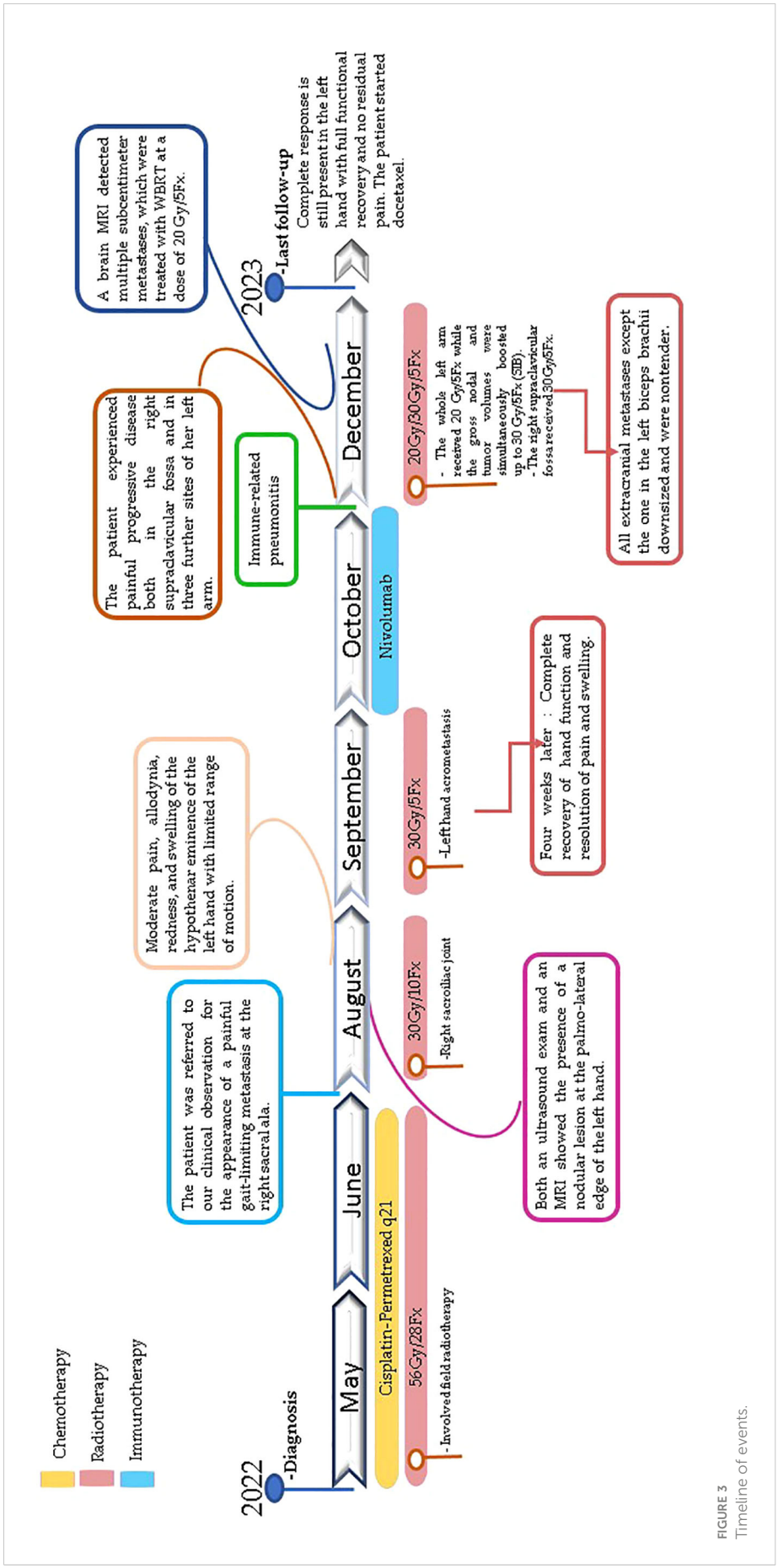

FIGURE 3
Timeline of events.

TABLE 1 Summary of case reports listing the prescribed radiation dose, fractionation scheme and clinical outcomes.

Authors, Year	Primary tumor histology	Acrometastasis Site	RT Dose/Fractions (Fx)	Outcomes
Khosla et al, 2012 (24)	Vaginal squamous cell carcinoma	Left fourth metacarpal	30Gy/10Fx	Good symptom palliation
De Smet L., 2004 (25)	Breast carcinoma	Right second metacarpal	30Gy/10Fx	Good symptom palliation
Sumodhee et al, 2014 (26)	Bronchogenic adenocarcinoma	Left ring finger	30Gy/10Fx	Good symptom palliation
Kumar et al, 2011 (27)	Cutaneous squamous cell carcinoma	Right tumb, distal phalanx	54Gy/27Fx	Good symptom palliation
	Esophageal squamous cell carcinoma	Left finger, distal phalanx	30Gy/10Fx	Modest pain control
Park et al, 2006 (6)	Gastric adenocarcinoma	Bilateral carpal bones	30Gy/10Fx	Minimal pain control and worsening of swelling
Vasic L., 2010 (28)	Sigmoid colon cancer	Right thumb, proximal and distal phalanges	30Gy/10Fx	Good symptom palliation and onset of soft tissue edema
Tabrizi et al, 2018 (29)	Bronchogenic adenocarcinoma	Left hamate	40Gy/20Fx	Good symptom palliation
Kodama et al, 2009 (30)	Bronchogenic adenocarcinoma	Left metacarpal	27Gy/NR	Complete pain resolution
Flynn et al, 2008 (3)	Bronchogenic non-small cell carcinoma	Left second metacarpal	8Gy/1Fx	Complete pain resolution
	Breast carcinoma	Right third and fifth metacarpal	8Gy/1Fx	Complete pain resolution
Asthana et al, 2001 (31)	Breast carcinoma	Left thumb, proximal phalanx	8Gy/1Fx	Good symptom palliation
Myrehaug and Bezjak, 2010 (32)	Bronchogenic adenocarcinoma	Right index finger, proximal phalanx	8Gy/1Fx	Good symptom palliation
Carvalho H.d.A. et al, 2002 (7)	Bronchogenic small cell carcinoma	Right thumb, distal phalanx	15Gy/3Fx	Transient pain relief
Bigot et al, 2007 (8)	Gastric adenocarcinoma	Right third metacarpal	20Gy/5Fx	No pain control
Verardino et al, 2011 (9)	Basaloid carcinoma of the anal canal	Right and left ring fingers, distal phalanges	20Gy/5Fx	No pain control
Kumar A., 2009 (33)	Gastric adenocarcinoma	Second left metacarpal	20Gy/5Fx	Complete pain resolution
Lambe et al, 2014 (34)	Bronchogenic squamous cell carcinoma	Right fifth finger, distal phalanx	NR	No pain control
Ferini et al, 2023	Lung adenocarcinoma	Soft tissues surrounding the fifth metacarpal	30Gy/5Fx	Complete pain resolution

RT, Radiation Therapy; NR, Not Reported.

acute skin toxicity, like in Dupuytren's disease treatment, and a greater risk of bone necrosis (37–39). Moreover, exposing a larger amount of the healthy lymphatic system to harmful radiation can produce chronic lymphedema culminating in function-limiting stiffness of the hand (40–42).

Our SBRT protocol was based on the use of the ExacTrac system, which, despite being specifically designed for intracranial and spine targets (17, 21, 43, 44), proved to be of great accuracy also in the treatment of appendicular skeleton in upper extremities (45). Other than the setup corrections, which notoriously reduce the toxicity rate when done on a daily basis (46), the ExacTrac system allows also intrafraction motion monitoring.

The characteristic tangential effect of rotational RT techniques like that used here reduces the need for a bolus to adequately irradiate even the most superficial layers of the target abutting the skin (47, 48). In agreement with this, we registered that 95% of the dose prescription covered 98,12% of the PTV.

Our patient achieved a rapid complete response in terms of both tumor regression and pain reduction with no significant toxicity, also restoring the full range of motion of her left hand. These findings encourage the introduction of SBRT among the therapeutic options available for the treatment of acrometastases.

The present case report has also the merit to describe an atypical cancer progression along the upper extremity after the appearance of the hand acrometastasis, alerting the practitioners about such a possible disease evolution. Interestingly, the tumor histology of our patient exhibited poor sensitivity to systemic drugs while being a good responder to radiation. This warrants further investigations

on the possible cancer cell targets to hit with radionuclide therapeutic agents (49).

Conclusions

SBRT might be characterized by the most favorable therapeutic profile among the currently available therapeutic options for the treatment of acrometastases. Larger series of patients are needed to confirm the results of our single case description.

Patient perspective

I am fully satisfied with the clinical result obtained in the hand, confident in achieving the same in the arm, and enormously grateful to the doctors who are supporting me in my fight against cancer.

Data availability statement

The original contributions presented in the study are included in the article/supplementary material. Further inquiries can be directed to the corresponding author.

Ethics statement

Ethical review and approval was not required for the study on human participants in accordance with the local legislation and institutional requirements. The patients/participants provided their written informed consent to participate in this study. Written informed consent was obtained from the participant/patient(s) for the publication of this case report.

Author contributions

GF: writing - original draft. VZ and GF: data collection. AV, MMA, MH, TV, PP: supervision. GF, SI, VV and GU writing - review and editing, also the treating doctors. All authors contributed to the article and approved the submitted version.

Acknowledgments

The authors thank Antonella Amato, Mariagrazia Marchese, and Gianluca Ciolino for their valuable technical support.

Conflict of interest

The authors declare that the research was conducted in the absence of any commercial or financial relationships that could be construed as a potential conflict of interest.

Publisher's note

References

1. Kerin R. The hand in metastatic disease. *J Handb Surg Am* (1987) 12(1):77–83. doi: 10.1016/s0363-5023(87)80164-8

2. Umana GE, Scalia G, Palmisciano P, Passanisi M, Da Ros V, Pompili G, et al. Acrometastases to the hand: a systematic review. *Medicina (Kaunas)* (2021) 57(9):950. doi: 10.3390/medicina57090950

3. Flynn CJ, Danjoux C, Wong J, Christakis M, Rubenstein J, Yee A, et al. Two cases of acrometastasis to the hands and review of the literature. *Curr Oncol* (2008) 15(5):51–8. doi: 10.3747/co.v15i5.189

4. Sebghati J, Khalili P, Tsagkozis P. Surgical treatment of metastatic bone disease of the distal extremities. *World J Orthop* (2021) 12(10):743–50. doi: 10.5312/wjo.v12.i10.743

5. Pergolizzi S, Cacciola A, Parisi S, Lillo S, Tamburella C, Santacaterina A, et al. An Italian survey on "palliative intent" radiotherapy. *Rep Pract Oncol Radiother* (2022) 27 (3):419–27. doi: 10.5603/RPOR.a2022.0052

6. Park KH, Rho YH, Choi SJ, Hong SJ, Lee JH, Choi IK, et al. Acute arthritis of carpal bones secondary to metastatic gastric cancer. *Clin Rheumatol* (2006) 25(2):258–61. doi: 10.1007/s10067-005-1096-7

7. Carvalho Hde A, Tsai PW, Takagaki TY. Thumb metastasis from small cell lung cancer treated with radiation. *Rev Hosp Clin Fac Med Sao Paulo* (2002) 57(6):283–6. doi: 10.1590/s0041-87812002000600007

8. Bigot P, Desbois E, Benoist N, Besnier L, Moui Y. Acrométastase révélée par une douleur isolée de la main. a propos d'un cas [Isolated pain of the hand revealing a metastatic tumor of the hand. report of a case]. *Chir Main* (2007) 26(6):300–2. doi: 10.1016/j.main.2007.09.001

9. Verardino GC, Silva RS, Obadia DL, Gripp AC, Alves Mde F. Rare cutaneous metastasis from a probable basaloid carcinoma of the colon mimicking pyogenic granuloma. *Bras Dermatol* (2011) 86(3):537–40. doi: 10.1590/s0365-05962011000300016

10. Sagiv P, Shabat S, Mann M, Ashur H, Nyska M. Rehabilitation process and functional results of patients with amputated fingers. *Plast Reconstr Surg* (2002) 110 (2):497–503; discussion 504-5. doi: 10.1097/00006534-200208000-00020

11. Cacciola A, Parisi S, Tamburella C, Lillo S, Ferini G, Molino L, et al. Stereotactic body radiation therapy and radiofrequency ablation for the treatment of liver metastases: how and when? *Rep Pract Oncol Radiother* (2020) 25(3):299–306. doi: 10.1016/j.rpor.2020.02.010

12. Vadalà RE, Santacaterina A, Sindoni A, Platania A, Arcudi A, Ferini G, et al. Stereotactic body radiotherapy in non-operable lung cancer patients. *Clin Transl Oncol* (2016) 18(11):1158–9. doi: 10.1007/s12094-016-1552-7

13. Palmisciano P, Ogasawara C, Ogasawara M, Ferini G, Scalia G, Haider AS, et al. Endocrine disorders after primary gamma knife radiosurgery for pituitary adenomas: a systematic review and meta-analysis. *Pituitary* (2022) 25(3):404–19. doi: 10.1007/s11102-022-01219-x

14. Inserra F, Barone F, Palmisciano P, Scalia G, DA Ros V, Abdelsalam A, et al. Hypofractionated gamma knife radiosurgery: institutional experience on benign and malignant intracranial tumors. *Anticancer Res* (2022) 42(4):1851–8. doi: 10.21873/anticanres.15661

15. Umana GE, Scalia G, Palmisciano P, Passanisi M, Pompili G, Amico P, et al. Spontaneous sacral fracture with associated acrometastasis of the hand. *Surg Neurol Int* (2021) 12:534. doi: 10.25259/SNI_917_2021

16. Gagliano A, Prestifilippo A, Cantale O, Ferini G, Fisichella G, Fontana P, et al. Role of the combination of cyclin-dependent kinase inhibitors (CDKI) and radiotherapy (RT) in the treatment of metastatic breast cancer (MBC): advantages and risks in clinical practice. *Front Oncol* (2021) 11:643155. doi: 10.3389/fonc.2021.643155

17. Ferini G, Viola A, Valenti V, Tripoli A, Molino L, Marchese VA, et al. Whole brain irradiation or stereotactic RadioSurgery for five or more brain metastases (WHOBI-STER): a prospective comparative study of neurocognitive outcomes, level of autonomy in daily activities and quality of life. *Clin Transl Radiat Oncol* (2021) 32:52–8. doi: 10.1016/j.ctro.2021.11.008

18. Ferini G, Castorina P, Valenti V, Illari SI, Sachpazidis I, Castorina L, et al. A novel radiotherapeutic approach to treat bulky metastases even from cutaneous squamous cell carcinoma: its rationale and a look at the reliability of the linear-quadratic model to explain its radiobiological effects. *Front Oncol* (2022) 12:809279. doi: 10.3389/fonc.2022.809279

19. Bauman GS, Corkum MT, Fakir H, Nguyen TK, Palma DA. Ablative radiation therapy to restrain everything safely treatable (ARREST): study protocol for a phase I trial treating polymetastatic cancer with stereotactic radiotherapy. *BMC Cancer* (2021) 21(1):405. doi: 10.1186/s12885-021-08020-2

20. Parisi S, Ferini G, Cacciola A, Lillo S, Tamburella C, Santacaterina A, et al. A non-surgical COMBO-therapy approach for locally advanced unresectable pancreatic adenocarcinoma: preliminary results of a prospective study. *Radiol Med* (2022) 127 (2):214–9. doi: 10.1007/s11547-021-01441-w

21. Pontoriero A, Iatì G, Cacciola A, Conti A, Brogna A, Siragusa C, et al. Stereotactic body radiation therapy with simultaneous integrated boost in patients with spinal metastases. *Technol Cancer Res Treat* (2020) 19:1533033820904447. doi: 10.1177/1533033820904447

22. Cuccia F, Pastorello E, Vitale C, Figlia V, Levra NG, Mazzola R, et al. Stereotactic body radiotherapy for a rare case of sinonasal metastasis arising from renal cell cancer. *In Vivo* (2023) 37(1):490–2. doi: 10.21873/invivo.13104

23. Lee CC, Soon YY, Cheo T, Vellayappan B, Tey J. Stereotactic body radiation therapy versus conventional external beam radiation therapy for painful bone metastases: a systematic review and meta-analysis of randomized trials. *Crit Rev Oncol Hematol* (2022) 178:103775. doi: 10.1016/j.critrevonc.2022.103775

24. Khosla D, Rai B, Patel FD, Sapkota S, Srinvasan R, Sharma SC. Acrometastasis to hand in vaginal carcinoma: a rare entity. *J Cancer Res Ther* (2012) 8(3):430–2. doi: 10.4103/0973-1482.103526

25. De Smet L. Late appearance and slow progression of a breast carcinoma metastasis of the index metacarpal. *Acta Chir Belg* (2004) 104(3):345–6. doi: 10.1080/00015458.2004.11679570

26. Sumodhee S, Huchot E, Peret G, Marchal C, Paganin F, Magnin V. Radiotherapy for a phalanx bone metastasis of a lung adenocarcinoma. *Case Rep Oncol* (2014) 7 (3):727–31. doi: 10.1159/000368345

27. Kumar N, Kumar R, Bera A, Kumar P, Angurana SL, Ghosal S, et al. Palliative and supportive care in acrometastasis to the hand: case series. *Indian J Palliat Care* (2011) 17(3):241–4. doi: 10.4103/0973-1075.92347

28. Vasić L. Osteolysis of hand bones due to metastatic deposits from colon cancer–a case report. *Med Pregl* (2010) 63(9-10):719–22. doi: 10.2298/mpns1010719v

29. Tabrizi A, Afshar A, Shariyate MJ, Gharalari FH, Aidenlou A. Isolated metastatic carcinoma to the hamate bone: the first manifestation of an occult malignancy. *J Handb Microsurg* (2019) 11(Suppl 1):S01–5. doi: 10.1055/s-0038-1645952

30. Kodama T, Kikuchi N, Satoh H, Ohtsuka M. Metacarpal bone metastasis from lung cancer. *Onkologie* (2009) 32(4):216–7. doi: 10.1159/000203347

31. Asthana S, Deo SV, Shukla NK, Raina V. Carcinoma breast metastatic to the hand and the foot. *Australas Radiol* (2001) 45(3):380–2. doi: 10.1046/j.1440-1673.2001.00943.x

32. Myrehaug S, Bezjak A. Rapidly progressive bone destruction of the finger as first presentation of systemic metastases from lung cancer. *BMJ Case Rep* (2010) 2010:bcr05. doi: 10.1136/bcr.05.2009.1912

33. Kumar A. Acrometastases to the hand in stomach carcinoma: a rare entity. *BMJ Case Rep* (2019) 12(8):e229390. doi: 10.1136/bcr-2019-229390

34. Lambe G, Le P, Clay TD. A finding with a diagnosis: I just can't put my finger on it. *BMJ Case Rep* (2014) 2014:bcr201420866. doi: 10.1136/bcr-2014-208665

35. Parisi S, Lillo S, Cacciola A, Ferini G, Valenti V, Viola A, et al. Non-stereotactic radiotherapy in older cancer patients. *Heliyon* (2022) 8(6):e09593. doi: 10.1016/j.heliyon.2022.e09593

36. Ferini G, Molino L, Bottalico L, De Lucia P, Garofalo F. A small case series about safety and effectiveness of a hypofractionated electron beam radiotherapy schedule in five fractions for facial non melanoma skin cancer among frail and elderly patients. *Rep Pract Oncol Radiother* (2021) 26(1):66–72. doi: 10.5603/RPOR.a2021.0013

37. Kadhum M, Smock E, Khan A, Fleming A. Radiotherapy in dupuytren's disease: a systematic review of the evidence. *J Handb Surg Eur Vol* (2017) 42(7):689–92. doi: 10.1177/1753193417695996

38. Rohde RS, Puhaindran ME, Morris CD, Alektiar KM, Schupak KD, Healey JH, et al. Complications of radiation therapy to the hand after soft tissue sarcoma surgery. *J Handb Surg Am* (2010) 35(11):1858–63. doi: 10.1016/j.jhsa.2010.08.030

39. Goitz RJ, Tomaino MM, Smith P, Hannallah D, Sinha R. Treatment of radiation-induced soft-tissue fibrosis and concomitant acetabular osteonecrosis: a case report. *Am J Orthop (Belle Mead NJ)* (2007) 36(4):E56–8.

40. Rayner CR. The results of treatment of two hundred and seventy-three carcinomas of the hand. *Hand* (1981) 13(2):183–6. doi: 10.1016/s0072-968x(81)80061-7

41. Avraham T, Yan A, Zampell JC, Daluvoy SV, Haimovitz-Friedman A, Cordeiro AP, et al. Radiation therapy causes loss of dermal lymphatic vessels and interferes with lymphatic function by TGF-beta1-mediated tissue fibrosis. *Am J Physiol Cell Physiol* (2010) 299(3):C589–605. doi: 10.1152/ajpcell.00535.2009

42. Brewer CF, Deutsch CJ, Jemec B. Is radiation therapy as a primary treatment modality for squamous cell carcinoma of the hand the best choice? case series and review of the literature. *Dermatol Online J* (2020) 26(6):13030/qt0mx961gq. doi: 10.5070/D3266049311

43. Ferini G, Palmisciano P, Scalia G, Haider AS, Bin-Alamer O, Sagoo NS, et al. The role of radiation therapy in the treatment of spine metastases from hepatocellular carcinoma: a systematic review and meta-analysis. *Neurosurg Focus* (2022) 53(5):E12. doi: 10.3171/2022.8.FOCUS2255

44. Palmisciano P, Ferini G, Khan R, Bin-Alamer O, Umana GE, Yu K, et al. Neoadjuvant stereotactic radiotherapy for brain metastases: systematic review and meta-analysis of the literature and ongoing clinical trials. *Cancers (Basel)* (2022) 14 (17):4328. doi: 10.3390/cancers14174328

45. Ferini G, Palmisciano P, Zagardo V, Viola A, Illari SI, Marchese V, et al. Combining a customized immobilization system with an innovative use of the ExacTrac system for precise volumetric modulated arc therapy of challenging forearm sarcomas. *Pract Radiat Oncol* (2022) S1879-8500(22):00328–9. doi: 10.1016/j.prro.2022.10.005

46. Ferini G, Tripoli A, Molino L, Cacciola A, Lillo S, Parisi S, et al. How much daily image-guided volumetric modulated arc therapy is useful for proctitis prevention with respect to static intensity modulated radiotherapy supported by topical medications among localized prostate cancer patients? *Anticancer Res* (2021) 41(4):2101–10. doi: 10.21873/anticanres.14981

47. Ferini G, Valenti V, Puliafito I, Illari SI, Marchese VA, Borzì GR. Volumetric modulated arc therapy capabilities for treating lower-extremity skin affected by several merkel cell carcinoma nodules: when technological advances effectively achieve the palliative therapeutic goal while minimising the risk of potential toxicities. *Medicina (Kaunas)* (2021) 57(12):1379. doi: 10.3390/medicina57121379

48. Cuccia F, Figlia V, Palmeri A, Verderame F, Lo Casto A, Mannino M, et al. Helical tomotherapy® is a safe and feasible technique for total scalp irradiation. *Rare Tumors* (2017) 9(1):6942. doi: 10.4081/rt.2017.6942

49. Pirooznia N, Abdi K, Beiki D, Emami F, Arab SS, Sabzevari O, et al. 177Lu-labeled cyclic RGD peptide as an imaging and targeted radionuclide therapeutic agent in non-small cell lung cancer: biological evaluation and preclinical study. *Bioorg Chem* (2020) 102:104100. doi: 10.1016/j.bioorg.2020.104100

Frontiers in Oncology

Advances knowledge of carcinogenesis and tumor progression for better treatment and management

The third most-cited oncology journal, which highlights research in carcinogenesis and tumor progression, bridging the gap between basic research and applications to imrpove diagnosis, therapeutics and management strategies.

Discover the latest Research Topics

See more →

Frontiers

Avenue du Tribunal-Fédéral 34
1005 Lausanne, Switzerland
frontiersin.org

Contact us

+41 (0)21 510 17 00
frontiersin.org/about/contact